

Enhancing Performance of Self-Compacting Concrete with Internal Curing Using Thermostone Chips

Amar Yahia Ebrahim AL-Awadi
Ministry of Municipalities
email: ammar.awady@gmail.com

Prof. Dr. Nada Mahdi Fawzi
University of Baghdad
email: naljalawi@yahoo.com

ABSTRACT

This paper is devoted to investigate the effect of internal curing technique on the properties of self-compacting concrete (SCC). In this study, SCC is produced by using silica fume (SF) as partial replacement by weight of cement with percentage of (5%), sand is partially replaced by volume with saturated fine lightweight aggregate (LWA) which is thermostone chips as internal curing material in three percentages of (5%, 10% and 15%) for SCC, two external curing conditions water and air. The experimental work was divided into three parts: in the first part, the workability tests of fresh SCC were conducted. The second part included conducting compressive strength test and modulus of rupture test at ages of (7, 28 and 90). The third part included the shrinkage test, at ages (7, 14, 21, 28) days. The results show that internally cured SCC has the best workability, and the best properties of hardened concrete which include (compressive strength and modulus of rupture) then the externally cured SCC with both water and air as compared with reference concretes. Also, the hardened properties of internally cured SCC with replacement percentage of (10%) by thermostone chips is the best as compared with that of percentages (5% and 15%) for both external curing conditions. In general, the results of shrinkage test, showed reduction in shrinkage of internally cured SCC as compared with reference concrete.

Key words: self-compacting concrete, internal curing, thermostone chips, silica fume.

تحسين اداء الخرسانة ذاتية الرص بواسطة الانضاج الداخلي باستعمال فتات الكتل الخرسانية الخلوية

أ. د. ندى مهدي فوزي
كلية الهندسة-جامعة بغداد

عمار يحيى إبراهيم العوادي
وزارة البلديات

الخلاصة

ان الغرض من هذا البحث هو التحري عن تأثير تقنية المعالجة الداخلية على خصائص الخرسانة ذاتية الرص. في هذه الدراسة تم انتاج الخرسانة ذاتية الرص باستعمال غبار السليكا كاستبدال جزئي من وزن السمنت بنسبة 5 % ، وتم استبدال الرمل جزئيا بركام ناعم خفيف الوزن ومشبع وجاف السطح هو فتات الكتل الخرسانية الخلوية كمادة معالجة داخلية وبثلاث نسب حجمية هي (5%، 10%، 15%) كاستبدال حجمي، طرفين للمعالجة الخارجية هما الماء والهواء. قسم العمل المختبري في هذه الدراسة الى ثلاثة اجزاء اساسية : في الجزء الاول تم اجراء الفحوص المختبرية للخرسانة ذاتية الرص الطرية لاجاد قابلية التشغيل. أما القسم الثاني فيتضمن اجراء فحوص مقاومة الانضغاط ومقاومة الانثناء للخرسانة ذاتية الرص المتصلبة بأعمار (7، 28، 90) يوم. والجزء الثالث يتضمن اجراء فحص الانكماش بأعمار (7، 14، 21، 28) يوم. لوحظ من استعراض نتائج فحوص الخصائص الطرية والمتصلبة للخرسانة ذاتية الرص المعالجة داخليا بفتات الكتل الخرسانية الخلوية حصول تحسن واضح في قابلية التشغيل وكذلك حصول تحسن ملحوظ في الخصائص المتصلبة والتي تشمل (مقاومة الانضغاط ومقاومة الانثناء) في كلا طرفي المعالجة الخارجية مقارنة بالخرسانة المرجعية. كما ان الخصائص المتصلبة للخرسانة ذاتية الرص باستعمال فتات الكتل الخرسانية الخلوية بنسبة استبدال (10%) هي الافضل قياسا بنسب الاستبدال الاخرى. وبشكل عام بينت النتائج حصول نقصان واضح في انكماش الخرسانة ذاتية الرص المعالجة داخليا.

كلمات رئيسية: الخرسانة ذاتية الرص، المعالجة الداخلية، فتات الكتل الخرسانية الخلوية، غبار السليكا.

1. INTRODUCTION

Self compacting concrete is characterized by high resistance to segregation that can be cast without compaction or vibration. It flows like honey, deaerates, self-compacts and has nearly a horizontal concrete level after placing, **Holm, and Bremner, 2000**.

The term internal curing means “supplying water throughout a freshly placed cementitious mixture using reservoirs, via pre-wetted lightweight aggregates, that readily release water as needed for hydration or to replace moisture lost through evaporation or self-desiccation” according to the definition provided in American Concrete Institute. Also, the hydration of cement continues because of the availability of internal water that is not part of the mixing water, refers to internal curing technique, **ACI 213-03R, 2003**.

The concept of SCC was first proposed by Professor Hajime Okamura, in 1986 in Japan as a solution to concrete's concerns. There are many advantages of using SCC, these include, **Bouzoubaa, and Lachemi, 2001. Horta, 2005**.

- No need for vibration.
- Reducing the construction time and labor cost.
- Reducing the noise pollution.
- Improving the filling capacity of highly congested structural member.
- Facilitating and ensuring good structural performance.

The use of SCC is spreading world wide because of its very attractive properties in the fresh state as well as after hardening. The use of SCC leads to reduce the technical costs of in situ concrete constructions and eliminate some of the potential human error. It replaces the manual compaction of fresh concrete with a modern semi-automatic placing technology that way improve health and safety on and around the construction site, **Selvamony, et al., 2010**.

It is possible to get benefit from the internal curing instead of traditional external curing. Internal curing has a significant contribution in shrinkage reduction and enhancing concrete performance as well as environmental friendly, **Munaz, et al., 2011**.

By replacing a portion of the normal weight aggregates with pre-wetted lightweight aggregates (LWA), additional internal curing water is provided to the concrete mixture. During the hydration of the cement paste within the concrete mixture, this internal curing water will be drawn from the LWA into the hydrating paste, maintaining a high degree of saturation (water-filled pores) in the cement paste and avoiding or at least reducing shrinkage stresses and their accompanying autogenous deformations, **Cusson, and Hoogeveen, 2005. Bentz, 2007**.

The main properties of lightweight aggregate (LWA) are its high porosity, high absorption, low specific gravity and cellular structure [Muhsen 1996] and [Dhaher 2001]. These properties make LWA a suitable material for internal curing technique, **Lura, et al., 2004**.

2. EXPERIMENTAL WORK

2.1 Materials

Taslua Ordinary Portland Cement complied with the Iraqi specification, **IQS No.5, 1984** was used. The coarse aggregate was brought from Al-Nibaii quarry with a nominal size of (14) mm. Al-Ekhaider natural sand is used as fine aggregate in concrete mixes. **Tables 1 and 2** show the sieve analysis and properties for the sand used throughout this work. The grading and properties of the used sand and coarse aggregate satisfies the requirements of the Iraqi specification, **IQS No.45, 1984**.

Thermostone chips is used as a lightweight aggregate in this study to be the internal curing material. Thermostone was from Karbala thermoston Factory as waste and broken into

smaller size particles. Then, the crushed thermostone is washed with water afterward dried by spread in air. The crushed particles are sieved and partially replaced by volume with the same size of sand with a certain percentage to have the same grading as the used sand which satisfies the grading requirements of the Iraqi specification, **IQS No.45, 1984**. Later, the thermostone aggregate is soaked in water for (24) hours to bring the aggregate particles to saturated condition. **Table 3** shows the physical properties of the used crushed thermostone aggregate.

Glenium 51 (G51) is used in this research as chemical admixture and complies with **ASTM C 494-05, 2005** type F.

Silica fume is used as a highly pozzolanic mineral admixture. The fineness (Blaine specific surface) of SF is (23000 m²/kg). The chemical analysis of SF which is used in this research conforms to the chemical requirements of **ASTM C 618-03, 2003** as shown in **Table 4**.

2.2 Mix Design and Proportions

The mix design method of the used SCC in this study is according to **ERMCO, 2005**. The proportions of materials were modified after obtaining a satisfactory self-compactability by evaluating through fresh concrete tests. The mix proportions of the SCC which was used throughout this research are shown in **Table 5**.

2.3 Tests of Fresh Concrete

Slump flow test, T50cm test, V- funnel test and L-box test were used for workability properties of SCC according to the European Federation Guidelines **ERMCO, 2005**.

2.4 Tests of Hardened Concrete

Tests of hardened concrete in this research are shown below:

- Compressive strength test was conducted according to the British Standard, **BS1881 part 116, 1985**. Three cubes (100*100*100) mm were tested for each mix at each age of (7, 28 and 90) days for determination of compressive strength using two sets of mixes for SCC, one of these sets is cured in water and the other is cured in air.
- Modulus of rupture test was performed on two (100x100x400) mm prisms according to **ASTM C 293-02, 2002**, with span of (300) mm at age of (7, 28 and 90) days. The average of two prism specimens of each mix was adopted.
- Shrinkage test was conducted according to **ASTM C 490-00, 2000**. A micrometer dial gauge with (0.001) mm reading accuracy was used in this test. Pins were fixed on prisms (100x100x400) mm after casting the specimens. The shrinkage test was conducted by using two sets of prisms specimens for SCC, the first set was cured for 7 days in water, after that it was taken out from water tank and left in air (laboratory conditions) for 21 days, the second set was cured in air along test period for 28 days. The changes in length were calculated at age of (7, 14, 21 and 28) days.

3. RESULTS AND DISCUSSION

3.1 Test Results of Fresh Concrete

The results of the slump flow test, V- funnel test and L-box test are shown in **Table 6**. These results indicate that in general, the workability of fresh SCC was improved with increasing thermostone chips as partial sand replacement percentage when it is compared with reference concrete mix. This is due to the pre-wetted fine lightweight aggregate (LWA) which provides a set of water-filled reservoirs within the concrete as additional moisture and in turn improves the workability of fresh SCC, **Friggle, and Reeves, 2008. Villareal, 2008**. These

results are within the acceptable criteria **EFNARC, 2002** for SCC and indicate also satisfactory deformability and filling ability without any segregation, bleeding and blocking.

3.2 Test Results of Hardened Concrete

The results of the properties of hardened concrete which include (compressive strength, modulus of rupture and shrinkage) of SCC are shown in **Tables 7 to 12**, and represented in **Fig. 1 to Fig. 6**. From these results, it can be seen that internally cured SCC by using pre-wetted thermostone chips as fine aggregate has better properties than that of externally cured SCC for both water and air curing as compared with reference concrete mix, as a result of internal curing technique. The highest increasing of compressive strength reaches 27.63% and 21.89% for SCC internally cured with thermostone chips as partial sand replacement with percentage of (10%) and cured in water and air respectively.

In general, the results of shrinkage test shows a reduction in shrinkage of internally cured SCC with thermostone chips as compared with reference concrete mix.

The mechanism of reduction of shrinkage by internal curing technique can be explained as follows, internal curing is a curing system that supplies water from pre-saturated porous LWA which has absorbed a huge amount of water when soaked in it. The pores of the cement paste absorb the water from the LWA by capillary suction as a result of the difference in water pressure in pores between LWA and cement hydrates, then an internal curing water leads to increase the final degree of hydration and decrease the unhydrated cement content and the capillary porosity by increase in the gel hydration products which cause increase in the crystallization pressure and reduce the shrinkage of concrete. The increased strength may be attributed to the increase in the degree of cement hydration as a result of internal curing water which leads to increase the hydration products, improve the interfacial transition zone by filling internal voids of concrete, reduction of shrinkage induce micro cracking and decrease the porosity of SCC. This complies with studies carried out by, **Lura, 2003. Cusson, et al., 2010. Al-Awadi, 2013.**

4. CONCLUSION

Depending on the results of this investigation, the following conclusions can be drawn:

- The internal curing technique may be achieved by using thermostone chips as partial sand replacement by volume as internal curing material.
- Improving the workability and the properties of the hardened concrete such as (compressive strength and modulus of rupture) may be achieved by internally curing SCC by using thermostone chips as partial sand replacement as compared with reference concrete.
- The SCC mixes are internally cured with thermostone chips as fine aggregate and externally cured in both water and air exhibit very low shrinkage as compared with reference concrete.
- It is useful to employ internal curing instead of traditional external curing due to its ease to use and its a significant contribution to shrinkage reduction, enhancing durability, sustainability and hence improving overall SCC performance.



REFERENCES

- ACI Committee 213R-03, 2003, *Guide for Structural Lightweight Aggregate Concrete*, Reported by ACI committee 213, ACI Manual of Concrete Practice, pp. 213R-1-38.
- AL-Awadi, A.Y., 2013, *Enhancing Performance of Self –Compacting Concrete with Internal Curing Using Lightweight Aggregate*, M.Sc. Thesis, University of Baghdad.
- ASTM C490-00, 2000, *Use of Apparatus for the Determination of Length Change of Hardened Cement Paste, Mortar, and Concrete*, Annual Book of ASTM Standards C490 – 00.
- ASTM C293-02, 2002, *Flexural Strength of Concrete (Using Simple Beam with Center – Point Load)*, Annual Book of ASTM Standards C293 – 02, pp. 1-3.
- ASTM C618-03, 2003, *Standard Specification for Coal Fly Ash and Raw or Calcined Natural Pozzolan for Use Concrete*, Annual Book of ASTM Standard, Vol. 04-02, pp. 296-298.
- ASTM C494-05, 2005, *Standard Specification for Chemical Admixtures for Concrete*, Annual Book of ASTM Standards.
- Bentz, D.P., 2007, *Internal Curing of High-Performance Blended Cement Mortars*, ACI Materials Journal, Vol. (104), No. (4), pp. 408-414.
- Bouzoubaa, N., and Lachemi, M., 2001, *Self-Compacting Concrete Incorporating High-Volumes of Class F Fly Ash: Preliminary Results*, Cement and Concrete Research, Vol. 31, No.3, pp413-420.
- British Standards Institution. B.S 1881, Part 116, 1985, *Method for Determination of Compressive Strength of Concrete Cubes*.
- Cusson, D., and Hoogeveen, T., 2005, *Internally-Cured High-Performance Concrete under Restrained Shrinkage and Creep*, in CONCREEP 7 Workshop on Creep, Shrinkage, and Durability of Concrete and Concrete Structures, Nantes, France, pp. 579-584.
- Cusson, Z., and Lounis, L., 2010, *Benefits of Internal Curing on Service Life and Life-Cycle Cost of High-Performance Concrete Bridge Decks – Case Study*.
- EFNARC, 2002, *Specification and Guidelines for Self-Compacting Concrete*, pp. 32, www.efrance.org.
- ERMCO, 2005, *The European Guidelines for SCC*, pp. 63, www.efca.info.
- Friggle, T., and Reeves, D., 2008, *Internal Curing of Concrete Paving: Laboratory and Field Experience*, in: *Internal Curing of High Performance Concrete: Laboratory and Field Experiences*, American Concrete Institute, Farmington Hills, MI, pp. 71-80.



- Holm, T.A., and Bremner, T.W., 2000, *State-of-the-Art Report on High-Strength, High-Durability Structural Low-Density Concrete for Applications in Severe Marine Environments*, Engineer Research and Development Center , ERDC/SL TR-00-3, C.116, Vicksburg.
- Horta, A., 2005, *Evaluation of Self-Consolidating Concrete for Bridge Structure Applications*, M.Sc. Thesis, Georgia Institute of Technology, pp.228.
- Iraqi Specifications, IQS No.5, 1984, *The Portland Cement*, Central Apparatus for Standardization and Quality Control. (Translated from Arabic).
- Iraqi Specifications, IQS No.45, 1984, *The Used Aggregate from Natural Sources in Concrete and Building*, Central Apparatus for Standardization and Quality Control. (Translated from Arabic).
- Lura, P., 2003, *Autogenous Deformation and Internal Curing of Concrete*, Ph.D. thesis, Technical University of Delft.
- Lura, P., Bentz, D.P., Lange, D.A., Kovler, K., and Bentur, A., 2004, *Pumice Aggregates for Internal Water Curing*, Proceeding International RILEM Symposium on Concrete Science and Engineering, Northwestern University, Evanston, Illinois. RILEM Publications S.A.R.L., pp. 137–151.
- Munaz, A.N., Bushra, I., and Rahman, S., 2011, *A State of Art Review on Internal Curing of Concrete and Its Prospect for Bangladesh*, BUET-Japan Institute of Disaster Prevention and Urban Safety, Bangladesh University of Engineering and Technology, Dhaka, Bangladesh, pp. 22-28.
- Selvamony, M.S., Ravikumar, S.U., and Basil, G., 2010, *Investigations on Self-Compacted Self-Curing Concrete Using Limestone Powder and Clinkers*.
- Villareal, V.H., 2008, *Internal Curing - Real World Ready Mix Production and Applications: A Practical Approach to Lightweight Modified Concrete*, in: *Internal Curing of High Performance Concrete: Laboratory and Field Experiences*, Eds. D. Bentz and B. Mohr, American Concrete Institute, Farmington Hills, MI, pp. 45-56.

**List of Abbreviations and Symbols**

IQS= Iraqi specification.
LWA= lightweight aggregate.
SCC= self-compacting concrete.
SF= silica fume.
T _{50cm} = slump flow time at diameter 50cm .
TV= flow time of v-funnel test.
TV _{5min} = flow time of v-funnel test after 5min. of filling.

Table 1. Sieve analysis of sand and thermostone chips.

Sieve size (mm)	Percent passing (%)	I.Q.S.45: 1984 Limits Zone (2)
10	100	100
4.75	99.8	90 - 100
2.36	84.4	75 - 100
1.18	65.6	55 - 90
0.60	41.8	35 - 59
0.30	11	8 - 30
0.15	2.2	0 - 10
Fineness modulus = 2.95		

Table 2. Physical and chemical properties of sand.

Property	Test result	I.Q.S.45: 1984 Limits
Apparent specific gravity	2.55	-----
Absorption, %	2.95	-----
Bulk density (kg/m ³)	1710	-----
Sulphate content (SO ₃)	0.19%	0.50% (max)

**Table 3.** Physical properties of thermostone chips.

Property	Test result
Shape	Crushed
Apparent specific gravity	1.14
Bulk density (kg/m^3)	675
Absorption, %	48

Table 4. Chemical composition of SF (with fineness is 23000 m^2/kg) and the chemical requirements of ASTM C 618-03.

Oxide composition	Oxide content %	Chemical requirements of ASTM C 618-03 class (N)
SiO_2	91.39	(SiO_2) plus (Al_2O_3) plus (Fe_2O_3) , min, = 70.0%
Al_2O_3	2.90	
Fe_2O_3	0.30	
SO_3	Nil	(SO_3) , max, = 4.0%
L.O.I	3.35	L.O.I, max, = 10.0%
CaO	Nil	-----
MgO	2.02	-----

Table 5. Mix proportions of SCC mixes*.

Index of Mixes	Sand kg/m^3	Thermostone Chips kg/m^3		
		5%	10%	15%
Mix-R	825	---	---	---
Mix-T5%	783.75	16.3	---	---
Mix-T10%	742.5	---	32.6	---
Mix-T15%	701.25	---	---	48.9

*Water (kg/m^3) = 185

Glenium 51 (liter per 100kg of cementitious materials) = 1.1

Table 6. The results of the slump flow test, V- funnel test and L-box test.

Index of Mixes	Slump flow		V-Funnel		L-Box	
	D (mm)	T50cm (sec)	TV (sec)	TV5min (sec)	Blocking Ratio (H2/H1)	T40cm (sec)
Mix-R	698	4.5	12	13.5	0.82	5
Mix-T5%	706	4.4	11.7	13	0.83	4.8
Mix-T10%	715	4.2	10.5	12	0.84	4.5
Mix-T15%	723	4	9.5	11.2	0.85	4.2

**Table 7.** Test results of compressive strength of SCC internally cured with thermostone chips and externally cured with water

Mixes	Compressive strength (MPa)		
	7 days	28 days	90 days
Mix-R	43.65	45.87	52.76
Mix-T5%	48.42	52.58	63.65
Mix-T10%	50.14	56.64	67.34
Mix-T15%	46.31	50.84	58.63

Table 8. Test results of compressive strength of SCC internally cured with thermostone chips and externally cured with air.

Mixes	Compressive strength (MPa)		
	7 days	28 days	90 days
Mix-R	40.84	42.96	48.43
Mix-T5%	43.69	48.04	55.90
Mix-T10%	45.73	51.14	59.03
Mix-T15%	42.68	45.59	52.92

Table 9. Test results of modulus of rupture of SCC internally cured with thermostone chips and externally cured with water.

Mixes	Modulus of rupture (MPa)		
	7 days	28 days	90 days
Mix-R	6.06	6.32	6.95
Mix-T5%	6.35	6.86	7.68
Mix-T10%	6.78	7.19	7.98
Mix-T15%	6.24	6.58	7.34

**Table 10.** Test results of modulus of rupture of SCC internally cured with thermostone chips and externally cured with air.

Mixes	Modulus of rupture (MPa)		
	7 days	28 days	90 days
Mix-R	5.74	5.98	6.65
Mix-T5%	6.06	6.40	7.18
Mix-T10%	6.29	6.65	7.44
Mix-T15%	5.90	6.24	6.91

Table 11. Test results of volume change of SCC internally cured with thermostone chips and externally cured with water for 7 days and with air until 21 days.

Mixes	Shrinkage $\times 10^{-6}$				
	Water curing		Air curing		
	4 days	7 days	14 days	21 days	28 days
Mix-R	+30	+35	-60	-165	-215
Mix-T5%	+35	+45	-40	-55	-80
Mix-T10%	+40	+50	-30	-40	-50
Mix-T15%	+45	+60	-20	-30	-35

Table 12. Test results of volume change of SCC internally cured with thermostone chips and externally cured with air until 28 days.

Mixes	Shrinkage $\times 10^{-6}$				
	Air curing				
	4 days	7 days	14 days	21 days	28 days
Mix-R	-130	-215	-245	-265	-285
Mix-T5%	-40	-70	-85	-100	-110
Mix-T10%	-30	-50	-70	-75	-85
Mix-T15%	-25	-40	-55	-65	-70

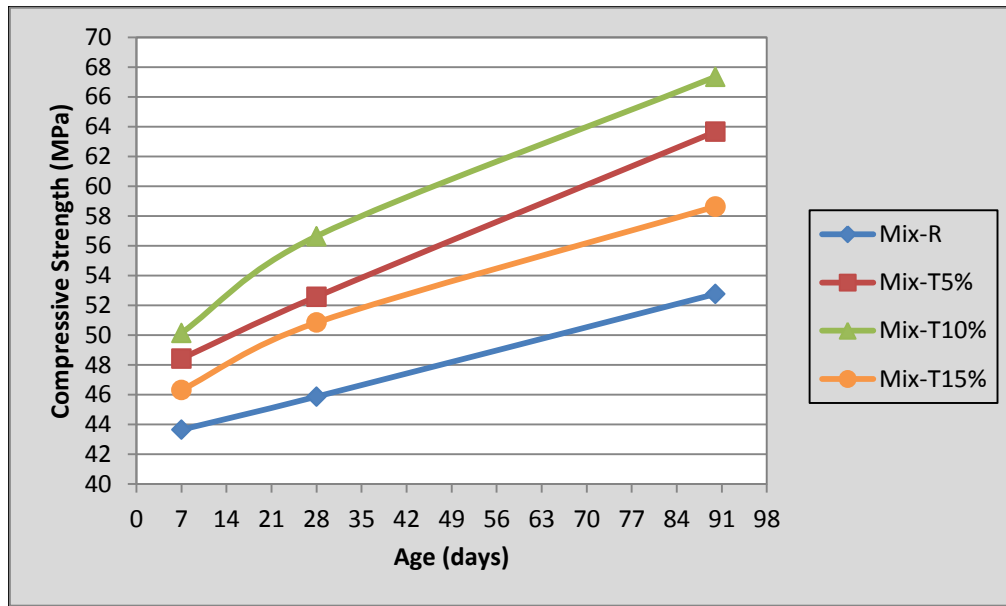


Figure 1. Compressive strength development of SCC internally cured with thermostone chips and externally cured with water.

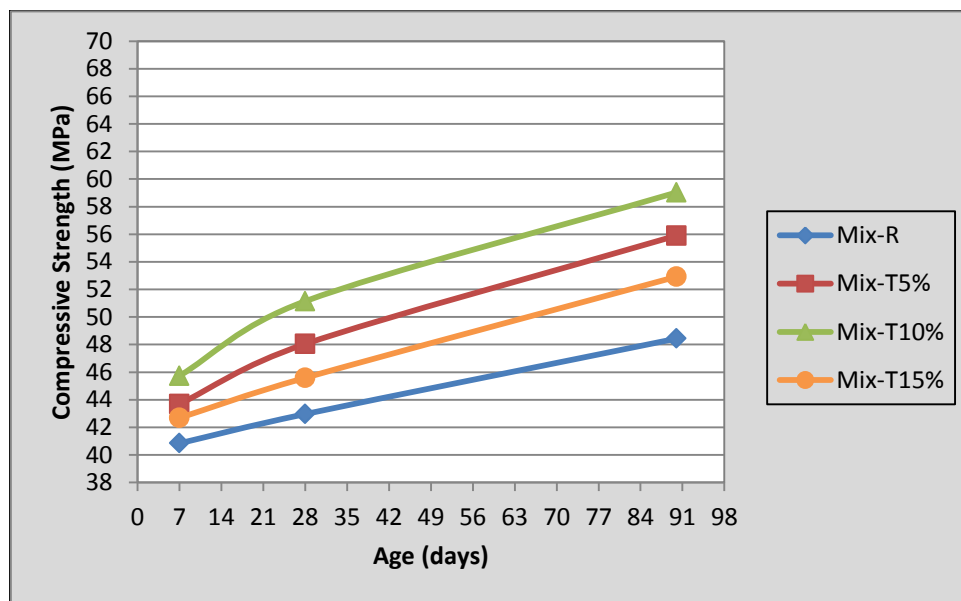


Figure 2. Compressive strength development of SCC internally cured with thermostone chips and externally cured with air.

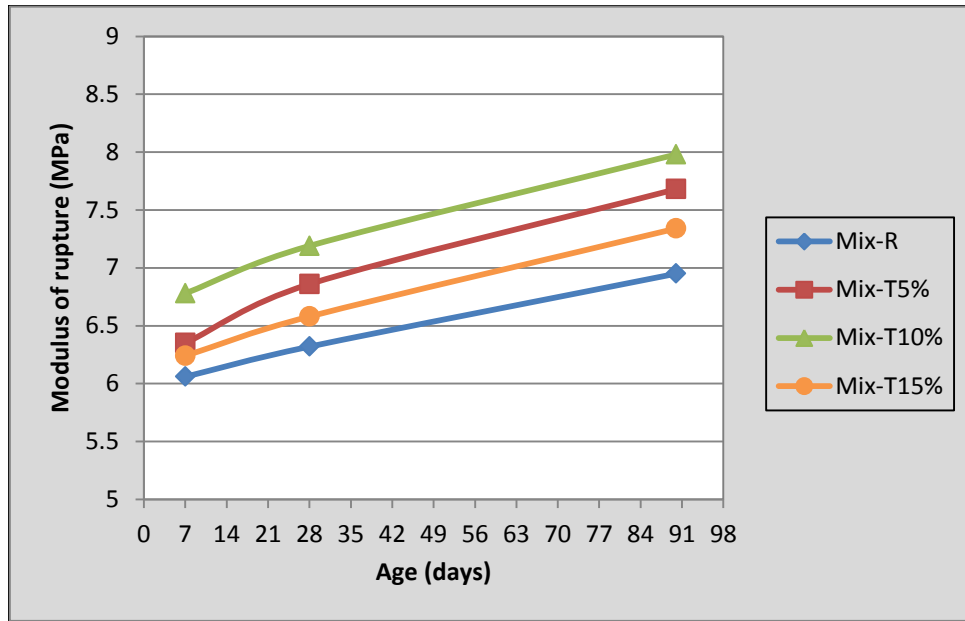


Figure 3. Modulus of rupture development of SCC internally cured with thermostone chips and externally cured with water.

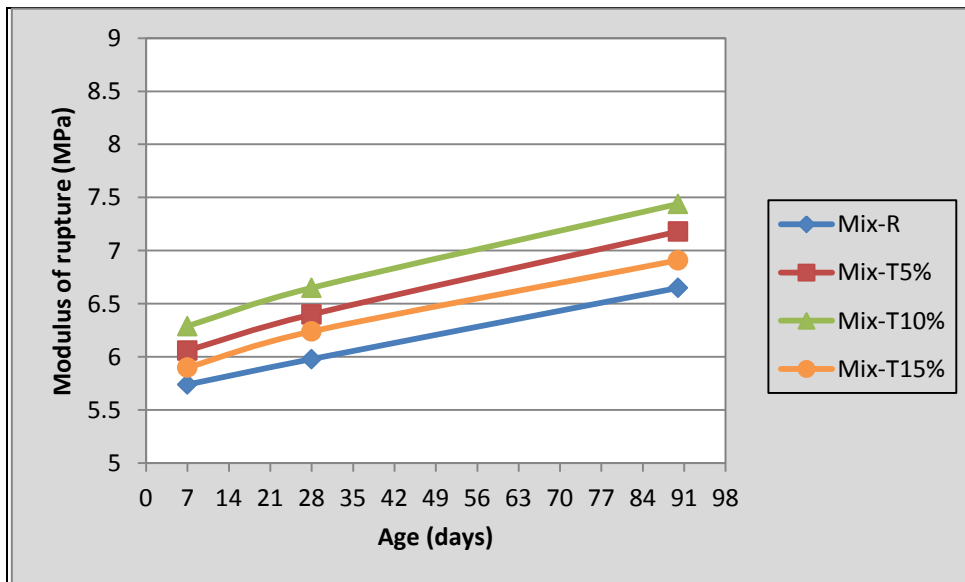


Figure 4. Modulus of rupture development of SCC internally cured with thermostone chips and externally cured with air.

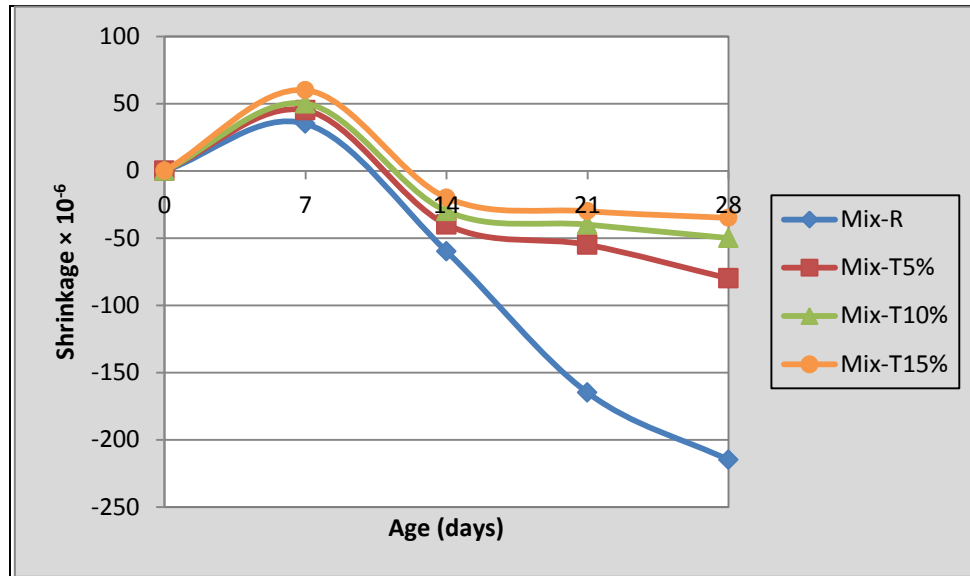


Figure 5. Volume change development of SCC internally cured with thermostone chips and externally cured with water for 7 days and with air until 21 days.

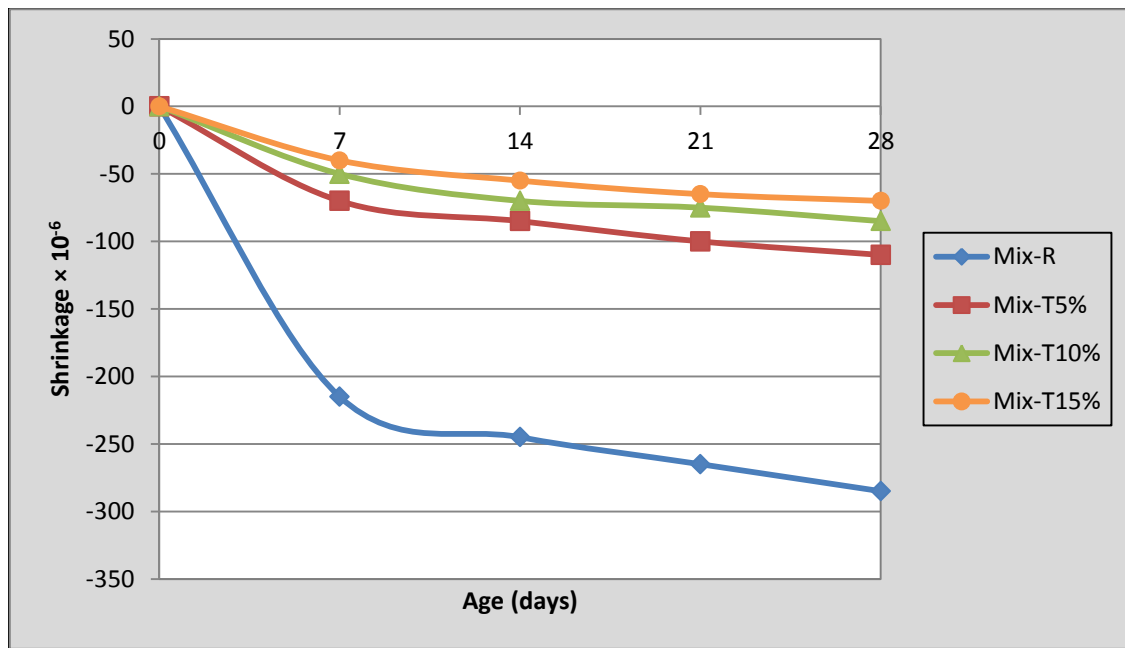


Figure 6. Volume change development of SCC internally cured with thermostone chips and externally cured with air until 28 days.

Influence of Temperature Upon Permanent Deformation Parameters of Asphalt Concrete Mixes

Dr. Amjad Hamad Albayati

Assistant. Professor

College of Engineering

University of Baghdad

Sirtransportation@yahoo.com

Aliaa Faleh Hamd Alani

M.Sc student /transportation engineerin

College of Engineering

University of Baghdad

Aliaa_falah@yahoo.com

ABSTRACT

The performance of asphalt concrete pavement has affected by many factors, the temperature is the most important environmental one which has a large effect on the structural behavior of flexible pavement materials. The main cause of premature failure of pavement is the rutting, Due to the viscoelastic nature of the asphalt cement, rutting is more pronounced in hot climate areas because the viscosity of the asphalt binder which is inversely related to rutting is significantly reduced with the increase in temperature resulting in a more rut susceptible paving mixtures. The objective of this study is to determine the effect of temperatures variations on the permanent deformation parameters (permanent strain (ϵ_p), intercept (a), slope (b), Alpha and Mu) as well as resilient strain (ϵ_r) and resilient modulus (M_r). To achieve this objective, one aggregate gradation with 12.5mm nominal maximum size, two grades of asphalt cements (40-50 and 60-70) brought from Al- Daurah refinery, limestone dust filler has been used to prepare the asphalt concrete mixtures. 30 Marshall specimens were prepared to determine the optimum asphalt cement content. Thereafter, 30 cylindrical asphalt concrete specimens (102mm in diameter and 203 mm in height) are prepared in optimum asphalt cement and optimum ± 0.5 percent. The prepared specimens were used in uniaxial repeated load test to evaluate the permanent deformation parameters of asphalt concrete mixes under the following testing temperature (5, 15, 25, 40 and 60°C). The test result analyses appeared that M_r is decrease 51 percent when temperature increased from 5 °C to 25 °C and then decrease 22 percent with further increase in temperature from 25 °C to 60 °C. Also, the Alpha value decreases by a factor of 1.25 and 1.13 when temperature increases from 5 °C to 25 °C and 25 °C to 60 °C, respectively. Finally, statistical models were developed to predict the Alpha and Mu parameters of permanent deformation.

Key word: Asphalt concrete, Marshall, permanent deformation, Alpha, Mu.

تأثير درجات الحرارة على معاملات التشوهات الدائمة للخلطات الإسفلتية

علياء فالح حمد العاني

طالبة ماجستير /هندسة طرق

جامعة بغداد- كلية الهندسة

د. أمجد حمد البياتي

استاذ مساعد

جامعة بغداد- كلية الهندسة

المستخلص

أداء التبليط الإسفلت يتأثر بعدة عوامل و درجة الحرارة هي واحدة من العوامل المناخية المهمة التي لها أكبر تأثير على أداء السلوك الانشائي لمواد الرصف المرنة. إن السبب الرئيسي للفشل المبكر للطرق هو التخذد ونظرا لطبيعة الاسفلت اللزجة/المرنة فالتخذد يظهر بكثرة في المناطق المناخية الحارة لان لزوجة الاسفلت ترتبط عكسيا مع التخذد

الذي يقل بشكل ملحوظ مع ارتفاع درجات الحرارة وبالنتيجة يعطي حساسية اكبر للتخدد لطبقات التبليط . ان الهدف من هذه الدراسة هو لتحديد تأثير درجات الحرارة المختلفة على معاملات التشوهات الدائمة ومعامل المرونة ولتحقيق هذا الهدف تم اختيار تدرج واحد للركام بمقاس اسمي اقصى (12.5) ملم ونوعين اسفلت ذو اختراق (40-50)(60-70) من مصفى الدورة وقد تم استخدام الحجر الجيري المطحون كمادة مالئة. استخدمت هذه المواد لتحضير (30) نموذج مارشال لغرض تعيين نسبة الاسفلت المثلى، وكذلك تم تحضير (30) نموذج اسطوانى من الخرسانة الاسفلتية (102 ملم قطر، 203 ملم ارتفاع) تم تهيئتها بنسبة الاسفلت المثلى وكذلك نسبة $\pm 0.5\%$ من النسبة المثلى . استخدم في الاختبار جهاز الحمل المتكرر لتقييم معاملات التشوه الدائمى لخلطات الاسفلت بدرجات حرارة (5, 10, 25, 40, 60)°م. نتائج الفحوصات وتحليل النتائج اظهرت ان معامل المرونة يقل بمقدار 51% عند زيادة درجة الحرارة من 5 الى 25°م ونقصان 22% مع زيادة درجة الحرارة من 25 الى 60°م وايضا قيمة الفا تقل بمقدار 1.25 و 1.13 عند زيادة درجة الحرارة (5-25)°م و (25-60)°م على التوالي. واخيرا تم تطوير موديلات احصائية للتنبؤ بقيم المعاملات الفا و Mu للتشوهات الدائمة.

1. INTRODUCTION

Asphalt concrete which is also called hot mix asphalt HMA due to its relatively high mixing and compaction temperature is a paving material that consists of asphalt cement (by weight of total mix its content range from 4 to 6 percent while by volume the contents range from 8.8 to 13.3 percent from the entire volume of mix) and mineral aggregate. The aggregate skeleton role is to withstand the traffic load whereas the asphalt cement acts as an adhesive material which holds the aggregate skeleton together. The combination of these materials forms a mixture that has viscoelastic behavior basically due to the viscoelastic nature of the adhesive asphalt cement. A viscoelastic material combines the behavior of an elastic solid and a viscous liquid. The proportions of the elastic and viscous components depend on the temperature as well as rate of shear. The viscous nature increases and the elastic nature decreases as the temperature increases and shearing rate decreases, and vice versa.

In the structural design of asphalt concrete pavement system, two climatic factors, temperature and moisture, are considered to influence the structural behavior of the pavement materials. Temperature, either their value which influences the stiffness (resilient modulus) and permanent deformation (rutting) parameters as well as low temperature fatigue behavior or their magnitude fluctuation within a day which can affect thermal fatigue cracking distribution within the asphalt concrete layers. Whereas in the other hand, moisture conditions influence the stiffness and strength of the granular pavement material (subbase course and subgrade). Based on aforementioned, the design procedure requires the determination of pavement temperature values within the asphalt concrete layers of pavement in order to characterize the materials of these layers in the laboratory under condition as close as possible to that anticipated in the field. **Albayati, 2006** conducted a local study to predict the temperature within the asphalt concrete layers at a different depth from the pavement surface and for varying air temperatures. The researcher concluded from the developed relationship at a depth of 2cm below the pavement surface, the asphalt concrete could reach to a temperature of 60°C when the air temperature is 50°C. In view of this findings, rutting mode of failure perhaps the most probable cause of failure for local pavement since this type of failure is more prevalent under hot climate condition. The

permanent deformation (rutting) is defined as the progressive accumulation of plastic strain in each layers of the pavement system that occurs under each load repetitions. Excessive permanent deformation will eventually result in reduction of pavement serviceability due to loss in riding comfort, **Bazlamit, 2005**.

Rutting is more pronounced in hot climate areas because the viscosity of the asphalt binder which is inversely related to rutting is significantly reduced with the increase in temperature resulting in a more rut susceptible HMA mix. **Fig.1** shows the effect of temperature on log asphalt viscosity for a wide range of asphalt cement grades, **Puzinauskas, 1979**. From this Figure, it is obvious that the viscosity of asphalts vary from less than one poise to more than one trillion poises. Within such extreme viscosity range, asphalts are transformed from low viscosity Newtonian liquids to materials exhibiting shear-dependent visco-elastic behavior, where with decreasing temperature the elastic component tends to be predominant. Thus, the gradually changing curvature of plots in **Fig.1** indicates that the viscosity of asphalt tends to change more rapidly at low temperatures, and such change becomes far less pronounced at higher temperatures when the viscous behavior is predominant.

Beside the asphalt consistency which can be characterized by viscosity grading, penetration grading or performance grading, the asphalt cement content also has an effect on the permanent deformation of asphalt concrete. Based on the indirect tensile strength test for dimetral Marshall specimens, **Zhaw, 2011**, concluded that the asphalt cement content variation evaluated in his study has a significant effect on the rutting performance of the mixtures. The mixes with lower binder content showed better rutting performance, he also stated that even deviations within a small range (± 0.25 percent) of binder content could significantly have an effect on rutting performance.

Based on the aforementioned preface, it can be postulated that the temperature have a significant effect on the rutting mode of distress in asphalt concrete paving materials, also the asphalt cement types (grades) which control the viscoelastic nature of mixture and asphalt cement content have some specific relations to this type of distress. Therefore, a need has been a rise to conduct a laboratory tests at temperatures approximately close to those which may be encountered in field under local environmental conditions after considering the type and asphalt cement content in consideration.

2. MATERIAL CHARACTERIZATION

The materials used in this study are asphalt cement, aggregate and mineral filler. The properties of these materials were evaluated using routine type of tests and the obtained results were compared with the **SCRB R/9, 2003**, specification requirements. All the materials used are locally available and widely employed in the pavement construction in the Iraq.

2.1 Asphalt cement

Two types of asphalt cement were employed with penetration grade (40-50) and (60-70) obtained from Al-Durra refinery, south-west of Baghdad. The physical properties of these binders are presented in **Table 1**.

2.2 Aggregate

The aggregate used in the laboratory work is crushed quartz from Al-Nibaie quarry which is widely used for asphalt mixes in Baghdad city. The coarse and fine aggregate used in this work were sieved and recombined in the proper proportion to meet the wearing course gradation type III A as required by SCRB specification, **SCRB R/9, 2003**. The gradation of aggregate with a nominal maximum size of 12.5mm (1/2inch) is shown in **Table 2** and the selected gradation with specification limits are presented in **Fig.2**. The physical properties of aggregate used are shown in **Table 3**.

2.3 Filler

The mineral filler is a non-plastic material passing sieve No.200 (0.075mm). The filler used in this work is limestone dust obtained from Amanat Baghdad asphalt concrete mix plant; its source is the lime factory in Karbala Governorate. The physical properties of the filler are presented in **Table 4**.

3.EXPERIMENTAL WORK

The experimental work was started by determining the optimum asphalt content for all the asphalt concrete mixes using Marshall design method and thereafter cylindrical asphalt concrete were prepared to evaluate the permanent deformation parameters using uniaxial repeated loading.

3.1 Marshall mix design

Standard method of Marshall as in (**ASTM D-1559**) specifications was used to find the optimum asphalt content for compacted asphalt concrete specimens. Marshall test was conducted on a cylindrical specimen of 102 mm (4 inch) diameter by 63.5 mm (2.5 inch) height. The optimum asphalt content of the mix (shown below in **Fig.4** and **Fig5**) was calculated as the numerical average of the values of asphalt contents corresponding to the following:

- Asphalt content at maximum unit weight
- Asphalt content at maximum stability
- Asphalt content at 4% air voids

3.2 Uniaxial repeated load

The dimensions of the cylindrical specimen used in this work were 102 mm (4 inch) in diameter and 203 mm (8 inch) in height. The axial compressive repeated loads test were conducted using the pneumatic repeated load system (PRLS) developed by, **Albayati, 2006** (shown below in **Fig.3**) applied in the form of rectangular wave with a constant loading frequency of 60 cycles per minute. A heavier sine pulse of 0.1 sec load duration and 0.9 sec rest period was applied over test duration of approximately 3 hour, history loading results in approximately 10,000 load cycles or when the specimen fractured. In these tests ,repetitive compressive loading with a stress level 20 psi and the uniaxial repeated loading tests were conducted at five temperature (5°,15°,25°,40°,and60°c).

The permanent strain (ϵ_p) is calculated by applying the following equation:

$$\epsilon_p = \frac{pd \times 10^6}{h} \quad (1)$$

where :

ϵ_p = axial permanent microstrain,(in/in)

Pd = axial permanent deformation and

H= specimen height.

The resilient deformation is determined at the load repetition of 200th , resilient strain (ϵ_r) is found according to following equation:

$$\epsilon_r = \frac{Rd}{h \times 10^6} \quad (2)$$

ϵ_r = axial resilient microstrain,(in/in)

Rd = axial resilient deformation and

$$Mr = \frac{\sigma}{\epsilon_r} \quad (3)$$

where :

M_r = resilient modulus (psi)

σ = repeated axial stress (psi)

ϵ_r = axial resilient strain (in/in) , **Huang, Y. H. 2004.**

The permanent deformation test results for this study are represented by the linear log-log relationship between the number of load repetition and the permanent microstrain with the form shown in Eqn.(4) below which is originally suggested by **Monismith et al.,1975 and Barksdale, 1972.**

$$\epsilon_p = aN^b \quad (4)$$

where :

p = permanent strain

N = number of stress applications

a = intercept coefficient

b = slope coefficient

4. TEST RESULTS AND DISCUSSION

4.1 Marshall properties

To satisfy the requirements of the experimental design, Marshall mix design procedure was performed according to AI's manual series No.2 (AI, 1981) using 75 blows of the automatic Marshall compactor on each side of the specimen which represent high tire pressure applied to roadway. Based upon this method, the optimum asphalt content is determined by averaging the three values shown below:

- Asphalt content at maximum unit weight.
- Asphalt content at maximum stability.
- Asphalt content at 4% air voids.

For each grade of asphalt cement, 15 Marshall specimens were prepared with a constant increment of 0.3 percent of asphalt cement content (3 replications for each content). The selected asphalt contents to perform the Marshall mix design were (4.3, 4.6, 4.9, 5.2 and 5.5) percent by weight of total mix, these values belong to the mix type IIIA of wearing course.

Fig.4 and **Fig.5** show the plots of the Marshall data for each type of asphalt cement, from these figures the calculated optimum asphalt content is 5 percent for asphalt cement grade (40-50) and 4.6 percent for grade (60-70).

4.2 Effect of temperature

The analysis of the results begins by identifying “sort” variable: i.e., temperature. Therefore, the entire data file is sorted according to test temperature. For example, to clearly show the effect of temperature on both the plastic and elastic properties the entire data is sorted by test temperatures and the mean values of permanent deformation parameters are calculated as presented in **Table 5**.

As may be seen from **Fig.6**, the permanent strain, intercept, slope, resilient modulus, $\alpha(1-b)$ and $\mu(a^b/\epsilon_r)$ are substantially influenced by temperature. For example, when the temperature increases from 5 to 25°C, the permanent strain and intercept increases by a factor of 6.77 and 1.55, respectively. The corresponding reduction in resilient modulus (M_r) is 51 percent. Further increase in the temperature from 25 to 60°C, results in permanent strain increases by a factor of 6.27 whereas the intercept by a factor 2.57. This findings has the implication that the temperature effects on both the permanent strain and intercept are not linearly varied, i.e., the highest the temperature the more the rate of plastic deformation.

As shown by the values in **Table 5** and **Fig.6** it appears that the temperature influences the slope and the resilient modulus in essentially the same manner.

Furthermore, increase in the temperature from 25 to 60°C, results in the resilient modulus decrease by 22 percent whereas the slope increase by a factor 1.85.

When the temperature increase from 5 to 25°C, Mu increase by a factor of 1.7 and Alpha decreased by a factor 1.25, whilst when the temperature increase from 25 to 60°C Mu increase by a factor of 1.13 and Alpha decrease by a factor 2.12. These findings besides that related to permanent strain and intercept confirm that the rutting mode of failure is enhanced in asphalt concrete pavement in hot summer temperature.

4.3 Effect of asphalt cement grade

Fig.7 shows the change in resilient modulus as well as the plastic deformation parameters with the variation of asphalt cement type. It can be seen from the presented data in Table 6, the asphalt grade has higher influence on the plastic strain as well as the intercept coefficient than other parameters. The variation of resilient modulus, slope and Mu values changes also with asphalt cement type but to lesser extent. For example, the average value of resilient modulus corresponding to asphalt grade 40-50 is almost 1.13 times the value for asphalt grade 60-70 at 5°C. The same is applicable to the permanent strain which is 1.85 times the value for asphalt grade 40-50 at the same degree.

4.4 Effect of asphalt cement content

Based on the data graphically shown in **Fig.8** and **Fig.9**, it appears that the examined asphalt contents have influence on the plastic response of the material. The higher plastic strain is associated with the increases in asphalt content from 4.5 to 5.5 and from 4.1 to 5.1 percent asphalt for AC (40-50) and AC (60-70) respectively. From **Fig.8** it can be seen that the increment of 1 percent in the asphalt content type (40-50) beyond 4.5 percent will result in 8 percent decrease in alpha value and 35 percent decrease in mu value. Whereas for the asphalt cement type (60-70) that shown in **Fig.9** the change in alpha and mu values are more sensitive for the change in asphalt content, the increasing in asphalt content from 4.1 percent to 5.1 percent resulted in a reduction in alpha value about 12 percent as well as in mu value about 52 percent. from the aforementioned findings, one can be concluded that the asphalt content variations have more effect on permanent deformation parameters alpha and mu when the asphalt cement grade is soft (60-70) as compared to relatively hard grade type (40-50). The resilient modulus decreases approximately 16 percent when there is an increment one percent beyond the 4.5 percent for AC 40-50, for the AC 60-70 the increment of one percent beyond the 4.1 percent resulted in a 15 percent reduction in the resilient modulus value.

4.5 Combined Effect of Variable on Rutting Parameters

Table 7 summarizes the trends in the observed data presented in the preceding sections. This table provides a qualitative description of the influence of the temperature and asphalt cement (type and content) on the resilient modulus and plastic strain as well as the permanent deformation parameters.

As shown in **Table 7**, the resilient modulus, M_r , is heavily dependent on temperature; also it is moderately dependent on asphalt content.

The plastic strain, ϵ_p , is very highly dependent on temperature, The asphalt content virtually have low effects on the plastic strain of asphalt concrete which is in turn moderately effected by asphalt grade.

The intercept coefficient “a”, which is directly related to rutting, is highly affected by temperature, and moderately dependent on asphalt properties (grade and content). Similarly, the slope coefficient “b” or alpha ($\alpha=1-b$) is highly dependent on temperature and to a lesser degree on asphalt properties (grade and content).

Mu appears to be influenced strongly by temperature and asphalt content, asphalt grade have moderate effect on Mu. **Fig.10** through **Fig. 15** show the histogram of collective effects of temperature, asphalt content and asphalt grade on permanent deformation parameters as well as resilient modulus.

4.6 Permanent Deformation Parameters Predictive Models:

Presented in this section, are the statistical models attempted for the permanent deformation parameters alpha and Mu. Stepwise regression technique is used for the purpose of model development using statistical software (SPSS version 19). It's shown that Mu can be predicted with moderate accuracy in terms of the variables cited in this research ($R^2=0.85$). In contrast to alpha, which is predicted excellently in terms of the test conditions and asphalt cement properties ($R^2=0.982$). The developed models are:

$$\text{Alpha} = -0.009T + 0.167L\eta - 0.06AC$$

$$\text{Mu} = 0.786 - 1.211\sqrt{AC} + 0.242\sqrt{T} - 0.021T + 0.256L\eta$$

where:

T = test temperature in degree centigrade ($^{\circ}\text{C}$)

η = viscosity at 135°C (cP)

AC= Asphalt content (percent by weight of total mix)

5.CONCLUSION AND RECOMMENDATIONS

5.1 Conclusions

According to the work presented in this research and within the limitation of test program, type of testing tools and type of materials used, the following main points are concluded:

- The asphalt concrete mixture with resilient modulus (M_r) value of 328036 psi at 5°C temperature loses approximately 88 percent of its strength in term of M_r when there is a rise in temperature up to 60°C . The variation in M_r value with

temperature was shown to have non-linear trend, the asphalt concrete mix lost about 51 and 22 percentages of its strength when the temperature changed from 5°C to 25°C and from 25°C to 60°C, respectively.

- The results of permanent deformation test support the allegation of "the higher the temperature the more the rate of plastic deformation". When the temperature increases from 5 to 25°C, Mu increases by a factor of 1.7 and Alpha decreases by a factor 1.25, whilst when the temperature increases from 25 to 60°C Mu increases by a factor of 1.13 and Alpha decreases by a factor 2.12.
- The increment of 1 percent in the asphalt content type (40-50) beyond 4.5 percent resulted in 8 percent decrease in alpha value and 35 percent decrease in mu value. Whereas for the asphalt cement type (60-70) the increasing in asphalt content from 4.1 percent to 5.1 percent resulted in a reduction in alpha value about 12 percent as well as in mu value about 52 percent
- Models were developed to predict the permanent deformation parameters alpha and Mu

$$\text{Alpha} = -0.009T + 0.167\text{Ln}\eta - 0.06\text{AC} \quad (R^2=0.982)$$

$$\text{Mu} = 0.786 - 1.211\sqrt{\text{AC}} + 0.242\sqrt{T} - 0.021T + 0.256\text{Ln}\eta \quad (R^2=0.85)$$

where:

T = test temperature in degree centigrade (°C)

η = viscosity at 135°C (cP)

AC= Asphalt content (%)

As an example when: T =25 °C , η = 498 cP , AC= 4.5 percent by weight of total mix , Alpha =0.64 and Mu =0.642

6. REFERENCES

- AI ,1981, *Thickness Design-Asphalt Pavements for Highways and Streets*, Asphalt Institute, Manual Series No.2, College Park, Maryland, USA.
- Albayati, A., 2006, *Permanent Deformation Prediction of Asphalt Concrete Under Repeated Loading*, Ph. D Thesis, Civil Engineering, University of Baghdad.
- ASTM, 2009, *Road and Paving Materials*, Annual Book of ASTM Standards, Volume 04.03, American Society for Testing and Materials," West Conshohocken, USA.
- Bazlamit, S.M. and F. Reza, 2005, *Changes in asphalt pavement friction components and adjustment of skid number for temperature*. J. Transp. Eng.131.

- Brule, B., Brion, Y. and Tanguy, A, 1988, *Paving Asphalt Polymer Blends: Relationships Between Composition, Structure and Properties*, Proc. AAPT Vol. 57, pp. 41-64.
- Huang, Y., 2004, *Pavement Analysis and Design*, 2nd Edition, Prentice Hall, USA.
- Monismith, C.L., Epps, J.K., Kasianchuk, D.A., McLean, D.B., 1971, *Asphalt Mixture Behavior in Repeated Flexure*, Report TE 70-5, University of California, Berkeley.
- Monismith, C., Ogawa, N. and Freeman, C., 1975, *Permanent Deformation Characteristics of Subgrade Soils due to Repeated Loadings*, TRR 537.
- Puzinauskas, V., 1979, *Properties of Asphalt Cements*, Proceedings, Association of Asphalt Paving Technologists (AAPT), USA.
- SCRB/R9, 2003, *General Specification for Roads and Bridges*, Section R/9, Hot-Mix Asphalt Concrete Pavement, Revised Edition. State Corporation of Roads and Bridges, Ministry of Housing and Construction, Republic of Iraq.
- Walid, M. N., 2001, *Utilization of Instrument Response of Superpave Mixes at the Virginia Smart Road to Calibrate Laboratory Developed Fatigue Equations*, PhD Dissertation, Virginia University, pp. 168.
- Witczak, M., 1972, *Design of Full Depth Air Field Pavement*, Proceedings, Third International Conference on the Structural Design of Asphalt Pavements, London.
- Zhao, W., 2011, *The effects of fundamental mixture parameters on hot-mix asphalt performance properties*. PhD Dissertation, Clemson University, South Carolina, USA.

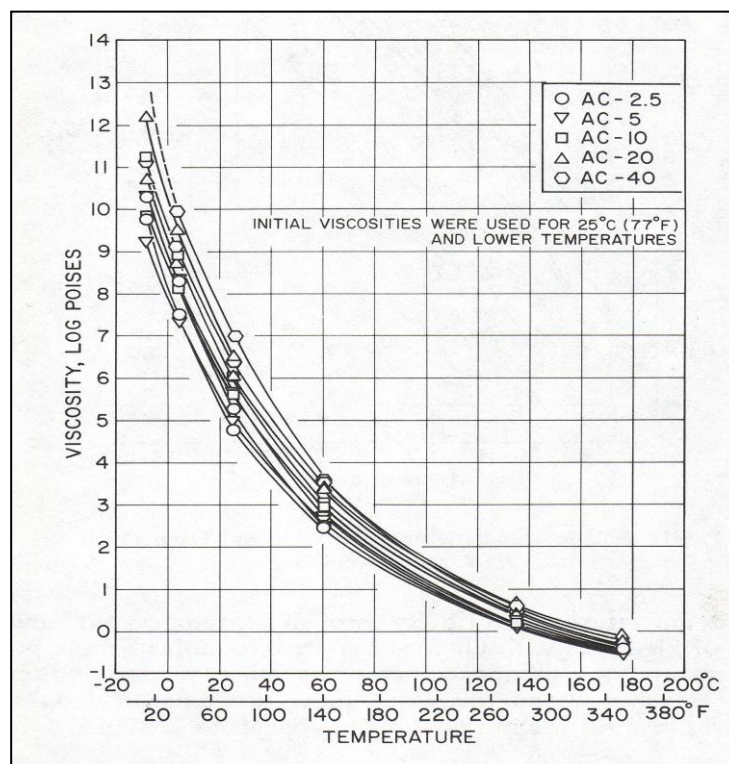


Figure 1. Relationship between viscosity and temperature for asphalt cements, Puzinauskas, 1979.

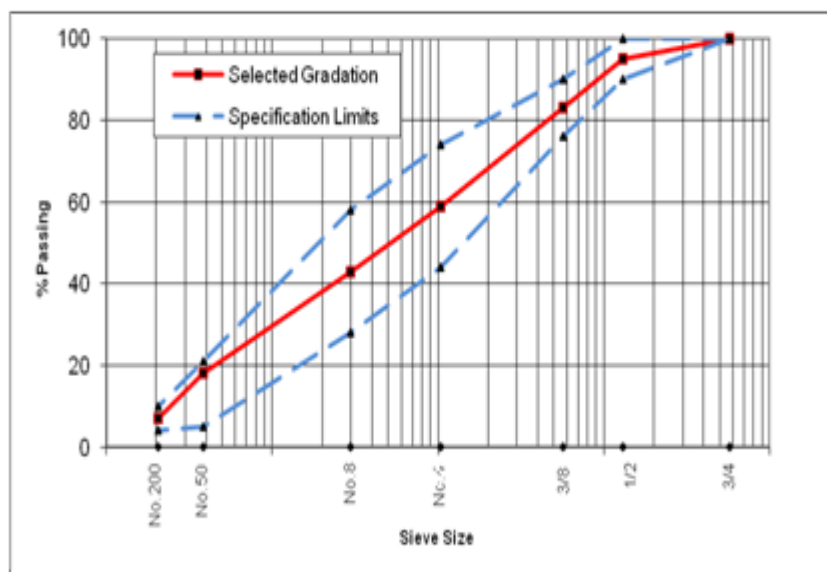


Figure 2. Aggregate Gradation Curve.



Figure 3. Photograph for PRLS.

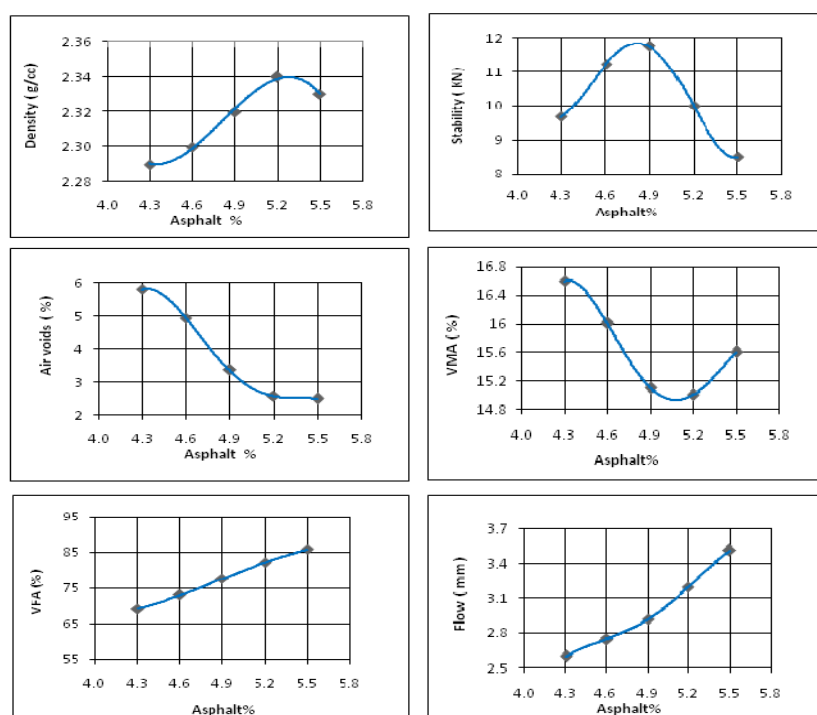


Figure 4. Marshall plots for mixtures with AC (40-50).

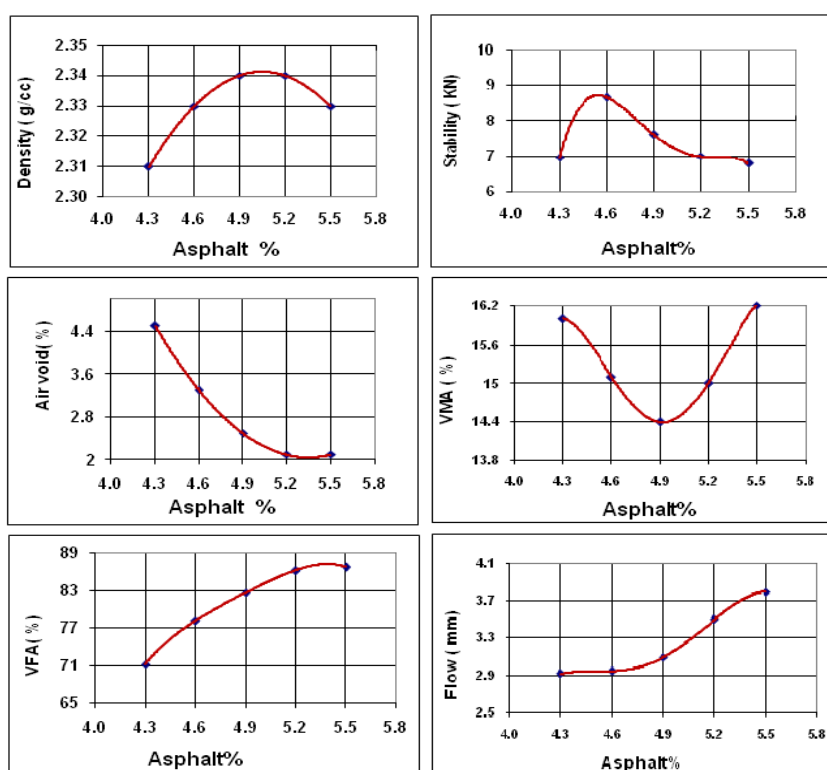


Figure 5. Marshall plots for mixtures with AC (60-70).

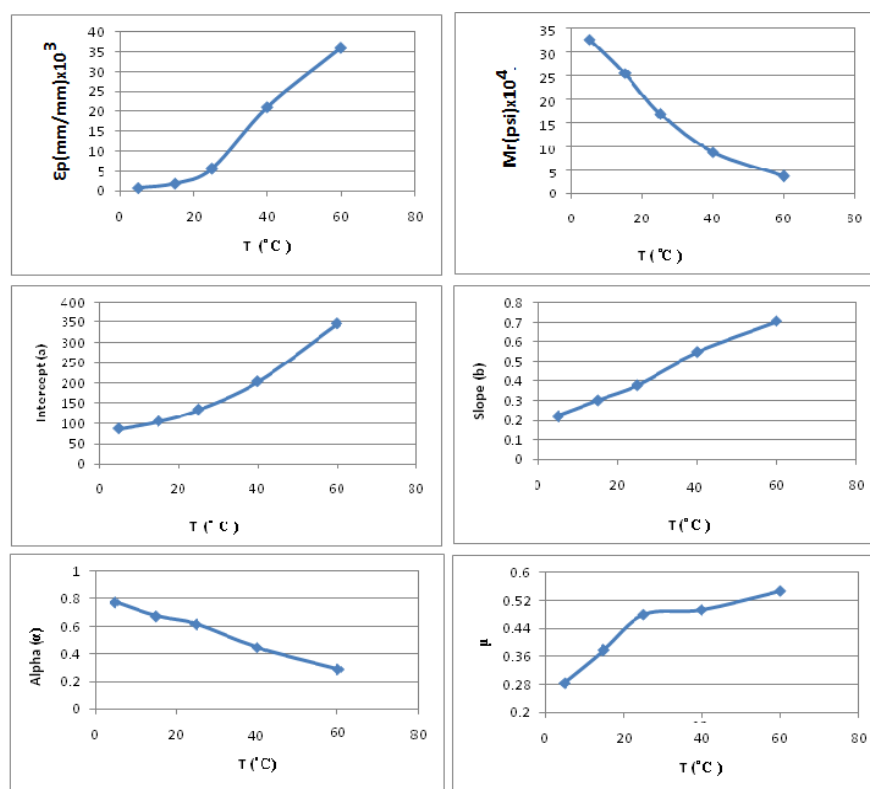


Figure 6. Effect of temperature on permanent deformation parameters.

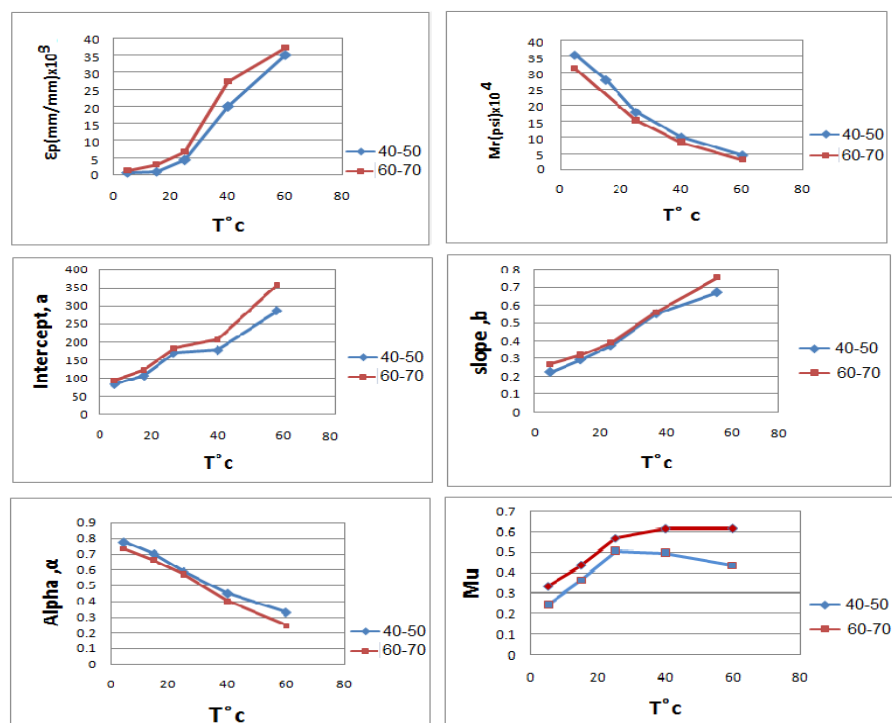


Figure 7. Effect of Asphalt Grade on Permanent Deformation Parameters.

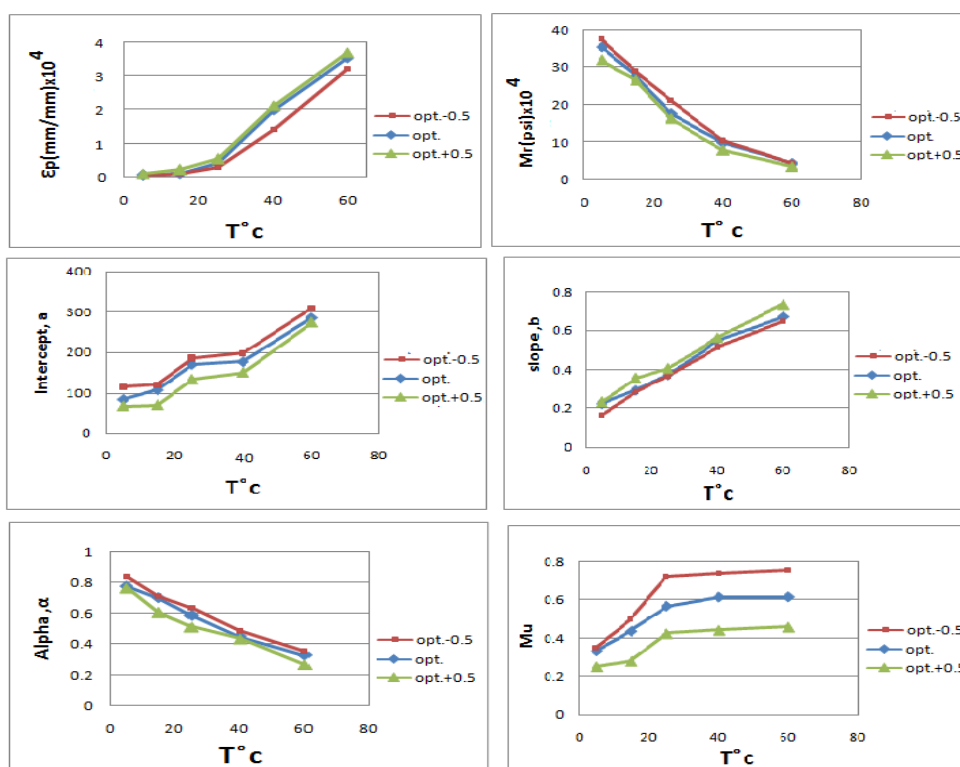


Figure 8. Effect of asphalt content on permanent deformation parameters for AC (40-50).

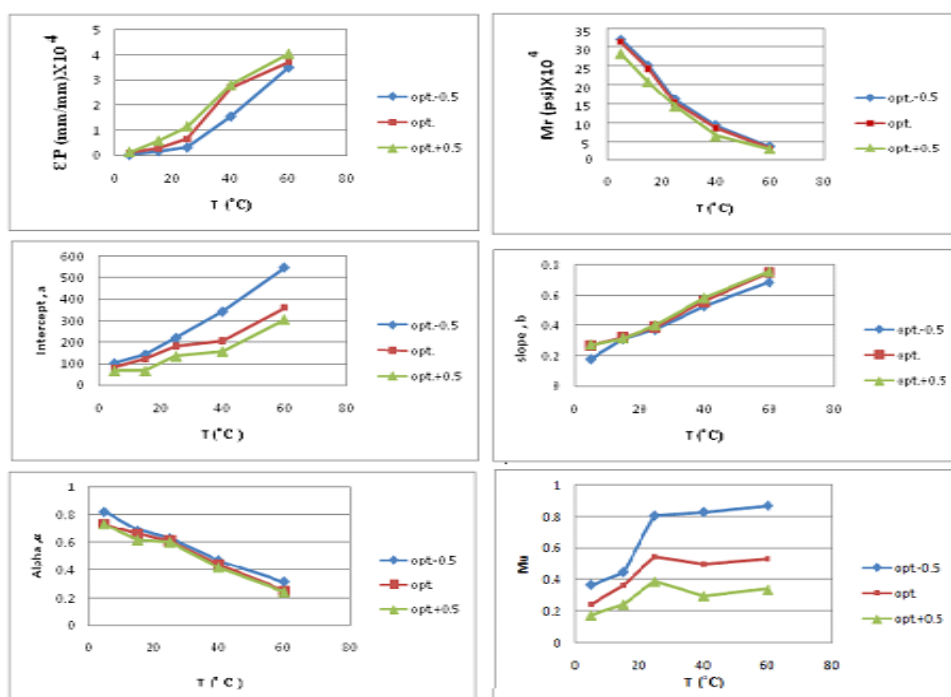


Figure 9. Effect of asphalt content on permanent deformation parameters for AC (60-70).

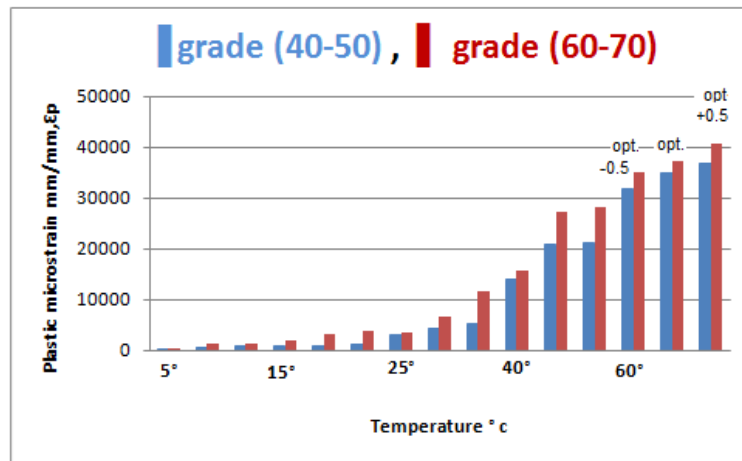


Figure 10. Effect of temperature, asphalt Content, asphalt grade on plastic microstrain.

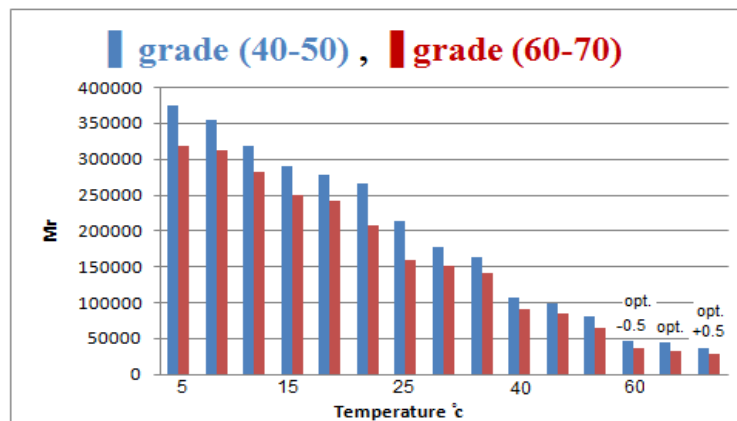


Figure 11. Effect of temperature, asphalt content, asphalt grade on Mu.

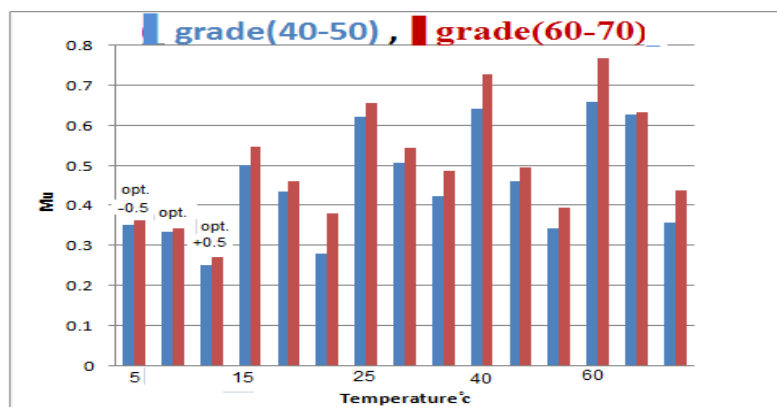


Figure 12. Effect of temperature, asphalt content, asphalt grade on Mu.

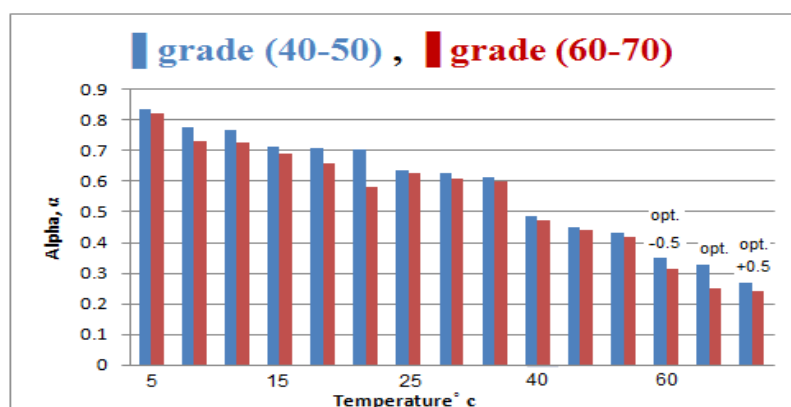


Figure 13. Effect of temperature, asphalt content, asphalt grade on alpha (α).

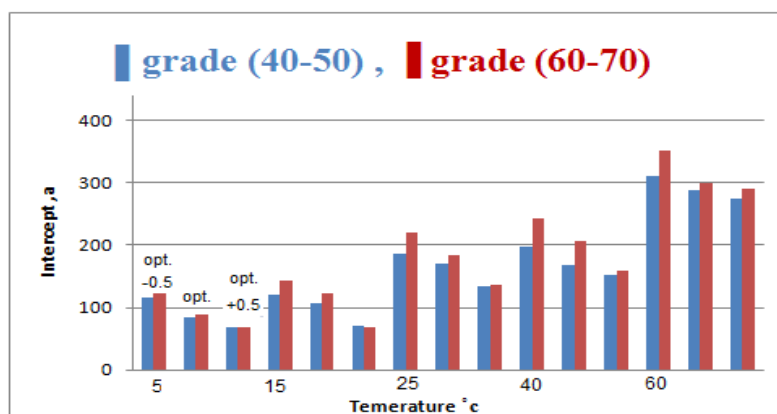


Figure 14. Effect of temperature, asphalt content, asphalt grade on intercept (a).

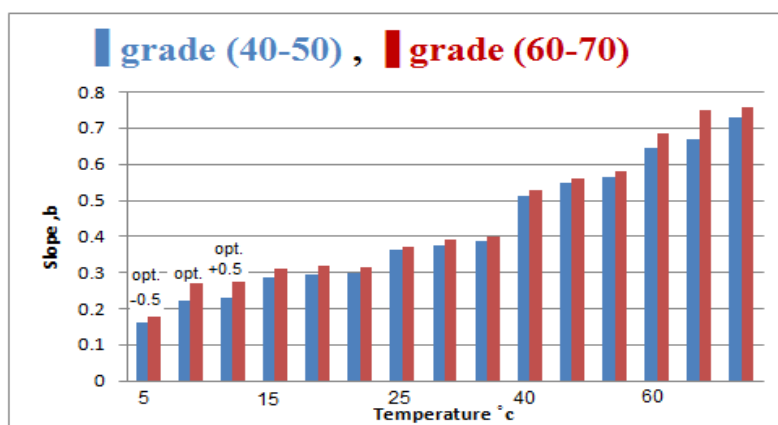


Figure 15. Effect of temperature, asphalt content, asphalt grade on slope (b).

**Table 1.** Physical properties of asphalt Cement (Baghdad University Lab).

Test	Test condition	ASTM Designation	Units	Asphalt Cement			
				40-50	SCRB specification	60-70	SCRB specification
Penetration	100 gm, 25 °C, 5 sec., 0.1 mm	D5	1/10 mm	44	40-50	63	60-70
Kinematic viscosity	135°C	D2170	Cst.	433	Min 400	318	Min 300
Specific Gravity	25 °C	D70	-----	1.03		1.02	
Ductility	25 °C, 5 cm/min.	D113	cm	>100	>100	>100	>100
Flash Point	----	D92	°C	234	232 min	245	232 min
Softening Point	(4±1) °C /min.	D36	°C	48		46	
After Thin Film Oven Test							
Penetration of Residue	100 gm, 25 °C, 5 sec., 0.1 mm	D5	1/10 mm	29		45	
Ductility of Residue	25 °C, 5 cm/min.	D113	cm	53	>25	75	>25
Softening point (Ring & ball) °C	(4±1) °C /min.	D36	°C	50.6		49	

Table 2. Surface or wearing course type.

Opening (mm)	Size(in)	passing by weight of total % aggregate + filler	Specification limits (SCRB-R9/3)
19	3/4	100	100
12.5	1/2	95	90-100
9.5	3/8	83	67-90
4.75	No.4	59	44-74
2.36	No.8	43	28-58
0.3	No.50	18	5-21
0.075	No.200	7	4-10
Asphalt Cement (% weight of total mix)		5	4-6

**Table 3.** Physical properties of aggregates (Baghdad University Lab).

No.	Laboratory Test	ASTM Designation	Test Results	SCRB Specification
Coarse Aggregate				
1	Apparent Specific Gravity	C-127	2.678	-
2	Bulk Specific Gravity	C-127	2.61	-
3	Water Absorption, %	C-127	0.21	-
4	Fractured pieces, %	-	96	90 Min.
5	Percent Wear (Los Angeles Abrasion), %	C-131	17.5	30 Max.
6	Soundness Loss by Magnesium Sulfate solution, %	C-88	3.83	18 Max.
Fine Aggregate				
1	Apparent Specific Gravity	C-128	2.683	-
2	Bulk Specific Gravity	C-128	2.621	-
3	Water Absorption, %	C-128	0.4	-
4	Sand Equivalent, %	D-2419	68.45	45 Min.

Table 4. Physical properties of mineral filler (Baghdad University Lab).

Property	Test Result
Specific Gravity	2.72
%Passing Sieve No.200 (0.075 mm)	96

Table 5. Mean values of permanent deformation parameters for different temperatures.

T(°C)	Mr (psi)	ϵ_p (mm/mm)	a	b	α	μ
5	328036	848.958	86.8617	0.22317	0.77683	0.28538
15	256205	1989.58	105.462	0.30417	0.67583	0.37759
25	168303	5755.21	134.983	0.38183	0.61817	0.48122
40	87904.8	21197.9	204.233	0.5505	0.4495	0.49441
60	37060.1	36125	347.717	0.70817	0.29183	0.5476

**Table 6.** Mean value of permanent deformation parameters with the variation of asphalt cement grade.

	ϵ_p		M_r		a		b		α		μ	
T °c	40-50	60-70	40-50	60-70	40-50	60-70	40-50	60-70	40-50	60-70	40-50	60-70
5	656.3	1218.75	355555	313333	83.75	94.02	0.224	0.27	0.776	0.73	0.24198	0.333
15	1000	3062.5	278260	242973	107.1	122.6	0.293	0.321	0.7	0.659	0.36157	0.436
25	4344	6687.5	177777	152381	170.9	183.1	0.374	0.391	0.586	0.569	0.50546	0.568
40	19875	27187.5	100000	85333.3	177.6	207.5	0.551	0.56	0.449	0.4	0.49579	0.615
60	35125	37187.5	44444	32000	286.9	359.1	0.671	0.752	0.329	0.248	0.43207	0.616

Table 7. Influence of temperature, mix components on strain and permanent deformation parameters for both grade.

Predictor variable	Criterion variable					
	Resilient modulus (M_r)	Plastic strain (ϵ_p)	Intercept coef. (a)	Slope coef. (b)	Alpha (α)	Mu (μ)
Temperature	High	Very high	High	High	High	High
Asphalt Content	Moderate	Low	Moderate	Low	Low	High
Asphalt Grade	Low	Moderate	Moderate	Low	Low	Moderate

Regulations Enforcement Mechanisms for Sustainable Housing Projects

Dr. Sawsan Rasheed Mohammed

Assistant Professor
Department of Civil Engineering
Engineering College- Baghdad University
Email: sawsan_2@yahoo.com

Ibtisam Abduljabbar Abdulridha

Ph.D Student-Principal Senior Engineer
Ministry of Construction and Housing
Email: Ibtisam3_5@yahoo.com

ABSTRACT

Regulations are one of the instruments that governments used to achieve objectives of their policies. Sustainable projects often face compliance problems when working to meet the applicable regulations. The challenge for governments is to develop and apply enforcement mechanisms that achieve the best possible outcomes by achieving the highest possible levels of compliance. The aim of this paper is to identify the most effective mechanisms that can be used to develop a framework for the regulations enforcement for the applications of sustainable housing projects. Accordingly, this paper reviews the common classification of building regulations and enforcement steering mechanisms, in addition to the related international tools of sustainable housing development. The researchers developed a questionnaire included proposals for legislation within five main themes: materials, energy efficiency, water efficiency, health and safety as well as management of residential complexes during the occupation and maintenance phase. Findings represented the highly importance and top preference of incentive mechanism for enhancing sustainable housing regulations. Furthermore, in the theme of health and safety is within the authority of the institution that set these regulations to be imposed on providers and developers of housing. While the results of both energy efficiency and management of housing complexes indicate that legislation be obligated through centralized Act and not as an institutional, so any institution must impose these legislations on housing developers.

Key words: regulations, enforcement, sustainable housing, mandatory regulation, incentives.

آليات انفاذ ضوابط مشاريع السكن المستدام

د. سوسن رشيد محمد
طالبة دكتوراه
رئيس مهندسين اقدم
وزارة الاعمار والسكان

د. سوسن رشيد محمد
استاذ مساعد
قسم الهندسة المدنية
كلية الهندسة-جامعة بغداد

الخلاصة

تعتبر التشريعات واحدة من الأدوات المستخدمة من الحكومات لتحقيق أهداف السياسات التي تضعها. وكثيراً ما تصادف المشاريع المستدامة مشاكل التنظيم والامتثال للقوانين في تلبية اللوائح بشكل أوسع. إن التحدي الذي تواجهه الحكومات هو تطوير وتطبيق آليات انفاذ التشريعات التي تحقق أفضل النتائج الممكنة من خلال تحقيق أعلى المستويات الممكنة من المطابقة. يهدف البحث الى تحديد الآليات الأكثر فاعلية التي يمكن استخدامها لوضع إطار لإنفاذ اللوائح لتطبيقات المشاريع الإسكانية المستدامة. يستعرض البحث مختلف انواع انظمة البناء وآليات الانفاذ فضلاً عن الأدوات العالمية الخاصة بالإسكان المستدام. طور الباحثون استبياناً شمل مقترحات لتشريعات ضمن خمسة محاور رئيسية هي: المواد وكفاءة الطاقة وكفاءة استخدام المياه والصحة والسلامة، فضلاً عن إدارة المجمعات السكنية خلال مرحلة الاشغال والصيانة. تمثلت النتائج بأهمية آلية التحفيز كأحد انواع التشريعات المعززة لنشر تطبيقات السكن الميسر حيث كانت الاعلى تفضيلاً. كما لوحظ في محور الصحة والسلامة حيث يقع ضمن سلطة المؤسسة التي تضع هذه تفرض على مقدمي ومطوري الإسكان. في حين أشرت نتائج كل من محوري كفاءة الطاقة وإدارة المجمعات السكنية أن تكون بشكل تشريع ملزم من خلال قانون مركزي، لذلك يجب على المؤسسات أن تفرض هذه التشريعات على مطوري الإسكان.

الكلمات المفتاحية: التشريعات، الانفاذ، الاسكان المستدام، التشريعات الملزمة، التحفيز.

1. INTRODUCTION

Over all centuries, the governments have developed regulations and rules to control buildings work to save and maintain life safety and quality from the common social and economic issues. The development of regulations is important to achieve the new requirements for applications such as sustainable objectives. This is because of the need for new considerations and changes.

The previous housing policies in Iraq which expanded from the fifteenth of last decay were almost as partial solutions other than effective housing policies lead to retreat the housing sector other than the quality of life, and not being harmony with the stress of population growth because of deceleration of construction industry caused from Iraq conditions that lead to housing deficit. Nowadays, Iraq is considered a developing country but heading towards sustainability development; this will accelerate all sectors move towards sustainability. Concerning housing sustainability, The Agenda No. 21 for Environment and Development of the United Nations Conference **UNCED, 1992**, identified a number of program areas for promoting sustainable human settlement development, including providing access to safe and healthy shelter.

Challenges stand against implementing sustainability within housing projects in Iraq lie in economical, institutional, technical and socio-cultural barriers. Lack of sustainability concerning regulations and lack of enforcement are challenges with higher impact. Ensuring effective compliance with regulations is an important factor in creating a well-functioning society and trust in government. As many issues for housing development, sustainability should be tackled from a regulations perspective. To promote sustainability within housing projects, it is often necessary to experiment with new initiatives and programs that break out of standard patterns.

2. CLASSIFICATION OF BUILDING REGULATION INSTRUMENTS

First of all, the researchers has to define the deferent instruments for regulating the building industry through the most common terms related to the subject of buildings which they are:

1. Acts: The act is a regulatory document that enacted by Congressional approval to make it a mandatory provision. In Iraq, the first Act was enacted for buildings works is the System of Roads and Buildings (SRB) No. 35 of year 1935 and was amended in 1964. **A1., 1964**
2. Building Regulations: Building regulation is characterized as an instrument utilized by a national or local government organization to direct building implementations through an arrangement of articulations of satisfactory least prerequisites. In Iraq, there are the building regulations that issued by the Morality of Baghdad, in addition to the Comprehensive plan of Baghdad. **A2., 2007**
3. Building Standards: Standards are created by an expansive scope of public or private institutions, however not by legislation bodies or by their agents. Standards for the most part manage how things have to be carried out and perform as “best perform”. There are various types of standards **Bukowski, e al., 2001**: calculation or test technique standards; product or system determination standards; and performance statement standards, including client needs or goals.
4. Guiding Rules: Guiding rules are tools regulate building works but without scores and ratings. The design guidelines set up a typical understanding of design principles and need to be integrated with the design process.
5. Assessments: Assessments may be utilized during the design phase of construction project less than building guidelines. Life cycle assessment (LCA) is one technique for assessment. It used in assessing the ecological impacts of systems, processes and products during entire life-cycle of them **Sonnemann, et al., 2003**.

6. Rating Systems: The rating system is considered the most market-oriented tool; it aims to assure the affirmation and public acknowledgment of prevalent building performance and design.
7. Code of Practice: Building codes build up the least measures for construction projects aiming to health and safety regards. For housing sector in Iraq, there is the Code of Practice of Pole Service-Report Two which is adopted for approval awarded for design documents of housing projects. **A3., 1983.**

3. REGULATIONS ENFORCEMENT SYSTEMS

It is very essential to the viability of any building regulatory framework that it ought to work to fulfill compliances with related acts and regulations either were prescriptive or performance based regulations. This would be built up by enforcement and compliance systems, which are necessary to get a building license for any construction works. It is the request for a license from the authorities which is the municipality that sets the system of compliance. In order to get a building license, plans have to be submitted that will reviewed and approved before issuing the license. This is regularly where various building practitioners and individuals communicate with the regulatory authorities in regards to the regulations and its necessities. There are different types of regulations that commonly in use, which illustrated in the following sections that are ordered according to their degree of centralized control from government.

3.1 Command-and-control regulation

This type of regulation is made for non-acceptable actions so it commands the working sectors or people by "not to do a specific action". So the government enacts a law for this command to make that action illegal. Enforcing this law will be by delegating authorities to impose fines to those who break the law. For examples, a law enacted for the allowed maximum levels of pollution emissions. **Cole, and Grossman, 1999.** The researchers supposed that is the control system used by the government.

3.2 Incentive-based regulation

An incentive is any approach, rule, evaluating instrument or strategy that looks to alter the conduct of people or organizations by changing the marginal expenses or marginal advantages associated with specific choices and exercises, through the essential idea of punishments for bad behavior such as polluting, or rewards for good action **Cambini, and Rondi, 2010.** An example, regulations of land use may include incentives for developers to provide affordable housing; in such a case, the localities must ensure that those who will benefit from the incentives, only the once that will fulfill or exceed the criteria of the particular sustainable housing. Incentives should be considered for specific terms, i.e. developers ought to be punished on the off chance that they neglect to maintain their end of the contract and do not meet the necessities of sustainable housing requirements **Kumar, 2015.**

3.3 Performance-based regulation (PBR)

This regulation is a type of incentive-based regulation when incentives are tied to enhancements in facility performance, price lessening and improving service quality. Performance-based regulation (PBR) intends to advance sharing of advantage between the facility and the customers. The utility will advantage from incentives and lower costs that prompt to higher and better profit on investments. While the customers get advantage from lower prices and improved service. PBR is additionally more dependent on external standards of performance and less touchy to organization particular activities. For example, PBR may enhance plant usage,

diminish operation and maintenance costs and enhance system reliability **Bukowski, and Rackliffe, 2001**.

3.4 Market regulations

There is a scope of market-based regulations, which can be utilized to manage activities. These regulations can demonstrate finance effective and lead to control and decrease the regulatory interference in everyday operation of business. The researchers find that this type can be used to promote the applications of sustainable construction by establishing such as the international tools for sustainable rating systems.

Monetary measures, for example, the utilization of taxes and subsidies are also generally utilized market-based instruments. Taxes are regularly forced on destructive activities to make them moderately more costly. While, subsidies can be utilized to support generation or utilization of activities or products which are viewed as attractive **Hepburn, 2009**.

3.5 Self-regulation

This regulation is characterized as relying substantially on the goodwill and cooperation of individual firms for their compliance. It regularly appears as a business or an exchange affiliation developing, monitoring and enforcing its own guidelines of performance **Sinclair, 1997**. There can be some oversight on the regulation by the government. Deferent industries used to have self-regulatory systems to govern industry practices, such as health care, nuclear power, higher education, and professional sports. **Gunningham, 1998**.

Heijden, 2007 found that because of critic on both command and control system and self regulations, and due to thoughts that private sector being more effective than government legislative sector, a solid concentrate on the possibility of self-regulation appears to have ascended from the 1970's.

4. SUSTAINABLE HOUSING REGULATIONS

Regulatory systems and codes concerning the sustainability objectives are significant in advancing support for sustainability to be integrated within practices of building projects **Luce, 2010**. As a result of the fragmented manner of construction projects with the various involved stakeholders and actors, regulations may consider as the main conceivable way for projects activities to continue **Häkkinen and Belloni, 2011**. Following sections review kinds of sustainability regulation tools for housing in particular.

4.1 Sustainable Building Instruments

Sustainable building instruments come in a wide assortment of advancing formats; each format achieves diverse objectives and makes distinctive impacts **Carmody, et al., 2009**. **Table 1** shows the international tools related to sustainable housing projects. Instruments reviewed in this paper come into five fundamental classes: building codes, standards, assessments, rating systems, guidelines,

In Some cases, guidelines of sustainable building are composed as recommendations or advise to help engineers, developers, and planners to design and construct the sustainable buildings. In other cases, governments and its different institutions may utilize these guidelines as obligatory methods. For example, The Sustainable Building Guidelines of Minnesota in United States is a case of a guideline that is obligatory for all buildings developed by financing from the state government **Carmody, et al., 2009**. This is to aim to guarantee that state money is utilized rationally to design buildings that are energy efficient, long lasting, and with few loads as could be expected on local infrastructure, e.g. roads and storm sewers.

4.2 Types of Indicators

Commonly, there are two types of sustainability indicators: prescriptive indicators and performance indicators. These both types have favorable circumstances. Indicators are typically used to determine the action or performance objective that must be met to fulfill a specific standard of work. Otherwise, there is an imperative distinction amongst prescriptive and performance indicators as discussed below.

4.2.1 Prescriptive Indicators

These indicators are used to determine specific arrangements for actions that must be made to fulfill the criteria. These arrangements are picked in advance by the institution that built up any of the deferent instruments i.e. guideline, assessment, or the rating system. Then these actions be prescribed and must be finished as composed. Since the indicator is not tied to a measurement, the ultimate result of a prescriptive indicator will not be known **Carmody, et al., 2009**. Contractors prefer prescriptive type since this type outline a progression of actions which are simple to follow. Similarly, organizations working with rating acknowledge prescriptive indicators because they are not difficult to enforce.

4.2.2 Performance Indicators

This type of indicators is used to measure the result of an arrangement of actions which is not prescribed. With these indicators, designers and specialists will choose how the required outcomes will be accomplished. Likewise, the performance indicator decides how the outcome will be measured. There are significant advantages of these indicators. First, these indicators maximize the flexibility designers need to accomplish objectives of sustainable building. In spite of that advantage, performance indicators necessitate extra work to measure the performance of accomplished works. Additionally, they compel designers and specialists to measure the outcomes of the choices they make. This helps them comprehend which choices really work to enhance performance.

In case of post-occupancy monitoring activities, performance indicators will be used to constrain building owners and occupants to measure environmental impacts of their actions. This can prompt improvement to behavior and procedures to enhance a building's performance. Additionally, these indicators can aid to measure compliance with centralized regulations such as energy use, levels of pollution. **Carmody, et al., 2009** found that most of building researchers have mostly agreed that performance indicators are the best method to achieve objectives of sustainability.

4.3 Regulation Enforcement Instruments

The shortage of correct instrument could be a barrier for the sustainable building practices. Different forms of instruments are getting used for steering the sustainable buildings projects. These forms include obligatory laws, incentives and voluntary actions. Accordingly, in order to enhance application of sustainability within building projects, it is important to find the right instruments and systems for enforcing the regulations whatever the type of them.

4.3.1 Obligatory regulations

In this form, the project will be more averse to be opposed by the regulatory institutions since requirements are considered previously, **Robichaud and Anantatmula, 2011**. The regulations may have either positive or negative consequences on an action. In the primary phase of

sustainable building development, regulations have to enforce the base required performance and this will definitely be effective to accomplish the outcomes **Häkkinen and Belloni, 2011**.

4.3.2 Incentives

Incentives are as motivation method to encourage people or institutions to do something, for example as tax diminishment which can impact positively the developers' desire to accomplish sustainability targets. As sustainability needs both regulations and innovations in the future as more in the housing development projects, incentives can persuade innovations and make requests for alternatives. As an example, in USA, several states enacted their own legislation to develop and implement LEED based tax discount incentives to create green building initiatives, by allowing property tax discount at a local level, as financial incentives that will be founded on accomplishing LEED accreditation **Prum, 2009**. As per this proposed enactment, a private client, who wants to develop a new building with LEED accreditation, he will get tax discount for up to 12 years.

The risk of Incentive programs is that they deviates markets and present need to comparison opportunities for developers. These programs require solid enforcement and checking by government powers. Such incentives additionally should be organized with clear points of reference and conditions and commitments, to necessitate the release of the incentives. In this manner, implementation the incentives should be actualized with great care.

For sustainable housing projects, right adjust is required between the cost and the value picked up by the developer. Development of sustainable housing may be postponed in case incentive is not satisfied. Incentive programs are also subject to be not active leading that developers may develop less-quality houses.

4.3.3 Voluntary activities

Voluntary activities are, for example, the green accreditations from various rating systems such as LEED system. **Häkkinen and Belloni, 2011** concluded that voluntary approach has not brought about huge changes, therefore, normative regulations are required. In the case of regulations that support the voluntary activities, they would be useful to enhance application of sustainable construction.

5 BUILDING THE ENFORCEMENT REGULATION FRAMEWORK

Regulators need to implement rules and instructions by delivering what they aim from concerning institutions and people, through providing guidance or any deferent forms of direction to achieve enforcement. They often enforce regulations through inspections and approved all stages outputs of design to assess whether development accords with regulations. There are two levels of influences required to be considered when planning for enforcing regulations; one of them is concerning the behavior of people, and the other will be required to influence the actions and activities of institutions when delivering their works related to housing projects.

For the aim of this paper concerning developing an enforcement steering mechanism for sustainable housing regulations, the researchers framed the following steps:

1. Identifying the scope of the regulations needed to be implemented for sustainable housing projects in Iraq;
2. Develop a questionnaire to test the themes needed to stimulate a framework for enforcement mechanisms. Those will be illustrated in section 5.2;
3. Discussing the results to advance recommendations for the aim of this paper

5.1 Regulations of Sustainable Housing

For the scope of this paper, the researchers concluded and extracted, from literature survey, five main domains which are crucial for sustainability within housing projects: Materials, Energy efficiency, Water efficiency and Health and safety. These domains are to be decided during the stage of planning and design of the project. In addition to the management domain which will be needed after completion of previous phase, i.e. the phase of occupation and maintenance. These domains are as shown in **Table 2**. The proposed regulations within those domains have to be decided how to be obligated. So the researchers appointed three main levels of obligation: Centralized regulations, institutional and guiding rules.

Additionally, the researchers developed incentives regulations for private investors to be used when developing sustainable housing projects as illustrated in **Table 3**; this is to examine how incentives would be viable to enforce sustainability practices for housing.

5.2 Developing the Questionnaire

The researchers used the questionnaire as an instrument considers the experience of professionals to examine the themes of the paper. Three questions were developed for three cores important for developing the intended framework for regulation enforcement mechanism. Questions and scale of evaluation are shown in **Table 4**. Themes of question 1 and question 3 were rated using the fifth scale of measurement, while for question 2, three types of obligation were proposed for each regulation of sustainable housing which determined in **Table 2**.

The questionnaire was delivered to professionals across all Iraq by using the technique of Google Drive to prepare and distribute the questionnaire and to receive the replied responses. Those professionals were choosing according to their sector of work, experience in housing sector, qualifications, and various disciplines ranging from planners, designers, managers, consultants, academics, legal and economists in addition to private investors. The researchers distributed the questionnaire to 44 professionals, but only 41 responses were replied, this is considered the sample size. Initially the questionnaire asked for the background profile of the professionals as shown in **Fig. 1**, which illustrates the working sectors ranging between public and private, and No. of experience years ranging from 16 years to more than 30 years which account for more than 52% of the total sample size of responses. While the qualifications ranged from Ph.D which accounts 35.50% of the sample size, in addition to MSc. accounts 24.85% and BSc. of 39.64%.

5.3 Discussion the Results of the Questionnaire

5.3.1 Testing the Reliability

It is known that the smallest acceptable value for Cronbach's alpha coefficient is (0.6) and the best value ranging from (0.7 to 0.9) while the higher value than (0.90) supposed to be the better but do not reach the correct value of (1) **A4., 2013**. Values of the reliability coefficients for the three questions are positive with maximum limit of (0.930) and the minimum limit of (0.644) as shown in **Table 5**.

5.3.2 Results of Question (1)

As noted from **Fig. 2** and **Fig. 3**, that the professionals are more satisfied with incentive and performance based systems to apply sustainable housing applications with some control required from government, and also they find that less control through self regulation and market control systems may be used for some types of regulations. These two types also gained some satisfaction from professionals with value of arithmetic mean exceeded (3.40) that means the "high" satisfaction.

5.3.3 Results of Question (2)

Values and symbols were given to the three levels of obligation, to examine the trends of responds for the regulations as follow:

"1" = (C) Central regulations

"2" = (I) Institutional regulations

"3" = (G) Guiding rules

The aim of this question is to test the considerations that researchers appointed for the three suggested levels to obligate the regulations of the five themes mentioned in **Table 2**. These considerations are:

- 1) All items will be implemented after the stage of development and construction of the housing project need to be legislated as centralized regulations.
- 2) Items that will be decided through the phase of development and construction will be either institutional-based regulations or design guiding rules. They will be obligated by the institution that gives the license for the project when these items are able to be implemented by the developers but these developers may not desire to implement them because of the possible related costs. Otherwise these items will be as guiding rules to the developers to implement them in the way they desire but have to accomplish the end targets.
- 3) Final evaluation for the level of regulations enforcement depended on the comparison between the researchers' considerations and the results from the questionnaire statistical analysis; this is because of discrete scale of the three levels of evaluation.

Tables 6a, b, c, d and e show the results of themes of the second question. The researchers noted that the centralized regulations were appointed by the professionals for actions that considered out of the authority of the institutions to control these actions and enforce them, i.e. these actions are interrelated to special named institutions must take action to regulate them.

For the non compatible final results with researchers' considerations, the researchers concluded that these regulations required to be included within the authority of the related institutions, as illustrated below for each proposed regulation:

- MR2- Recyclable and re-usable materials for a specific portion from total materials: the researchers supposed that this item need to be legislating as centralized regulations because it needs more obligations to be executed. As per, this will lead to establish stations for recycling and reusing of building materials and components. While the results shows the favor type of obligation is that regulation be as guiding rules for designers and this will not persuade the developers to implement this item because of non available required infrastructure for this item to be realized, and because of non interest and awareness of the important of recycling and reusing for sustainability. Accordingly, the researchers suggested that this item will be as guiding rule and to be studied for long term mandatory legislation in the future.
- MR4- Cavity external walls, double glazing, low emission glass and heat isolated materials: according to the professionals, this item required to be obligated for housing developer by an institution, while the researchers appointed this item to be as guiding rules. The recommendation is that this item be as institutional obligated or as guiding rule as per the project orientation and briefing.
- MR5- standard material and product sizes and unified window shapes and sizes for easy replace when need to maintenance: professionals indicated this item to be as guiding rules, while the researchers indicated it to be obligated by the institution. So, the researchers suggested that this

item firstly has to be as guiding rules with term that it will be obligated by institutions in the later time and not to stay as guiding rules.

- MR7: low shining concrete or materials with reflecting factor used for car parking surfaces to reduce the heat island: the result is as same as MR4. This item recommended to be obligated by institutions.
- For themes of energy efficiency, water efficiency and health and safety, the results are compatible for both researchers' consideration and results of the questionnaire.
- For themes of Occupation and Maintenance Management, only one item has conflict result which is the OMR3: Create programs for residents to engage them in the programs of utilizing and/or maintaining water and energy; the professionals indicated this item would be obligated as per institutions, while the other two items; OMR1 and OMR2 were indicated as centralized obligated.

5.3.4 Results of Question (3)

As noted from **Fig. 4**, the professionals highly encourage using incentive regulations for investors to promote the applications of sustainable housing. The three items: IR1, IR2 and IR3 concerning using the vacant and contaminated lands and enhancing mixed use zoning for housing within commercial buildings scored more than 4.20 which indicate "very high satisfaction" from the respondents. While the results of the other three regulations: IR4, IR5 and IR6 concerning rainwater tank and recycling techniques for grey water, floating zone and brownfield sites, also indicated high score which is higher than 3.40, leading to conclusion that the respondents are with high satisfaction with promoting incentives for these regulations but need more binding terms when contracting.

6 CONCLUSIONS

From the literature review of this paper and the results of the practical work, the researchers concluded that to promote sustainability practices within housing projects, it is necessary to establish programs and mechanisms out of the ordinary model. Enforcement mechanism should be standing on the concept of not treat all regulated issues in a uniform method. Based on that, differentiation should be based on the overall actions of the regulated issue. That means the enforcement approach would base on the status of the housing project and its briefing.

Furthermore, they concluded that incentive regulations can be determined and controlled by the authorized bodies. Also moving toward performance-based regulation (PBR) is highly recommended to be adopted in the reforming regulations of sustainable housing, but with using the four types of enforcement levels to promote the sustainable practices: centralized; institutional and guiding rules, in addition to incentive regulations. For some regulations, it is as per a locality to decide how would like to obligate them within contracts with developers to fulfilling their vision.

Also the researchers found that to create programs for residents to engage them in the programs of utilizing and/or maintaining water and energy need to be centralized obligated, so the researchers recommended that this item firstly be obligated as an institution decides to, with condition that it will be legislated centralized in the long term strategy.

Another recommendation is that the government has to promote actions to be as supported activities for establishing an enforcement mechanism for sustainable housing projects through maximizing the awareness of practitioners who either work within the regulatory bodies or the private sectors who work in developing housing projects in addition to the households that will be the users of the sustainable housing projects.

REFERENCES

- Bukowski, R, Hirano, Y., and Rackliffe, T., 2001, *Standards Linkages to a Performance-Based Regulatory Framework*, Proceedings CIB World Congress, Wellington, NZ, CIB 2001
- Cambini, C. and Rondi, L., 2010, *Incentive regulation and investment: evidence from European energy utilities*, Journal of Regulatory Economics, Volume 38
- Carmody, J., Weber, W. and Jacobson, R., 2009, *Design guidelines for Sustainable housing*, Center for Sustainable Building Research (CSBR), Korea
- Cole, Daniel H. and Grossman, Peter Z., 1999, *When Is Command-and-Control Efficient? Institutions, Technology, and the Comparative Efficiency of Alternative Regulatory Regimes for Environmental Protection*, Articles by Maurer Faculty, Indiana University, Paper 590
- Gunningham, N., 1998, *Smart Regulation. Designing Environmental Policy*, Clarendon Press, Oxford
- Häkkinen, T., & Belloni, K., 2011, Barriers and drivers for sustainable building. Building Research & Information, 39(3), 239-255.
- Heijden, J., 2007, *Enforcement of Building Regulations: From Public Regulation to Self regulation; A Theoretical Approach*, International Conference for Sustainable Urban Areas, 2007, Rotterdam
- Hepburn, G., 2009, *Alternatives To Traditional Regulation*, OECD report for the OECD Regulatory Policy Division
- Kumar, Tej K., 2015, *Mandatory Versus Incentive-Based State Zoning Reform Policies for Affordable Housing in the United States: A Comparative Assessment*, Journal of Housing Policy Debate, V. 25
- Luce, Z., 2010, *Project Management and Sustainability*, Retrieved 11th October
- Sinclair, D., 1997, *Self-Regulation versus Command and Control? Beyond False Dichotomies*, Law & Policy Journal, Vol. 19, No. 4
- Prum, D., 2009, *Creating State Incentives for Commercial Green Buildings: Did the Nevada Experience Set an Example or Alter the Approach of Other Jurisdictions?*, William & Mary Environmental Law and Policy Review /vol34/iss1
- Robichaud, L. B., & Anantatmula, V., 2011, *Greening project management practices for sustainable construction*, Journal of Management in Engineering
- Sonnemann, G.; Castells, F.; Schuhmacher, M., 2003, *Integrated Life-Cycle and Risk Assessment for Industrial Processes*, Lewis Publishers: Boca Raton, USA
- UNCED, 1992, The Agenda No. 21 of the United Nations for Environment and Development Conference.

المصادر العربية

- A1., 1964: وزارة الداخلية في العهد الملكي، نظام الطرق والابنية رقم 44 لسنة 1935، معدل في 1964، العراق
- A2., 2007: امانة بغداد، 2007، مجموعة الضوابط التخطيطية للبناء وتقسيم الاراضي في مدينة بغداد، العراق
- A3., 1983: مؤسسة بول سيرفس البولونية، 1983، معايير الاسكان الحضري ووالريفي، المؤسسة العامة للاسكان السابقة، العراق
- A4., 2013: عبد المجيد، احمد عودة، 2013، كتاب مفاهيم التقييم والقياس والاداء، كلية التدريب، الرياض

ABBREVIATIONS

PBR= performance based regulations

CAC= command and control

ER= energy efficiency regulations

HSR = health and safety regulations

MR = materials regulations

OMR= occupation and maintenance regulations

Q = question

Sys = system of enforcement

S.D = standard deviation

WR = water efficiency regulations

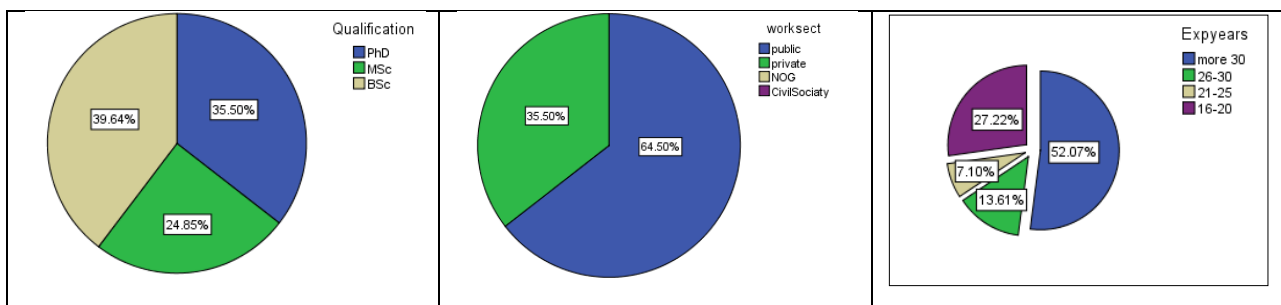


Figure 1. Qualifications and work place of the respondents, **Researchers.**

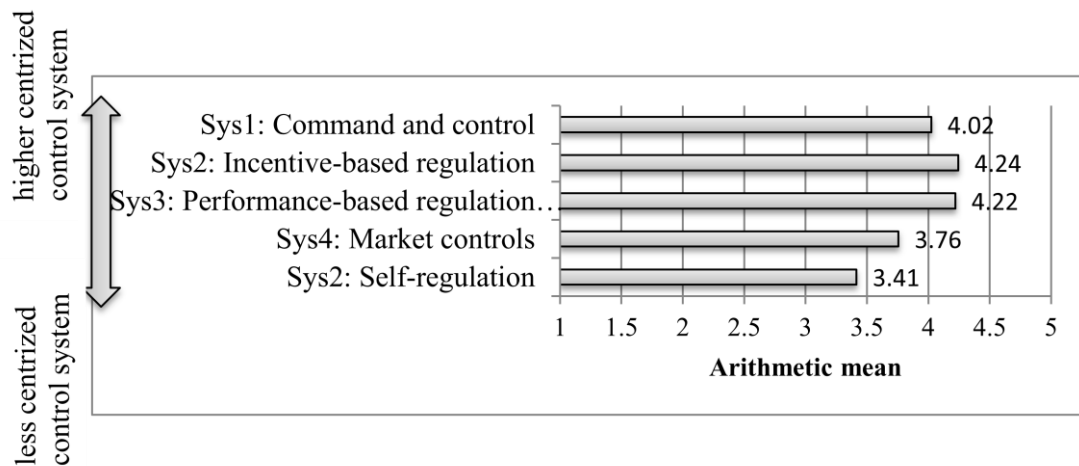


Figure 2. Descriptive analysis for respondent's evaluation of supposed regulations enforcement systems, **Researchers.**

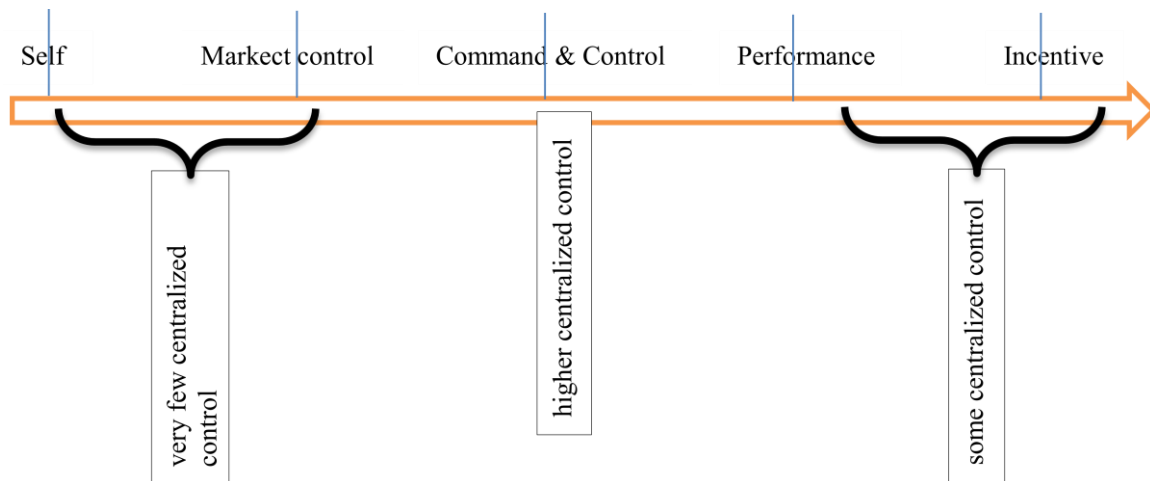


Figure 3. Spectrum of satisfaction with degree of centralized control by regulations, **Researchers.**

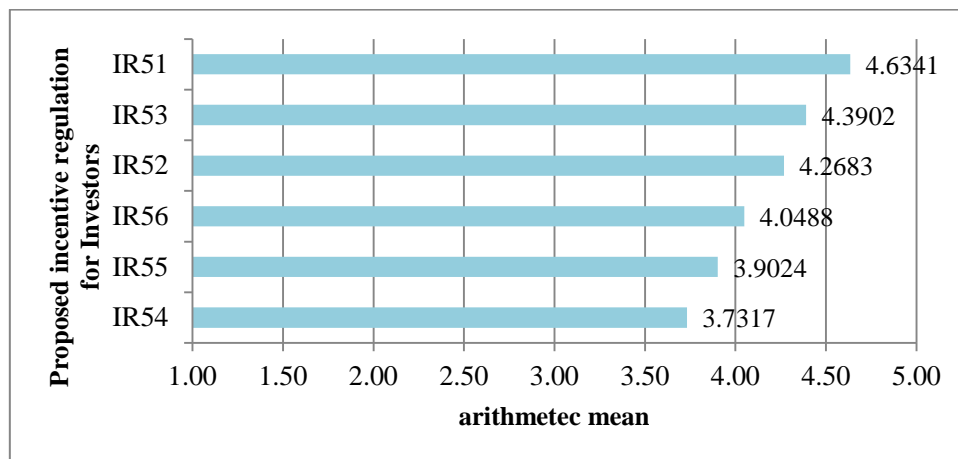


Figure 4. Descriptive analysis for respondent's evaluation of proposed incentive themes for regulations for housing investors, **Researchers.**

Table 1. Indicators in the international tools for sustainable housing development ,Researchers depend on, **Carmody, et al., 2009**.

International tools for sustainable housing development															
		LEED for Neighborhoods	LEED for Homes	CASBEE-Homes	HK--BEAM	GBCS -MUNRBs	Green Globes	Austin Energy Green Building	Passive Haus	NABERS - Homes	Living Building Challenge	UK Code for Sustainable Home	MN B3 Guidelines	SB-tool	SBAT Ilite
Year		2007	2008	2002	1996	2002	2004	1992	1996	2005	2006	2007	2004	1997	1997
Country		USA	USA	Japan	Hong Kong	Korea	USA	USA	Germany	Australia	USA	United Kingdom	USA	Canada	South Africa
Formats	Building Code											●			
	Standard						●								
	Assessment								●	●	●		●	●	
	Rating	●	●	●	●	●	●	●		●		●		●	●
	Guideline										●		●	●	
Performance Indicators	Bio - diversity	√	√	√	√	√	√	√			√	√	√		
	Land use	√	√		√	√	√	√			√	√	√		√
	Heat island effect	√	√	√	√		√						√		
	Vehicle miles travelled	√	√		√	√	√	√				√	√		√
	Energy use – total building	√	√		√	√	√	√	√	√	√	√	√	√	
	Energy use – HVAC		√	√			√	√	√						√
	Energy use – others		√	√	√		√	√				√	√	√	√
	Energy use – renewable	√	√	√	√	√	√	√					√	√	√
	Water use – building	√	√	√	√	√	√	√			√	√	√	√	√
	Water use – landscape	√	√	√	√	√	√	√			√	√	√		√
	Waste water				√	√	√				√		√		√
	Storm water	√	√	√	√	√	√				√	√	√		√
	Solid waste	√	√	√	√	√	√	√			√	√	√		√
	Light pollution	√			√		√	√					√		
	Sound pollution			√	√	√									
	Carbon footprint				√		√				√	√	√	√	√
	Human health IEQ	√	√	√	√	√	√	√				√	√	√	

Table 2. The proposed regulations within the five domains for sustainable housing, Researchers.

Main domains	Proposed Regulations
Materials Enact a standardized national code to promote using:	MR1: local building materials for a specific portion from total materials
	MR2: recyclable and reusable materials with for a specific portion from total materials
	MR3: low volatile organic compound (VOC) building materials
	MR4: Cavity external walls, double glazing, low emission glass and heat isolated materials
	MR5: standard material and product sizes and unified window shapes and sizes for easy replace when need to maintenance
	MR6: energy saving construction materials for a specific portion from total materials
	MR7: low shining concrete or materials with reflecting factor used for car parking surfaces to reduce the heat island
Energy Efficiency	ER1: Determine a portion of the total electric power needed to whole housing project to be generated from renewable energy recourses
	ER2: Using Solar system for water heating
	ER3: Installing energy efficient appliances for heating, cooling, cooking, lighting and ventilation
	ER4: A specific percentage of total dwelling units must be oriented correctly
Water Efficiency	WR1: Water recycling based strategies: rain water storage and re-use, and Gray water re-use and recycling system
	WR2: installing water efficiency appliances and fittings
	WR3: Impose strict levies and penalties for the quantity of used water by specify the upper limit for the permitted quantity of water
	WR4: establish limits for out-door water use
Health and Safety	HSR1: make the main living areas of the dwelling unit away from roads and car parking to avoid exposure to car fumes
	HSR2: Enhancing using fire network System and design for escaping roots
	HSR3: Using materials and building components of a non- combustible and flammable content in order to reduce the risk of the rapid spread of fire and toxic gases inside the house
	HSR4: Using smart appliances such as: Combustion appliances (venting Measures), Indoor contaminant control, Moisture Control devices and Occupant controls/ease of use (CO Monitors installed in each unit
	HSR5: Using hard or natural barriers and trees to avoid and eliminate the outside noises
Occupation and Maintenance Management	OMR1: Establish housing association in order to set and conduct a long term Programs for housing and facilities maintenance and management within the housing development or district.
	OMR2: set and conduct a waste management plan for the housing development
	OMR3: Create programs for residents to engage them in the programs of utilizing and/or maintaining water and energy.

Table 3. Incentives regulations for private investors, **Researchers.**

	Proposed Incentives regulations for investors
IR1	Vacant lands: Reduce costs and facilitate the approvals and licenses for investors for the purpose of developing vacant land within the urban fabric assigned for residential use to establish affordable housing but must be with sustainability applications for energy, water and materials using efficiency.
IR2	Contaminated lands: Granting subsidies for the rehabilitation of contaminated lots for housing complex projects with sustainable practices
IR3	Inclusionary Zoning-Mixed Use: allow apartments over stores to create powerful incentives for private developers and investors to produce more affordable housing but with sustainable practices.
IR4	Brownfield sites: Using land with existing infrastructure more effectively: reducing the need to invest in costly new infrastructure expansion, lowers land and service costs thereby contributing to housing affordability and sustainability
IR5	Floating zone: Identifying specific regions and lands to apply specific floating legislation previously agreed that differ from what is stipulated in the general regulations such as density, number of floors, elevations, coverage ratios, setbacks and subdivisions and others, to create a motivational environment for investors to set up projects with sustainable applications for affordable housing
IR6	Rainwater tank and recycling techniques for grey water: Developers are entitled to an amount as remission on their development contribution for approved installation of rainwater tanks, and using recycling for grey water to encourage the wise and sustainable reuse of water resource.

Table 4. Themes and scale of evaluating the themes of the questionnaire.

Questions	Theme	Scale
Q1	Enforcement systems mentioned in Section 3	Rated from 1 to 5, where (1) represents the "not satisfy" and (5) represents the highest satisfaction. The calculated scale to represent the results are: - Not satisfy: 1.00 - 1.80 - Little: 1.81 – 2.60 - Medium: 2.61 – 3.40 - high: 3.41 – 4.20 - Very high: 4.21 – 5.00
Q2	Proposed regulations for five themes: 1)Materials, 2)Energy efficiency, 3)Water efficiency, 4)Health and safety, and the 5)management	three main levels of obligation: • Centralized regulations; • institutional; • guidelines

Q3	Proposed incentive regulations for housing private investors	<p>Rated from 1 to 5, where (1) represents the "not satisfy with viability of the proposal" and (5) represents the highest satisfaction. The calculated scale to represent the results are:</p> <ul style="list-style-type: none"> - Not satisfy: 1.00 - 1.80 - Little: 1.81 – 2.60 - Medium: 2.61 – 3.40 - high: 3.41 – 4.20 - Very high: 4.21 – 5.00
----	--	---

Table 5. Reliability statistics test for the main themes of the questionnaire using Cronbach's Alpha as internal consistency.

Question	Number of items of the question	Standard lower bound	Actual values	Assessment
Q1	5	0.60	0.644	Pass
Q2	33	0.60	0.930	Pass
Q3	10	0.60	0.729	Pass

Table 6a. Results for the theme of Materials.

Proposed Regulations	Supposed mandatory level by researchers	Centralized regulations (C)	Institutional /sectoral regulations (I)	Guiding rules (G)	Mean	S. D	assess
MR1	Centralized	15	13	13	1.95	.835	Centralized
MR2	Centralized	12	11	18	2.15	.853	Guidelines
MR3	Centralized	19	12	10	1.78	.822	Centralized
MR4	Guidelines	11	20	10	1.98	.724	Institutional
MR5	Institutional	4	16	21	2.41	.670	Guidelines
MR6	Guidelines	8	13	20	2.29	.782	Guidelines
MR7	Guidelines	12	17	12	2.00	.775	Institutional

Table 6b. Results for the theme of Energy efficiency.

Proposed Regulations	Supposed mandatory level by researchers	Centralized regulations (C)	Institutional /sectoral regulations (I)	Guiding rules (G)	Mean	S. D.	assess
ER1	Centralized	13	21	7	1.85	.691	Centralized
ER2	Centralized	15	15	11	1.90	.800	Centralized
ER3	Centralized	15	14	12	1.93	.818	Centralized
ER4	Guidelines	6	18	17	2.27	.708	Guidelines

Table 6c. Results for the theme of Water efficiency.

Proposed Regulations	Supposed mandatory level by researchers	Centralized regulations (C)	Institutional/sectoral regulations (I)	Guiding rules (G)	Mean	S. D.	assess
WR1	Institutional	11	21	9	1.95	.705	Institutional
WR2	Centralized	11	18	12	2.02	.758	Institutional
WR3	Centralized	21	11	9	1.71	.814	Centralized
WR4	Centralized	10	20	11	2.02	.724	Institutional

Table 6d. Results for the theme of Health and safety.

Proposed Regulations	Supposed mandatory level by researchers	Centralized regulations (C)	Institutional/sectoral regulations (I)	Guiding rules (G)	Mean	S. D.	assess
HSR1	Guidelines	14	14	13	1.98	.821	Institutional
HSR2	Centralized	20	16	5	1.63	.698	Centralized
HSR3	Centralized	15	15	11	1.90	.800	Centralized
HSR4	Guidelines	10	17	14	2.10	.768	Institutional
HSR5	Guidelines	10	16	15	2.12	.781	Institutional

Table 6e. Results for the theme of Occupation and maintenance management.

Proposed Regulations	Supposed mandatory level by researchers	Centralized regulations (C)	Institutional/sectoral regulations (I)	Guiding rules (G)	Mean	S. D.	assess
OMR1	Centralized	18	20	3	1.63	.623	Centralized
OMR2	Centralized	18	19	4	1.66	.656	Centralized
OMR3	Centralized	11	17	13	2.05	.773	Institutional

Adsorption of Mefenamic Acid From Water by Bentonite Poly urea formaldehyde Composite Adsorbent

Dr.Basma Abbas Abdel Majeed

Professor

College of Engineering-University of Baghdad

basma1957@yahoo.com

Dr.Raheem Jameel Muhseen

Assistance Professor

college of Pharmacy-University of Basra

raheemjamail@yahoo.com

Nawras Jameel Jassim

Assistance Lecturer

Basra Technical Institute -Southern Technical University

nawras.jassim@gmail.com

ABSTRACT

Poly urea formaldehyde –Bentonite (PUF-Bentonite) composite was tested as new adsorbent for removal of mefenamic acid (MA) from simulated wastewater in batch adsorption procedure. Developed a method for preparing poly urea formaldehyde gel in basic media by using condensation polymerization. Adsorption experiments were carried out as a function of water pH, temperature, contact time, adsorbent dose and initial MA concentration. Effect of sharing surface with other analgesic pharmaceuticals at different pH also studied. The adsorption of MA was found to be strongly dependent to pH. The Freundlich isotherm model showed a good fit to the equilibrium adsorption data. From Dubinin–Radushkevich model the mean free energy (E) was calculated and the value of 5 KJ/mole indicated that the main mechanism governing the adsorption of MA on PUF-Bentonite composite was physical in nature. The kinetics of adsorption tested for first order, pseudo second order models and Elovich's equation, results showed the adsorption followed the pseudo-second-order model.

Key Words: Mefenamic acid adsorption, Bentonite ,Analgesic ,Poly urea formaldehyde.

امتزاز حامض الميفيناميك من الماء بواسطة خليط البنتونيت البولي يوريا فورمالدهايد كمادة ممتزة

د.رحيم جميل محسن

استاذ مساعد- كلية الصيدلة جامعة البصرة

د.بسمه عباس عبد المجيد

استاذ – كلية الهندسة جامعة بغداد

نورس جميل جاسم

مدرس مساعد – المعهد التقني في البصرة

الخلاصة

تم اختبار مزيج بولي يوريا فورمالدهايد (PUF) بنتونيت كمادة ممتزة جديدة لإزالة حمض الميفيناميك (MA) حيث أجريت تجارب الامتزاز بالدفعات لنموذج من الماء الملوث معد مختبريا. تم تطوير طريقة جديدة لتحضير بوليمر اليوريا فورمالدهايد في وسط قاعدي باستخدام البلمرة التكثيفية. أجريت تجارب الامتزاز من خلال دراسة متغيرات التأثير المختلفة مثل الدالة الحامضية (pH)، الحرارة، زمن التلامس، كمية المادة الممتزة وتركيز الحامض الابتدائي. درس كذلك تأثير مشاركة السطح الممتز مع مواد مسكنة صيدلانية أخرى عند قيم مختلفة من pH. وجد ان امتزاز MA يعتمد بصورة اساسية على pH. اظهرت بيانات توازن ايزوثيرم الامتزاز تطابقها مع نموذج Freundlich. من نموذج

Dubinin Radushkevich تم حساب متوسط الطاقة الحرة (E) وكانت قيمتها 5 KJ/mole والتي تشير الى ان طبيعة امتزاز حامض الميفيناميك على خليط البولي يوريا فورمالديهايد بينتونايت هي ذات طبيعة فيزيائية . تم تطبيق نماذج دراسة حركيات الامتزاز الرتبة الاولى والرتبة الثانية ومعادلة Elovich's وأشارت النتائج الى ان الامتزاز يخضع الى نموذج حركية الرتبة الثانية.

الكلمات الرئيسية : امتزاز حامض الميفيناميك ، بنتونايت ، مثبط ، بولي يوريا فورمالديهايد.

1. INTRODUCTION

An increasing number of emerging contaminants have been detected in surface waters, sediment, soil and ground water in different locations in the world, which is a new environmental challenges need an actual concern for international scientific and legislative communities **Álvarez , et al. 2015**. Generally, these compounds, e.g., pharmaceuticals, personal care products surfactants, pesticides, and brominated flame retardants are not totally removed by conventional wastewater treatment plants (WWTP), due to its existing everywhere and stability against biodegradation. The effect of these pollutants in the environment does not only depend on its concentration level in the environment, but also on other factors, such as bioaccumulation , lipophilicity increases or persistence, exposition time and mechanisms of biotransformation and elimination , **Esplugas ,et al. 2007**. From the other hand a wide range of these compounds are suspected to have endocrine-disrupting effects, possibly at long-term, in living organisms, including humans , **Nikolaou ,et al. 2007**.

Pharmaceuticals and their metabolisms are the most important emerging contaminants detected in environmental systems. Approximately 3,000 different compounds, with wide range of different chemical structures, are used in human and veterinary medicine ,**Halling-Sørensen ,et al. 1998**. Several researches focused on detection of pharmaceuticals at different therapeutic classes, analgesics, lipid-lowering agents, antipyretics, broncholitics, antidepressants, synthetic steroidal hormones, human and veterinary antibiotics, etc. in surface water, soil and ground water, with this purpose accurate and sensitive analytical method have to be developed capable to monitor these compounds in ng/L level ,**Farré ,et al. 2001; Hernando, et al. 2007; Hao , et al. 2008; Silva, et al. 2008 ; Gracia-lor, et al. 2010; Du , et al. 2014 ; K'oreje ,et al. 2016** .

Among the pharmaceuticals reported in environment ,Analgesic and non-steroid anti-inflammatory drugs (NSAID) have been detected in the concentration ranges from ng/L to $\mu\text{g/L}$ in surface and wastewater due to very high use of these pharmaceuticals also without prescription **Tauxe-Wuersch, et al. 2005; Fatta, et al. 2007; Durán-Alvarez, et al. 2009; Ziylan & Ince 2011; Carmona, et al. 2014; Lolić ,et al. 2015; Jung, et al. 2015**. Mefenamic acid [2-(2,3-dimethyl phenyl)amino] benzoic acid **Table 1** is a non-steroidal drug which has analgesic, anti-inflammatory and antipyretic actions and it is used specially in the treatment of rheumatoid arthritis and osteoarthritis and other muscular-skeletal diseases, **Reynolds, J.E.F., Prasad 1982**.

The present water and wastewater treatment plants have been designed for the treatment and removal of contaminants and eutrophication pollution loads, which are specified in the existing regulations. However, the occurrence of the new unregulated contaminants requires advanced treatment ,**Bolong ,et al. 2009**. The removal technologies can be classified as three main classes' physiochemical treatments such as adsorption, biodegradation such as membrane bioreactor (MBR), and advance technologies such as advance oxidation by ozone. A Comparison for removal capacities between membrane bioreactor and conventional activated-sludge process showed a maximum removal of 74.8 % and 29.4% respectively ,**Radjenovic ,et al. 2007**.

Elimination of mefenamic acid MA by photolysis, ozonation, adsorption onto activated carbon (AC) was investigated **Gimeno ,et al. 2010** .The results showed that the addition of activated carbon don't enhanced removal process and get a removal efficiency of 60% in 120 min by combination of ozone and UV radiation .**Rodrigo, et al., 2014**, used adsorption of mefenamic acid with activated carbon and red mud then oxidation with chlorine ,they go to removal of 100% for activated carbon and 96 % for red mud . Different oxidative processes (H_2O_2 , H_2O_2/UV , Fenton and Photo-Fenton) were investigated for mefenamic acid removal from water **Colombo, et al. 2016**.The results, shows that the photo-Fenton process is the best to get maximum removal efficiency of 95.5 at pH 6.1 and 60 min oxidation time .

Bentonite was used as adsorbent for different pollutants in aqueous media ,**Hefne ,et al. 2008; Hefne ,et al. 2010 ; Al-Khatib, et al. 2012; Chmielewska ,et al. 2013 ; Aljlil & Alsewilem 2014 ; Moradi ,et al. 2015**.From other side composite bentonite with other polymer or organic material were studied ,**Ulusoy & Şimşek 2005 ; Anirudhan, et al. 2008;Anirudhan ,et al. 2010;Anirudhan & Suchithra 2010;Zhao, et al. 2010;Dalida ,et al. 2011;Anirudhan & Rijith 2012**.

Polymeric adhesive poly urea formaldehyde (PUF) gel is a condensation product of the chemical reaction of formaldehyde with urea, considered as one of the most important wood adhesives. Urea formaldehyde gel have been greatly used in wood based industries due to it low cost, low cure temperature, lack of color and ease of use under a wide variety of curing conditions , **Gürses, et al. 2014**.The composite mixture of poly urea formaldehyde and bentonite(PUF-Bentonite) will be studied as anew adsorbent .

There are very limited studies on the adsorption and removal of mefenamic acid from water and waste water. This study focused on the adsorption of mefenamic acid using new composite adsorbent poly urea formaldehyde and bentonite clay in a step to enhancement the surface with low cost adsorbent and minimize the waste treatment cost .The optimum bentonite dose in composite adsorbent , effect of contact time, temperature ,initial concentration , solution pH , adsorbent dose and sharing surface with other analgesic were investigated. Equilibrium and kinetic parameters were also determined to help provide a better understanding of the adsorption process and application it in a large and industrial scale.

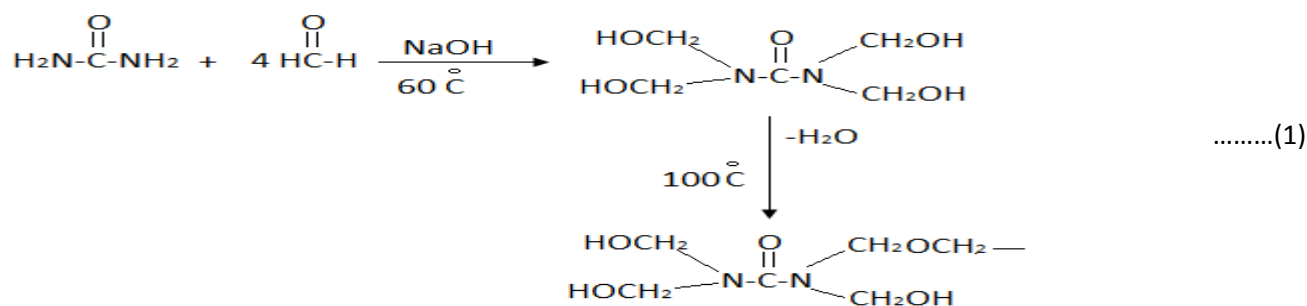
2. EXPERIMENTAL

2.1 Materials

The materials and chemicals used in this study, listed in **Table 2**, the solvents and reagent grade and used without further purifications.

2.2 Preparation of Poly Urea Formaldehyde Gel

Five grams of urea dissolve in 50 ml formaldehyde using 250 round flask with reflux, after completely dissolved adding a drops of 1M sodium hydroxide solution to adjust pH to 9 .The round put on a hot plate mixing stirrer, the temperature set to 60 °C. Left the condensation reaction for 3 hours and with pH control to 9.A viscous fluid formed after three hour of condensation reaction then left in oven at temperature 40 °C for 48 hour to remove excess water. Finally the urea formaldehyde gel store in glass container at room temperature for further use.The proposed equation for preparation polyureaformaldehyde clarified in **Eq.1**



2.3 Preparation Urea Formaldehyde Bentonite Composite

Bentonite washed in deionized distill water for three times and then dried in an oven at 100 °C for two hours .Different masses ratios of bentonite to poly urea formaldehyde 0,1 ,2,3,4, and 5 took to prepare composite of PUF –Bentonite .The composite mixed vigorously at temperature 60°C for 15 minutes , then put composite in an oven at 110 °C for 24 hour to solidification .The composite washed many times with deionized water finally dried in an oven to remove water . The sample was crushed and screened through a 200-mesh for further use.

2.4 Adsorbate

Mefenamic acid is poorly soluble in water and several solvents. In this study many solvent checked to test total solubility of MA such as methanol and ethanol.50 mg of MA dissolved in 250 ml of water solution 0.01 M NaOH at temperature 37° C for 12 hour to prepare 200 µg/ml MA solution .This stock solution used in next time to prepare different concentrations of MA by dilution in 0.01 M NaOH solution.

2.5 Calibration and Method Validation

UV spectrophotometer type Apel pd-303 UV were used to quantification of MA concentration , 30 µg/ml concentration solution of MA were used to tested maximum wave length from 200-400 nm **Fig.1** the results showed that the maximum wave length occurs at 285nm this results fit with , **Singh ,et al. 2011**,study . From the respective stock solution (200µg/ml) different concentration of 2.5, 5, 10, 20, 30, 40 and 50 µg/ml MA were prepared and scanned in UV at 285 nm region. Calibration curve were plotted as absorbance vs concentration and their linearity range was determined **Fig.2**.

2.6 Characterization

The mineralogical composition of bentonite samples and bentonite poly urea formaldehyde composite was determined using X-ray Diffraction (XRD) technique. X-ray analyses of the samples was performed on the (PAN ALYTICAL); a copper (Cu) anode was used in the X-ray tube and operated at current 20 Ma and power level of 4 kW. The surface morphology of each samples was determined by scanning electron microscopy (SEM) photography (INSPECT-550) was normally performed at 10 Kv . FTIR spectra were recorded in the region of 4000-400 cm⁻¹ (SHIMADZU).

2.7 Adsorption Studies

The adsorption studies were conducted with 0.050 g of adsorbent and 20 mL of mefenamic acid solution at desired concentration, pH and temperature on a constant speed of 180 rpm. The solution was filter in 0.2 microns Millipore filter syringe and the concentration of MA in the supernatants was examined with a spectrophotometer at the wavelength of 285nm at which the maximum absorbency occurred. Then the amounts of MA adsorbed per unit mass of adsorbent were calculated from the differences between the initial and final MA concentrations in solution by the following equation Eq(1):

$$q = \frac{(C - C_e) \times V}{M} \quad \dots \dots (2)$$

Where q is the adsorption capacity of mefenamic acid mg/g at any time t C and C_e is initial and equilibrium concentration respectively, V (L), the volume of MA solution used in adsorption experiment, M(g), the mass of the adsorbent used in the present study.

For the investigation of effect of composite mass ratio Bentonite/poly urea formaldehyde content on adsorption capacity, 50 mg of the adsorbent with 20 ml of 40 μ g/ml MA solution was put into the flask with fitted cub and stirred at 180 r.p.m for 240 min in water bath shaker (Polyscience) type .Temperature adjusted to 27 °C using chiller type DHC , pH set to 7 by using 0.01 M HCL or 0.01 M NaOH solution using pH meter type (HANNA pH 211) . To investigate the effect of contact time on adsorption, time changed between 15 to 120 minutes. Temperature effect studied with changing temperature from 15 to 64 °C at contact time 60 min. To investigate the effect of pH on adsorption, MA solution with an initial concentration of 40 μ g/ml with pH in the range of 1.5–12.5 for contact time 60 min and temperature 47° C. A series of MA solutions with different concentrations (20–200 μ g/ml) at pH = 2 and temperature of 47°C were prepared to investigate the adsorption isotherms. To investigate the effect adsorbent dose on adsorption, the concentration of MA 200 μ g/ml used with the same previous conditions by changing the dose from 50 – 300 mg in 20 ml MA solution. The effect of sharing surface with other analgesic, used a complex wastewater containing other NSAIDs acetaminophen 40 μ g/ml , diclofenac sodium 40 μ g/ml, acetylsalicylic acid 40 μ g/ml, ibuprofen 40 μ g/ml and indomethacin 200 μ g/ml this complex prepared at different pH values from 2-12, with contact time 60 min, temperature 47°C and 50 mg adsorbent in 20 ml MA solution will be used .All experiment repeated double time and the average of absorbance took as a final reading.

3. RESULTS AND DISCUSSION

3.1 Characterization

Bentonite is considered one of the most abundant natural materials available in nature that can be used for adsorption pollutant from wastewater and other application **Al Khatib,et al. 2012**. The chemical composition of natural bentonite is different depending on the source of collection. The commercial bentonite XRD shown in **Fig.3** . Bentonite poly urea formaldehyde composite predominantly had a dark brown appearance. A typical XRD pattern of bentonite poly urea formaldehyde composite after mixing shown in **Fig.4** .FTIR spectra for bentonite , poly urea formaldehyde and bentonite polymer composite shown in **Fig.5 ,6,7** its seems shifting and missing groups as illustrated in **Table.3**.SEM image for raw material and composite shown in **Fig.8 a&b** it can be seen gathering of many microfine particles in

bentonite -PUF composite compare with bentonite surface which lead to rough surface with presence of pore structures.

3.2 Effect of Composite Mass Ratio

The adsorption of MA by composite adsorbents with different mass ratios of bentonite and PUF shown in **Fig.9**. It could be observed that the adsorption capacity is 2.4, 5.7, 6, 9.6, 6.6 and 5.9 mg/g for composite with bentonite to PUF (bentonite only ,1:1,2:1,3:1,4:1 and 5:1) respectively. It observed that the adsorption capacity increase by increasing bentonite content until reaching the best ratio of 3:1(3g bentonite/1g PUF) then the increasing of bentonite reduce the adsorption capacity. This may attributed to increase organic /inorganic interaction between PUF and bentonite which responsible to convert the surface from hydrophilic to organophilic by urea groups. Increasing PUF in composite compare with bentonite weight caused also decrease in adsorption capacity because surface became more amorphous and reduce crystalline structure .This confirmed by previous investigator focused on mixing organic group with clay **Moazed & Viraraghavan 2005 & Oleiwi 2014** . The best composite ratio bentonite to PUF will be used for further experiments is 3:1 for bentonite to PUF ratio.

3.3 Effect of Contact Time

Contact time is important parameter because it can determine the time required to achieve equilibrium of the adsorption system and predict the feasibility of an adsorbent for its use in wastewater treatment. Except for high adsorption capacity, fast adsorption rate is also indispensable for practical application. The effect of contact time on adsorption of MA onto PUF -Bentonite composite was studied over a contact time of 0–120 min.**Fig.10** shows that the amount of MA adsorbed per unit mass of adsorbent increased rapidly within 45 min . Further increase in contact time did not enhance the adsorption. Equilibrium was achieved around 45 min and increased slightly to 60 min .A contact time of 60 min was chosen as equilibrium time in further experiments . The initial rapid increased may be due to greater number of adsorbent active sites available for MA adsorption which caused higher driving force that made fast transfer. With increase in contact time, the availability of MA to the active sites on the PUF-Bentonite surface would be limited, which fixed the adsorption capacity. The contact equilibrium time achieved in this study is shorter than the contact time using different adsorbent in many researches focused on selected NSAIDs **Gimeno et al. 2010 ;Khatem et al. 2015&Jodeh et al. 2016** .

3.4 Effect of Temperature

Fig. 11 illustrates the variation of MA adsorption capacity with temperature in the range from 15 to 67 °C. From the figure it is seen that temperature had a limited influence on adsorption capacity. The adsorption capacity of MA increased with increase in temperature in the range from 15- 49° C , then was observed at 50 °C it gradually decreases with again increase in temperature. The enhancement in adsorption with rise in temperature may be attributed to increases the rate of diffusion of the adsorbate molecules across the boundary layer and within the internal pores of the adsorbent particle, due to decrease in the viscosity of the solution from the other hand increasing temperature increase in the number of active surface sites available for adsorption, pore volume and the porosity of the adsorbent. The decrease in adsorption capacity with further increase in temperature is due to reduce the

boundary layer thickness and increase the kinetic energy of MA molecules, this gave a tendency to escape from active site to fluid bulk. From the other hand MA is hydrophobic and water structuring existing around hydrophobic part of MA molecules, at high temperature water structuring decreasing and make the molecule more free to diffusion and increased diffusion rate **Steinby et al. 1993 & Nam et al. 2014**. Previous literatures working with temperature range from 30 to 40 °C for same group of NSAIDs have similar behavior **Cabrita et al. 2010 ;Álvarez, R.S. Ribeiro, et al. 2015 & Mohd et al. 2015**.

3.5 Effect of pH

Generally pH is considered to be an important parameter that controls the adsorption at water-adsorbent interfaces. Results of the influence of pH on adsorption are illustrated in **Fig.12**, pH seems had significant influence on adsorption capacity of MA. Experiments were conducted varying the solution pH from 1.5 -13 while rest of the factors were kept constant. The maximum capacity was observed at pH range 1.5-3.5. Result indicated a pH less than the pK_a of MA ($pK_a = 4.20$), is efficient for MA removal. The solubility of MA with carboxylic acid groups decrease when pH decrease then 'van der Waal' interaction between MA and the adsorbent surface increased. At pH more than 6 MA are quantitatively dissociated, increasing their water solubility and decreasing their interaction by hydrogen bonds **Bui & Choi 2009 ; Guedidi et al. 2014 & Jodeh et al. 2016**.

3.6 Effect of Initial Concentration

The initial concentration provides an important driving force to overcome all mass transfer resistances of all molecules between the aqueous and solid phases **Malkoc & Nuhoglu 2007**. From the other hand pharmaceutical pollutant are variable concentrations in water then the understanding the variation in concentration is important to control the adsorption process. MA acid concentration changed from 20 to 200 µg/ml with adjusted pH value to 2. It seems from **Fig.13** that the adsorption capacity increase with increasing initial MA concentration. This is a result of the increasing driving force resulting from increment in concentration gradient to reduce the mass transfer resistance between solid and liquid phases and raised the number of available molecules per adsorption site. It's important to show in this situation that the percent removal of MA from aqueous phase decrease with increasing initial concentration due to saturated the adsorbent active sites **Khalaf et al. 2013**.

3.7 Effect of Adsorbent Dose

The effect of adsorbent dose on the adsorption capacity of MA is shown in **Fig.14** the adsorbent mass changed from 50 to 350 mg with 40µg/ml initial concentration. It was observed that as the mass of PUF- Bentonite composite increased the adsorption capacity decrease and increasing percent removal. This is mainly due to an increase in the adsorption surface area and the availability of more active sites on the surface. The reverse trend of adsorption capacity would be attribute to the gathered and unsaturated adsorption sites **Nam et al. 2014 & Mupa M et al. 2015**.

3.8 Effect of Surface Sharing

In previous parameter checked the effect of different parameters regarding MA adsorption on PUF-Bentonite surface, if water contain only MA as pollutant. In this part investigate the effect of present of other pollutants in water to adsorption of MA at different pH values. Adsorption experiment were carried out for water containing MA (40µg/ml) and other analgesic acetaminophen 40µg/ml, diclofenac sodium 40µg/ml, acetylsalicylic acid

40µg/ml, ibuprofen 40µg/ml and indomethacin 200 µg/ml at different pH value of 2,5,7 and 12. The results illustrated in **Fig.15**, and it seems that the adsorption capacity decrease with existing of other pollutant in water, this due to sharing the free sites in the adsorbent surface with other pollutant and solute-surface interactions and competition of pollutant with each other to attack surface and overcoming mass transfer resistance **Bui & Choi 2009**.

3.9 Adsorption Isotherm and Kinetic Study

Adsorption isotherm is important to sketch how adsorbate interact with adsorbent, and it is critical in optimizing an adsorption process to suggest how the adsorbed molecules distribute between the liquid phase and solid phase until the adsorption process achieve an equilibrium at a constant temperature **Buckley1992**. Adsorption isotherms are basic requirements for the design of adsorption systems. In order to understanding the adsorption isotherm of MA on bentonite PUF adsorbent the experimental data were applied to the Langmuir, Freundlich, Tempkin and Dubinin–Radushkevich equations. The constant parameters of the isotherm equations for adsorption process were calculated by regression using linear form of the isotherm equations (R^2). The constant parameters and correlation illustrated in **Table. 4**.

3.10 Error analysis

The use R^2 is limited to describe the fitting to linear behavior, and doesn't describe the nonlinear behavior. In this study used chi-square test (χ^2) obtained by judging the sum squares differences between the experimental and the calculated data, with each squared difference is divided by its corresponding value (calculated from the models). Small χ^2 value indicates its similarities while a larger number represents the variation of the experimental data **Boulinguez, et al. 2008**. The value of (χ^2) for different isotherms listed in **Table .5**. It's clear from **Fig.16** and **Table 5** that the Freundlich isotherm was the fit to the experimental behavior, describing the non-ideal and reversible adsorption, not restricted to the formation of monolayer. This empirical model can be applied to multilayer adsorption, with non-uniform distribution of adsorption heat and affinities over the heterogeneous surface. A favorable adsorption is when Freundlich constant (n) is between 1 and 10. When n is higher than that range it implies stronger interaction between the adsorbent and the adsorbate. From **Table. 5**, it can be seen that the (n) value was between 1 and 10 showing favorable adsorption of MA. The constant k_{ad} in Dubinin –Radushkevich model gives an idea about the mean adsorption energy, E, which is defined as the free energy transfer of 1 mole of solute from infinity of the surface of the adsorbent and can be calculated using the relationship :

$$E = \frac{1}{\sqrt{2k_{ad}}} \dots\dots\dots(3)$$

The parameter gives information about the type of adsorption mechanism as chemical ion-exchange or physical adsorption. If the magnitude of E is between 8 and 16 kJ /mole, the sorption process is supposed to proceed via chemisorption, while for values of $E < 8$ kJ /mole, the sorption process is of physical nature. The magnitude of E in this study is 5 kJ/mole indicates the adsorption of MA in PUF-Bentonite adsorbent is physical adsorption via physical binding forces **Kundu & Gupta 2006 ;Das et al. 2013**.

Adsorption kinetic models were applied to the experimental data, in order to analyze the rate of adsorption and possible adsorption mechanism of MA on PUF-Bentonite composite. Adsorption process is normally controlled by three diffusion steps for adsorbate transport first from the bulk of water to the solid liquid film, the next step from the film to the surface of

adsorbent then from the surface to vacant site in the adsorbent then binding of MA molecules with active site. The kinetic models applied in this study are the Lagergren first order, pseudo-second order and Elovich's equation listed in **Table. 5**. The results of kinetics plots showed in **Fig.17, 18 and 19** for three models and results listed in **Table. 5**, it seems the pseudo second order model is nearly to describe adsorption of MA on PUF-Bentonite adsorbent.

4. CONCLUSION

PUF-Bentonite composite prepared from mixing commercial bentonite with poly urea prepared in basic media in mixing ration of bentonite to polymer of 3 is efficient for removal of MA acid from water .pH is the significant parameter affecting the adsorption capacity gives maximum capacity at pH 2 .Also the adsorbent concentration is a significant effect on adsorption capacity. Other parameters temperature, adsorbent dose and contact time studied at different values .Maximum adsorption capacity of 16 mg/g achieved at 47 °C and pH 1.5 .Adsorption isotherms model applied and kinetics model and adsorption of MA fit to Freundlich model and pseudo second order model .

5. REFERENCES

- Aljlil, S. a. & Alsewailem, F.D., 2014. Adsorption of Cu & Ni on Bentonite Clay from Waste Water. Athens Journal of Natural & Formal Sciences, 1(March), pp.21–30.
- Al-Khatib, L. et al., 2012. Adsorption from aqueous solution onto natural and acid activated bentonite. American Journal of Environmental Sciences, 8(5), pp.510–522.
- Álvarez, S., Ribeiro, R.S., et al., 2015. Synthesis of carbon xerogels and their application in adsorption studies of caffeine and diclofenac as emerging contaminants. Chemical Engineering Research and Design, 95, pp.229–238.
- Anirudhan, T.S. & Rijith, S., 2012. Synthesis and characterization of carboxyl terminated poly(methacrylic acid) grafted chitosan/bentonite composite and its application for the recovery of uranium(VI) from aqueous media. Journal of Environmental Radioactivity, 106, pp.8–19.
- Anirudhan, T.S., Rijith, S. & Tharun, A.R., 2010. Adsorptive removal of thorium(IV) from aqueous solutions using poly(methacrylic acid)-grafted chitosan/bentonite composite matrix: Process design and equilibrium studies. Colloids and Surfaces A: Physicochemical and Engineering Aspects, 368(1), pp.13–22.
- Anirudhan, T.S. & Suchithra, P.S., 2010. Humic acid-immobilized polymer/bentonite composite as an adsorbent for the removal of copper(II) ions from aqueous solutions and electroplating industry wastewater. Journal of Industrial and Engineering Chemistry, 16(1), pp.130–139.
- Anirudhan, T.S., Suchithra, P.S. & Rijith, S., 2008. Amine–modified polyacrylamide–bentonite composite for the adsorption of humic acid in aqueous solutions. Colloids and Surfaces A: Physicochemical and Engineering Aspects, 326(3), pp.147–156.
- Bolong, N. et al., 2009. A review of the effects of emerging contaminants in wastewater and options for their removal. Desalination, 239(1-3), pp.229–246.
- Boulinguez, B., Le Cloirec, P. & Wolbert, D., 2008. Revisiting the Determination of Langmuir Parameters and Application to Tetrahydrothiophene Adsorption onto Activated Carbon. Langmuir, 24(13), pp.6420–6424.
- Buckley, C., 1992. Membrane technology for the treatment of dyehouse effluents. , 25(10), pp.203–209.

- Bui, T.X. & Choi, H., 2009. Adsorptive removal of selected pharmaceuticals by mesoporous silica SBA-15. *Journal of Hazardous Materials*, 168(2-3), pp.602–608.
- Cabrita, I. et al., 2010. Removal of an analgesic using activated carbons prepared from urban and industrial residues. *Chemical Engineering Journal*, 163(3), pp.249–255.
- Carmona, E., Andreu, V. & Picó, Y., 2014. Occurrence of acidic pharmaceuticals and personal care products in Turia River Basin: From waste to drinking water. *Science of The Total Environment*, 484, pp.53–63.
- Chmielewska, E., Hodossyová, R. & Bujdoš, M., 2013. Kinetic and Thermodynamic Studies for Phosphate Removal Using Natural Adsorption Materials. *Pol. J. Environ. Stud.*, 22(5), pp.1307–1316.
- Colombo, R. et al., 2016. Removal of Mefenamic acid from aqueous solutions by oxidative process: Optimization through experimental design and HPLC/UV analysis. *Journal of environmental management*, 167, pp.206–13.
- Dada, A. et al., 2012. Langmuir, Freundlich, Temkin and Dubinin – Radushkevich Isotherms Studies of Equilibrium Sorption of Zn²⁺ onto Phosphoric Acid Modified Rice Husk. *IOSR Journal of Applied Chemistry*, 3(1), pp.38–45.
- Dalida, M.L.P. et al., 2011. Adsorptive removal of Cu(II) from aqueous solutions using non-crosslinked and crosslinked chitosan-coated bentonite beads. *Desalination*, 275(1), pp.154–159.
- Das, B. et al., 2013. Removal of copper from aqueous solution using alluvial soil of indian origin: Equilibrium, kinetic and thermodynamic study. *Journal of Materials and Environmental Science*, 4(4), pp.392–409.
- Du, B. et al., 2014. Comparison of contaminants of emerging concern removal, discharge, and water quality hazards among centralized and on-site wastewater treatment system effluents receiving common wastewater influent. *Science of The Total Environment*, 466, pp.976–984.
- Durán-Alvarez, J.C. et al., 2009. The analysis of a group of acidic pharmaceuticals, carbamazepine, and potential endocrine disrupting compounds in wastewater irrigated soils by gas chromatography–mass spectrometry. *Talanta*, 78(3), pp.1159–1166.
- Esplugas, S. et al., 2007. Ozonation and advanced oxidation technologies to remove endocrine disrupting chemicals (EDCs) and pharmaceuticals and personal care products (PPCPs) in water effluents. *Journal of Hazardous Materials*, 149(3), pp.631–642.
- Farré, M. et al., 2001. Determination of drugs in surface water and wastewater samples by liquid chromatography-mass spectrometry: Methods and preliminary results including toxicity studies with *Vibrio fischeri*. In *Journal of Chromatography A*. pp. 187–197.
- Fatta, D. et al., 2007. Analytical methods for tracing pharmaceutical residues in water and wastewater. *TrAC Trends in Analytical Chemistry*, 26(6), pp.515–533.
- Fierro, V. et al., 2008. Adsorption of phenol onto activated carbons having different textural and surface properties. *Microporous and Mesoporous Materials*, 111(1), pp.276–284.
- Foo, K.Y. & Hameed, B.H., 2010. Insights into the modeling of adsorption isotherm systems. *Chemical Engineering Journal*, 156(1), pp.2–10.
- Gimeno, O. et al., 2010. Application of Advanced Oxidation Processes to Mefenamic Acid Elimination. , 4(6), pp.1104–1106.
- Gracia-lor, E., Sancho, J. V & Hernández, F., 2010. Simultaneous determination of

acidic , neutral and basic pharmaceuticals in urban wastewater by ultra high-pressure liquid chromatography-tandem mass spectrometry. , 1217, pp.622–632.

- Guedidi, H. et al., 2014. Adsorption of ibuprofen from aqueous solution on chemically surface-modified activated carbon cloths. *Arabian Journal of Chemistry*, pp.1–11.
- Gürses, A. et al., 2014. Preparation and Characterization of Urea/Formaldehyde/Rosa Canina sp. Seeds Composites. *Acta Physica Polonica A*, 125(2), pp.368–373.
- Halling-Sørensen, B. et al., 1998. Occurrence, fate and effects of pharmaceutical substances in the environment- A review. *Chemosphere*, 36(2), pp.357–393.
- Hao, C. et al., 2008. Optimization of a Multiresidual Method for the Determination of Waterborne Emerging Organic Pollutants Using Solid-Phase Extraction and Liquid Chromatography/Tandem Mass Spectrometry and Isotope Dilution Mass Spectrometry. *Environmental Science & Technology*, 42(11), pp.4068–4075.
- Hefne, J. et al., 2010. Removal of Silver (I) from Aqueous Solutions by Natural Bentonite. *Journal of King Abdulaziz University-Science*, 22(1), pp.155–176.
- Hefne, J.A. et al., 2008. Kinetic and thermodynamic study of the adsorption of Pb (II) from aqueous solution to the natural and treated bentonite. *International journal of physical sciences*, 3(11).
- Hernando, M.D. et al., 2007. LC-MS analysis of basic pharmaceuticals (beta-blockers and anti-ulcer agents) in wastewater and surface water. *TrAC Trends in Analytical Chemistry*, 26(6), pp.581–594.
- Jodeh, S. et al., 2016. Adsorption of diclofenac from aqueous solution using Cyclamen persicum tubers based activated carbon (CTAC). *Journal of the Association of Arab Universities for Basic and Applied Sciences*, 20, pp.32–38.
- Jung, C. et al., 2015. Competitive adsorption of selected non-steroidal anti-inflammatory drugs on activated biochars: Experimental and molecular modeling study. *Chemical Engineering Journal*, 264, pp.1–9.
- K'oreje, K.O. et al., 2016. Occurrence patterns of pharmaceutical residues in wastewater, surface water and groundwater of Nairobi and Kisumu city, Kenya. *Chemosphere*, 149, pp.238–244.
- Khalaf, S. et al., 2013. Efficiency of membrane technology, activated charcoal, and a micelle-clay complex for removal of the acidic pharmaceutical mefenamic acid. *Journal of Environmental Science and Health - Part A Toxic/Hazardous Substances and Environmental Engineering*, 48(13), pp.1655–1662.
- Khatem, R., Ojeda, R. & Bakhti, A., 2015. Use of synthetic clay for Removal of Diclofenac Anti-inflammatory. *Eurasian Journal of Soil Science*, 4(2), pp.1–11.
- Kundu, S. & Gupta, A.K., 2006. Arsenic adsorption onto iron oxide-coated cement (IOCC): Regression analysis of equilibrium data with several isotherm models and their optimization. *Chemical Engineering Journal*, 122(1-2), pp.93–106.
- Lolić, A. et al., 2015. Assessment of non-steroidal anti-inflammatory and analgesic pharmaceuticals in seawaters of North of Portugal: occurrence and environmental risk. *The Science of the total environment*, 508, pp.240–50.
- Malkoc, E. & Nuhoglu, Y., 2007. Determination of kinetic and equilibrium parameters of the batch adsorption of Cr(VI) onto waste acorn of *Quercus ithaburensis*. *Chemical Engineering and Processing: Process Intensification*, 46(10), pp.1020–1029.
- Moazed, H. & Viraraghavan, T., 2005. Removal of Oil from Water by Bentonite Organoclay. *Practice Periodical of Hazardous, Toxic, and Radioactive Waste Management*, 9(2), pp.130–134.



- Mohd, N., Sudirman, M.F.A.E. & Draman, S.F.S., 2015. Isotherm and thermodynamic study of paracetamol removal in aqueous solution by activated carbon. *ARPN Journal of Engineering and Applied Sciences*, 10(20), pp.9516–9520.
- Moradi, M. et al., 2015. Application of modified bentonite using sulfuric acid for the removal of hexavalent chromium from aqueous solutions. *Environmental Health Engineering And Management Journal*, 2(3), pp.99–106.
- Mupa M, M.T., M, M. & F, G.U. and D., 2015. Preparation of Rice Hull Activated Carbon for the Removal of Selected Pharmaceutical Waste Compounds in Hospital Effluent. *Journal of Environmental & Analytical Toxicology*, s7.
- Nam, S.-W. et al., 2014. Adsorption characteristics of selected hydrophilic and hydrophobic micropollutants in water using activated carbon. *Journal of hazardous materials*, 270(January), pp.144–52.
- Nikolaou, A., Meric, S. & Fatta, D., 2007. Occurrence patterns of pharmaceuticals in water and wastewater environments. In *Analytical and Bioanalytical Chemistry*. pp. 1225–1234.
- Oleiwi, H.B., 2014. Treatment and Reuse of Produced Water from Al-Ahdab Iraqi Oilfields. University of Baghdad.
- Radjenovic, J., Petrovic, M. & Barceló, D., 2007. Analysis of pharmaceuticals in wastewater and removal using a membrane bioreactor. In *Analytical and Bioanalytical Chemistry*. pp. 1365–1377.
- Reynolds, J.E.F., Prasad, A.B. (eds. ., 1982. *Martindale-The Extra Pharmacopoeia*. 28th ed. London: The Pharmaceutical Press, 1982., p. 61. *Martindale-The Extra Pharmacopoeia*, p.61.
- Silva, A.R.M., Portugal, F.C.M. & Nogueira, J.M.F., 2008. Advances in stir bar sorptive extraction for the determination of acidic pharmaceuticals in environmental water matrices. Comparison between polyurethane and polydimethylsiloxane polymeric phases. *Journal of Chromatography A*, 1209(1-2), pp.10–16.
- Singh, H., Kumar, R. & Singh, P., 2011. Development of UV Spectrophotometric Method for Estimation of Mefenamic Acid in Bulk and Pharmaceutical Dosage Forms. , 3(2), pp.2–3.
- Steinby, K., Silveston, R. & Kronberg, B., 1993. The Effect of Temperature on the Adsorption of a Nonionic Surfactant on a PMMA Latex. *Journal of Colloid and Interface Science*, 155(1), pp.70–78.
- Tauxe-Wuersch, A. et al., 2005. Occurrence of several acidic drugs in sewage treatment plants in Switzerland and risk assessment. *Water research*, 39(9), pp.1761–72.
- Ulusoy, U. & Şimşek, S., 2005. Lead removal by polyacrylamide-bentonite and zeolite composites: Effect of phytic acid immobilization. *Journal of Hazardous Materials*, 127(1), pp.163–171.
- Zhao, G. et al., 2010. Sorption of copper(II) onto super-adsorbent of bentonite-polyacrylamide composites. *Journal of Hazardous Materials*, 173(1-3), pp.661–668.
- Ziylan, A. & Ince, N.H., 2011. The occurrence and fate of anti-inflammatory and analgesic pharmaceuticals in sewage and fresh water: Treatability by conventional and non-conventional processes. *Journal of Hazardous Materials*, 187(1), pp.24–36.

Table 1.Physical, chemical and pharmacological properties of MA.

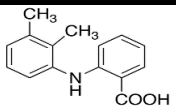
Structure	
Formula	C ₁₅ H ₁₅ NO ₂
Usage	For the treatment of rheumatoid arthritis, osteoarthritis, dysmenorrhea, and mild to moderate pain, inflammation, and fever.
Molecular weight	241.285 g/mol
Water solubility	20 mg/L (at 30 °C)
Pk _a	4.2
Elimination half-life	2 hour
Excretion	52% by urine ,20% in faeces from the dose
Metabolites in urine	hydroxymethyl mefenamic acid, 3-carboxymefenamic acid ,

Table 2. Chemical used in Experiment.

Material	Manufacture
Formaldehyde solution 37%	Merck
Urea powder (MW=60.06)	Romil
Hydrochloric acid 37%	Scharlau
sodium hydroxide pellets	Analytical Rasayan
Deionized water with conductivity less than 0.07μS/cm	Al-Najebia gas station from EDI effluent /Basra
Pure Mefenamic acid	SIGMA life science
Acetylsalicylic acid >99% crystalline	SIGMA life science
Acetaminophen 98-101 %(USP XXIV),Powder	SIGMA life science
Diclofenac Sodium	SIGMA life science
Indomethacin 99%(TLC)	SIGMA life science
Ibuprofen 98%(GC)	SIGMA life science

Table 3. FTIR spectra for Bentonite, Poly urea formaldehyde and Bentonite polyuria formaldehyde composite.

Functional groups	(cm ⁻¹)		
Resin	Bentonite	PUF	B-PUF Composite
O-H	3300-3600w	3200-3500s	3400-3500w
CH ₂ ,CH ₃ asym	-----	2960-3000w	2960-3000w
CH ₂ ,CH ₃ sym	-----	2800-2950s	2800-2950w
C=O	1650w	1650-1660s	-----
N-H bending	-----	1350-1540s	-----
O-H bending	1176-1180	1000-1150	1000-1100
Si-O	1083-1100	-----	1083-1100

Table 4. Definition of adsorption isotherm models and kinetics models used in this study.

Isotherm model	Linear form	Parameters	Reference
Langmuir	$\frac{1}{q_e} = \frac{1}{Q_0} + \frac{1}{Q_0 b C_e}$	Q ₀ : maximum monolayer coverage capacities (mg/g)	Foo & Hameed 2010
Freundlich	$\ln q_e = \ln K_f + \frac{1}{n} \ln C_e$	K _f : Freundlich isotherm constant (mg/g) (L/g) related to adsorption	Dada ,et al. 2012
Tempkin	$q_e = \frac{RT}{b_T} \ln A_T + \frac{RT}{b_T} \ln C_e$	A _T : Tempkin isotherm equilibrium binding constant	Tempkin and Pyzhev,194
Dubinin–Radushkevich	$\ln q_e = \ln q_s - K_{ad} \epsilon^2$	Q _s : theoretical isotherm saturation capacity (mg/g)	Dubinin and Radushkevi
Kinetics' models	Linear form	Parameters	Reference
pseudo-first order		q:capacity at time t mg/g q _e : capacity at equilibrium	Álvarez, et al. 2015
pseudo-second order	$\frac{t}{q} = \frac{1}{q_e^2} + \frac{t}{q_e}$	q:capacity at time t mg/g q _e : capacity at equilibrium	Álvarez, et al. 2015



Elovich's equation	$q = \frac{1}{b} \ln(ab) + \frac{1}{b} \ln(t)$	q:capacity at time t mg/g a: is the initial adsorption	Fierro ,et al. 2008
--------------------	--	---	----------------------------

Table 5. Parameters results for application of adsorption isotherm models and kinetics models used in this study.

Model	Parameters	value
Langmuir	q_0	28.01mg/g
	b	12.3 L/mg
	R^2	0.9189
	χ^2	7
Freundlich	K_f	29.17(mg/g)(L/g)
	n	2.5
	R^2	0.97
	χ^2	0.63
Tempkin	A_T	63.8 L/g
	b_T	360
	R^2	0.8929
	χ^2	3.87
Dubinin–Radushkevich	Q_s	29.9 mg/g
	K_{ad}	2.00E-08
	R^2	0.83
	χ^2	6.28
	E	5 KJ/mole
Pseudo-first order	q_e experimental	10.51 mg/g
	q_e calculated	6.42 mg/g
	K_1	0.0422min ⁻¹
	R^2	0.78
	χ^2	12.6
Pseudo-second order	q_e experimental	10.51 mg/g
	q_e calculated	12.2 mg/g
	K_2	0.0069 g/mg. min
	R^2	0.9381
	χ^2	0.67
Elovich's equation	a	0.6 mg/g.min
	$1/b$	1.3 mg/g
	R^2	0.7129
	χ^2	17.2

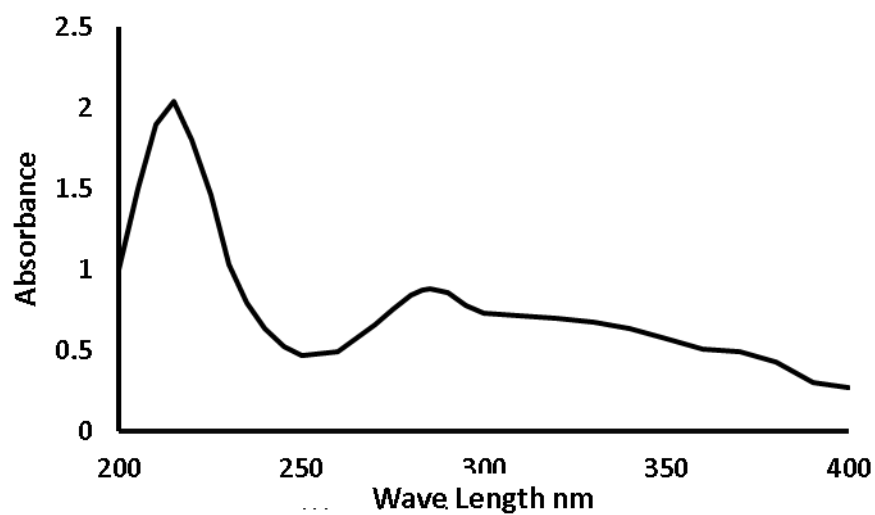


Figure 1. UV spectra of MA.

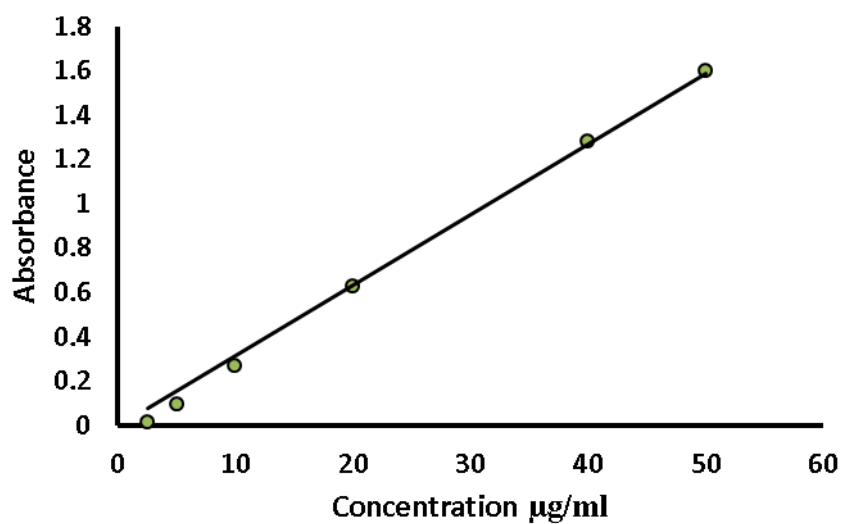


Figure 2. Standard Calibration curve of MA.

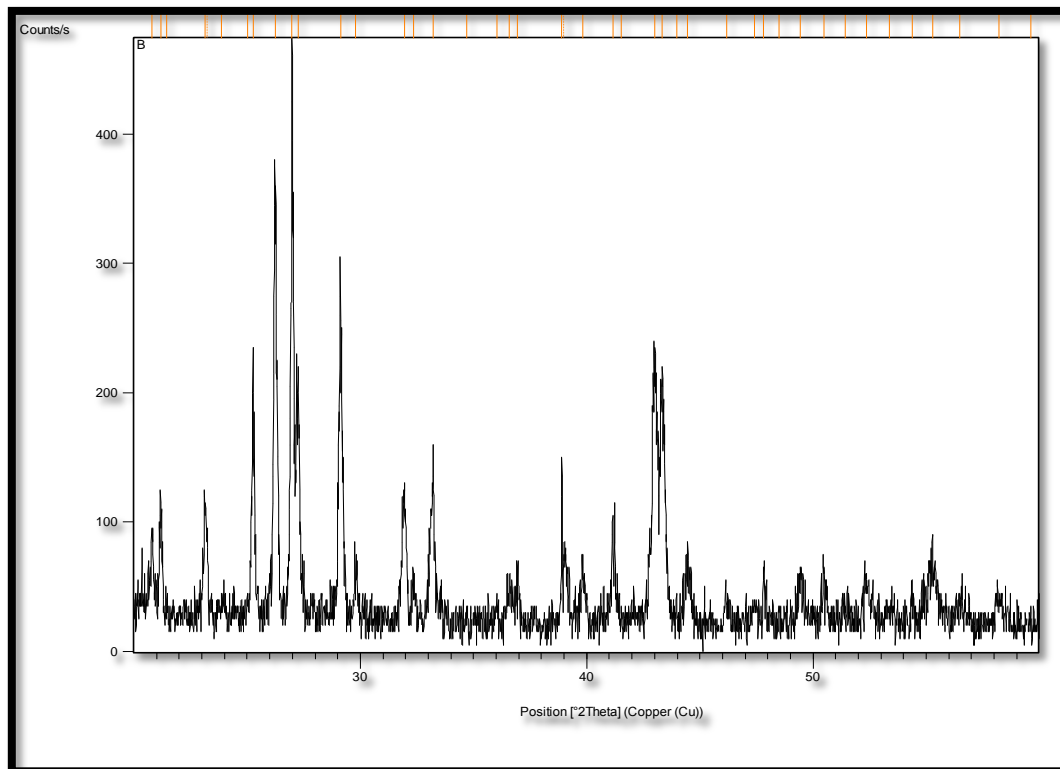


Figure 3. XRD of Bentonite.

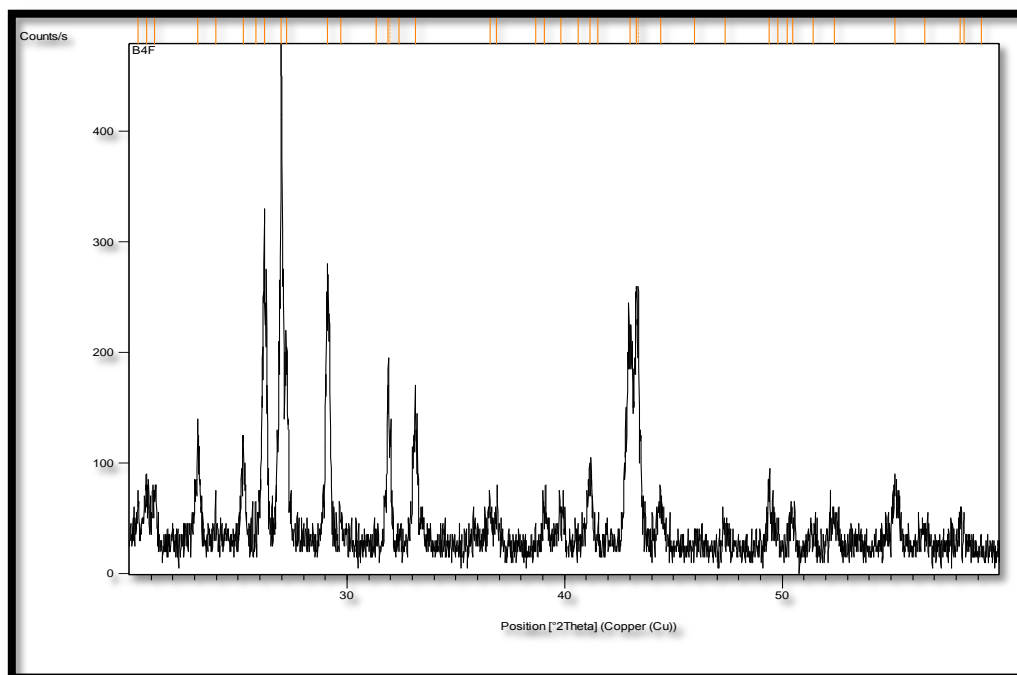


Figure 4. XRD for Bentonite poly urea formaldehyde composite.

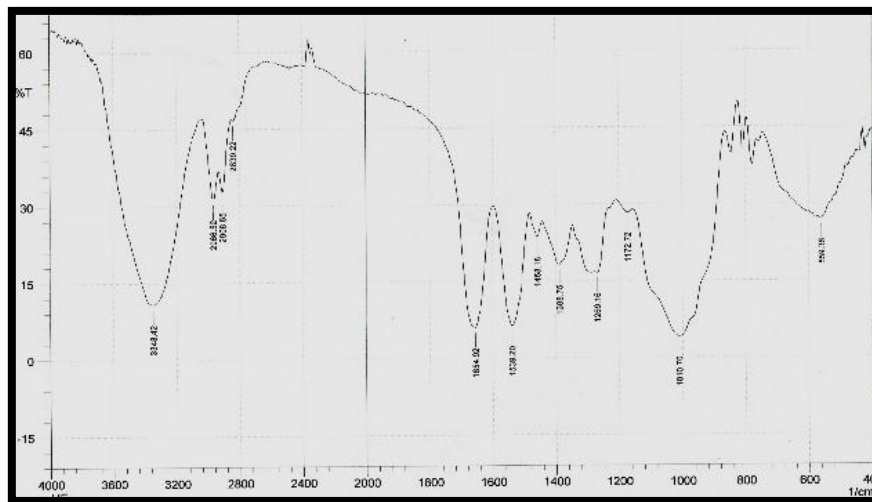


Figure 5. FTIR spectra for ureaformaldehyde resin.

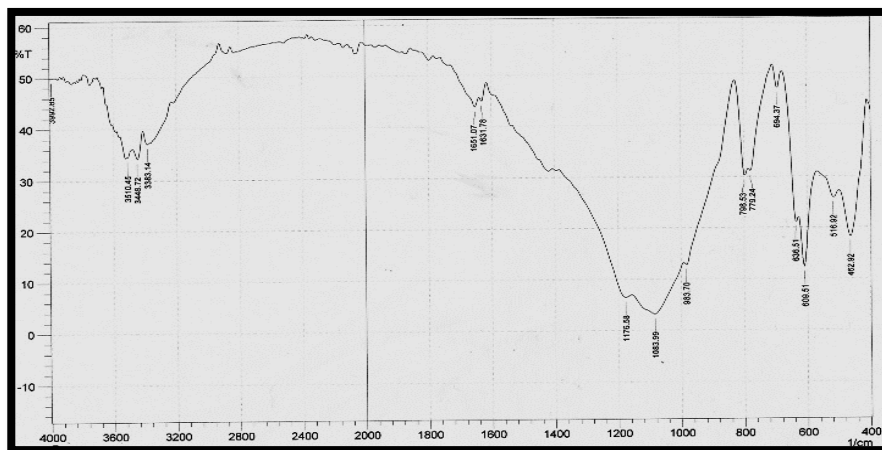


Figure 6. FTIR spectra for bentonite.

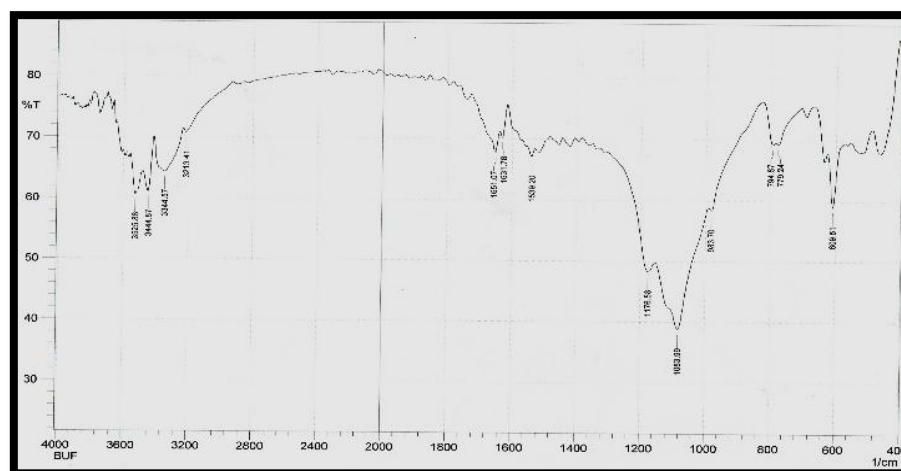


Figure 7. FTIR spectra for bentonite -PUF composite.

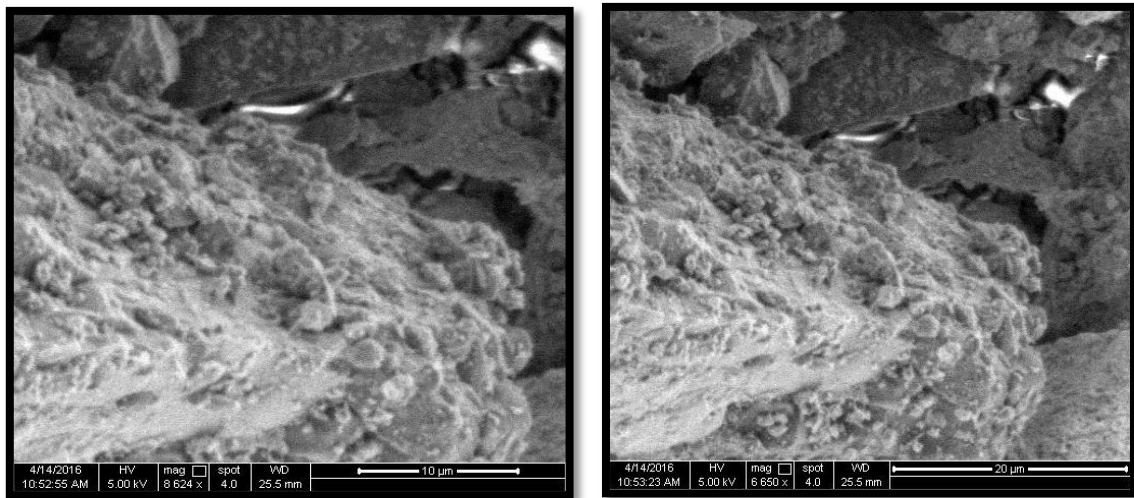
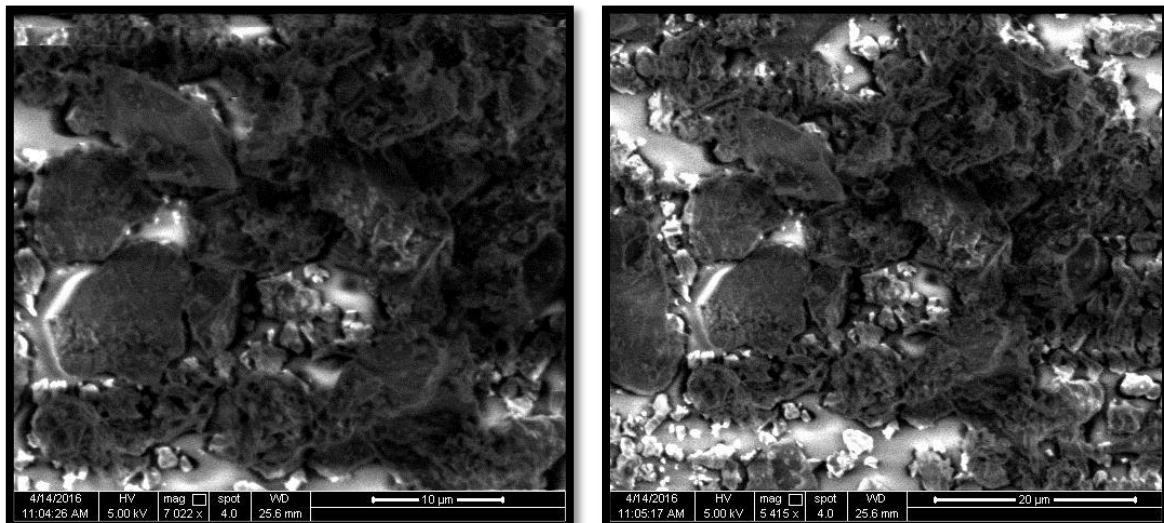
**a****b**

Figure 8. SEM image for (a) bentonite (b) bentonite-PUF composite.

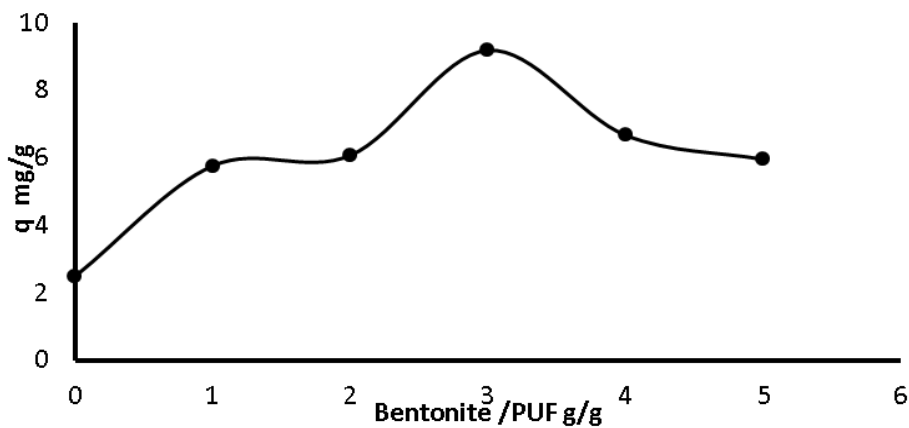


Figure 9. Effect of bentonite mass on adsorption capacity pH=7,R.P.M =180,T=27°C ,adsorbent mass =0.05 g, contact time 240 min and initial concentration 40µg/ml.

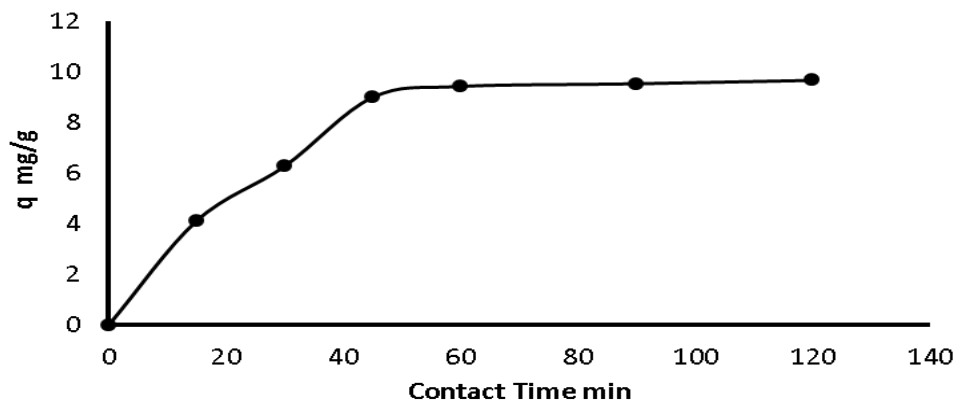


Figure 10. Effect of contact time on adsorption capacity pH=7,R.P.M =180,T=27°C ,adsorbent mass =0.05 g and initial concentration 40µg/ml.

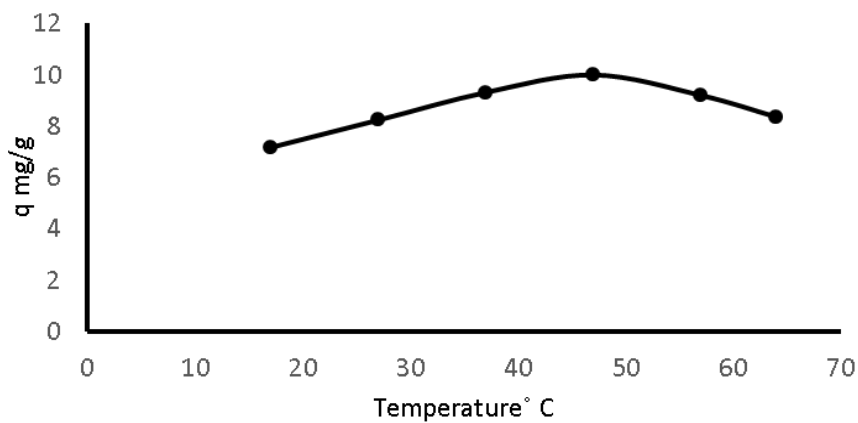


Figure 11. Effect of Temperature on adsorption capacity pH=7, R.P.M =180, contact time = 60 min, adsorbent mass =0.05 g and initial concentration 40µg/ml.

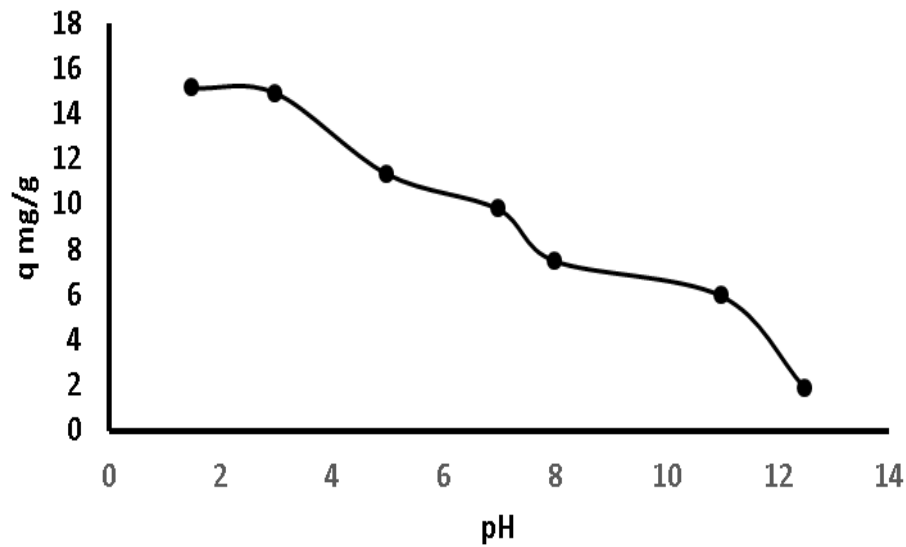


Figure 12. Effect of pH on adsorption capacity ,Temp.=47°C, R.P.M =180, contact time = 60 min, adsorbent mass =0.05 g and initial concentration 40 μ g/ml.

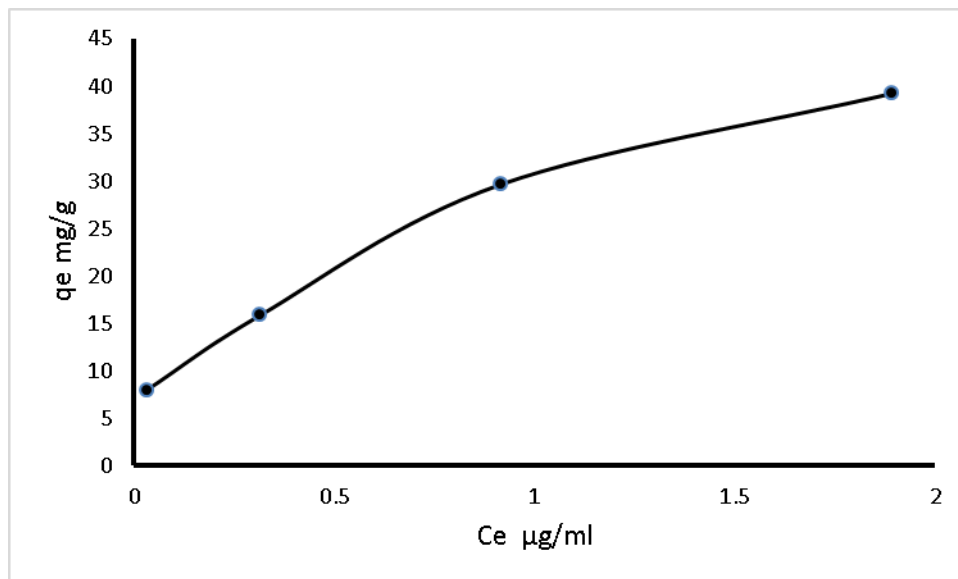


Figure 13. Effect of initial concentration on adsorption capacity, Temp.=47°C, R.P.M =180, contact time = 60 min, Adsorbent mass =0.05 g and pH = 2.

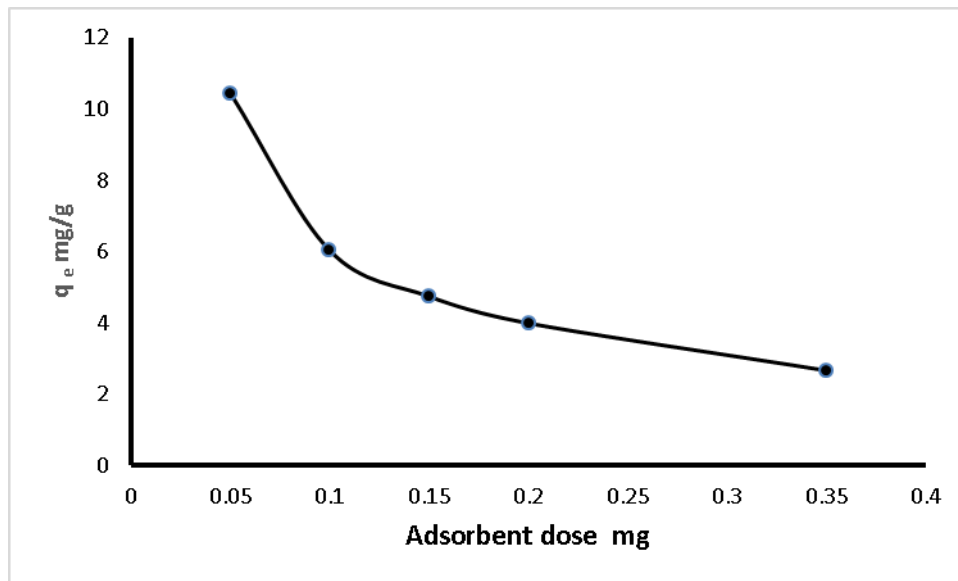


Figure 14. Effect of Adsorbent dose on adsorption capacity, Temp.=47°C, R.P.M =180, contact time = 60 min, Adsorbate initial concentration =40 μ g/ml and pH = 7.

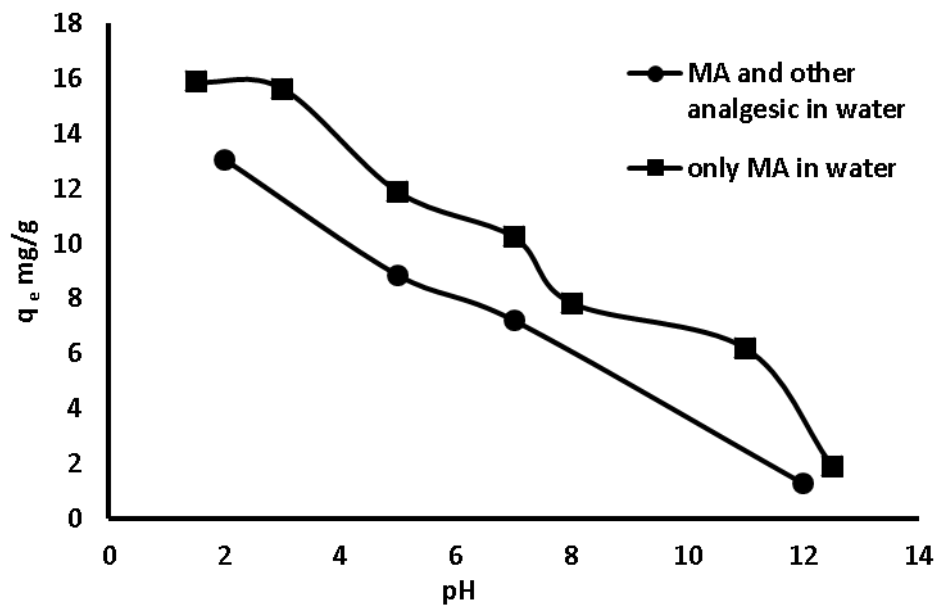


Figure 15. Effect of sharing adsorbent surface on adsorption capacity, Temp.=47°C, R.P.M =180, contact time = 60 min, Adsorbate initial MA concentrations =40 μ g/ml and adsorbent mass =0.05 g.

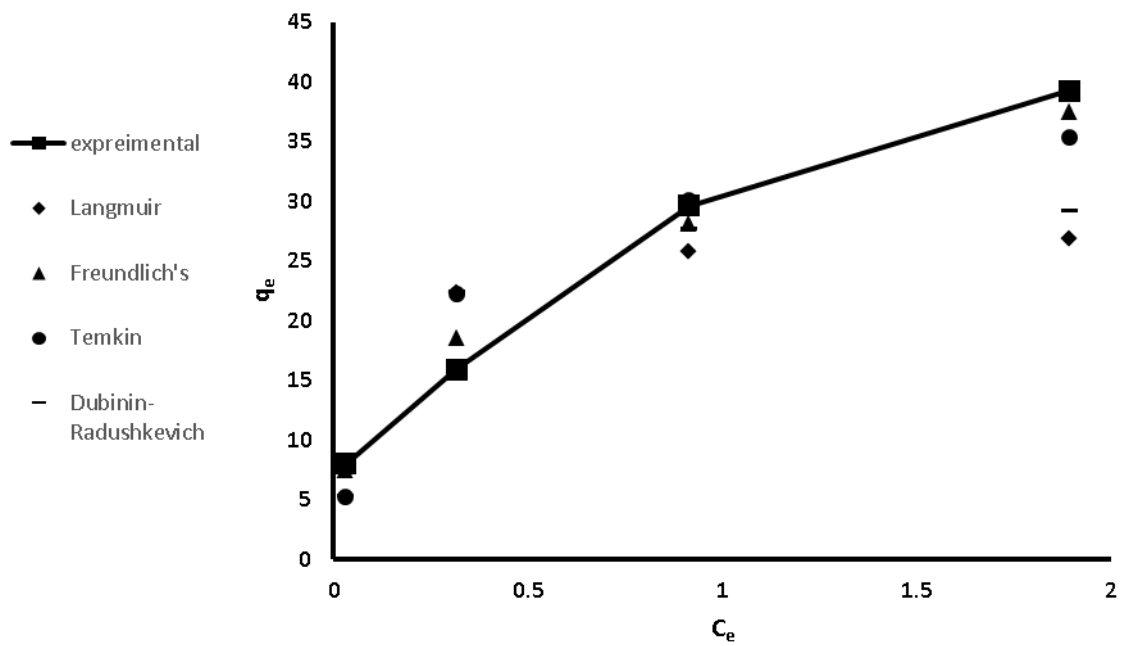


Figure 16. Experimental and isotherm models data for MA adsorption on PUF - Bentonite composite.

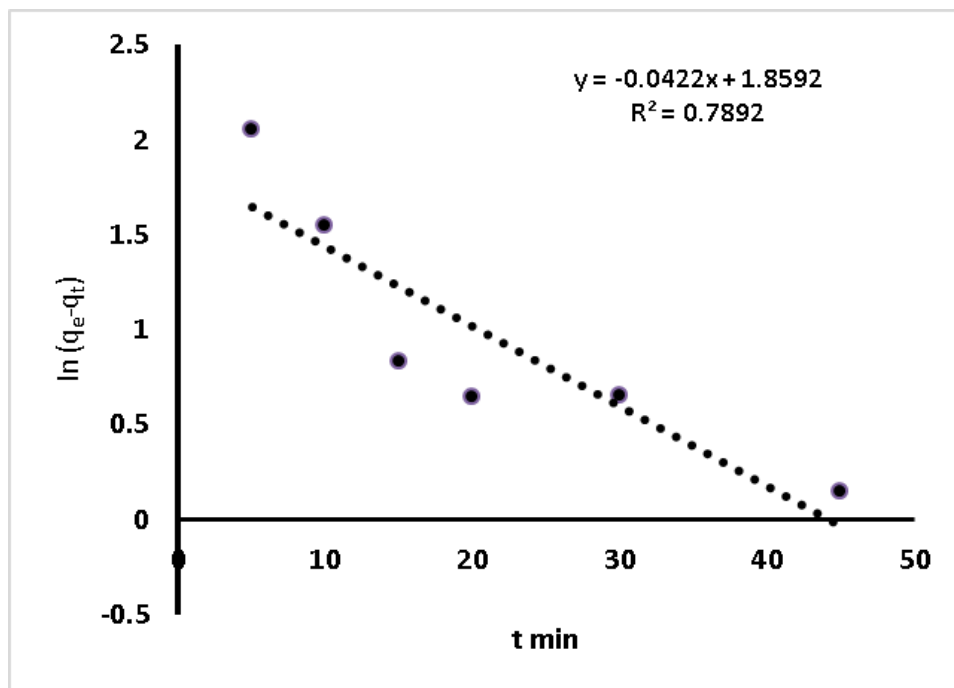


Figure. 17. linear form of first order kinetics.

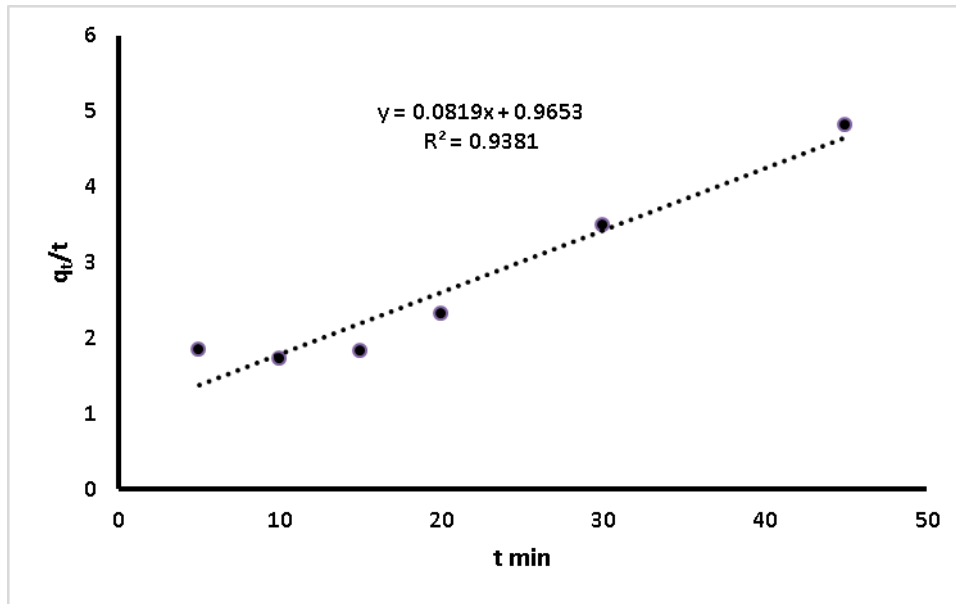


Figure. 18. linear form of second order kinetics.

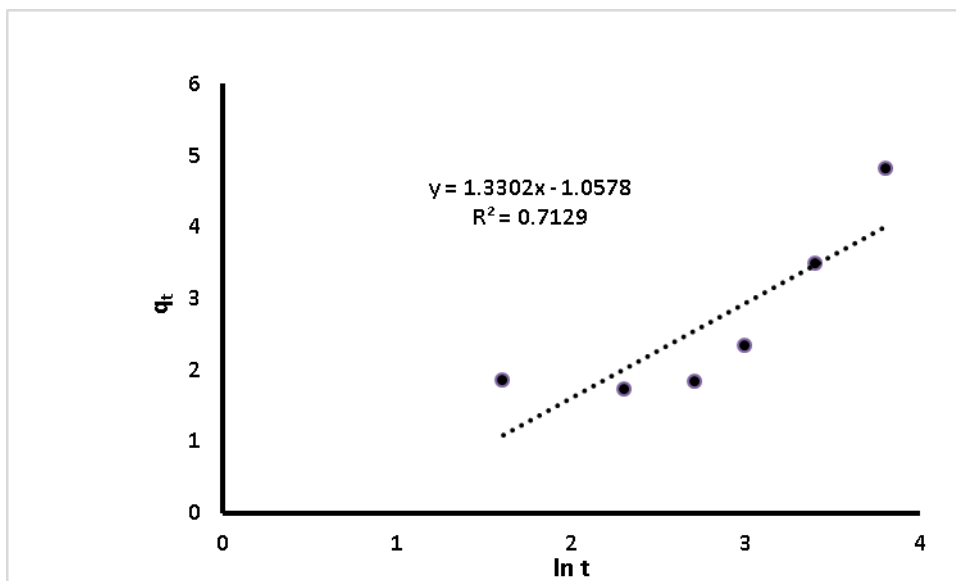


Figure. 19. linear form of Elovich's equation.

Performance Evaluation of a PID and a Fuzzy PID Controllers Designed for Controlling a Simulated Quadcopter Rotational Dynamics Model

Laith Jasim Saud

Assistant Professor
Control & Systems Eng. Dept.
University of Technology
Laithjasim15@yahoo.com

Rasha Shehab Mohammed

M.Sc. Student
Control & Systems Eng. Dept.
University of Technology
rasha_shehab@yahoo.com

ABSTRACT

This work is concerned with designing two types of controllers, a PID and a Fuzzy PID, to be used for flying and stabilizing a quadcopter. The designed controllers have been tuned, tested, and compared using two performance indices which are the Integral Square Error (ISE) and the Integral Absolute Error (IAE), and also some response characteristics like the rise time, overshoot, settling time, and the steady state error. To try and test the controllers, a quadcopter mathematical model has been developed. The model concentrated on the rotational dynamics of the quadcopter, i.e. the roll, pitch, and yaw variables. The work has been simulated with "MATLAB". To make testing the simulated model and the controllers more realistic, the testing signals have been applied by a user through a joystick interfaced to the computer. The results obtained indicated a general superiority in performance for the Fuzzy PID controller over the PID controller used in this work. This conclusion is based by the following figures: 70%, 70%, and 52% lesser ISA for the roll, pitch, and yaw consequently, 70.5%, 70.5%, 56.4% lesser IAE for the roll, pitch, and yaw consequently, 53%, and 80.6% lesser rise time and settling time for the roll and pitch consequently, and 77% lesser settling time for the yaw. Moreover, the FPID gave zero overshoot versus 18%, 18%, and 25% in the PID case for the roll, pitch, and yaw consequently. Both controllers gave zero steady state error with close rise times for the yaw. This superiority of the FPID controller is gained as the fuzzy part of it continuously and online adapts the parameters of the PID part.

Key words: unmanned aerial vehicle quadcopters, quadcopter modeling, PID controller, fuzzy PID controller, performance indices.

تقييم اداء مسيطر تناسبي تكاملي تفاضلي و مسيطر تناسبي تكاملي تفاضلي ضبابي مصممان للتحكم بنموذج
للديناميكا الدورانية لمروحية رباعية محاكى رقمية

رشا شهاب محمد

قسم هندسة السيطره والنظم
الجامعة التكنولوجية

الاستاذ المساعد الدكتور ليث جاسم سعود

قسم هندسة السيطره والنظم
الجامعة التكنولوجية

الخلاصة

يتضمن هذا البحث تصميم نوعين من المسيطرات، اولهما المسيطر التناسبي التكاملي التفاضلي، وثانيهما والمسيطر التناسبي التكاملي التفاضلي الضبابي، مستخدمان لتحقيق طيران مستقر لمروحية رباعية. لقد تم تنعيم المسيطرات المصممة واختبارها و مقارنة اداؤها باستخدام معياري اداء احدهما تكامل مطلق الخطأ وثانيهما تكامل مربع الخطأ، إضافة الى استخدام بعض خصائص الاستجابة مثل زمن الصعود و تجاوز الحد وزمن الاستقرار وقيمة الخطأ عند الاستقرار. لتجربة واختبار المسيطرات، تم بلورة

نموذج رياضي للمروحية الرباعية و الذي يركز تحديدا على الديناميكا الدورانية للمروحية. وقد تم محاكاة المنظومة رقميا باستخدام الكيان البرمجي (MATLAB). ولجعل عملية اختبار النموذج المحاكى والمسيطرات المصممة أكثر واقعية فقد تم ادخال اشارات التحكم عبر عصا تحكم تربط مع الحاسوب. لقد عكست النتائج المستحصلة من المحاكاة تفوق واضح في الاداء للمسيطر التناسبي التكاملي التفاضلي الضبابي على المسيطر التناسبي التكاملي التفاضلي. إن هذا الاستنتاج مبني على المعطيات التالية: تكامل مربع الخطأ أقل بنسبة 70%، 70%، 52% لكل من زوايا العطوف والخطران والانعراج على التوالي، وتكامل مطلق الخطأ أقل بنسبة 70.5%، 70.5%، 56.4% لكل من زوايا العطوف والخطران والانعراج على التوالي، وزمني صعود و استقرار أقل بنسبة 53% و 80.6% لكل من زوايا العطوف والخطران على التوالي، وزمن استقرار أقل بنسبة 77% لزوايا الانعراج. وإضافة لهذا فان نسبة الطفرة مع المسيطر التناسبي التكاملي التفاضلي الضبابي كانت صفرا مقابل 18%، 18%، و 25% مع المسيطر التناسبي التكاملي التفاضلي ولكل من زوايا العطوف والخطران والانعراج على التوالي. أما بالنسبة لخطأ حالة الاستقرار فكانت صفراً لكلا المسيطرين ولكل الحالات. وأما بالنسبة لزمن الصعود لزوايا الانعراج فان المسيطرين أعطيا نتائج متقاربة. إن الافضلية في الاداء التي ابداهما المسيطر التناسبي التكاملي التفاضلي الضبابي على المسيطر التناسبي التكاملي التفاضلي متأتية من قيام الجزء الضبابي فيه بالتعديل المستمر وخلال عمل المنظومة لقيم معاملات الجزء التناسبي التكاملي التفاضلي.

الكلمات الرئيسية: المروحيات الرباعية من دون طيار، نمذجة المروحية الرباعية، المسيطر (التناسبي+التكاملي+المشتقة)، المسيطر (التناسبي+التكاملي+المشتقة) الضبابي، مؤشرات الاداء.

1. INTRODUCTION

In control, modeling represents a very important issue as it can serve the process of system testing, analysis, as well as the design process. It reduces effort, cost, problems, and provides the possibility of getting fair solutions in considerably shorter times. Mathematical modeling of systems provides the possibility of numerical simulation with computers with its well-known capability and software versatility which eases and speeds up the test, analysis, and design of well controlled systems that obey the targeted performance objectives. That is why a lot of efforts have been done through simulation work. Some of the researches focused on modeling the quadcopter **Benic, et al., 2016**. Some concentrated on developing and evaluating different controllers **Anjum, et al., 2016, Ribas and Engel, 2014. Abbasi, and Mahjoob, 2013. Bouadi, et al., 2007. and Harrag, et al., 2012**. And some dealt with the two issues, i.e. the model and the controllers, **Mahdi, 2006. Bouabdallah, 2007. Brito, 2009. and Basta, 2012**. In addition, practical implementation issues got part of the research interest, **Hystad, 2015**. as well as the trajectory tracking problems, **Luis, 2016**.

In this work, a mathematical model will be derived specifically for the quadcopter rotational dynamics. The derivation will be carried out using Newton Euler equations. The quadcopter model will be then, through simulation and software, used in the process of testing the quadcopter action and designing and trying different controllers that can help in achieving the goal of flying the quadcopter accurately and stably. For the control part, two controllers are used, the Proportional+Integral+Derivative (PID) controller, and the fuzzy PID controller. The controllers are to be designed to achieve the goal of flying the quadcopter accurately and stably.

For evaluating the controllers' performance and to compare among them, four response characteristics will be used which are the rise time, the overshoot, the settling time, and the steady state error. That is besides two performance indices which are the ISE and the IAE.

2. THE QUADCOPTER MODEL

Before derivation, some important relevant terms and concepts will be defined or clarified.

2.1 Definitions

- i- The coordinates system: There are two coordinate systems; Earth frame and Body frame, **Mahdi, 2006**. These two frames are shown in **Fig.1**
- ii- Kinematics description model: In this description, any point in the body frame can be defined with the following relation:

$$S = R * v$$

where; S represents the displacement vector in the Earth frame, R represents the rotation matrix, and v represents the displacement vector in the body frame. The velocity equation is found through derivation of the displacement equation.

- iii - Dynamics description model: the dynamics of a quadcopter can be derived by Lagrange Euler equations and Newton Euler equations. The dynamics of the quadcopter take into consideration the mass and the moments of inertia about the axes.

2.2 Notes about modeling the quadcopter

The motion of the quadrotor can be divided into two subsystems; rotational subsystem (roll, pitch and yaw) and translational subsystem (z, x, and y positions), and as shown in **Fig.2**, It is worth it to mention that the rotational subsystem is fully actuated while the translational subsystem is under-actuated **Nagaty, et al., 2013**.

The aim here will be the model derivation of the rotational subsystem of the quadcopter dynamics, that is, developing the equations of the roll (ϕ), pitch (θ), and yaw (ψ) for the quadcopter. In the derivation, the quadcopter body and earth fixed frames considered in the derivation are shown in **Fig.1**. In this figure, B represents the body fixed frame, and E represents the earth fixed frame. The quadcopter orientation in space is given by a rotation from B to E, and as clarified in **Fig.1**.

2.3 Modeling with Newton-Euler equation

The mathematical model for the quadcopter dynamics and motion could be developed either using either Euler Lagrange equations or Newton-Euler equations. The results obtained in both cases will be the same, but the procedure with the Newton-Euler equations is shorter, and that is why it will be used in this section.

In order to derive a model for the quadcopter motion, the various moments and forces on the quadcopter must be taken into consideration. Both forces and moments on the quadcopter can be derived using Newton-Euler equations and as given in Eq. (1).

$$\begin{bmatrix} F \\ \tau \end{bmatrix} = \begin{bmatrix} mI_{3 \times 3} & 0 \\ 0 & I_{3 \times 3} \end{bmatrix} * \begin{bmatrix} \dot{v} \\ \dot{w} \end{bmatrix} + \begin{bmatrix} w \times mv \\ w \times Iw \end{bmatrix} \quad (1)$$

where; m represents the mass of the quadcopter, \dot{v} represents the linear acceleration vector, \dot{w} represents the angular acceleration vector, F represents the force vector acting on the quadcopter, \mathcal{T} represents the torque vector acting on the quadcopter, all with the respect to the body frame, and $I_{3 \times 3}$ represents the moments of inertia matrix and is given as:

$$I = \begin{bmatrix} I_{xx} & 0 & 0 \\ 0 & I_{yy} & 0 \\ 0 & 0 & I_{zz} \end{bmatrix} \quad (2)$$

The equations for the quadcopter motion can be developed using Eq. (1), with the individual moments and forces described for all degrees of freedom **Schmidt, 2011**.

From Eq. (1), the equivalent moments' equation is given by:

$$\mathcal{T} = I\dot{w} + (w \times Iw) \quad (3)$$

$$\begin{bmatrix} \mathcal{T}_\phi \\ \mathcal{T}_\theta \\ \mathcal{T}_\psi \end{bmatrix} = \begin{bmatrix} I_{xx} & 0 & 0 \\ 0 & I_{yy} & 0 \\ 0 & 0 & I_{zz} \end{bmatrix} * \begin{bmatrix} \ddot{\phi} \\ \ddot{\theta} \\ \ddot{\psi} \end{bmatrix} + [(\dot{\phi}i + \dot{\theta}j + \dot{\psi}k) \times (I_{xx}\dot{\phi}i + I_{yy}\dot{\theta}j + I_{zz}\dot{\psi}k)] \quad (4)$$

where $i \times i = 0, j \times j = 0$ and $k \times k = 0$, the moments for the roll, pitch, and yaw are obtained:

$$\begin{bmatrix} \mathcal{T}_\phi \\ \mathcal{T}_\theta \\ \mathcal{T}_\psi \end{bmatrix} = \begin{bmatrix} I_{xx}\ddot{\phi} \\ I_{yy}\ddot{\theta} \\ I_{zz}\ddot{\psi} \end{bmatrix} + \begin{bmatrix} \dot{\theta}\dot{\psi}(I_{zz} - I_{yy}) \\ \dot{\phi}\dot{\psi}(I_{xx} - I_{zz}) \\ \dot{\phi}\dot{\theta}(I_{yy} - I_{xx}) \end{bmatrix} \quad (5)$$

the moments acting round x, y, and z axis are given by:

$$\mathcal{T}_x = bl(-\Omega_1^2 + \Omega_2^2 + \Omega_3^2 - \Omega_4^2) \quad (6)$$

$$\mathcal{T}_y = bl(-\Omega_1^2 - \Omega_2^2 + \Omega_3^2 + \Omega_4^2) \quad (7)$$

$$\mathcal{T}_z = d(-\Omega_1^2 + \Omega_2^2 - \Omega_3^2 + \Omega_4^2) \quad (8)$$

where; b represents the thrust factor of the quadcopter, d represents the drag factor of the quadcopter, l represents the distance from the center of gravity to the center of a motor, and $(\Omega_1^2, \Omega_2^2, \Omega_3^2$ and $\Omega_4^2)$ represents the squared angular velocities of the propellers. The given moment equations are for "X" configuration adopted in this work. Some researches, like **Gopalakrishnan, 2016**, adopts the "+" configuration.

The configuration used for the quadcopter is the (X) configuration and as depicted in **Fig.3**. Considering this configuration, the speed equations are given by the following equations:

$$\Omega_1^2 = Throttle - Ur - Up - Uy \quad (9)$$

$$\Omega_2^2 = Throttle + Ur - Up + Uy \quad (10)$$

$$\Omega_3^2 = Throttle + Ur + Up - Uy \quad (11)$$

$$\Omega_4^2 = Throttle - Ur + Up + Uy \quad (12)$$

where; Ur, Up , and Uy represents the control signals for each of the roll, pitch, and yaw motion. These equations take the correction command for the roll, pitch, yaw and throttle and combine them in a way to allow all corrections be sent to the motors. An important point to state here is that the signals of all parts in all of the equations depend on each axis reference as well as where each motor is located **Ribas, and Engel, 2014**.

The gyroscopic effect resulting from the propellers rotation for roll is defined as:

$$\text{The gyroscopic effect for roll} = -Jr * wy(-\Omega_1 - \Omega_3 + \Omega_2 + \Omega_4)$$

and, the gyroscopic effect resulting from the propellers rotation for pitch is defined as:

$$\text{The gyroscopic effect for pitch} = Jr * wx(-\Omega_1 - \Omega_3 + \Omega_2 + \Omega_4)$$

where; wx, wy represents the body axis angular rate, and Jr represents the rotor inertia of the quadcopter. And considering that:

$$\begin{bmatrix} \tau_\phi \\ \tau_\theta \\ \tau_\psi \end{bmatrix} = \begin{bmatrix} \tau_x \\ \tau_y \\ \tau_z \end{bmatrix} \quad (13)$$

The following equation can be obtained:

$$\begin{bmatrix} I_{xx}\ddot{\phi} \\ I_{yy}\ddot{\theta} \\ I_{zz}\ddot{\psi} \end{bmatrix} = \begin{bmatrix} \tau_x \\ \tau_y \\ \tau_z \end{bmatrix} - \begin{bmatrix} \dot{\theta}\dot{\psi}(I_{zz} - I_{yy}) \\ \dot{\phi}\dot{\psi}(I_{xx} - I_{zz}) \\ \dot{\phi}\dot{\theta}(I_{yy} - I_{xx}) \end{bmatrix} \quad (14)$$

Then, the dynamics of the subsystem can be written as follows:

$$\ddot{\phi} = \left[\frac{\dot{\theta}\dot{\psi}(I_{yy}-I_{zz})}{I_{xx}} \right] + \frac{\tau_x}{I_{xx}} - \frac{Jr * wy * (-\Omega_1 - \Omega_3 + \Omega_2 + \Omega_4)}{I_{xx}} \quad (15)$$

$$\ddot{\theta} = \left[\frac{\dot{\psi}\dot{\phi}(I_{zz}-I_{xx})}{I_{yy}} \right] + \frac{\tau_y}{I_{yy}} + \frac{Jr * wx * (-\Omega_1 - \Omega_3 + \Omega_2 + \Omega_4)}{I_{yy}} \quad (16)$$

$$\ddot{\psi} = \left[\frac{\dot{\theta}\dot{\phi}(I_{xx}-I_{yy})}{I_{zz}} \right] + \frac{\tau_z}{I_{zz}} \quad (17)$$

Although this work is based on the dynamics given by Eqs. (15) to (17), it is important to state that many researchers, like **Kotarski, et al. 2016**. and **Bresciani, 2008**. simplify the dynamics by keeping the terms with the moments and ignoring the others. Such simplifications are based on justifications which in turn are based on assumed conditions. For example, ignoring coupling terms is justified by assuming the motion of the quadrotor to be close to the hovering condition, which means small angular changes occur (especially for roll and pitch). And so, these terms can be simplified because they are smaller than the main ones. In reality, to work close to the hovering condition can help a lot in analysis and design. One other simplification example based on the

“close to hovering” condition, is that the angular accelerations which are referred to the angles of the quadrotor measured in its fixed frame, can be referred directly to the Euler angle accelerations that are referenced to the earth frame.

3. THE QUADCOPTER MODEL WITH THE CONTROLLERS

To test the quadcopter rotational dynamics and control its rotational variables ϕ , θ , and ψ , the closed loop control system shown in **Fig.4** has been suggested.

Before going into the controllers details, some important points will be clarified about the system:

- The system outputs or controlled variables are ϕ , θ , and ψ .
- There are three input signals to the system which are ϕ_d , θ_d and ψ_d . These signals represent the desired values for the outputs
- The throttle signal is intended to play the role of the control signal responsible for altitude control. And as the simulation is intended for the quadcopter rotational dynamics, the throttle value is kept constant throughout the simulation.
- During testing the quadcopter model and the controllers used, the input signals (ϕ_d , θ_d and ψ_d) will be input to the computer by a user through a joystick connected to the computer. This arrangement is used to resemble the actual case when a person is controlling a real quadcopter through a joystick.
- The (X) configuration will be used for the quadcopter and as depicted in **Fig.3**.

3.1 The PID and the Fuzzy PID Controllers

In this part, two controllers will be suggested for controlling the quadcopter. A justification for this suggestion will be given, and an analysis for its performance will be covered, and also their feasibility will be discussed.

The PID control is one of the early used control methods. Its first version was an analog pneumatic one, and its latest version is the digital PID that is implemented as software. The PID with the proportional, derivative, and integral manipulation of the error signal, represents a mixture that aims at fast response with minimum overshoot and minimum if not null steady state error **Ribas, and Engel, 2014**. The reason for the wide and surviving use of PID is because it offered an easy structure that was simple to understand and operate with, and the more important is that it does well with a lot of systems **Basta, 2012**. Not for just this reason the PID has been adopted in this research for quadcopter fly control, but for many other reasons, like:

- It is still an efficient controller that can meet, when tuned, the design objectives (not for just the quadcopter, but for a lot of other systems).
- It has some sort of robustness.
- It can be tuned manually or with many procedural methods.
- It is easy to implement by software in real time applications.
- Its execution time is small which makes it suitable for real time applications with strict timing conditions.
- The huge number of researches and researchers, it is considered as a reference to compare the performance of other controllers with it.

To do well, the PID controller must be tuned. Different methods exist for tuning like the manual, Tyreus-Luyben, close loop Ziegler-Nichols, open loop Ziegler-Nichols, damped oscillation, Cohen-

Coon, and C-H-R **Shahrokhi**, and **Zomorodi**, 2010. Besides these methods, there are newer ways that depend non classical optimization methods, and the GA algorithm is just one of many examples.

The approach of the tuning methods mentioned above is to tune the controller parameters and then use them in the real time work of the system. A different magnificent way of tuning is introduced with the fuzzy PID controller. With this controller, the fuzzy logic part continuously tunes and adjusts the PID parameters while the controlled system is in its actual long run real time work. In other words, the Fuzzy part adapts the PID parameters moment by moment at each sampling instant. Although some concentrates when talking about tuning methods on the capability of minimizing cost and training time, like **Dicesare, et al.,2009**. who suggests the use of Ziegler-Nichols method or the manual method, in the opinion of researchers in this paper, it is more important to get a method with adaptive online tuning that provides the controller with capability of self-adapting to go on with the nonlinear nature of the quadcopter dynamics and other external effects, for example. The Fuzzy logic is nonlinear and can adapt tuning to suffice the quadcopter control needs, as will be seen.

A lot could be found in the literature about the PID controller and the fuzzy logic **Seidabad, et al., 2014. Abbasi, and Mahjoob, 2013. Tanaka, 1996. Ross, 2010. and Harris, 2000.** and so, the focus here will be on issues relating to use them.

3.2 The Quadcopter System with the PID Controller

The overall control system for the quad copter with the PID controllers for the three basic quadcopter motions, roll, pitch, and yaw is shown in **Fig.5** Three controllers' outputs are used to control these variables; Ur , Up , and Uy respectively. These three control signals together with the "throttle" signal will be used to calculate the actual signals needed to control the quadcopter four motors, and as given by Eqs. (9) to (12).

3.2.1 The roll controller

The PID control equation for the roll of the quadcopter is defined by:

$$Ur = K\phi_p * e(t) + K\phi_i * \int_0^t e(\tau) dt + K\phi_d * \frac{de(t)}{dt} \quad (18)$$

The error equation is given by:

$$e(t) = (\phi_d - \phi) \quad (19)$$

where; $K\phi_p$, $K\phi_i$, and $K\phi_d$, are three roll PID controller parameters, ϕ_d represent the roll desired value, and ϕ represent the roll actual value.

3.2.2 The pitch controller

The PID control equation for pitch of the quadcopter is defined by:

$$Up = K\theta_p * e(t) + K\theta_i * \int_0^t e(\tau) dt + K\theta_d * \frac{de(t)}{dt} \quad (20)$$

The error equation is given by:

$$e(t) = (\theta_d - \theta) \quad (21)$$

where; $K\theta_p$, $K\theta_i$, and $K\theta_d$, are the three pitch PID controller parameters, θ_d represents the pitch desired value, and θ represents the pitch actual value.

3.2.3 The yaw controller

The PID control equation for yaw of the quadcopter is defined by:

$$U_y = K\psi_p * e(t) + K\psi_i * \int_0^t e(\tau) dt + K\psi_d * \frac{de(t)}{dt} \quad (22)$$

The error equation is given by:

$$e(t) = (\psi_d - \psi) \quad (23)$$

where; $K\psi_p$, $K\psi_i$, and $K\psi_d$ are the three yaw PID controller parameters, ψ_d represent the yaw desired value, and ψ represent the yaw actual value.

3.2.4 PID manual tuning procedure

In this method, which is much like Ziegler-Nichols method, the tuning takes place while the system is running. Initially, K_i and K_d values are set to zero, and K_p value is changed until the output of the loop oscillates. The value of K_p should be set to half of the value that caused the oscillation. Then K_i value is to be changed to minimize settling time without causing instability. Finally, the K_d value is to be changed until the overshoot is as small as possible without damping the system. The advantage of this method lies in that the PID parameters can be changed online; and no calculations are needed. The main disadvantage is that it is not as precise as other methods **Dicesare, et al., 2009**.

3.3 The Quadcopter System with the Fuzzy PID Controller

The overall control system for the quad copter with the Fuzzy PID controllers for the three basic quadcopter motions, roll, pitch, and yaw is shown in **Fig.6**. The FPID controller contains two parts, the fuzzy logic tuner, and the PID controller. The fuzzy part is used to tune the PID controllers' parameters. Each fuzzy tuner system contains two inputs; error and error derivative, and three outputs; K_p , K_i and K_d . The triangular membership function has been used for each of the inputs and the outputs and for all of the controllers. The inputs, the error and the error derivative, are defined by five membership functions: NB (negative big), NS (negative small), Z (zero), PS (positive small), and PB (positive big). On the other hand, each of the outputs is defined by three membership function: S (small), M (medium), and B (big). The range of the fuzzy set for the error input has been chosen as $[-2, 2]$, and for the error derivative as $[-4, 4]$. **Fig.7** shows the membership functions for the inputs.

The range for the outputs fuzzy set has been chosen as follows:

- [1, 75] for K_p , and is the same for roll, pitch, and yaw, and as indicated in **Fig.8**.
- [0, 0.02] for K_i , and is the same for roll, pitch, and yaw, and as indicated in **Fig.9**.
- [2, 18] for K_d , and is the same for roll, and pitch, and as indicated in figure **Fig.10**.
- [36, 72] for K_d for yaw case and as is indicated in **Fig.11**.

After defining the inputs and the output for each fuzzy tuner, the next step is to set the rules base. In this case, 25 rules are needed. This is because there are two inputs each of which contains five membership functions. The number of rules equal five multiplied by five. **Tables 1** and **2** show the rules for K_p , K_i , and K_d for each controller.

The outputs of each fuzzy tuner system provide gains values for the PID controllers used to control the roll, pitch, and yaw of the quadcopter. After using the fuzzy tuner to calculate the optimal gains, these gains are used by the PID controllers to find the U_r, U_p, U_y control signals via the three closed control loop as shown in **Fig.6** These three control signals, together with the “throttle” signal, will be used to calculate the actual signals needed to control the quadcopter four motors, and as given by Eqs. (9) to (12).

4. THE SIMULATION RESULTS

The quadcopter model and the controllers developed in sections 2 and 3 will be simulated and results will obtained using “MATLAB” software. The outputs or the controlled variables will be the roll, pitch, and yaw. The desired values for these variables will be entered to the “MATLAB” environment through a joystick interfaced to the computer running the “MATLAB” to resemble of actual quadcopter control, **Fig.12** shows the joystick and the computer used.

The quadcopter parameters used in the simulation are given in **Table 3**. These parameters are based on a quadcopter designed and built by the researchers of this work.

To get close to a realistic situation, the quadcopter model parameters used in the simulation are those of an actual quadcopter being designed and implemented by the researchers of this work.

4.1 The Result Obtained with the PID Controller

In this case, each parameter of the PID controller has been tuned to get a stable system and improved performance. **Tables 4** and **5** show the parameters values for each of the PID controllers, and **Figs. 13** to **15** show the response for each PID controller.

4.2 The Fuzzy PID Controller

In this part, the fuzzy logic system has been used to tune the PID controller’s parameters in such a way to get a stable response with good characteristics. **Figs. 16** to **19** show the parameters for each PID controller during the tuning/response time. **Figs. 20** to **22** show the quadcopter responses for the roll, pitch, and yaw signals.

5. PERFORMANCE EVALUATION

Two performance indices have been used to judge the performance of the two controllers used. The two indices are the Integral Square Error (ISE) and the Integral Absolute Error (IAE). The time over

which each of these two indices has been measured is (20 seconds) for the roll and pitch cases, and (40 seconds) for the yaw case. **Table 6** shows the values for the ISE and the IAE for each controller, with attention to that the results obtained for the PID controller regards the PID after being manually tuned.

Moreover, the system performance has been evaluated using four response characteristics which are the rise time, the overshoot, the steady state error, and the settling time. The results obtained are summarized in **Table 7**. It must be pointed out here that the results obtained for the PID controller regards the PID after being manually tuned. The results given in **Tables 6** and **7** indicates a clear superiority of the FPID.

6. RESULTS DISCUSSION

The results obtained for controlling the rotational dynamics variables, the pitch, the roll, and the yaw, with the PID controller have been compared to those obtained with the FPID controller to judge the performance of each controller. Doing the comparison required calculating some performance indices and response characteristics and as given in **Tables 6** and **7**. The comparison indicates that the FPID is more capable than the PID in reducing the ISA and the IAE. And this is true whether for the roll or the pitch or the yaw. Also, the FPID showed the capability of reducing rise and settling times and at the same time reducing the overshoot in the response. This was the case for the pitch and the roll. For the yaw case, the FPID managed to reduce the settling time and the overshoot, but with no improvement regarding the rise time. Considering the steady state error, both of the controllers managed to eliminate it.

The percentage of improvement in the responses, with the FPID controller, for the different evaluation cases considered ranged (approximately) between 50% and 80%.

The main feature of the FPID which gave it this efficiency is its capability in adapting the PID parameters from sample to sample, and so, giving it the capability to cope with changes in the system working conditions keeping in mind that it is a nonlinear one. It is important to point out here that the fuzzy part of the FPID, could itself be tuned to be capable of achieving better tuning of the PID part.

7. CONCLUSIONS

In this work adopted the software simulation approach and aimed at testing, evaluating, and comparing two controllers, namely the PID and the FPID, when used to control the pitch, roll, and yaw of a quadcopter. Two performance indices, the Integral Square Error (ISE) and the Integral Absolute Error (IAE), and four response characteristics, the rise time, the overshoot, the settling time, and the steady state error, have been used for evaluation and compare. The obtained results indicated a superiority in performance for the FPID over the PID, and this is because the FPID involves continuous adjusting of the PID parameters over the entire response time to cope with the changing situation in a way to achieve best possible response. This conclusion about performance superiority is based by the following figures that are calculated using the results obtained: 70%, 70%, and 52% lesser ISA for the roll, pitch, and yaw consequently, 70.5%, 70.5%, 56.4% lesser IAE for the roll, pitch, and yaw consequently, 53%, and 80.6% lesser rise time and settling time for the roll and pitch consequently, and 77% lesser settling time for the yaw. In addition, the FPID gave zero overshoot versus 18%, 18%, and 25% in the PID case for the roll, pitch, and yaw

consequently. Apart from this, both controllers gave zero steady state error with close rise times for the yaw.

The FPID fits quite great for simulation cases. For control of quadcopter in real time, the processing unit must be capable and fast enough to compute the control signals using the FPID controller. And this is because the computations needed for the FPID controller is much greater than that for the PID.

One more important thing to point out is that the fuzzy part itself could be tuned with the aim of a compromise between an improved efficiency and a reduced computation time.

8. REFERENCES

- Abbasi, E. and Mahjoob, M., 2013, *Controlling of Quadrotor UAV Using a Fuzzy System for Tuning the PID Gains in Hovering Mode*, Mechanical Engineering, University of Tehran, College of Engineering Journal, Vol.12, No.5.
- Anjum, A., Sufian, R., Abbas, Z., and Qureshi, I., 2016, *Attitude Control of Quadcopter Using Adaptive Neuro Fuzzy Control*, International Journal of Hybrid Information Technology, Vol.9, No.4.
- Basta, P. O., 2012, *Quadcopter Flight*, M. Sc. Thesis, Electrical Engineering, University of California, USA.
- Benic, Z., Piljek, P., and Kotarski, D., 2016, *Mathematical Modeling of Unmanned Aerial Vehicles with Four Rotors*, Interdisciplinary Description of Complex Systems, Vol.14, No.2 pp.88-100.
- Bouabdallah, S., 2007, *Design and Control of Quadrotors with Application to Autonomous Flying*, M.Sc. Thesis, Faculty of Science, Engineering and Technology, University of Aboubekr Belkaid.
- Bouadi, H., Bouchoucha, M., and Tadjine, M., 2007, *Modeling and Stabilizing Control Laws Design Based on Sliding Mode for an UAV Type-Quadrotor*, Engineering Letters, Vol.15, No.2, pp. 42-47.
- Brito, J. M., 2009, *Quadcopter Prototype*, M.Sc. Thesis, Department of Mechanical Engineering, University of tecniciac de Lisboa, Portugal.
- Bresciani, T., 2008, *Modelling, identification and control of a quadrotor helicopter*, Thesis, Lund university, Sweeden.
- Dicesare, A., Gustafson, K., and Lindenfelzer, P., 2009, *Design Optimization of a Quad-Rotor Capable of Autonomous Flight*, B.Sc. Thesis, Department of Mechanical Engineering, Institute Worcester Polytechnic, USA.
- Gopalakrishnan, E., 2016, *Quadcopter flight mechanics model and control algorithms*, Thesis, Czech Technical University, Czech.
- Harrag, A., Zeghlache1, S., Saigaa, D., Kara, K., and Bouguerra, A., 2012, *Fuzzy Sliding Mode Control with Chattering Elimination for a Quadrotor Helicopter in Vertical Flight*, in Corchado et al. (Eds), *Hybrid Artificial Intelligent System*, Berlin Heidelberg: Springer, Vol.10, No.4, pp.125-136.
- Hystad, A., 2015, *Model, design and control of a quadcopter*, Thesis, Norwegian University of Science and Technology, Norway.
- Harris, J., 2000, *An Introduction to Fuzzy Logic Applications*, Springer.

- Kotarski, D., Benic, Z., and Krznar, M., 2016, *Control design for unmanned aerial vehicles with four rotors*, journal of Interdisciplinary Description of Complex Systems, Vol.14, No.2, Croatia.
- Luis, C., 2016, *Design of a trajectory tracking controller for a nano quadcopter*, Technical report, Polytechnique Montreal, Canada.
- Mahdi, O., 2006, *Modeling and Control of Unmanned Aerial Vehicle of Technology*, M.Sc. Thesis, Department of Automation and Robotics, Poznan University of Technology, Poland.
- Nagaty, A., Saeedi, S., Thibault, C., Seto, M., and Li, H., 2013, *Control and Navigation Framework for Quadrotor Helicopters*, Journal of Intelligent and Robotic Systems, Vol.70, No.1.
- Ribas, F., and Engel, P. M., 2014, *Complete System for Quadcopter*, B.Sc. Thesis, Computer Engineering, Federal University of Rio Grande do Sul, Brazil.
- Ross, T. J., 2010, *Fuzzy Logic with Engineering Applications*, 3rd. ed., John Wiley & Sons.
- Schmidt, M. D., 2011, *Simulation and Control of Quadcopter Unmanned Aerial Vehicle*, M.Sc. Thesis, University of Kentucky, USA.
- Seidabad, E. A., Vandaki, I., Kamyad, I. V., 2014, *Designing Fuzzy PID Controller for Quadrotor*, International Journal of Advanced Research in Computer Science and Technology, Vol.2, No.4.
- Shahrokhi, M. and Zomorodi, A., 2010, *Comparison of PID Controller Tuning Methods*, Project Report, Chemical and Petroleum Engineering, Sharif University of Technology, Iran.
- Tanaka, K., 1996, *An Introduction to Fuzzy Logic for Practical Applications*, Newyork: Springer.

Table 1. The rules for K_p and K_i for each of the three PID controllers.

$\begin{matrix} e \\ \text{de} \end{matrix}$	NB	NS	Z	PS	PB
NB	M	S	S	S	M
NS	B	M	S	M	B
Z	B	B	M	B	B
PS	B	M	S	M	B
PB	M	S	S	S	M

Table 2. The rules for K_d for each of the three PID controllers.

$\begin{matrix} e \\ \text{de} \end{matrix}$	NB	NS	Z	PS	PB
NB	M	B	B	B	M
NS	S	M	B	M	S
Z	S	S	M	S	S
PS	S	M	B	M	S
PB	M	B	B	B	M

**Table 3.** The parameters of the quadcopter.

Parameter	Description	Value	Units
m	mass	0.79	kg
L	Distance from the center of gravity to the center of a motor	0.27	m
I_{xx}	Roll inertia moment	$7.035 * 10^{-3}$	$kg * m^2$
I_{yy}	Pitch inertia moment	$7.035 * 10^{-3}$	$kg * m^2$
I_{zz}	Yaw inertia moment	$1.4 * 10^{-2}$	$kg * m^2$
J_r	Rotor inertia	$6.5 * 10^{-5}$	$kg * m^2$
b	Thrust factor	$3.13 * 10^{-5}$	-
d	Drag factor	$7.5 * 10^{-7}$	-

Table 4. The tuned simulation parameters of the PID controllers for roll and pitch cases.

Parameter	Value
k_p	3
k_i	0.01
k_d	2.5

Table 5. The tuned simulation parameters of the PID controller for the yaw case.

Parameter	Value
k_p	10
k_i	0.01
k_d	18

Table 6. The ISE and IAE values for the responses with the PID and the FPID controllers.

Controller	ISE	IAE
Roll PID	0.5702	0.9852
Pitch PID	0.5702	0.9852
Yaw PID	1.834	3.554
Roll fuzzy PID	0.1747	0.2998
Pitch fuzzy PID	0.1747	0.2998
Yaw fuzzy PID	0.8836	1.55

Table 7. The response characteristics values with the PID and the FPID controllers.

Roll and Pitch cases	PID controller	FPID controller	Yaw case	PID controller	FPID controller
Rise time (sec)	1.7	0.8	Rise time (sec)	4.5	4.7
Overshoot (%)	0.18	0	Overshoot (%)	0.25	0
Steady state error	0	0	Steady state error	0	0
Settling time (sec)	4.9	0.95	Settling time (sec)	25	5.73

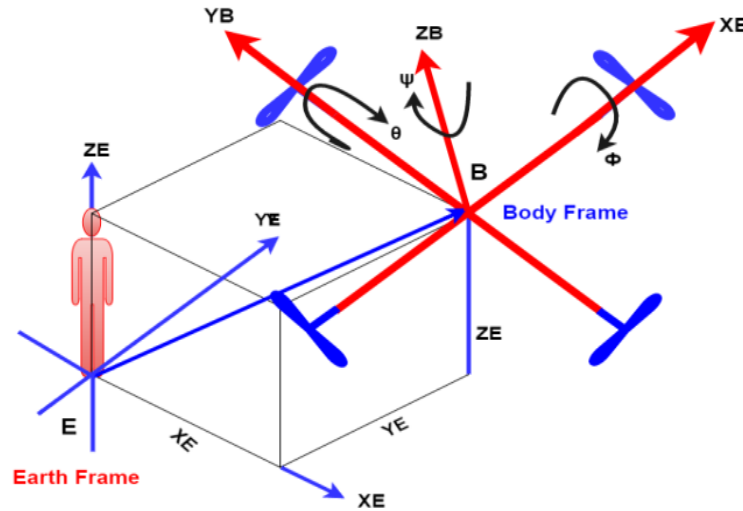


Figure 1. Body and earth fixed frame.

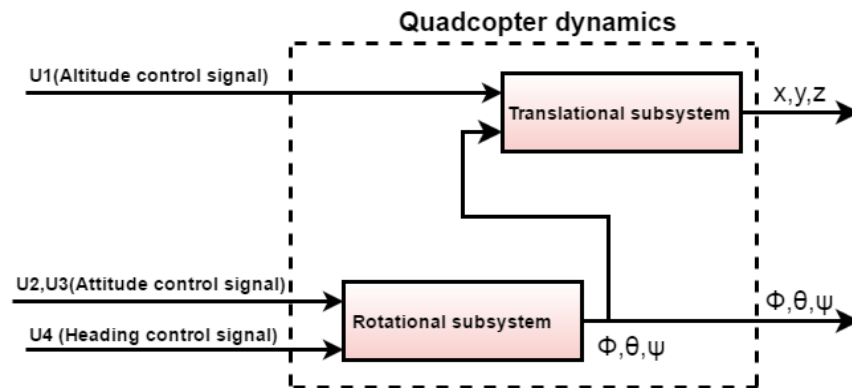


Figure 2. The quadcopter dynamics subsystems being given within a general block diagram for a quadcopter control system.

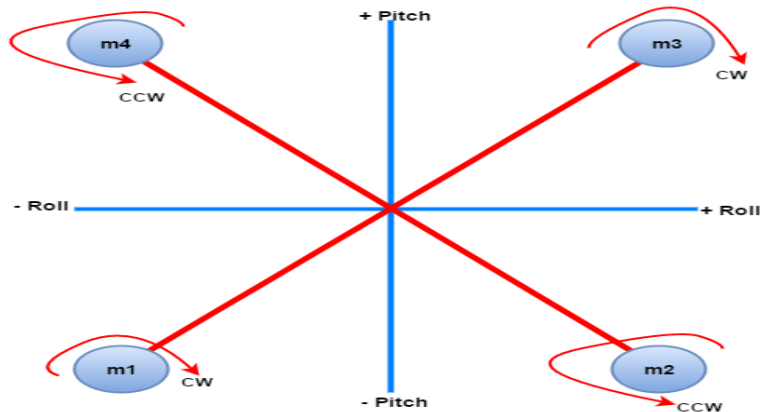


Figure 3. Quadcopter (X) configuration.

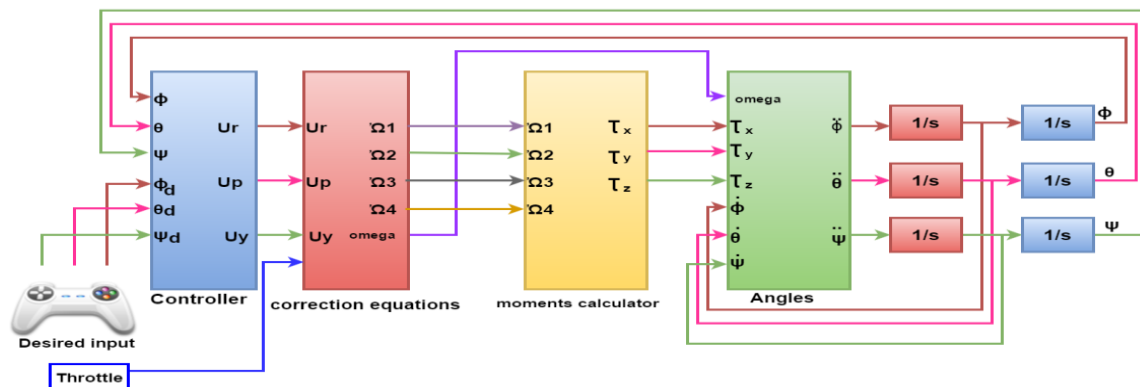


Figure 4. A picture giving an overall depiction of the closed loop quadcopter control system.

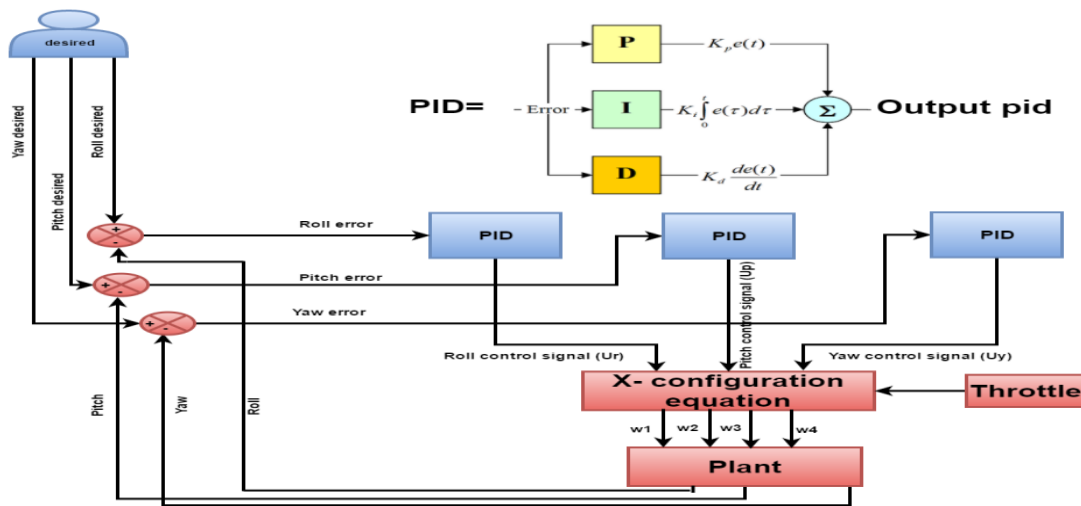


Figure 5. The quadcopter system with three PID controllers.

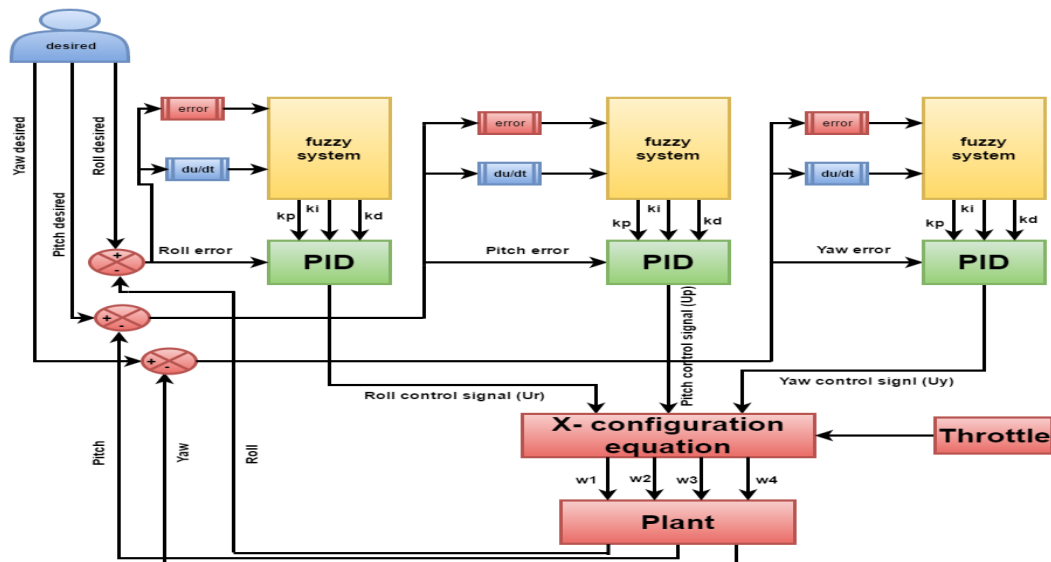


Figure 6. The quadcopter system with three fuzzy PID controllers.

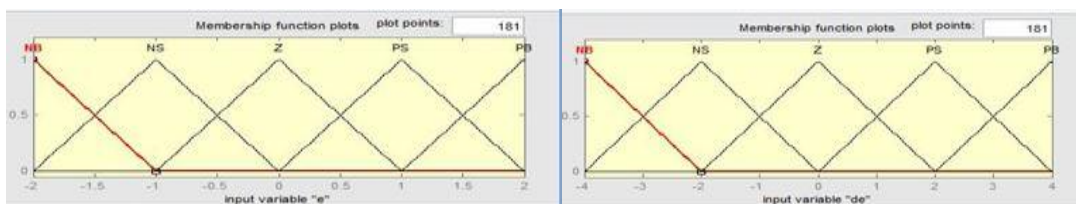


Figure 7. The membership functions for the inputs.

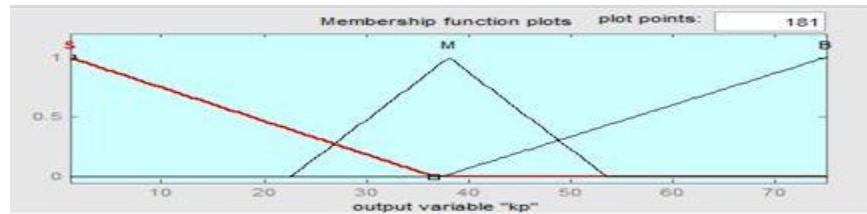


Figure 8. The memberships for the parameter K_p for roll, pitch, and yaw cases.

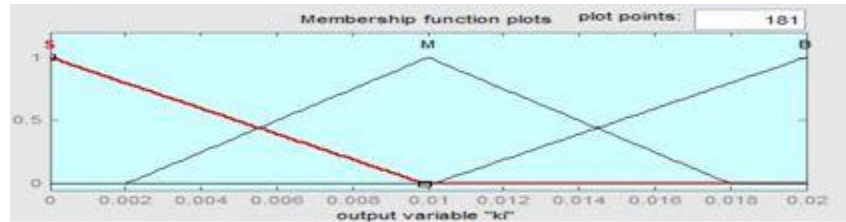


Figure 9. The memberships for the parameter K_i for roll, pitch, and yaw cases.

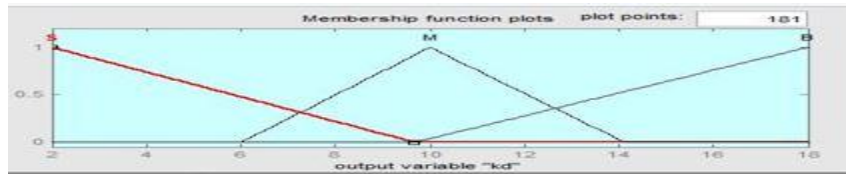


Figure 10. The memberships for the parameter K_d for roll, and pitch.

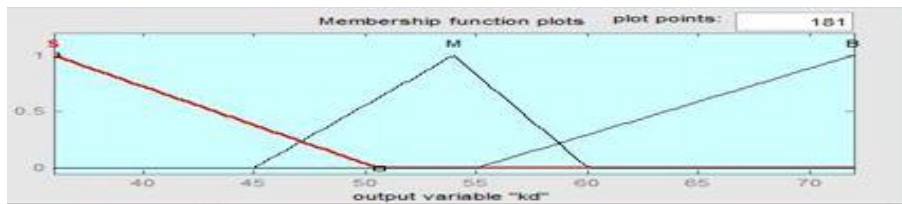


Figure 11. The memberships for the parameter K_d for yaw case.



Figure 12. The joystick interfaced to the computer for inputting the desired roll, pitch, and yaw values.

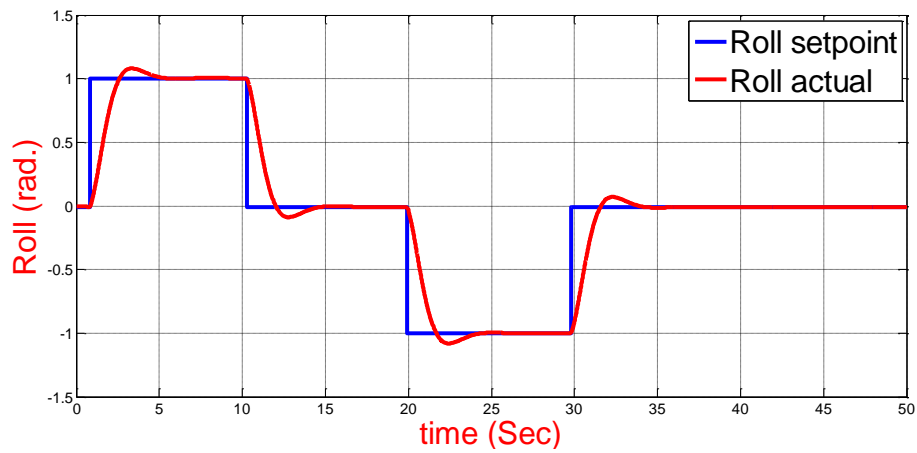


Figure 13. The roll signal Response.

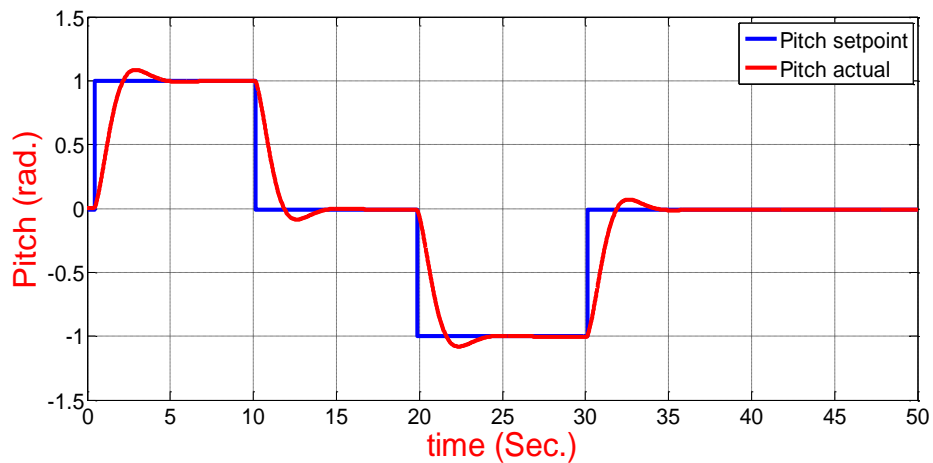


Figure 14. The pitch signal Response.

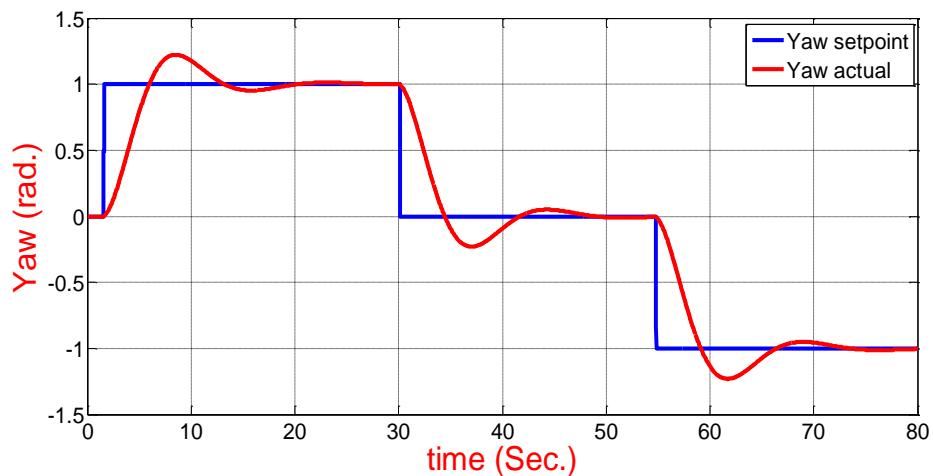


Figure 15. The yaw signal Response.

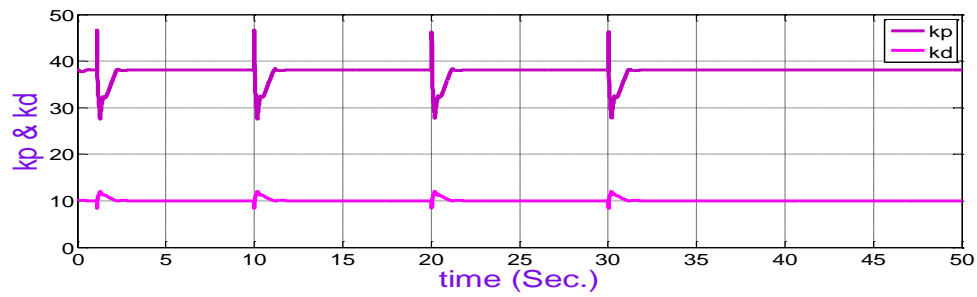


Figure 16. The k_p and k_d values for the roll and the pitch signals for the fuzzy PID controller case.

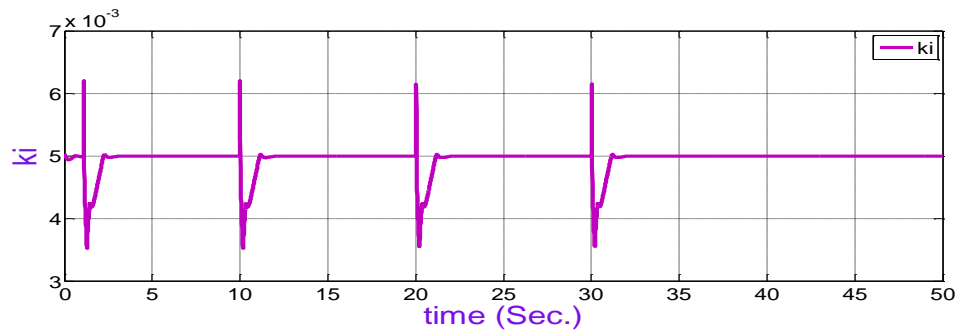


Figure 17. The k_i value for the roll and the pitch signals for the fuzzy PID controller case.

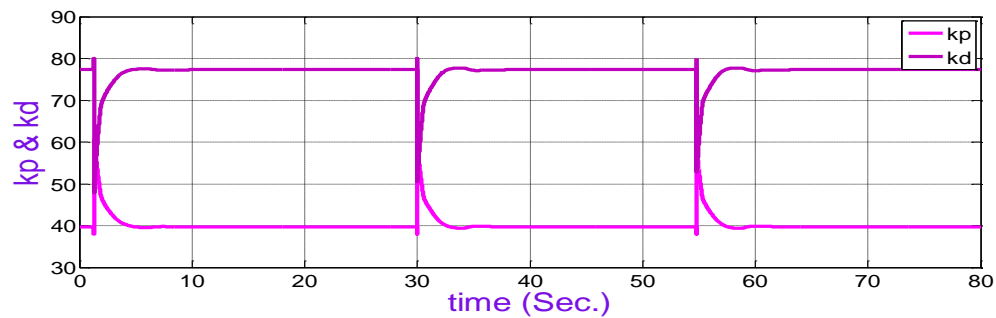


Figure 18. The k_p and k_d values for the yaw signal for the fuzzy PID controller case.

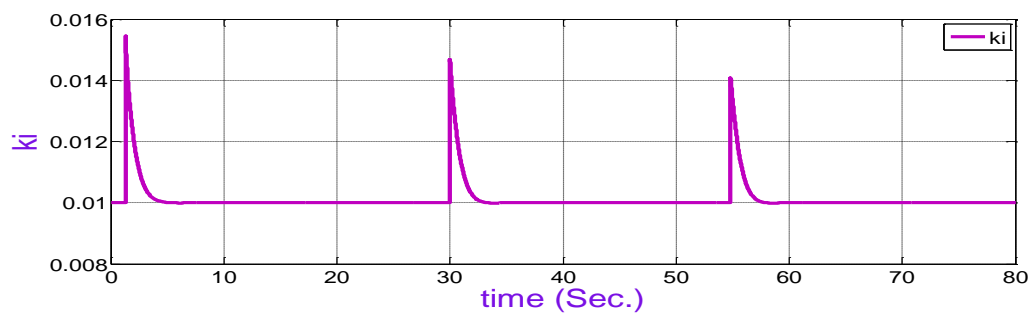


Figure 19. The k_i value for the yaw signal for the fuzzy PID controller case.

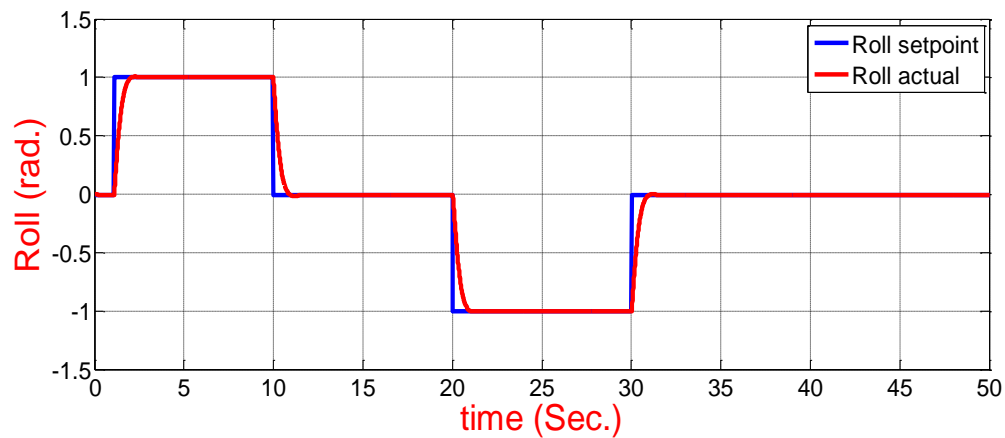


Figure 20. The roll response for the Fuzzy PID controller case.

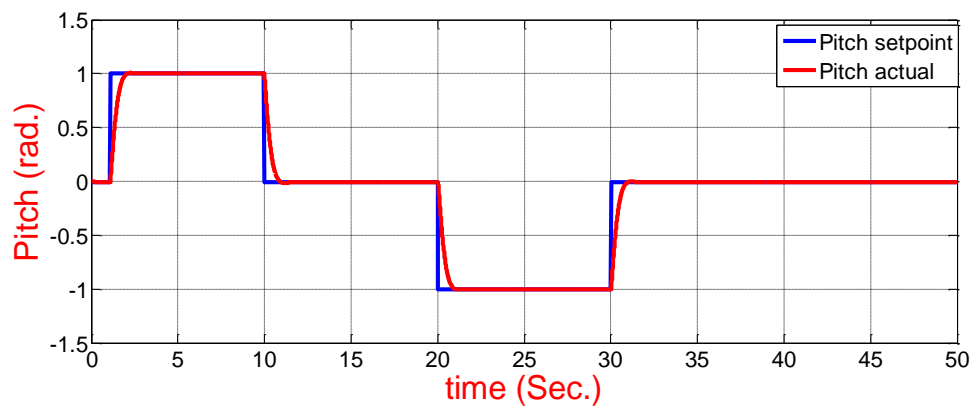


Figure 21. The pitch response for the Fuzzy PID controller case.

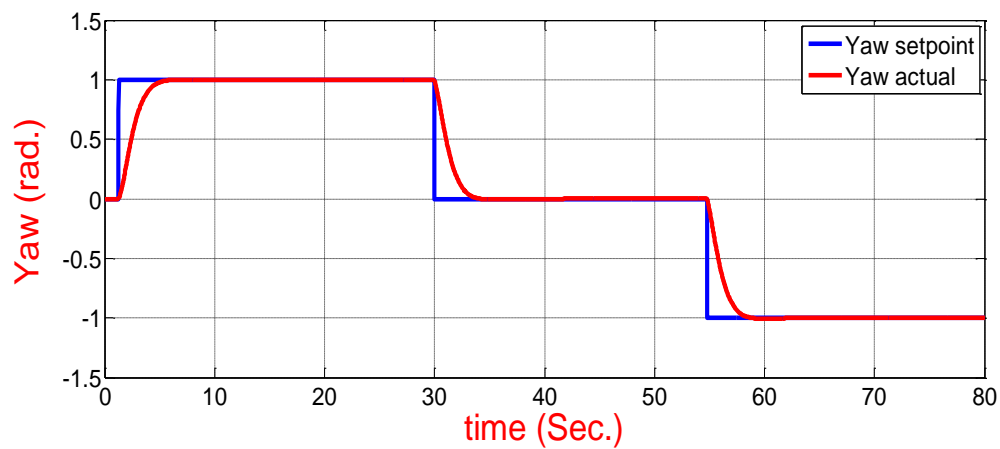


Figure 22. The yaw response for the Fuzzy PID controller case.

Simulation of Groundwater Movement for Nuclear Research Center at Al-Tuwaitha Area in Baghdad City, Iraq

Ayad Sleibi Mustafa
Assistant Professor
Engineering College-Anbar University
ayad_eng2001@yahoo.com

Ahmed Hazem Abdulkareem
Assistant Professor
Engineering College-Anbar University
ahm1973ed@yahoo.com

Rasha Ali Sou'd
Master Student
Engineering College-Anbar University
rasha.aliraqi90@gmail.com

ABSTRACT

The simulation of groundwater movement has been carried out by using MODFLOW model in order to show the impact of change of water surface elevation of the Tigris river on layers of the aquifer system for Nuclear Research Center at Al-Tuwaitha area, in addition to evaluate the ability of the proposed pumping well to collect groundwater and change the direction of flow at steady-state. The results of the study indicated that there is a good match between the values of groundwater levels that calculated in the model and measured in the field, where mean error is 0.09 m.

The study also showed that the increasing of water surface elevation of the Tigris river led to increase in the hydraulic head of observed wells, while the use proposed pumping well reduced the hydraulic head and intercepted the movement of groundwater flow. The flow direction is toward the Tigris river, and the velocity of flow is clear in the third layer identified medium sand which is 0.0015 m/day. The using of the proposed pumping well has changed the direction of groundwater, especially in the area around the well.

Key words: groundwater, MODFLOW, Al-Tuwaitha, and Tigris River.

محاكاة حركة المياه الجوفية لمركز البحوث النووي في منطقة التويثة، مدينة بغداد، العراق

رشا علي سعود
طالبة ماجستير
جامعة الانبار - كلية الهندسة

احمد حازم عبد الكريم
استاذ مساعد
جامعة الانبار - كلية الهندسة

اياد صليبي مصطفى
استاذ مساعد
جامعة الانبار - كلية الهندسة

الخلاصة

تم محاكاة حركة المياه الجوفية باستخدام نموذج MODFLOW لبيان تأثير تغيير منسوب الماء السطحي لنهر دجلة على الطبقة الجوفية لمركز البحوث النووي في منطقة التويثة اضافة الى تقييم قدرة بئر الضخ المقترح لتجميع الماء الجوفي وتغيير اتجاه الجريان بالحالة المستقرة مع الزمن. أشارت نتائج الدراسة الى وجود توافق جيد بين قيم مناسيب الماء الجوفي المحسوبة في الموديل والقيم المقاسة، حيث معدل الخطأ كان 0.09 م . كما بينت الدراسة ان زيادة منسوب الماء السطحي لنهر دجلة ادى الى زيادة المنسوب الهيدروليكي لإبار المراقبة ، بينما استخدام بئر الضخ ادى الى تقليل المنسوب الهيدروليكي واعتراض حركة الجريان . اتجاه التدفق كان باتجاه نهر دجلة ، والسرعة تكون واضحة بالطبقة الثالثة المميزة (رملية متوسط) 0.005 م/يوم . استخدام بئر الضخ غير اتجاه التدفق وخاصة بالمنطقة حول البئر .

1. INTRODUCTION

Groundwater is predominantly a new able resource which ensures the supply for a long term to meet the increasing requests and mitigate the impacts of anticipated climate change, and it is closely interrelated with other components of the environment, **Guzha, 2008**. The movement of groundwater may be overlapping with each other, or the direction of flow may be in the river or the sea. Therefor the effective management of water sources requires a comprehensive knowledge of hydrologic processes.

The model of groundwater flow is a clear representation for a groundwater system (a real phenomenon) and simplified it with maintaining the required accuracy and ensuring high reliability of the results. The models incorporated restrictive assumptions, such as spatial variability, dimensionality, and interaction of various components of flow and transport processes.

The modeling of groundwater flow applied by several researchers in Iraq for different purposes, for example : **Al-Ajaaj, 2007**, studied the impact of the environmental of Badush dam on groundwater flow by using Visual MODFLOW. The results showed that the dam has a negative impact on the foundation of the nearby building after 20 years after construction. **Attea, et al, 2007**, used Processing MODFLOW software to describe the behavior of groundwater flow at sandy Dibdiba formation in Safwan region. The results showed enhancing in the water elevation for wells and using artificial recharge for rehabilitation of formation for an aquifer. **Al-Maimuri, and Mohammed, 2009**, developed the mathematical model for groundwater motion by applying the theory of superposition. The superposition gave a good concordance between the time and distance down the curves of theoretical and numerical solution in heterogeneous hydrogeologic media. **Al-Dabbas, et al, 2016**, explained the impact of the climatic change on the groundwater. They found that the climatic change led to decrease the water table in the unconfined aquifer in Salah Din.

In this research, the modeling of groundwater flow is applied for Nuclear Research Center at Al-Tuwaitha area to determine the distribution of the hydraulic head and to evaluate the impact of the proposed pumping well on groundwater levels. Processing MODFLOW software version 5.3.1 is used to simulate groundwater flow, MODFLOW model is used to calculate and distribute the hydraulic heads, and PMPATH model is used to show the flow direction of the aquifer in Al-Tuwaitha.

2. MATERIALS AND METHODS

2.1 Site Description

The Nuclear Research Center is located in Al-Tuwaitha site about 18 kilometers (km) south of the southern edge of Baghdad Governorate, between (44°27'-44°35') Longitude and (33°10'-33°15) Latitude. It is characterized by a flat floor surface, surrounded by earthen dikes and ranging from 30-32m above mean sea level and the topography factor has no significant impact on water level and groundwater movement, **Copland, and Cochran, 2013**. The Tigris river passes near it about 1km from it, **Fig. 1**. The typical lithology of the site is a loamy clay from 0 to 16 m bls (below land surface), silt fine sand from 16 to 30 m bls, and medium sand from 30 to 50 m bls, **Al-Daffaie, 2014**. It has a hot, dry climate, vassal to Baghdad climate that's considered one of the hottest cities in the world. The warmest month is July with an average high of 44 °C and an average low of 25.5°C, while the coolest month is January with an average high of 16°C and an average low of 3.8°C.

2.2 Data Collection

Water level data for six observation wells located at Al-Twaitha area is used for ground water modeling, as in **Table 1**. The recharge is applied to top grid layer and the input parameter is assumed to be constant during the time stress period, and the principal source is the rainfall. The value of recharge rate was 2×10^{-5} m/day, **Bashoo, et al, 2005**. Aquifer properties for each layer were given as input to the model in **Table 2**.

2.3 Groundwater Flow Equation

The process of groundwater flow is based on Darcy's law and the conservation of mass, which describes the three dimensional movement of groundwater flow of constant density through the porous media is, **Rushton, 2004**.

$$\frac{\partial}{\partial x} \left(k_x \frac{\partial h}{\partial x} \right) + \frac{\partial}{\partial y} \left(k_y \frac{\partial h}{\partial y} \right) + \frac{\partial}{\partial z} \left(k_z \frac{\partial h}{\partial z} \right) = S_s \frac{\partial h}{\partial t} - W \quad (1)$$

Where:

K_x , K_y & K_z are components of the hydraulic conductivity [LT^{-1}], S_s is the specific storage [L^{-1}], $W(x,y,z,t)$ is the rate of ground water discharge/recharge per unit area [LT^{-1}] general sink/source term that is intrinsically positive and defines the volume of inflow to the system per unit volume of aquifer per unit of time [T^{-1}], h is the ground water head [L], x , y , z are Cartesian coordinate directions [L] and t is time [T].

In this research the groundwater flow ran at steady-state, where the term $S_s \frac{\partial h}{\partial t}$ was equal to zero.

2.4 Numerical Model

The finite-difference flow code existed within processing MODFLOW software, is used to perform this simulation. Processing MODFLOW for Windows (PMWIN) is designed with a professional graphical user-interface, the supported models and programs and several other useful modeling tools. The graphical user-interface allows to simulate and create models with ease. It handles models with up to 1,000 stress periods, 80 layers and 250,000 cells in each layer. The output of simulation included hydraulic heads, draw downs, subsidence, Darcy velocities, concentrations and mass terms, **Chiang, and Kinzelbach, 1998**.

The finite-difference is used to solve the groundwater flow equation in MODFLOW model, where the model domain is divided into a number of equal-sized cells-usually by specifying the number of rows and columns. Hydraulic properties are assumed to be uniform within each cell, and an equation is developed for each cell, based on the surrounding cells. Steady-state and transient flow conditions can simulate in MODFLOW. PMPATH Code is an advective transport model running to represent flow lines and paths lines of groundwater. It links with the groundwater models and outputs of the simulation from MODFLOW. It uses a semi-analytical particle tracking scheme, **Lu, 1994**, to calculate the groundwater paths and performs particle tracking with just a few clicks of the mouse. It gives different on screen graphical options involving head contours, and velocity vectors, **Chiang, 2005**.

2.5 Discretization of the Model

The model consists of 28 rows and 57 columns in each layer as in **Fig. 2** with cell size 80 m x 80 m. Based on the acquired information the model is divided into a three layered, top layer which has loam clay with a thickness of 16 m (approx.), the middle layer is 14 m thick silt fine sand and bottom layer is made up of predominantly medium sand with a thickness of 20 m. MODFLOW is used to estimate the distribution of hydraulic heads in steady-state, and PMPATH is used to calculate the ground water flow paths.

The boundaries of flow model were based on physical features and the hydraulic conditions, the cells that represent the Tigris river are defined as a constant head boundary and the neighbored cells for the Tigris river from the north-west are considered inactive cells, while other cells were defined as variable head boundaries, as in **Fig. 2**. The value of water surface elevation of the Tigris river is specified as a value of initial hydraulic head with 27.6 m.a.s.l, **Copland, and Cochran, 2013**.

3. STEADY STATE MODEL CALIBRATION

The model is operated with the initial conditions and hydraulic conductivities, which is adjusted during the calibration of the model using manual calibration. The final calibration process gave a good match between the observed and calculated head. **Table 3** and **Fig. 3** show a fairly good match between the calculated and observed heads. The model calibration error can be expressed qualitatively by mean error (ME), mean absolute error (MAE), root mean square error (RMSE), **Anderson, and Woessner, 2002**.

The ME error for observed head versus calculated head is 0.09 m, is very close to 0, and it is the best statistical value compared with MAE and RMSE which are 0.16 m and 0.24 m, respectively. Since it is impossible to obtain an exact match for calculated and observed heads therefore the model can be accepted with an acceptable error ratio.

4. THE RESULT AND DISCUSSION

The equipotential lines of groundwater flow in the first, second, and third layers are shown in **Fig. 4**. It has a high value in the eastern part of the aquifer of 27.82 m, while the smallest value of the area that neighboring the river is 27.61 m, which is the grade towards the river, therefore the groundwater will move toward the river.

It has been noticed when the groundwater flow is drawn by PMPATH model that groundwater movement of groundwater is slow, especially in the first layer identity type of loam clay, **Ou, 2006**, but its highest in the third layer, where the velocity of groundwater flow in the first, second, and third layer were 9.77×10^{-6} , 3.6×10^{-4} , and 0.0015 m/day, respectively. **Fig.5 (a,b,c)** shows the behavior of groundwater flow direction in the aquifer system, where water flow towards the river because the less head at area neighbored the river.

5. THE SCENARIOS OF GROUNDWATER FLOW

After the final calibration process, two scenarios are tested in order to check the influence of variation in water surface elevation of the Tigris river and pumping well proposed on the head of the aquifer system.

In the scenario1 is run with an average water surface elevation of the Tigris river of 28.7 m.a.s.l, to predict the impact of the Tigris river on groundwater aquifer, and also on hydraulic head of observation wells. The results shown that the increase of water elevation of the Tigris

river creates to increase in the calculated head values of the groundwater levels as compared with the values of the observation wells, as **Fig. 6**.

While the model in the scenario 2 is run with an average of water surface elevation of the Tigris river of 28.7 m.a.s.l as in scenario 1 and used the proposed pumping well. The use of pumping well led to reduce the water level in the observed wells as compared with the value of the results in scenario 1, as **Fig. 6**. The direction of groundwater flow became toward the pumping well as shown in **Fig.7 (a,b,c)**. So the movement of contaminant will follow the groundwater movement and it will be toward the pumping well and this is noted from the output of this scenario, which operated with proposed pumping well to limit the movement of water contaminant toward the Tigris river and thereby reducing the movement of contamination deposited to aquifer from the surface for Nuclear Research Center at Al-Tuwaittha area near the Tigris river. **Fig. 8** shows the effect of pumping well on the equipotential lines.

6. CONCLUSIONS AND RECOMMENDATION

The simulation of groundwater flow shows that there is a good result between the observed and calculated heads, where the value of mean error is 0.09 which is close to zero. Any increase in the water elevation of the Tigris river leads to increase the hydraulic heads aquifer, while the use of proposed pumping well leads to reduce the hydraulic heads, and also to capture the flow lines of groundwater. Groundwater flow movement is slowly toward the Tigris river which, influenced by soil type. This is more pronounced in the third layer due to its high permeability value, the velocity of groundwater is 0.0015 m/day in the third layer compared with the first and the second layer, the velocity are 0.00036 m/day and 0.00000977 m/day respectively. The recommendations may be taken into consideration for further, as using transient simulations to show the change of aquifer levels with time, also using more parameters and changing boundary conditions by making the water surface elevation of the Diyala River as a boundary condition.

7. REFERENCE

- Al-Ajaaj, A., (2007), *Environment A Impact Assessment Numerical Model Of Proposed Badush Dam On A Groundwater*, M.Sc. Thesis, College of Engineering, University Of Technology, 74p.
- Al-Dabbas, M.A., Al- Khafaji, R.M., and Hussain, G.A., (2016), *Evaluation Of Climate Changes Impact on The Hydrological Properties Unconfined Aquifers : A case Study From Samara –Baljl Area, Iraq*, International Journal of Advanced Scientific and Technical Research, Vol.1, No.6, pp376-391.
- Al-Daffaie, H.S.A., (2014), *Investigation and Design Of Clay Liner For Radioactive Waste Landfill IN AL-Tuwatha Site _ Iraq*, M.Sc. thesis, Civil Engineering, University Allahabad, 94 p.
- Ali, S. M., (2012), *Hydrogeological Environmental Assessment of Baghdad Area*, Diss. PhD Thesis, College of Science, University of Baghdad, 303p.
- Al-Maimuri, N. M. L., and Mohammed, K. A. ,(2009), *A Model For Groundwater Motion In 3D Random Hydrogeologic Heterogeneous Media*, AL- Taqani, Vol. 24, No. 3, pp139-155.
- Anderson, M. P., and Woessner, W.W., (2002), *Applied groundwater modeling*, Academic Press, 338p.

- Attea, A. M., Bana, D. S., Mutasher, W. R., and Flayh, Q. M., (2007), *Simulation of influence of artificial recharge on ground water elevations of Sandy Dibdiba Formation in Safwan region, southern Iraq*, Basrah Journal of Science, Vol. 25, No. 1, pp 17-27.
- Bashoo, D., Lazim, S., and Alwan, M., (2005), Hydrogeology of Baghdad province, General Directorate of Water Well Drilling, Baghdad, (internal report), 51p.
- Chiang, W. H., (2005), *3D Groundwater Modeling With PMWIN: A Simulation System for Modeling Groundwater Flow and Transport Process*, Springer Science & Business Media, 397p.
- Chiang, W. H., and Kinzelbach, W., (1998), *Processing MODFLOW: a simulation system for modeling groundwater flow and pollution*, Instrukcja programu, Hamburg-Zurich.
- Copland, J. R., and Cochran, J. R., (2013), *Groundwater monitoring program plan and conceptual site model for the Al-Tuwaitha Nuclear Research Center in Iraq (No. SAND2013-4988)*, Sandia National Laboratories (SNL-NM), Albuquerque, NM (United States).
- Guzha, A. C., (2008), *Integrating Surface and Sub Surface Flow Models of Different Spatial and Temporal Scales Using Potential Coupling Interfaces*, (Doctoral dissertation, Utah State University).
- Heath, R. C., (1983), *Basic ground-water hydrology*, Prepared in cooperation with the North Carolina Department of Natural Resources and Community Development (Vol. 2220). US Geological Survey.
- Lu, N., (1994), *A semianalytical method of path line computation for transient finite-difference groundwater flow models*, Water Resources Research, Vol. 30, No. 8, pp. 2449-2459.
- Osterbaan, R. J., and Nijland, H. J., (1986), *12 Determining The Saturated Hydraulic Conductivity*, www.waterlog.info.
- Ou, Chang-Yu, (2006), *Deep excavation: theory and practice*, CRC Press, 552p.
- Rushton, K. R., (2004), *Groundwater Hydrology: Conceptual and Computational Models*, John Wiley & Sons.
- Todd, D. K., and Mays, L. W., (2005), *Ground-water hydrology*, Third Edition, Wiley International Edition.

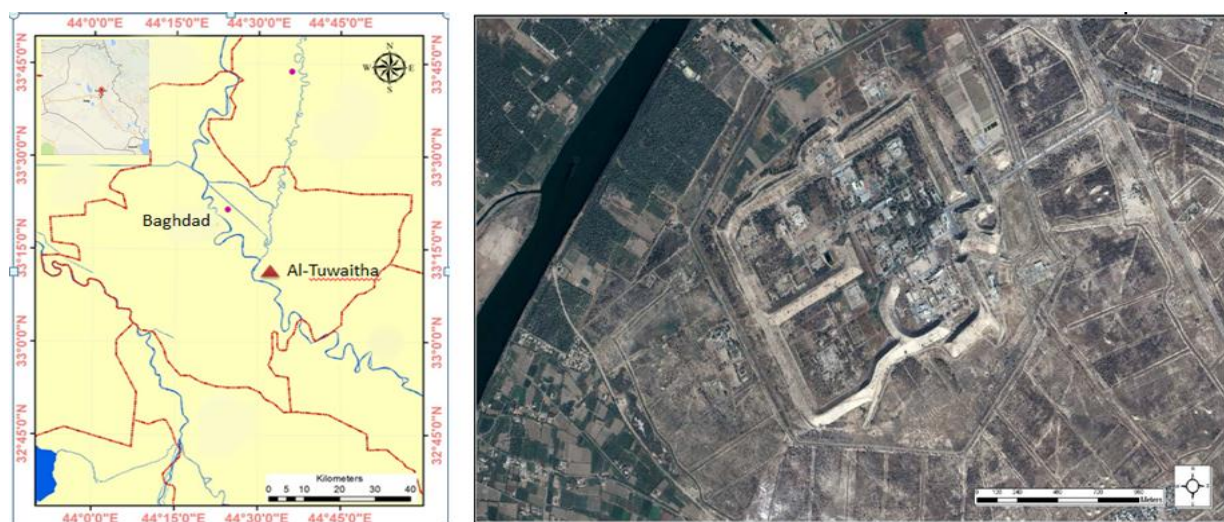


Figure 1. Location of Nuclear Research Center at Al-Tuwaitha site, Al-Daffaie, 2014.

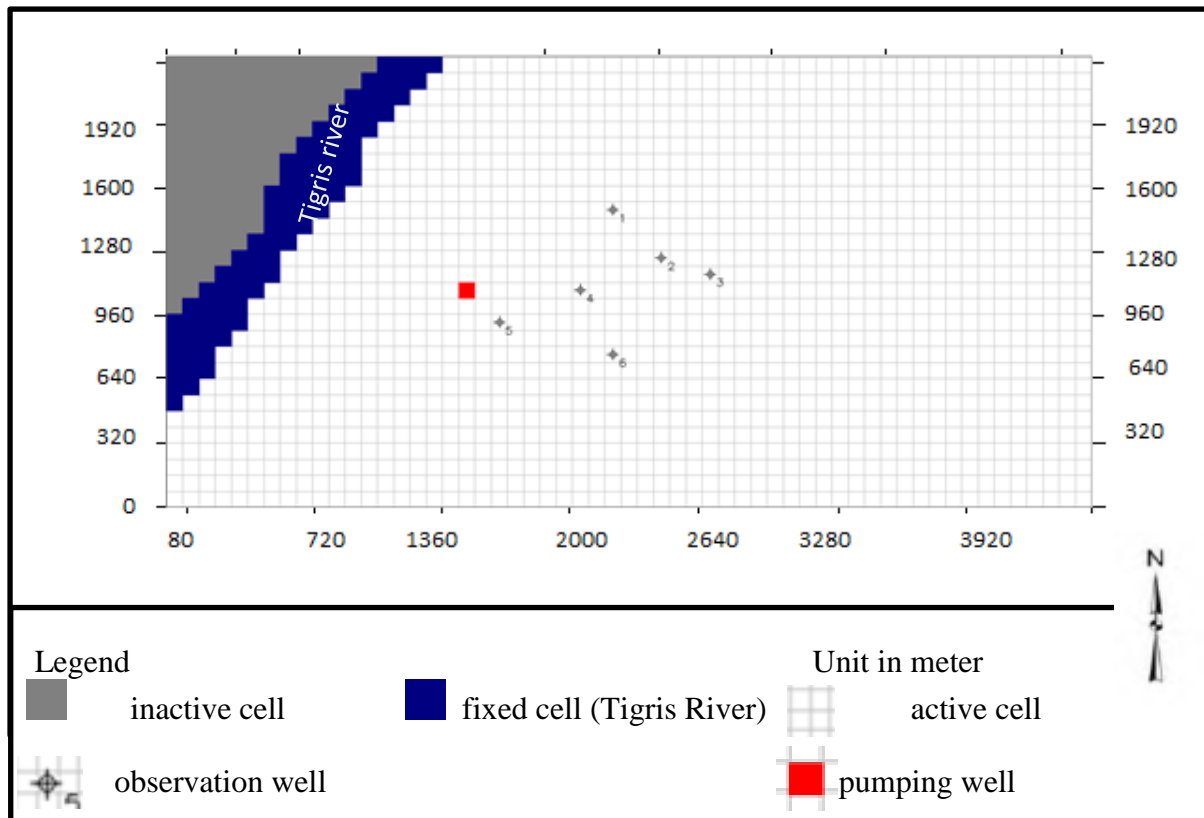


Figure 2. Plane view of the model.

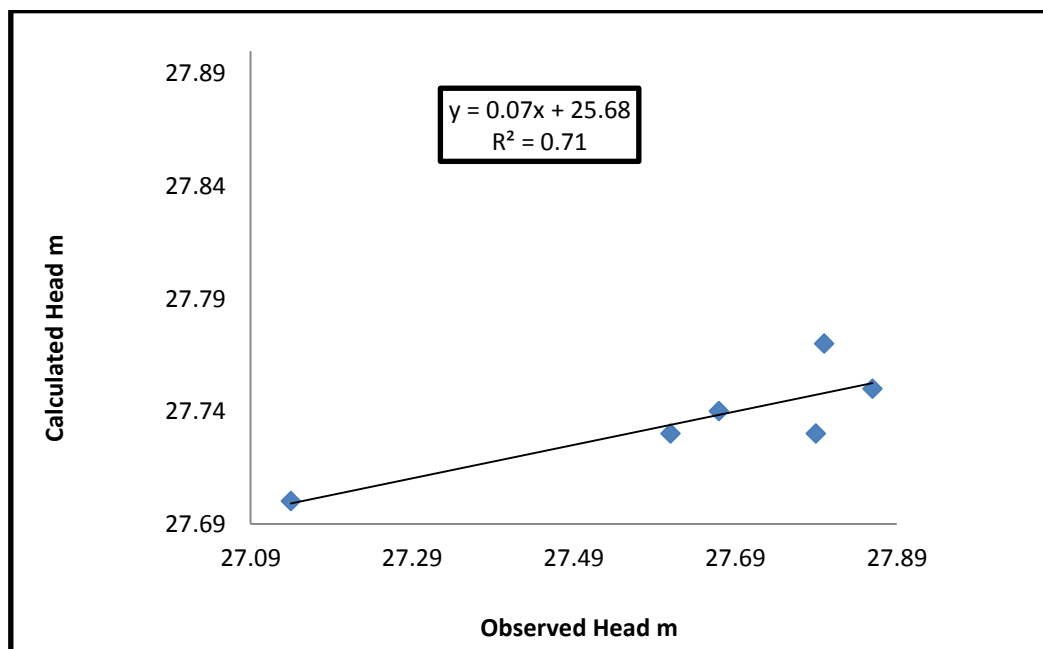


Figure 3. Calculated and observed heads (m) of Nuclear Research Center at Al-Tuwaitha site.

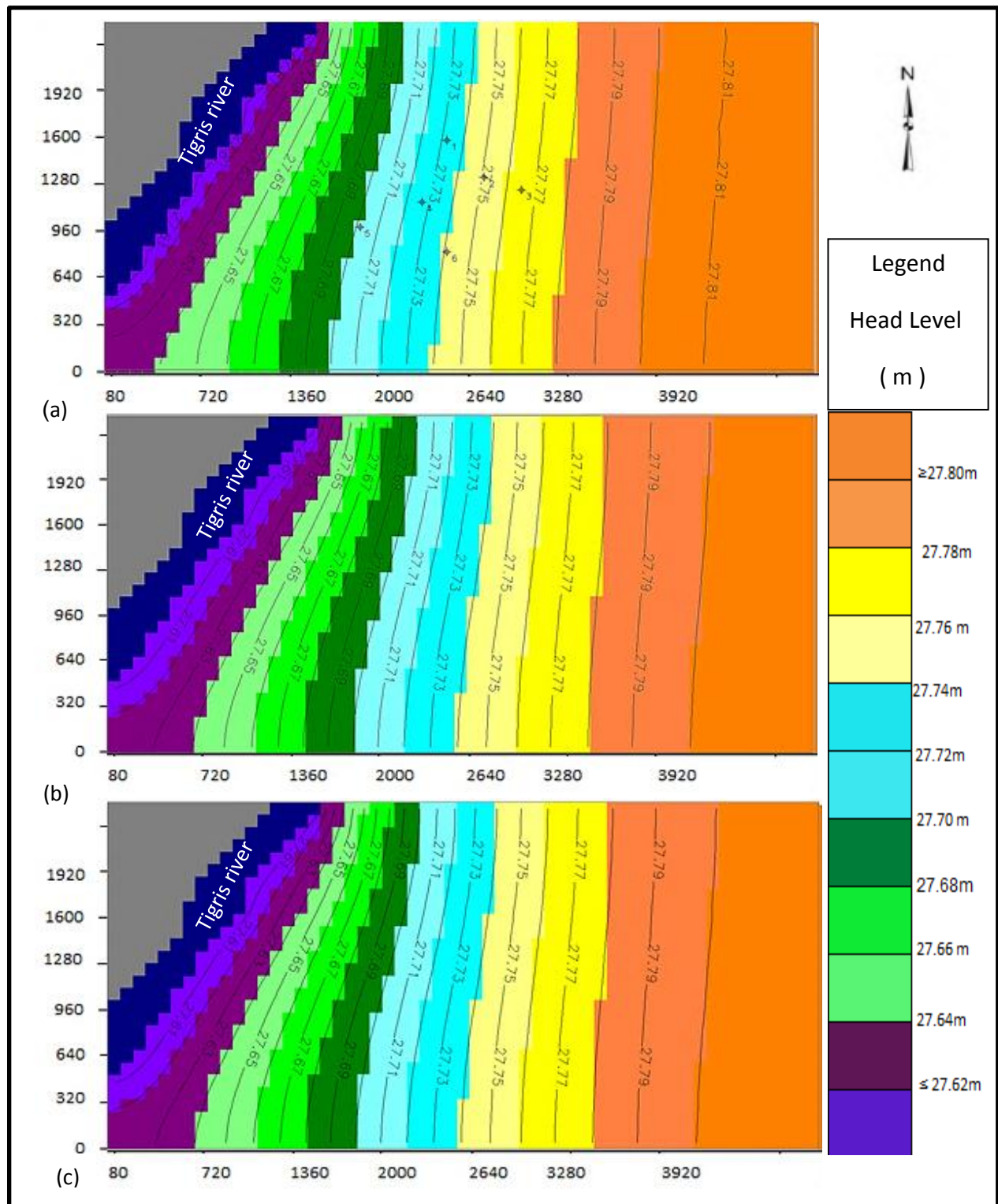


Figure 4. Simulated steady-state of the heads for the study area with 27.6 m as value of water surface elevation of the Tigris river, (a): contours of hydraulic heads in the first layer, (b): contours of hydraulic heads in the second layer, (c): contours of hydraulic heads in the third layer.

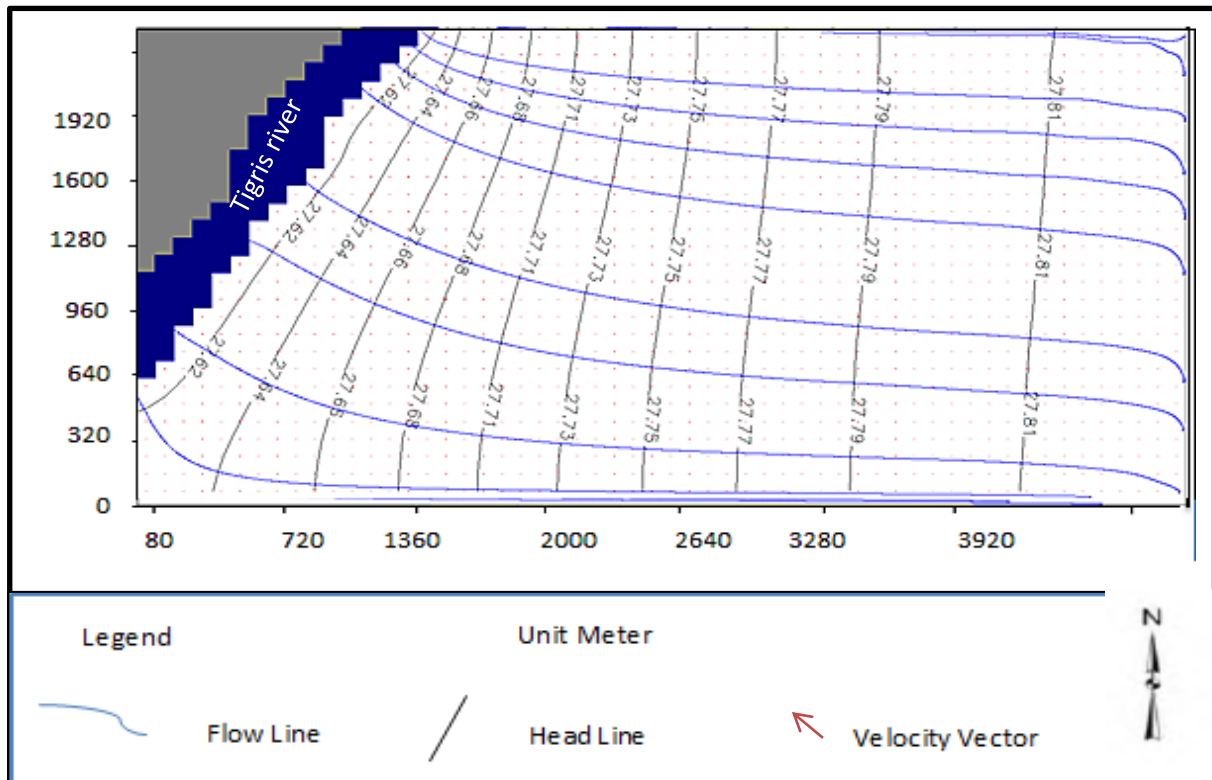


Figure 5a. Groundwater flow net direction in the first layer.

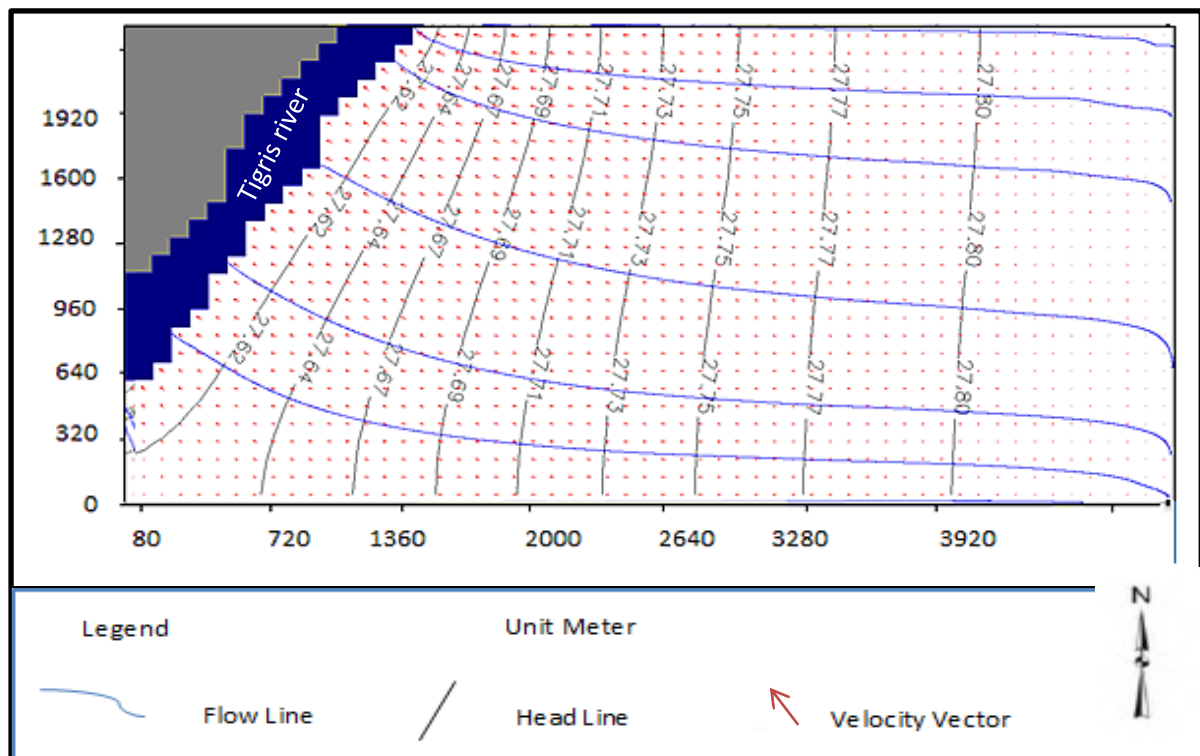


Figure 5b. Groundwater flow net direction in the second layer.

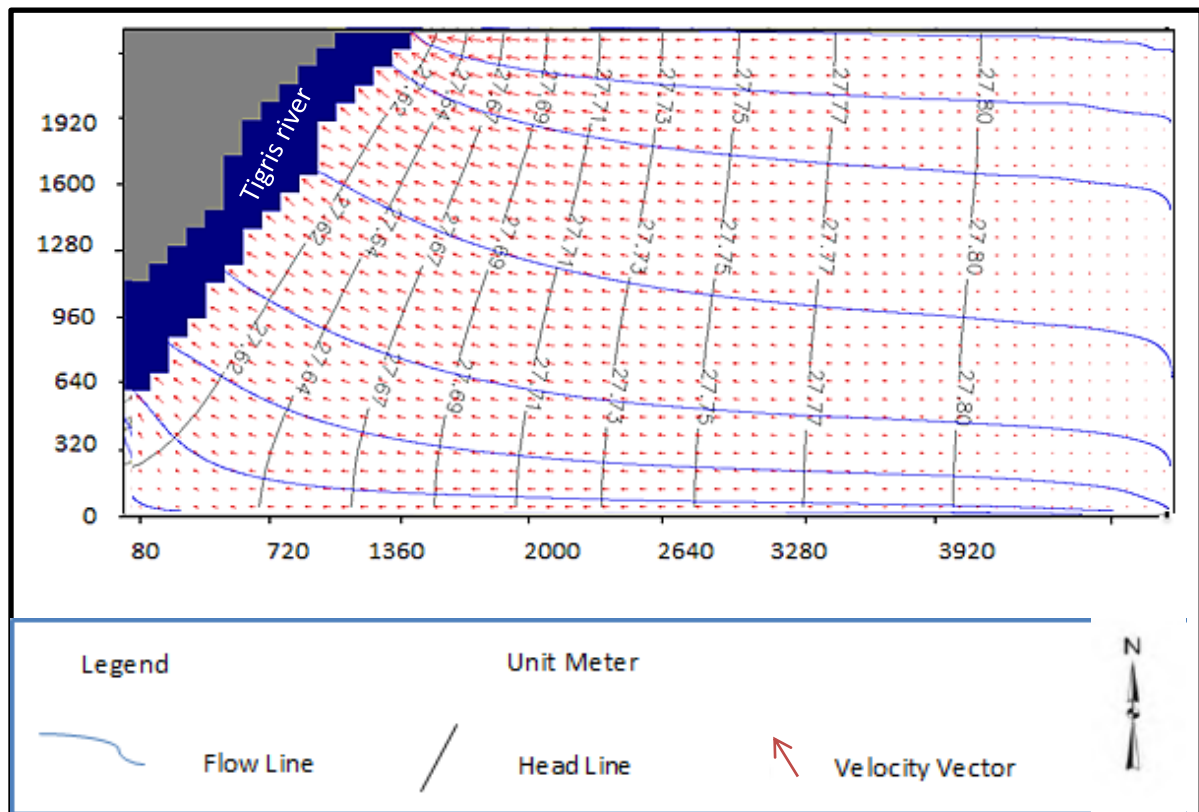


Figure 5c. Groundwater flow net direction in the third layer.

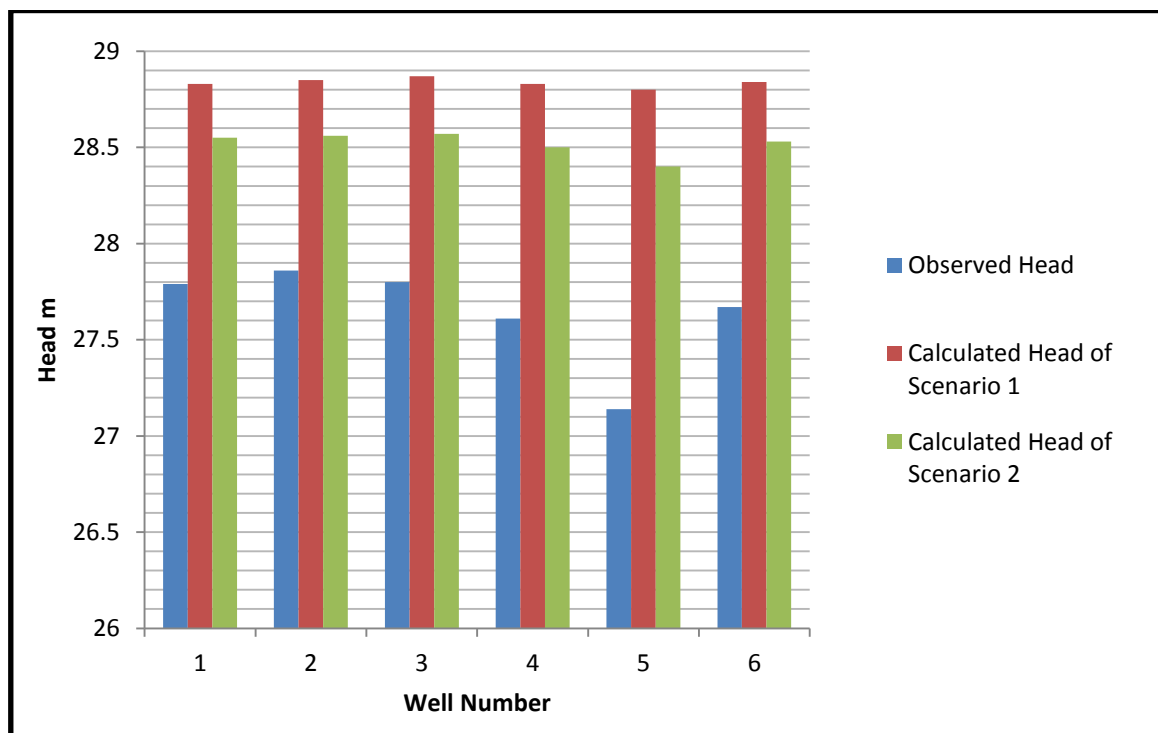


Figure 6. Calculated and observed heads (m) of Nuclear Research Center at Al-Tuwaittha site of scenario 1 and scenario 2.

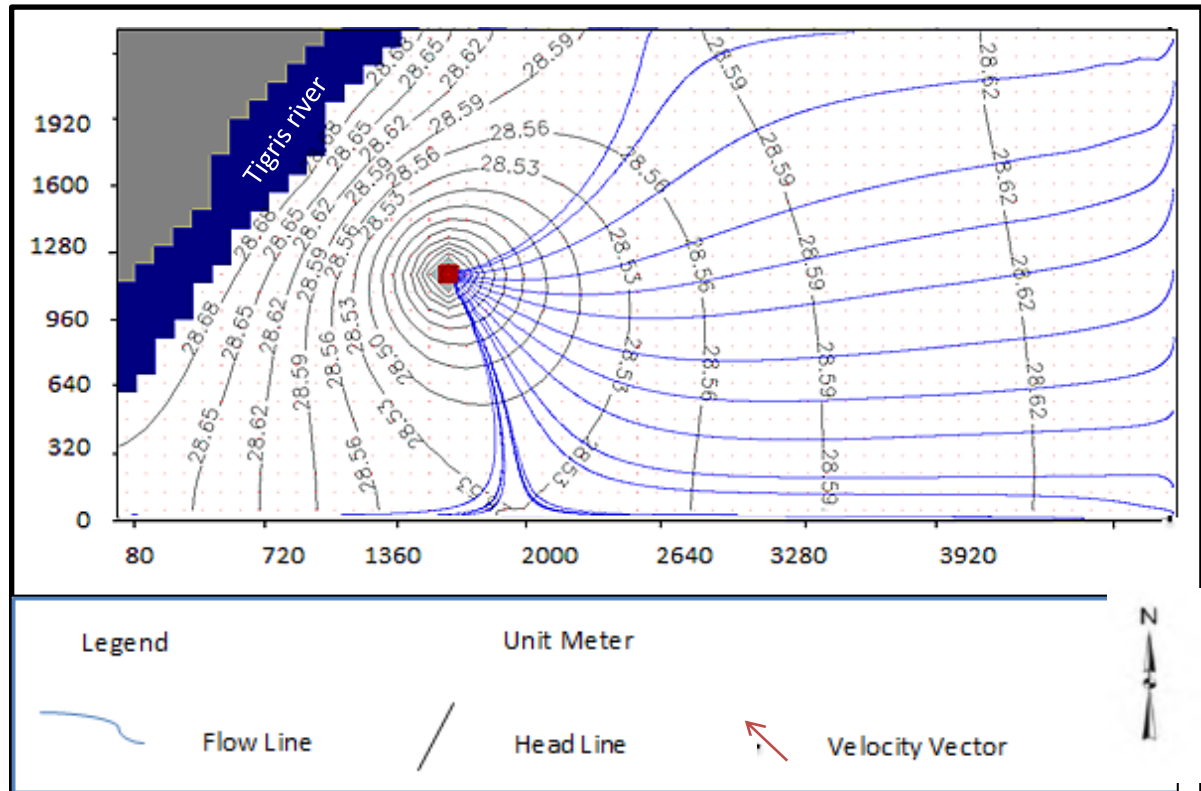


Figure 7a. Groundwater flow net direction in the first layer.

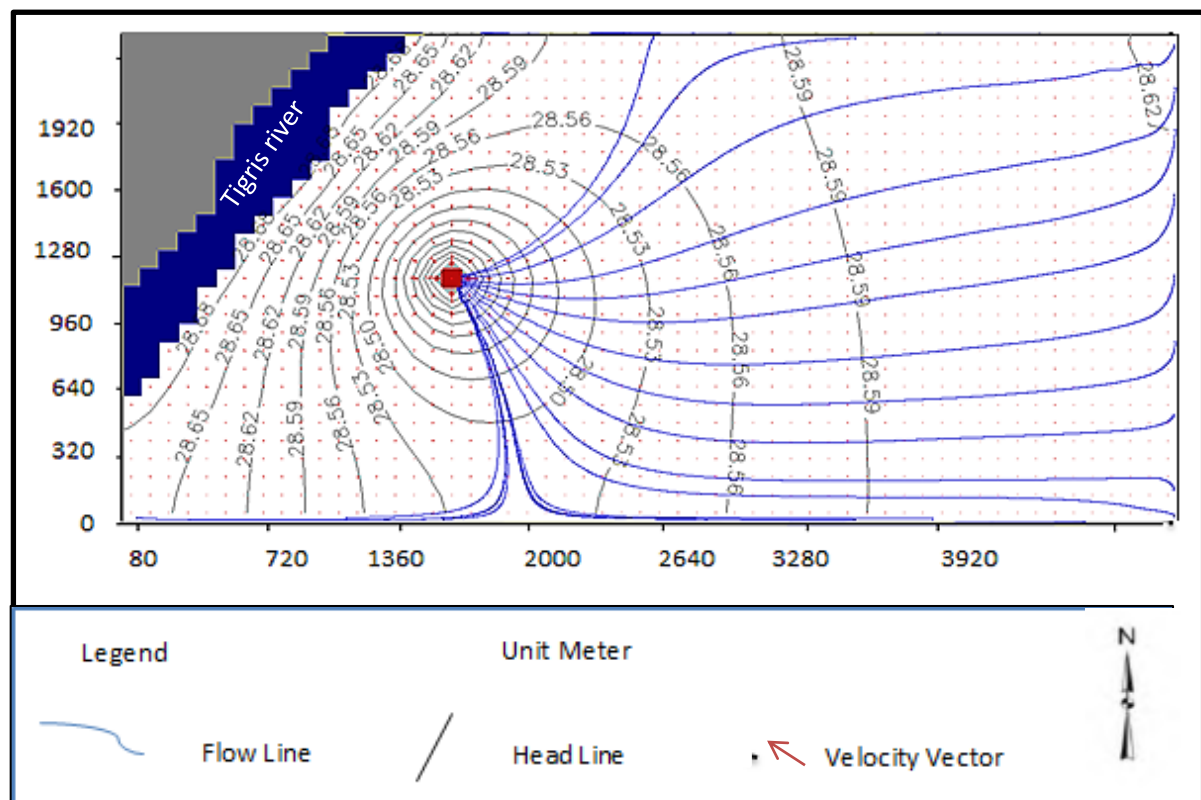


Figure 7b. Groundwater flow net direction in the second layer.

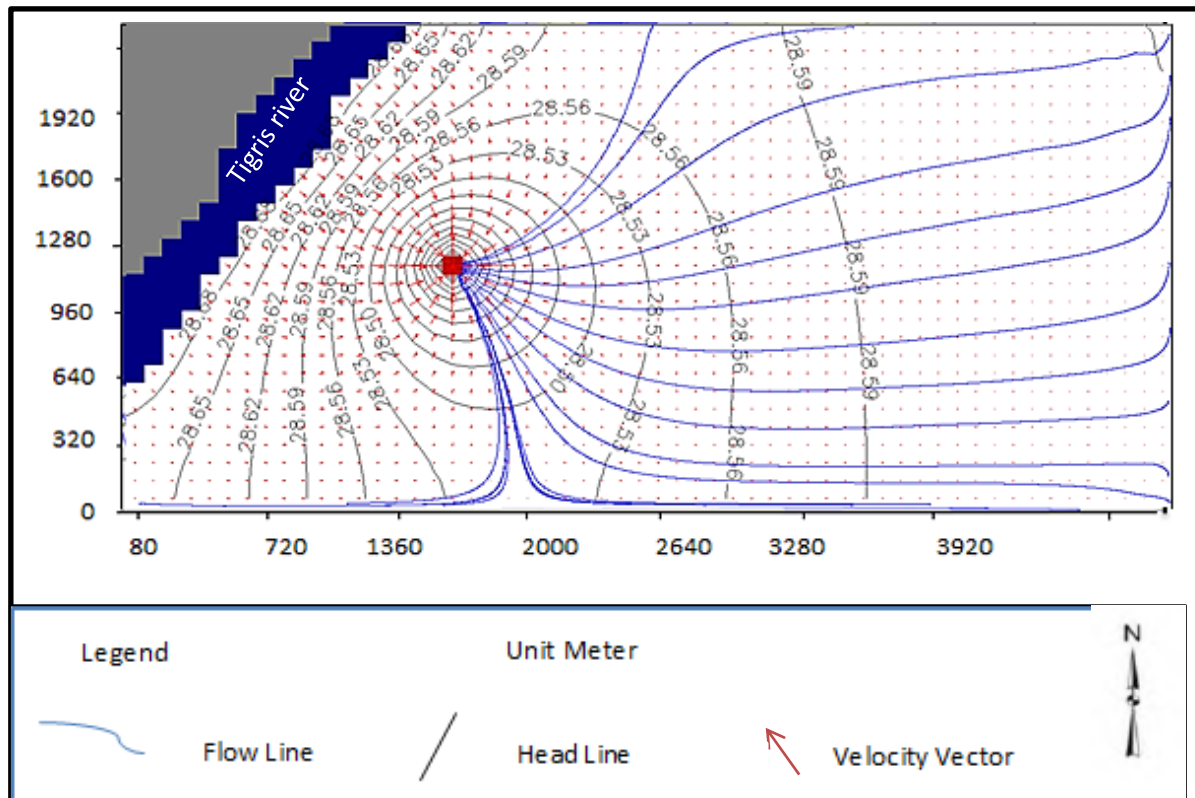


Figure 7c. Groundwater flow net direction in the third layer.

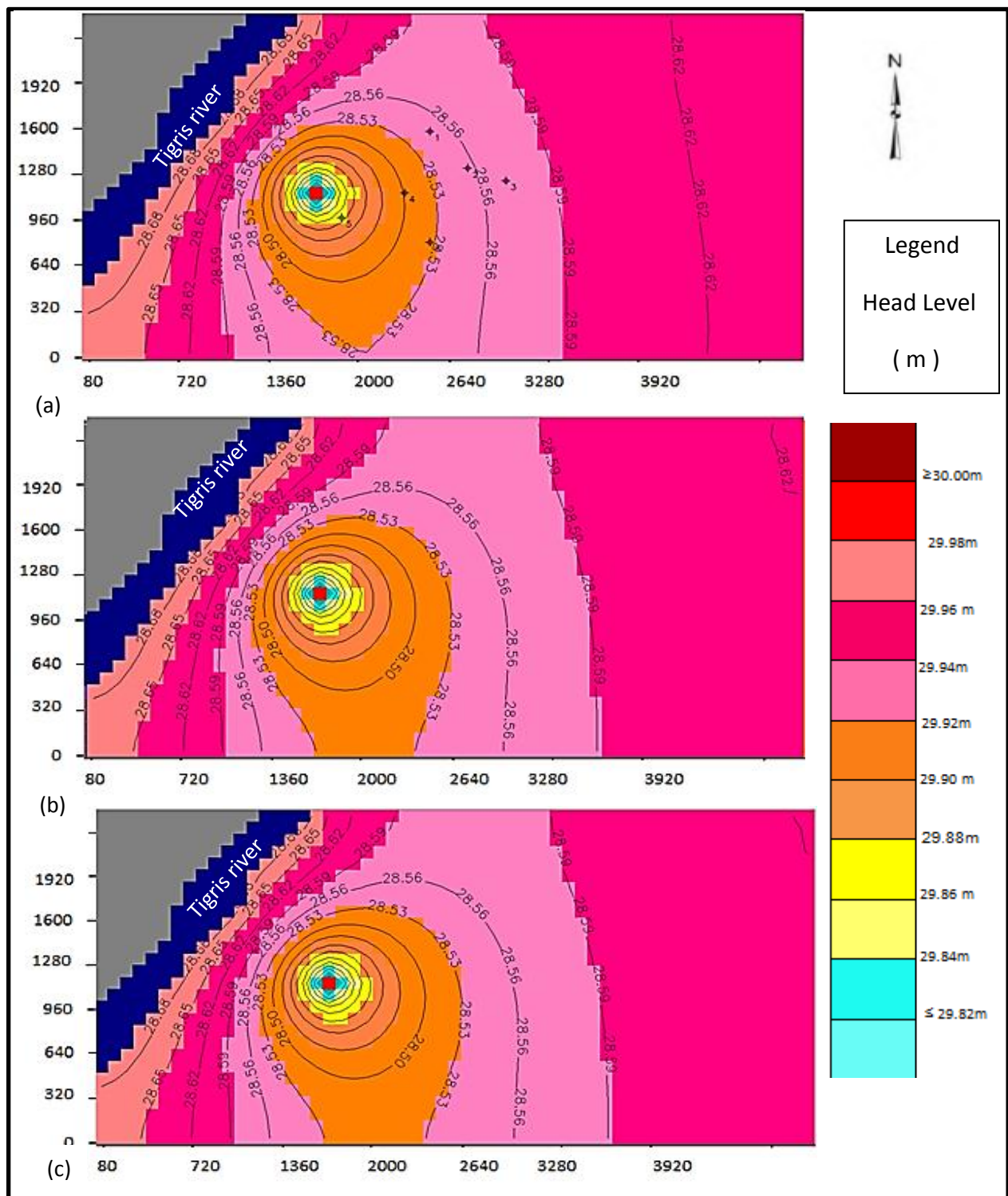


Figure 8. Simulated steady-state of the heads for the study area, (a): contours of hydraulic heads in the first layer, (b): contours of hydraulic heads in the second layer, (c): contours of hydraulic heads in the third layer.

**Table 1.** Water elevation of observation wells, Copland, and Cochran, 2013.

Observation Well	Ground Surface Elevation (m)	Water Table m.a.s.l.	Observation Well	Ground Surface Elevation (m)	Water Table m.a.s.l
W1	31.81	27.79	W4	31.56	27.61
W2	31.57	27.86	W5	31.14	27.14
W3	32.02	27.80	W6	31.88	27.67

Table 2. The aquifer properties.

No. Layer	Soil Type	Layer Type	Hydraulic Conductivity m/s	
			KH	KV
1	Loam /Clay	Unconfined	2×10^{-6}	2×10^{-7}
2	Silt /Fine sand	Confined / Unconfined, Transmissivity varies	7×10^{-5}	7×10^{-6}
3	Medium sand	Confined / Unconfined, Transmissivity varies	3×10^{-4}	3×10^{-5}
Source	Al-Daffaie, 2014	Ali, 2012	Osterbaan, 1986, and Heath, 1983.	Todd, 2005

Table 3. The values of calculated steady-state and observed heads (m) in Nuclear Research Center at Al-Tuwaitha site.

Well No.	Observed Head m.a.s.l	Calculated Head m.a.s.l	Well No.	Observed Head m.a.s.l	Calculated Head m.a.s.l
1	27.79	27.73	4	27.61	27.73
2	27.86	27.75	5	27.14	27.7
3	27.80	27.77	6	27.67	27.74

Aluminium Matrix Composites Fabricated by Friction Stir Processing

A Review

Hussein Burhan Mohammed

Assistant Lecturer

Engineering College Diyala-University

hussein.burhan80@gmail.com

ABSTRACT

Aluminum alloys widely use in production of the automobile and the aerospace because they have low density, attractive mechanical properties with respect to their weight, better corrosion and wear resistance, low thermal coefficient of expansion comparison with traditional metals and alloys. Recently, researchers have shifted from single material to composite materials to reduce weight and cost, improve quality, and high performance in structural materials. Friction stir processing (FSP) has been successfully researched for manufacturing of metal matrix composites (MMCs) and functional graded materials (FGMs), find out new possibilities to chemically change the surfaces. It is shown that the technique of FSP is very promising to modify the microstructure of strengthened metal matrix composite materials. There has the benefit of decline in distortion and flaw of material when FSP uses instead of other manufacturing processes. The aim of the present work is to give a review of technology of (FSP) as a method to produce the aluminium matrix composite, and conclusions of this review will be demonstrated.

Keywords: frictions stir processing, metal matrix composite materials, aluminium alloys.

عرض للمواد المركبة ذات الاساس من الالمنيوم والمصنعة بواسطة عملية الخلط الاحتكاكي

حسين برهان محمد

مدرس مساعد

كلية الهندسة- جامعة ديالى

الخلاصة

تستخدم سبائك الالمنيوم بشكل واسع في صناعات الفضاء والسيارات بسبب كثافتها المنخفضة والخواص الميكانيكية الجيدة و مقاومة البليان والتآكل الافضل وانخفاض معامل التمدد الحراري مقارنة بالسبائك والمعادن التقليدية. انتقل الباحثين مؤخرا من المادة المنفردة الى المواد المركبة لتقليل الوزن والكلفة وتحسين الجودة والاداء العالي للمواد الانشائية. المعالجة بالخلط الاحتكاكي كانت وما زالت تبحث بشكل ناجح لتصنيع المواد المركبة ذات الاساس المعدني والمواد المصنفة وظيفيا والذي كشفت امكانيات حديثة لاجراء تعديل السطوح كيميائيا. يبدو ان تقنية المعالجة بالخلط الاحتكاكي واعدة جدا في تعديل البنية المجهرية للمواد المركبة ذات الاساس المعدني. مقارنة مع عمليات التصنيع الاخرى، المعالجة بالخلط الاحتكاكي لها الافضلية في تقليل التشوه والعيوب في المواد. ان الهدف من هذه الدراسة هو استعراض تقنية المعالجة بالخلط الاحتكاكي كطريقة لتكوين المواد المركبة ذات الاساس من الالمنيوم، ومن ثم توضيح الاستنتاجات من هذا الاستعراض.

الكلمات الرئيسية: عملية الخلط الاحتكاكي، المواد المركبة ذات الاساس المعدني، سبائك الالمنيوم.

1. INTRODUCTION

Composites of metal matrix strengthened by particles with micro or nano size are so effective materials, proper for a many uses. These composites fabricated from metal matrix reinforced with nano particles or fibers show different physical properties and different mechanical properties compare with those of the base metal.

The composites of metal matrix (MMCs) strengthened by particles with nano-size, also called Metal Matrix nano-Composites (MMnCs), are being studied globally in late years, because they have attractive properties suitable for a many applications of function and structure. The interaction between reduced size particles and dislocations has important value because of the nano-scale of strengthening phase, when incorporated with other reinforced influences typically existed in traditional MMCs, lead to a exceptionally enhancement of mechanical properties. **Zhang, and Chen, 2008; Zhang, and Chen, 2006; Sanaty-Zadeh, 2012; Luo, et al. 2012.** Metal matrix composites with micron-size reinforcements have been used with outstanding success in the automotive and aerospace industries, in addition in small engines and electronic packaging applications. In the case of metal matrix nanocomposites, insertion of as little as one volume percentage of nanosize ceramics has led to a much greater increase in the strength of aluminum and magnesium base composites than was achieved at much higher loading levels of micron-sized additions **Rohatgi, and Schultz, 2007**. The greatest challenges facing the development of MMnCs for wide applications are the cost of nanoscale reinforcements and the cost and complexity of synthesis and processing of nanocomposites using current methods. As with conventional metal matrix composites with micron-scale reinforcements, the mechanical properties of a MMnC are strongly dependent on the properties of reinforcements, distribution, and volume fraction of the reinforcement, as well as the interfacial strength between the reinforcement and the matrix. Due to their high surface area, nanosize powders and nanotubes will naturally tend to agglomerate to reduce their overall surface energy, making it difficult to obtain a uniform dispersion by most conventional processing methods. In addition, due to their high surface area and surface dominant characteristics, these materials may also be highly reactive in metal matrices.

Saravanan, et al., 2010. Alloys of aluminum are very attractive for structural applications in aerospace, military and transportation industries because they are lightweight, high strength-to-weight ratio and excellent resistance to corrosion. Nevertheless, the low hardness and low strength of aluminium alloys limit their use, particularly for tribological applications. Thus, to

improve these properties, several properties improvement techniques can be used, from them one is (FSP), **Deepak, et al., 2013**. Rotating pin is particular designed for FSP, as explained in **Fig.1**, it is firstly inserted into the metal to be processed with a suitable tool tilt angle and then moves along the designed paths. The pin generates heat by frictional and plastic deformation within the processing zone. When the tool pin moves, this forces the material to flow around the pin. The forced material flows to the back of the pin, where it is extruded and forged behind the tool, consolidated and cooled under hydrostatic pressure conditions.

Friction stir processing is most commonly used with aluminum, **Johannes et al., 2007. Ma, and Liu, 2008**. Specifically, the effects of processing parameters on the microstructure evolution, deformation behaviors and mechanical properties were investigated, **Cavaliere, et al., 2008; and Cavaliere, et al., 2009**. The use of ceramic particles, such as silicon carbide and aluminum oxide, as reinforcements to form aluminum matrix composites, has been well studied, **Alpas, et al., 1994; Sannino, and Rack, 1995; Deuis, et al., 1997; Gustafson, et al., 1997; Kouzeli, and Mortensen, 2002**. From recent research, it can be illustrated that, for a fixed concentration, fine particles usually give stronger and harder composites, **Kouzeli, and Mortensen, 2002**. Many studies for developing nano- or sub-micro-particles strengthened aluminum composites have been adopted owing to this finding. Techniques of FSP have been successfully used to promote the structure and surface of composite with fine-grains, materials with modified microstructure, and synthesizing the composite and intermetallic compound in situ. For instance, by FSP, it was obtain on a finegrained microstructure for high-strain-rate superplasticity in the commercial 7075Al alloy, **Ma, et al., 2002**. Moreover, the technique of FSP has been used to create a surface composite on aluminum substrate, **Mishra, et al., 2002** and the homogenization of powder metallurgy (PM) aluminum alloys, metal matrix composites, and cast aluminum alloys, **Berbon, eta l., 2001; Ma , et al., 2003**.

This work can be considered a reference of FSP and it supplies a review of (FSP) technique for fabrication the aluminium metal-matrix composite as well.

2. FABRICATION MMCS USING FSP

It is well documented that the volume fraction and size of reinforcing phases also the characteristics of base metal-reinforcement interface control the mechanical properties of MMCs, **Shafiei-Zarghani, et al., 2009**. Powder metallurgy (P/M) method or processing of molten metal has been the main routes to fabricate particle-reinforced metal matrix composites.

However, obtaining a uniform dispersion of fine reinforcement particles within the matrix is especially challenging through traditional casting or P/M processing. It is mainly because of the natural trend of fine particles to agglomeration during blending of the matrix and the reinforcement powders. It has been shown that FSP can be employed to fabricate aluminum matrix composites *in-situ* without supplementary consolidation process. The application of FSP to produce MMCs has the following advantages, **Yang, et al., 2010**:

- a. Inducing severe plastic deformation to further mixing and refining of constituent phases in the material.
- b. Generation of high temperature to ease the *in-situ* reaction to develop reinforcing particles.
- c. Causing hot consolidation to establish fully dense solid.

On the other hand, the presence of the reinforcement particles in the metallic matrix leads to brittleness, which generally is not desirable. Therefore, instead of bulk reinforcement, incorporation of the particles to the surface enhances the wear properties, which is a surface dependent degradation mode, without sacrificing the bulk properties, **Dixit, et al., 2007**. Nevertheless, it is challenging to effectively distribute particles of ceramic on a metallic surface by conventional surface treatments. The processing techniques existent to produce surface composites are rely on processing during liquid phase at elevated temperatures. However, it is tough to prevent the reaction at interface between the reinforcement and base metal and the development of some harmful phases. In addition, to achieve a perfect solidified microstructure in surface layer monitor of processing parameter seems to be crucial. Apparently, processing of surface composite at low temperature, below the melting point, can prevent these problems, **Lim, et al., 2009**. In this case, FSP, as a solid state processing technique, can be successfully employed to produce surface composites.

3. FRICTION STIR PROCESSING TO FABRICATE ALUMINIUM MATRIX COMPOSITES

3.1 Fabrication Micro Composites

3.1.1 Aluminium Matrix Composite with Fine Grained and Modified

Due to substantial friction heating and severe plastic deformation during FSP, dynamic recrystallization occurs in the stirred zone (SZ), resulting in fine and equiaxed recrystallized grain of absolutely uniform size, **Mishra, et al., 2003**. **Hsu et al., 2005** observed that the Al-

Al₂Cu composite fabricated by in-situ became ultra-fine-grained composite after FSP. For the Al-Cu sintered billet, the reaction between Al and Cu was not achieved at sintering temperature 500 °C for 20 min. The reaction was significantly enhanced when sintering temperature reached at 530 °C. However, the initial coarse Cu or resultant Al₂Cu particles were heterogeneously dispersed in the aluminium matrix, **Fig.2** (a). This pointed out, that although a higher sintering temperature and a longer time can result in carry out the reaction between aluminium and copper, Heterogeneity distribution and coarseness of resultant particles of Al₂Cu are clear feature. Ultra-fine-grained Al-Al₂Cu composite obtained at two-pass FSP on the billets sintered at both 500 °C and 530 °C was owing to complete Al-Cu reaction and a uniform dispersion of the resultant Al₂Cu particles in the matrix of aluminum, **Fig.2** (b). This ultra-fine grained Al-Al₂Cu composite exhibited higher hardness and compressive strength. Lately, **Hsu, et al., 2006**, studied the influence of FSP on the in-situ reaction way between Al and Ti in an Al-Ti sintered billet. They observed that sintering at 610 °C temperature could achieve just a little amount of Al-Ti reaction came about around the Ti particles, **Fig.3** (a). The reaction the in-situ was importantly accelerated by the FSP. When a four-pass FSP occurred, the reaction between aluminium and titanium completed fundamentally, and dispersion of the Al-Ti nano-particles formed in situ in the ultra-fine-grained aluminum matrix was obviously revealed, as demonstrated in **Fig.3** (b). From results of tensile test, it can be seen that, the resultant composite of Al-Al₃Ti shows high strength and modulus Table 1. The modulus and strength increased with increase in the Ti content, while the ductility decreased. The Al-10 at. pct Ti composite showed a interconnection of high strength/modulus and good ductility. **Ma et al., 2006** investigated the effect of common parameters of FSP on sand-cast A356 plates. The results showed that coarse primary aluminum dendrites and coarse acicular particles of Si were broken up due to effect of FSP, in addition the closure of casting porosities, and the uniform spread of broken particles of Si in the aluminum matrix, as shown in **Fig.4** (b). With increase passes number of FSP and rotational speed, the size and aspect ratio of the Si particles and the level of porosity decreased as result of the effect of intensified stirring (see Table 3). Similarly, **Santella, et al., 2005** indicated that the coarse and heterogeneous cast structure of A319 and A356 was destroyed and then, a uniform distribution of broken second-phase particles is created due to influence of FSP, see **Fig.5** (b). In addition, the images of TEM showed the creation of a fine-grained structure of 5 to 8 μ m in FSP A356 and 2 to 3 μ m in FSP ADC12, **Ma, et al. 2006**. Also, they observed that the size of grain in the FSP specimens is much smaller than that in the as-cast structures, pointing

out the occurrence of dynamic recrystallization during FSP. **Tewari et al. Lakshminarayanan, and Balasubramanian, 2008** investigated the influence of SiC particle orientation modified owing to FSP. The information of microstructure for SiC/A6061 composite materials with and without FSP single step was obtained through high-resolution, large-area images. Anisotropic shape with an average aspect ratio approximately 1.6 to 1.8 was observed for the particles of SiC. The image of the composite by scanning electron microscopic in **Fig.6 (a)** explained such a morphological feature. Orientation statistics of particle indicated that there are preferred orientations for the nonequiaxed particles of SiC after extrusion processing. As illustrated in **Fig.6 (b)**, the arrangement of the SiC particles is parallel to the direction of extrusion. The axis of extrusion is vertical. The passage of the friction stir tool maybe modified the preferred orientation. From **Fig.6 (c)**, it can be observed, that the particles were redistributed at 45° to the extrusion and transverse directions. The tool motion of FSP is horizontal, left to right. The microstructural information consistently point out that important microstructural change occur during FSP, contain re-orientation of the reinforcement particles, and an important decline in the levels of microstructural heterogeneity and microstructural anisotropy.

3.1.2 Friction-Stir Surface/Bulk Composite

Since altering the parameters of FSP, vertical pressure, tool design, and active cooling/heating influence on the grain microstructure, it seems that the mechanical properties of a metallic material can be custom-made through FSP. An increase in both hardness and yield strength (YS) has been reported due to continuously reduction in the grain size of aluminum alloys by changing the FSP parameters. FSP has been also studied to develop layers of hard materials on soft matrix, as alloys of aluminium based.

Wang et al. Wang, et al., 2013 they used FSP to fabricate bulk SiC-reinforced aluminum MMCs. The rolled plate of 5A06Al and commercial powder of SiC were employed in this work. In the side of advancing at the pin edge a groove was machined, which had depth and width 1.0 and 0.5-mm respectively. At a distance 2.8 mm from the centerline, the groove was, and before processing, the powder of SiC was put into the groove. The high-speed steel was used to make the cylindrical tool of FSP with with a screwed pin. The plate was penetrated by the tool until the head face of shoulder reached 0.5 mm under the upper surface. The travel speed was 95 mm/min along the centerline and the rotational speed of tool was 1180 rpm. The dispersion of produced MMCs did not restrict to surface composites under the shoulder of tool but, the particles of SiC

could flow upwards of the thermomechanical affected zone (TMAZ) under the shoulder of tool, and it covered the range at a distance 1.5 mm of the pin edge at the advancing side. Nevertheless, the in deeper position, width became narrower, and the dispersion of MMCs was about 2.5 mm at the depth of 2 mm, which was in the pin range at the advancing side. Roughly, 88 HV the value of microhardness of matrix was. The microhardness was constant, 10% higher than the matrix, on the depth of 0.5 and 1.0 mm under surface owing to integral distributed SiC.

3.2 Fabrication Nano Composites

3.2.1 Fine grained and modified structure of aluminium matrix composite

Shahraki et al., 2013 used the friction stir processing (FSP) to produce AA5083/ZrO₂ nanocomposite layer. The sheet of 5083- H321 aluminum alloy with 5 mm thickness was used for the FSP experiments. The rectangular sheets with 300 mm in length and 300 mm in width were used as samples in this work. Commercially, powder of ZrO₂ with nano average diameter ~ (10 to 15) nm and purity ~99.9 pct was provided by the TECNON, S.L. Company. A groove of 1 mm width and 2 mm depth was machined on the AA5083 plate and then filled by the ZrO₂ powder before the FSP was carried out. The 2436 steel alloy was used to make the rotational tool in the process, encompasses a concave shoulder with a diameter of 18 mm and a triangle pin with diameter and length of 6 and 3.3 mm, respectively. The angle of tilt was approximately 3°. The pin was inserted into the groove filled with the nanopowder of ZrO₂. Two passes of the FSP was carried out at traverse speeds of 40, 80, 125, and 160 mm/min and tool rotation rates of 800, 1000, and 1250 rpm. It was indicated that the best choice to distribute the nanoparticles homogeneously in the matrix could be increasing the passes number of FSP. **Faraji et al., 2011** to investigate the microstructures of Al/ZrO₂, both optical microscopy (OM) and scanning electron microscopy (SEM) were used, as shown in **Fig.7** (a). also, VEGA II LMH SEM (Tescan, a.s., Brno, Czech Republic) equipped with an energy dispersive X-ray spectroscopy (EDS) analysis system was used to analysis the chemical composition of local areas in the specimens. In **Fig.7** (b), it can be seen the nanosized ZrO₂ particles distribution in the SZ. Depending on the parameter of Zener-Holoman, the grain size decreases with increasing the volume fraction of ZrO₂ particles, **El-Danaf, et al., 2010**. The corresponding mechanical properties of FSP specimens were assessed through tensile test and microhardness measurements. Samples of tensile were machined to the depth that FSP was applied along the longitudinal direction. The samples of the FSP with nano-particles of ZrO₂ showed that microstructures refined to a much smaller scale than the base metal alloy. The recrystallized

grains were equiaxed and had a similar size dispersion. The substrates microhardness was clearly increased after the FSP with ceramic particles. In majority of the processed samples, the hardness was greater with the maximum rise to be approximately 30 pct. The maximum value of microhardness for Al/ZrO₂ composite was approximately 134 HV, whilst that of the parent alloy was about 93 HV, as shown in **Fig.8 (a)**. For the samples without any defect and with uniform dispersion of ZrO₂ particles, FSP increased the ultimate strength of the parent material by approximately 10 pct this, as shown in **Fig.8 (b)**. **Zarghani, et al., 2009**. Used nanosized powder of Al₂O₃ with 50 nm average diameter and a extruded rod of commercial 6082 Al with 7 mm a thickness as reinforcement particulates and matrix, respectively. The Quenched H-13 tool steel was used to fabricate the pin with length and diameter 4 and 5 mm respectively. The pin traverse speed was set to be 135 mm/min and its rotational speed was 1000 rpm. To insert nano powder of Al₂O₃, a groove was machined with a width of 1mm and depth of 4 mm, in which the required amount of Al₂O₃ particles was crammed in. A tool without pin was used to close the groove to prevent sputtering of powder during the process. Various numbers of passes FSP from one to four have been carried out on the specimens, with and without powder of Al₂O₃. After each pass, at room temperature air-cooling was used. **Fig.9 (a)**. illustrated the optical micrograph of the parent 6082 Al. The using of FSP resulted in refine the size of grain of matrix, as explained in **Fig.9 (b)**. The distribution of Al₂O₃ particles in the surface composite layer was better when three FSP passes than that one FSP pass. Aggregation of nanosized Al₂O₃ particles occurred in some region. Furthermore, it could be observed that the FSP carried out by four passes, resulted in layer of surface composite with good distribution of nano-sized particles of Al₂O₃, as explain in **Fig.9 (c)**. As indicated by other researchers **Java, et al., 2002; Sato and Kokawa, 2001**, it was reported that the dynamic recrystallization occurred during FSP resulted in grain refinement. In fact, the FSP with the nanosized particles of Al₂O₃ has seen to be significant in reduction of the grain size of the 6082 Al matrix up to less than 300 nm this can be seen clearly in **Fig.9 c** and **d**. It has been considered that, the pinning impact by the nanosized Al₂O₃ particles prevent the growth of the grains for the considered 6082 Al matrix. the considered microhardness results have been obtained from the central cross-sectional zones of the friction stir processed specimens as shown in **Fig.10 (a)**. the hardness value have increased by about three times as compared to its value in the parent Al alloy. This has been carried out in the surface composite layer produced by four FSP passes. In the case of 6082 Al alloy where no alumina powder is added, after four passes of FSP, the microhardness image depicted a softening and decline of

hardness in the SZ contrary to that of the base Al metal. In this work, the wear kinetics have been compared due to the weight loss as the specimen has been used to be the pin and the material of disk from the GCr15 steel, as can be seen in **Fig.10** (b). The wear weight loss has increased with sliding distance. For the parent Al metal, the wear rate (weight loss/sliding distance) was of low value at the initial period of wear as it is increased then. At the nanocomposite layer surface produced by four FSP passes, the wear rate tends to be constant within sliding time. The wear resistance against a steel disk has been enhanced by about two to three times in the Al/ Al₂O₃ surface nanocomposite layer produced by four FSP passes. This has been in comparison to with the base Al metal. In fact, the wear mechanism was considered to be a combination of abrasive and adhesive wear. The enhancement in the wear resistance of the surface composite layer might be explained due to the lower coefficient of friction and hardness increment.

3.2.2 Surface/Bulk aluminium matrix composite

Sahraeinejad, 2014 used friction stir processing for fabricating of Surface Metal Matrix Composites. Different particles at sizes ranged between 130 nm and 4.3 µm, and different process parameters, were employed to have a uniform distribution of particles within the processed region. In this study, the FSP was used to fabricate the composite by insert the reinforcement powders into the matrix of aluminum through a groove machined with 4 mm width and 2 and 4-mm depth in the matrix to contain the reinforcement. A cylindrical tool without pin was used with plate of material to close the groove to prevent the powder from sputtering out the groove. Mechanical properties of the composites of Al 5059 matrix reinforced with Al₂O₃, SiC, and B₄C were got and compared. From results of tensile tests, it cab observed that demonstrated yield strength increases by 20, 32, and 38 percent compared to the matrix alloy for composites containing Al₂O₃, SiC, and B₄C, respectively, three passes of FSP were carried out using different tools explained in Table 4, also the Process parameters are summarized in Table 5.

The effect of particle type and size dispersion was investigated in Al alloy matrix composites fabricate by FSP. The mechanical and fracture behaviour was compared between the composites, and the main results were that:

- ❖ Reinforcement particles were homogenously distributed in the lower and upper parts of the stir zone when the number of FSP passes increased.

- ❖ 3-pass FSP composites made with a 2-mm groove and reinforced by particles illustrates an increase of ~15% in the hardness profile as compared with FSP composite with no powder. This obviously proves the influence of powder inclusion on the hardness profile.
- ❖ Composites reinforced by B₄C particles showed the highest tensile yield strength; however, their ductility drastically declined to 2.5% elongation in comparison to the parent considered
- ❖ When using 4.3- μm Al₂O₃ particles, the FSP technique lead to a 10 multiply refinement in the particle, whilst 1.1- μm Al₂O₃ particles are only refined to about half of their original size owing to the less effective attrition within the severely deformed stir zone.

Samiee et al., 2011 FSP was employed to fabricate surface layer of Al/AlN nano-composite on 6061 Al alloy matrix. FSP was carried out on 10 mm thick rolled plates of commercial 6061 aluminum alloy as base metal, chemical composition of Al alloy is shown in Table 6. Nano-sized AlN particles with an average diameter of ~50 nm and 99.9% purity was used as particulate reinforcement. The tool was machined with 16 mm shoulder diameter, pin tool 5 mm diameter and 4 mm length. A 3° tilt angle of the fixed pin tool was used. Nano-sized AlN particles were inserted in matrix through a groove machined with 1 and 3 mm width and depth respectively. The FSP were carried out with two passes at travel speed of 310 mm/min and rotation rates of 900, 1120 and 1800 rpm, respectively. From optical micrographs, it can be observed that the SZ contain fine, uniform and equiaxed grains, **Fig.11** (c), because of the dynamic recrystallization. The grain became smaller compared to the parent metal, this due to serious plastic deformation and high temperature. The stirred zone is surrounded by the thermo-mechanically affected zone (TMAZ), **Fig.11** (d) and by a small heat affected zone, (HAZ), **Fig.11** (e). Since recrystallization doesn't occur in this region owing to low temperature, the grains of the TMAZ are larger and less equiaxed than the stirred zone. In **Fig.12**, it can be seen that the agglomeration of nano-sized AlN particles observed in the SZ owing to decrease in rotational speed. Uniform dispersion of nano-sized AlN particles and less agglomeration of nano-sized AlN particles in the SZ have arisen from the higher rotational speed **Faraji and Asadi, 2010 Barmouz, et al., 2010**. From **Fig.12** (c) and **Fig.11** (c), it can be reported that the grain refinement in the SZ has arisen from presence the powder of the nano-sized AlN.

5. CONCLUSIONS

FSP has been one of successful and significant processes for fabrication of Aluminium Matrix Composite (AMC) and modification the microstructure of reinforced metal matrix composite

materials. Most of the results revealed that for different alloys of aluminium, FSP produces grain refinement equiaxed as a result of dynamic recrystallization and homogeneous grain structure. These resulted in enhancement of the mechanical properties of aluminium alloys, such as hardness and tensile characteristics. The new advances in adding reinforcing particles to manufacture surface alloys and base metal composites are a breakthrough in this technology finding new possibilities to manufacture composites nanostructured with huge and attractive properties. FSP parameters such as rotational speed of tool, travel, linear speed of tool, spindle tilt angle, and depth are decisive parameters to prepare the MMCs with good properties (mechanical properties and structural characteristics) and product free defects. In addition, the type and vol. pct of ceramic powder as well as the interfacial strength between the base metal and the reinforcement powder play role to improve the properties of MMCs.

REFERENCES

- Alpas, A. T., and Zhang, J., 1994, *Effects of microstructure (particulate size and volume fraction) and counter face material on the sliding wear resistance of particulate reinforced aluminum matrix composites*, Metallurgical and Materials Transactions, Vol. 25, pp. 969–983.
- Asadi, P., Faraji, G., and Besharati M. K., 2010, *Producing of AZ91/SiC composite by friction stir processing*, Int J Adv Manuf Technol, 51; pp. 247–260.
- Barmouz, M., Besharati Givi, Seyfi, J., 2010, Materials characterization, Vol. 62, pp. 108- 117.
- Cavaliere, P., De Santis, A., Panella, F., and Squillace, A., 2009, *Effect of welding parameters on mechanical and microstructural properties of dissimilar AA6082-AA2024 joints produced by friction stir welding*, Mater. Des., 30, pp. 609–616.
- Cavaliere, P., Squillace, A., and Panella, F., 2008, *Effect of welding parameters on mechanical and microstructural properties of AA6082 joints produced by friction stir welding*, J. Mater. Process. Technol., 200, pp. 364–372.
- Deepak, D., Sidhu, S. R., and Gupta, V. K., 2013, *Preparation of 5083 Al-SiC surface composite by friction stir processing and its mechanical characterization*, International Journal of Mechanical Engineering ISSN: 2277-7059 Vol.3.
- Deus, R. L., Subramanian, C., and Yellup, J. M., 1997, *Dry sliding wear of aluminum composites—A review*, Composites Science and Technology, Vol.57, pp. 415–435.
- Dixit, M., Newkirk, J. W. and Mishra, R. S., 2007, *Properties of friction stir-processed Al 1100-NiTi composite*, Scripta Materialia, Vol. 56, pp. 541-544.
- El-Danaf, E. A., El-Rayes, M. M., and Soliman, M. S., 2010, *Friction stir processing: An effective technique to refine grain structure and enhance ductility*, Mater. Des., Vol. 31, pp. 1231–36.
- Faraji, G., Asadi, P., 2010. *Characterization of AZ91/alumina nanocomposite produced by FSP*, Materials Science and Engineering, A528, pp. 2431-2440.

- Faraji, G., Dastani, O., and Mousavi S. A., 2011, *Effect of Process Parameters on Microstructure and Micro-hardness of AZ91/Al₂O₃ Surface Composite Produced by FSP*, *J. Mater. Eng. Perform.*, Vol. 20, pp. 1583–90.
- Gustafson, T. W., Panda, P. C., Song, G., and Raj, R., 1997, *Influence of microstructural scale on plastic flow behavior of metal matrix composites*, *Acta Materialia*, Vol. 45: pp. 1633–1643.
- Hsu, C. J., Chang, C. Y., Kao, P. W., Ho, N. J., and Chang, C. P., 2006, *Al–Al₃Ti nanocomposites produced in situ by friction stir processing*, *Acta Mater.*, Vol. 54, pp. 5241–49.
- Hsu, C. J., Kao, P. W., and Ho, N. J., 2005, *Ultrafine-grained Al–Al₂Cu composite produced in situ by friction stir processing*, *Scripta Mater.*, Vol. 53, pp. 341–45.
- Java, K. V., Sankaran, K. K., and Rushau, J. J., (2000), *Friction-stir welding effects on microstructure and fatigue of aluminum alloy 7050-T7451*, *Metall Mater Trans A* 31A, pp. 2181–2188.
- Johannes, L. B., Charit, I., Mishra, R. S., and Verma, R., 2007, *Enhanced superplasticity through friction stir processing in continuous cast AA5083 aluminum*, *Mater. Lett*, 464, pp. 351–357.
- Kouzeli, M., and Mortensen, A., 2002, *Size dependent strengthening in particle reinforced aluminum*, *Acta Materialia*, Vol. 50, pp. 39–51.
- Lakshminarayanan, A. K., and Balasubramanian, V., 2008, *Process parameters optimization for friction stir welding of RDE-40 aluminium alloy using Taguchi technique*, *Trans. Nonferrous Met. Soc. China*, Vol.18, pp. 548–554.
- Lim, D. K. Shibayanagi, T. and Gerlich, A. P., 2009, *Synthesis of multi-walled CNT reinforced aluminium alloy composite via friction stir processing*, *Materials Science and Engineering*, vol. 507, pp. 194–199.
- Luo, P., McDonald, D.T., Xu, W., Palanisamy, S., Dargusch, M.S., and Xia. K. A., 2012, *Modified Hall–Petch Relationship In Ultrafine-Grained Titanium Recycled From Chips By Equal Channel Angular Pressing*, *Scripta Mater*, 66, pp. 785–788.
- Ma, Z. Y., and Liu, F. C., 2008, *Achieving exceptionally high superplasticity at high strain rates in a micrograined Al-Mg-Sc alloy produced by friction stir processing*, *Scr. Mater*, 59, pp. 882–885.
- Ma, Z. Y., Mishra, R. S., and Mahoney, M. W., 2002, *Superplastic deformation behaviour of friction stir processed 7075Al alloy*, *Acta Mater.* Vol. 50, pp. 4419.
- Ma, Z. Y., Sharma, S. R., Mishra, R. S., and Mahoney, M. W., 2006, *Microstructural modification of as-cast Al-Si-Mg alloy by friction stir processing*, *Metall. Mater. Trans.*, vol. 37A, pp. 3323–36.
- Mishra R. S., Ma, Z. Y., and Charit, I., 2003, *Friction stir processing: a novel technique for fabrication of surface composite*, *Mater. Sci. Eng.*, Vol. A341, pp. 307–10.
- Sahraeinejad, S., 2014, *Fabrication of Surface Metal Matrix Composites Using Friction Stir Processing*, Thesis of MSc, Mechanical Engineering, University of Waterloo, Ontario, Canada.
- Sammiee, M., Honarbakhsh-Raouf, A., and Kashani, S. F., 2011, *Microstructural and Mechanical Evaluations of Al/AlN Nano-Composite Surface Layer Produced via Friction Stir Processing*, *Australian Journal of Basic and Applied Sciences*, 5(9): 1622–1626.

- Sanaty-Zadeh, A., 2012, *Comparison between current models for the strength of particulate-reinforced metal matrix nanocomposites with emphasis on consideration of Hall–Petch effect*, Mat. Sci. Eng., 531, pp. 112–118.
- Sannino, A. P., and Rack, H., 1995, *Dry sliding wear of discontinuously reinforced aluminum composites: Review and discussion*, Wear, 189, pp 1–19.
- Santella, M. L., Engstrom, T., Storjohann, D., and Pan, T. Y., 2005, *Effects of friction stir processing on mechanical properties of the cast aluminum alloys A319 and A356*, Scripta Mater., Vol. 53, pp. 201–06.
- Saravanan, C., Subramanian, K., Sivakumar, D. B., Sathyanandhan, M., and Narayanan, S. R., 2005, *Fabrication of Aluminium Metal Matrix Composite –A Review*, Journal of Chemical and Pharmaceutical Sciences www.jchps.com. ISSN: 0974-2115. pp 82-87.
- Sato, Y. S., and Kokawa, H., 2001, *Distribution of tensile property and microstructure in friction stir weld of 6063 aluminum*, Metall Mater Trans A 32A, pp. 3023–3031.
- Shafiei-Zarghani, A., Kashani-Bozorg, S. F., and Zarei-Hanzaki, A., 2009, *Microstructures and mechanical properties of Al/Al₂O₃ surface nano-composite layer produced by friction stir processing*, Materials Science and Engineering, Vol. 500, pp. 84-91.
- Shahraki, S., Khorasani, S., Behnagh, R. A., Fotouhi, Y., and Bisadi, H., 2013, *Producing of AA5083/ZrO₂ Nanocomposite by Friction Stir Processing (FSP)*, Metallurgical and Materials Transactions, Vol.44B, No. 4. Pp 1546-1553.
- Sharma, Z. Y., Ma, S. R., Mishra, R. S., and Manohey, M. W., 2003, *microstructural modification of cast aluminum alloys via friction stir processing*, Mater. Sci. Vol. 426, pp. 2891–2896.
- Wang, W., Shi, Q., Liu, P., Li, H., and Li, T., 2013, *A novel way to produce bulk SiCp reinforced aluminum metal matrix composites by friction stir processing*, J Mater Process Technol, Vol. 209, pp. 2099-2103.
- Y. Morisada, Y., Fujii, H., Nagaoka, T., Nogi, K., and Fukusumi, M., 2007, *Fullerene/A5083 composites fabricated by material flow during friction stir processing*, Composites Part A: Applied Science and Manufacturing, Vol. 38, pp. 2097-2101.
- Yang, M., Xu, C., Wu, C., Lin, K. C., Chao, Y. J., and An, L., 2010, *Fabrication of AA6061/Al₂O₃ nano ceramic particle reinforced composite coating by using friction stir processing*, Journal of Materials Science, Vol. 45, pp. 4431-4438.
- Zarghani S. A., Kashani-Bozorg S. F., and Zarei-Hanzaki A., 2009, *Microstructures and mechanical properties of Al/Al₂O₃ surface nano-composite layer produced by friction stir processing*, Mater Sci Eng, Vol. 500, pp. 84–91.
- Zhang, L., Chandrasekar, R., Howe, J. Y., West, M. K., Hedin, N. E., and Arbogast, W. J., 2009, *A Metal Matrix Composite Prepared from Electrospun TiO₂ Nanofibers and an Al 1100 Alloy via Friction Stir Processing*, Applied Materials and Interfaces, Vol. 1, pp. 987-991.
- Zhang, Z., and Chen, D. L., 2006, *Consideration of Orowan strengthening effect in particulate-reinforced metal matrix nanocomposites: A model for predicting their yield strength*, Scripta Mater, 54, pp. 1321–1326.
- Zhang, Z., and Chen, D. L., 2008, *Contribution of Orowan strengthening effect in particulate-reinforced metal matrix nanocomposites*, Mat. Sci. Eng., pp. 483–484, 148–152.

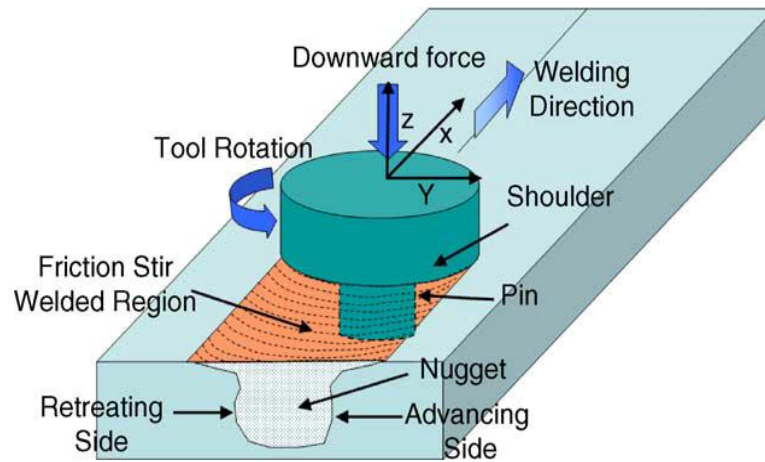


Figure 1. Schematic drawing of friction stir processing. **Mishra, et al., 2003.**

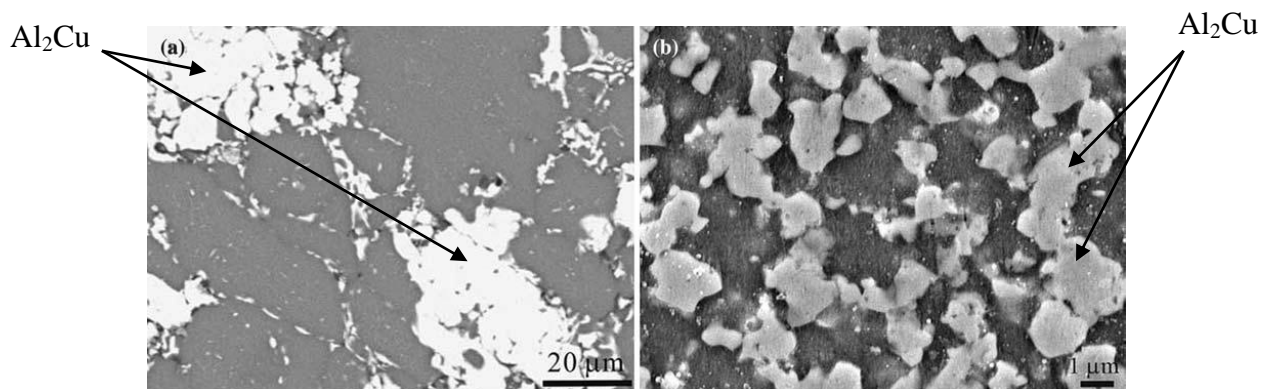


Figure 2. Backscattered electron imaging (BEI) of Al-15 at. pct Cu samples sintered at 530 °C, showing (a) coarse $\text{Al}_2\text{Cu}/\text{Cu}$ particles under as-sintered condition and (b) fine and uniformly distributed Al_2Cu particles after a subsequent two-pass FSP. **Hsu, et al. 2005.**

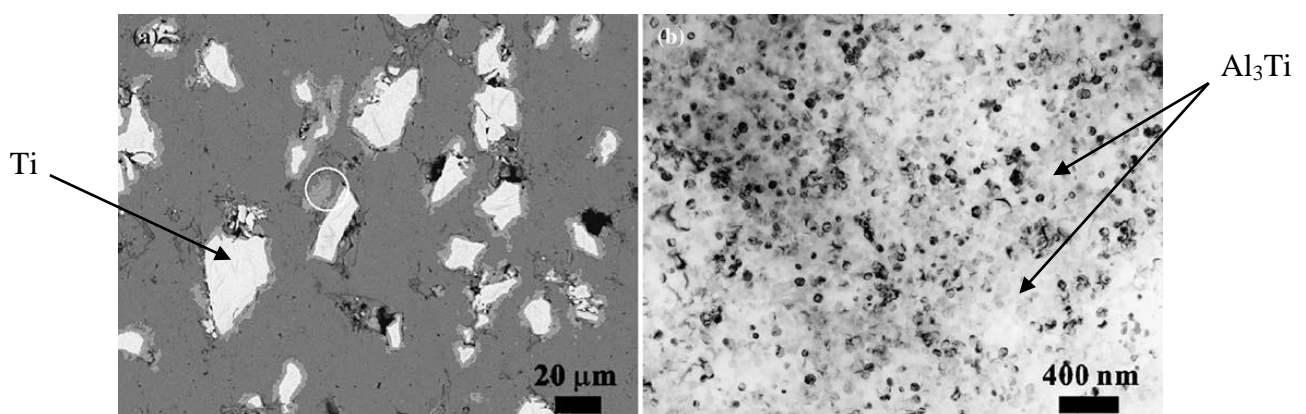


Figure 3. (a) BEI showing coarse unreacted Ti particles in Al-15 at. pct Ti sample sintered at 610 °C and (b) TEM bright-field image showing uniformly distributed nanosized Al_3Ti particles in four-pass FSP Al-10 at. pct Ti sample. **Hsu, et al., 2006.**

Table 1. Tensile Properties of Al-Al₃Ti Composites Prepared by Four-Pass FSP. **Hsu, et al., 2006.**

Materials	E (GPa)	YS (MPa)	UTS (MPa)	El. (Pct)
Al-5 at. pct Ti	82	277	313	18
Al-10 at. pct Ti	95	383	435	14
Al-15 at. pct Ti	108	471	518	1

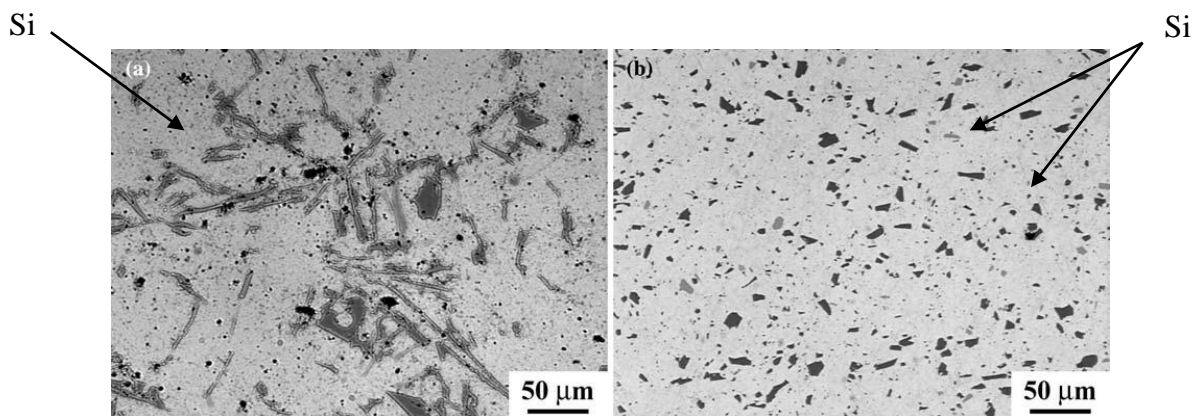


Figure 4. Optical micrographs showing morphology and distribution of Si particles in A356 samples: (a) as-cast and (b) FSP at 900 rpm and 203 mm/min. **Ma, et al. 2006.**

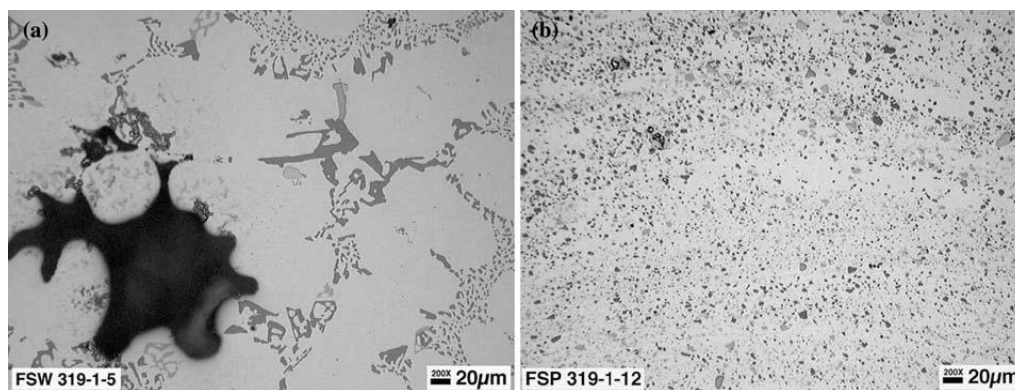


Figure 5. Optical micrographs showing (a) as-cast microstructure and (b) SZ of A319 (1000 rpm, 102 mm/min). **Ma, et al. 2006.**

Table 3. Size and Aspect Ratio of Si Particles and Porosity Volume Fraction in FSP and As-Cast A356 Ma, et al. 2006.

Materials	Particle Size (lm)	Aspect Ratio	Porosity Volume Fraction (Pct)
As-cast	16.75	5.92	0.95
FSP, 300 rpm, 51 mm/min	2.70	2.30	0.087
FSP, 900 rpm, 203 mm/min	2.50	1.99	0.032
FSP, 900 rpm, 203 mm/min, 2 pass	2.43	1.86	0.020

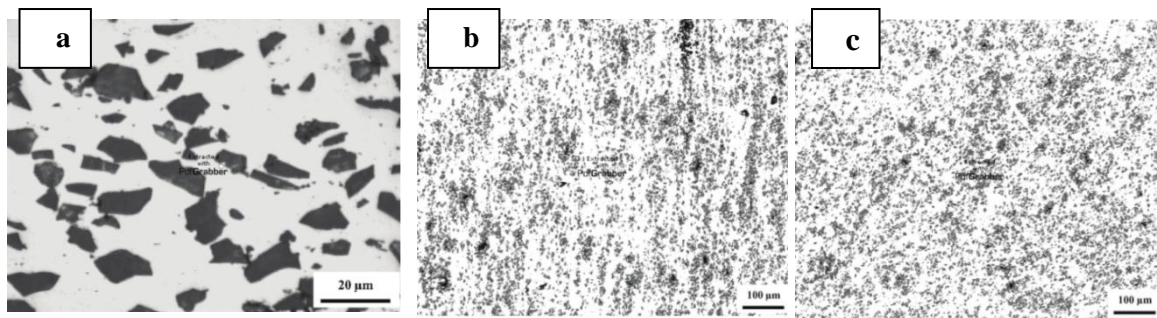


Figure 6. Microstructure change in SiC particle reinforced A6061 due to FSP (after Tewari et al. Lakshminarayanan, and Balasubramanian, 2008): (a) scanning electron microscopic image of the composite showing the anisotropic shape of SiC particles; (b) as-extruded SiC/Al; (c) after FSP.

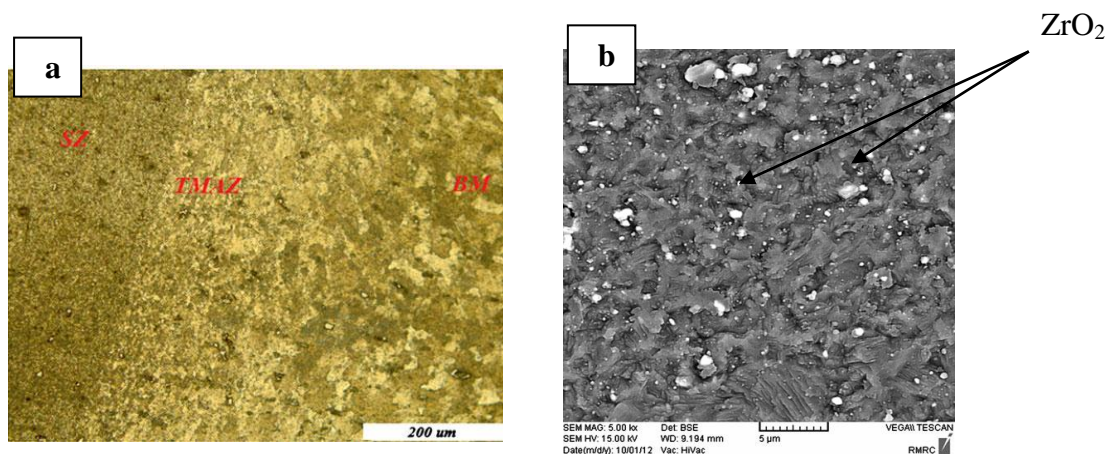


Figure 7. a) Micrograph of various zones with high magnification of Al/ZrO₂, process parameters: 1250 rpm, 80 mm/min b) distribution of ZrO₂ particles in the SZ. Shahraki et al., 2013.

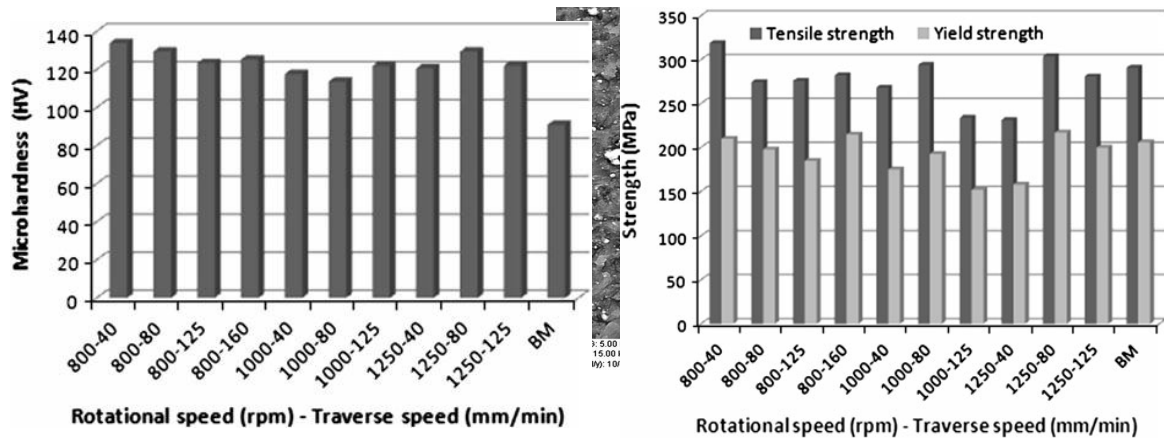


Figure 8. a) Hardness values of BM and SZ. b) Mechanical properties of BM and FSP samples Shahraki et al., 2013.

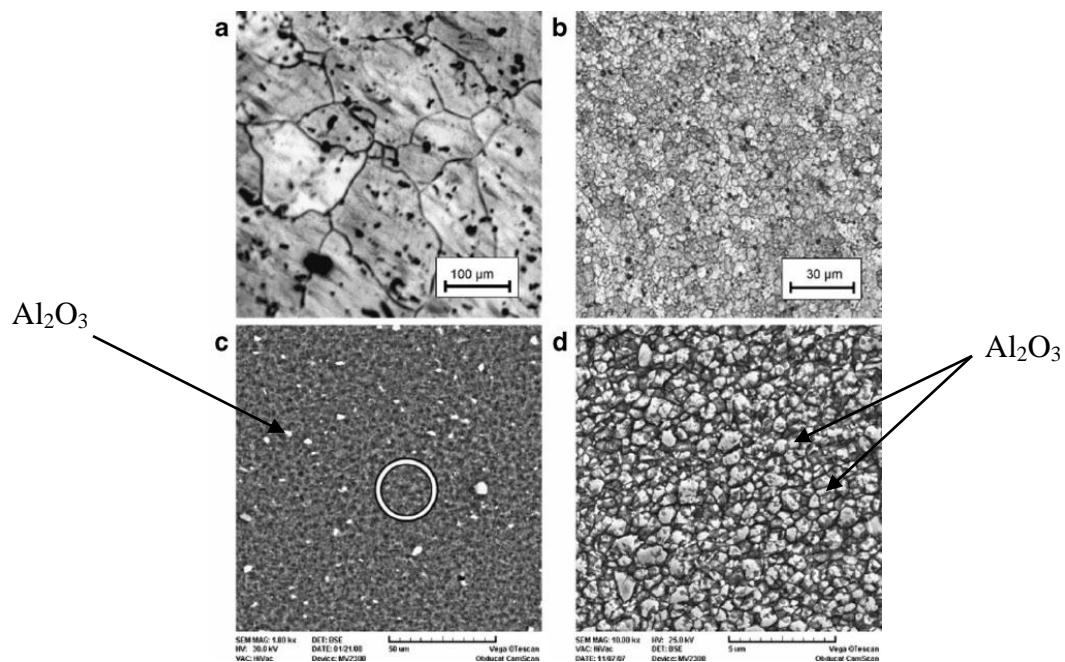


Figure 9. Optical micrographs showing the grain size of as-received 6082 Al (a) and Al 6082 before FSP (b) after four FSP passes. (c and d) SEM images showing the microstructure of the Al/Al₂O₃ surface composite layer produced by four FSP passes. Panel (d) is enlargement inside a circle for panel (c). Zarghani, et al., 2009.

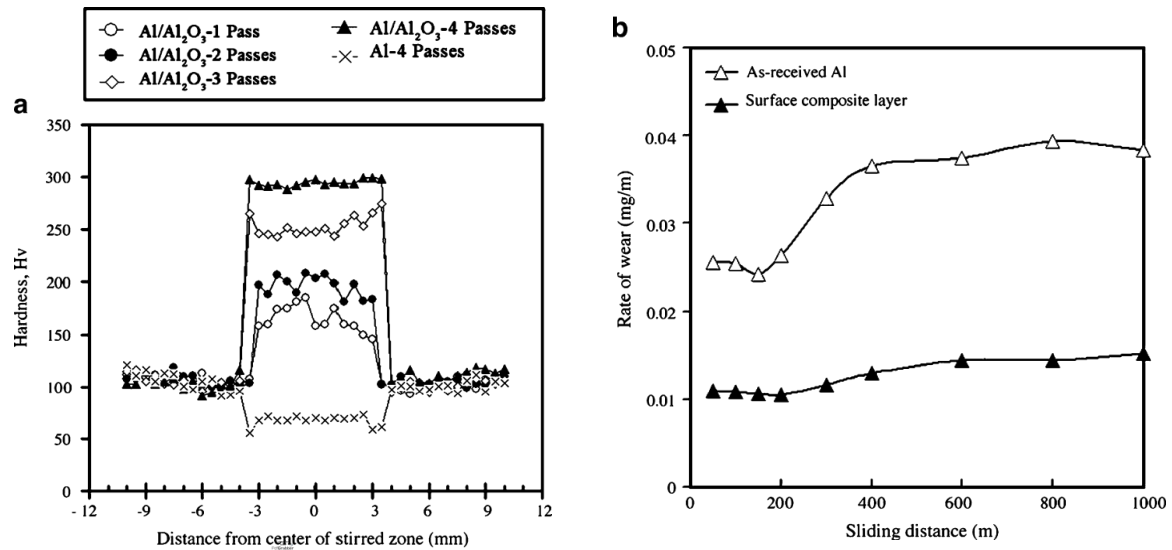


Figure 10. (a) Typical variation of the microhardness HV distributions of the FSPed 6082 Al alloy (no Al₂O₃) and surface composite layers. (b) Change in the reduction in pin weight with sliding distance for as received Al and surface nanocomposite layer produced by four FSP passes. **Zarghani, et al., 2009.**

Table 4. Processing parameters used in the FSP operations with 3-pass technique; travel speeds were 30 mm/min. **Sahraeinejad, 2014.**

Pass Number		Groove Depth (mm)	Shoulder Diameter D1 (mm)	Pin Diameter D2 (mm)	Pin Length L1 (mm)
0	Capping	N/A	15	N/A	N/A
1	Spiral Pin		10, 15	5	2.2, 4.0
2	3-flat	2 and 4	12, 15	5	2.2, 4.0
3	3-flat		12, 15	5	2.0, 3.8

Table 5. Summary of FSP Parameters applied. **Sahraeinejad, 2014.**

Pass Number		Tool	RPM	Rotation Direction	Inclination (°)	Travel Speed (mm/min)
0	Capping	Capping	1800	CW		
1	Pass 1	Spiral pin	1120	CCW	2.5	30
2	Pass 1	3 flat	450	CCW	2.5	
3	Pass 1	3 flat	450	CW	2.5	

Table 6. Chemical composition (wt %) of the base metal 6061 Aluminum alloy. **Samiee et al., 2011.**

Mg	Si	Fe	Cu	Cr	Mn	Zn	Ti	Al
1.05	0.36	0.41	0.23	0.05	0.07	0.12	0.01	Base

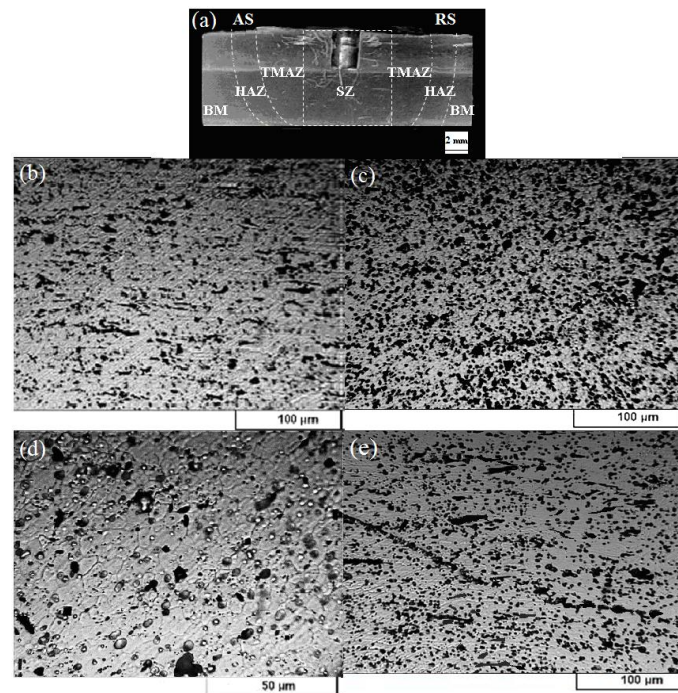


Figure 11. Cross section of the F1800: (a) the stirred zone, the TMAZ and the base metal interface, (b) the base metal, (c) the stirred zone, (d) the TMAZ and (d) the HAZ. **Samiee et al., 2011.**

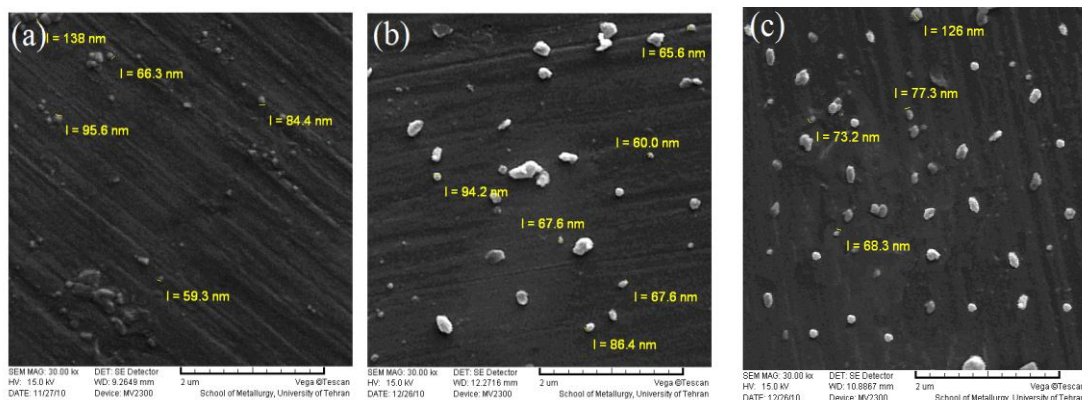


Figure 12. Effect of the rotary speed on the nano-sized AlN powder distribution and aluminum nitride cluster size in the surface Al/AlN nano-composite of the: (a) F900, (b) F1120 and (c) F1800 at a magnification of 30.00 kx. **Samiee et al., 2011.**

اعداد قواعد بيانات المكانية للتربة وحساب مساحاتها في العراق للإغراض الصناعية باستخدام نظم المعلومات الجغرافية (GIS)

نغم عامر عبداللطيف

مدرس مساعد
قسم المساحة
كلية الهندسة/جامعة بغداد

الخلاصة

تعد عملية تصنيف التربة في العراق للإغراض الصناعية من المواضيع المهمة التي تحتاج إلى دراسات واسعة ومتخصصة من أجل النهوض بالواقع الخدمي والصناعي في بلدنا العزيز، إن الكثير من البحوث العلمية تطرقت إلى تصنيف التربة في المجالات الزراعي والتجارية وغيرها من المجالات الأخرى إلا أننا لم نجد أي من المصادر والبحوث التي تطرقت إلى تصنيف الأراضي للإغراض الصناعية بصورة مباشرة. تم في هذا البحث استخدام برامج متخصصة مثل برنامج نظم المعلومات الجغرافية يتيح إمكانية دراسة التوزيع المكاني للظواهر والنشاطات والأهداف التي يمكن تحديدها في المحيط المكاني كالنقاط والخطوط والمساحات، حيث يقوم النظام بمعالجة المعلومات المرتبطة بتلك النقاط أو الخطوط أو المساحات لجعل البيانات جاهزة لاسترجاعها لغرض تحليلها أو الاستفسار عن معلومات معينة من خلالها. يهدف البحث إلى توفير الإمكانيات التي يتيحها نظام المعلومات الجغرافية لاستخدامها في مجال إعداد قواعد بيانات مكانية لتصنيف التربة في العراق للأغراض الصناعية من خلال تحويل الخرائط الورقية التقليدية إلى الصيغة الرقمية ومن ثم تكوين الطبقات المكونة للخريطة وإعداد قاعدة البيانات المكانية المناسبة لها. وإجراء تحليلات لهذه البيانات بما يسهل من تقليل الجهد والكلفة وزيادة الإنتاج والسرعة والدقة.

الكلمات الرئيسية: نظم المعلومات الجغرافية، تصنيف التربة للأغراض الصناعية، قاعدة بيانات، خرائط.

Prepare rules spatial data for soils and the Calculation of an Area in Iraq for Industrial Purposes using Geographic Information Systems (GIS)

Nagham Amer Abdleateef
Department of Surveying Engineering
College of Engineering
Baghdad University
husain_yousif@yahoo.com

ABSTRACT

The process of soil classification in Iraq for industrial purposes is important topics that need to be extensive and specialized studies. In order for the advancement of reality service and industrial in our dear country, that a lot of scientific research touched upon the soil classification in the agricultural, commercial and other fields. No source and research can be found that touched upon the classification of land for industrial purposes directly. In this research specialized programs have been used such as geographic information system software The geographical information system permits the study of local distribution of phenomena, activities and the aims that can be determined in the local surrounding like points, lines and areas, where the geographical information system treats the data related to these points, lines and areas to make the data ready to be returned for analysis or asking about certain information by using it.

The research aims to employ the potential given by GIS use in the field for building geo data based for soil classification in Iraq and transferring the traditional paper maps into digital maps. Then making the layers that the maps made of and preparing the geo data base that are appropriate. After that analysis of these data is done which permits for less effort and cost and finally increasing in the production speed and accuracy.

Key words: GIS, soil classification for industrial purposes, database, maps.

1- المقدمة

أجريت العديد من البحوث العلمية تطرقت إلى تصنيف التربة في المجالات الزراعي والتجارية وغيرها من المجالات الأخرى. البحث تطرق إلى تصنيف الأراضي للإغراض الصناعية بصورة مباشرة. إن التربة العراقية تحتوي على معادن وثروات مهمة وباحتياطات متميزة جعلت العراق في بعضها يحتل مواقع متقدمة من حيث الاحتياطي والإنتاج على المستوى الدولي، كما أن استخدامها محلياً يوفر العمل لنسب معينة من السكان ويفتح المجال أمام استثمار الرأسمال الوطني لإقامة المصانع المختلفة من أجل استغلال الموارد الطبيعية واستثمارها اقتصادياً.

واعتماداً على ما تقدم تبرز أهمية دراسة تصنيف التربة في العراق واثراً ومن خلال هذه الدراسة للتوزيع الجغرافي للتربة وكميات احتياطها، كما تم دراسة أهمية الصناعات الاستخراج الموارد المعدنية في محافظات، فضلاً عن دراسة الأفق المستقبلي للمعادن والثروات المتوافرة في العراق (Barzanji,1984).

إن معرفة التركيب الجيولوجي ونوعية الصخور تؤدي إلى تحديد نوعية وكمية الثروة المعدنية الموجودة في أي إقليم جغرافي فضلاً إلى توزيعها الجغرافي (Konecny,2003). تم إنشاء خارطة لتصنيف التربة للإغراض الصناعية في العراق باستخدام نظام المعلومات الجغرافية، إذ إن تصنيف التربة يمكن القول عنه هو لغة التخاطب الأولى بين المهتمين بعلم التربة ويعد من الأمور المهمة التي يلزم معرفتها والإلمام بها، فالتصنيف يعتمد على الغرض من استخدام التربة فقد يكون التصنيف لأغراض زراعية أو جيولوجية أو هندسية أو غير ذلك. وبمعرفة نوع التربة يمكن حل المشاكل التي قد تظهر عند استخدامها (Chang,2006).

2- أهمية التصنيف:

معرفة أنواع التربة مهمة جداً للاستعمالات في الميدان الزراعي أو العمراني أو مد المواصلات أو تهيئة البيئة بصفة عامة. وإذا كانت البلدان المتطورة قد مسحت أراضيها ودرست تربتها، فحددت أنواعها ورسمت لها خرائط منذ مطلع القرن الحالي، فإن بلدان كثيرة في العالم خاصة البلدان النامية ومنها البلدان العربية لازالت في معظم الحالات لم تغط دراسة تربتها، حيث أن هناك مساحات شاسعة من سطح أراضيها لازالت في طي المجهول أو هي مدروسة دراسة عامة وأن معظم خرائط التربة للعالم العربي أن وجدت فهي ذات مقاييس صغيرة لا تعطي إلا فكرة موجزة، كثيراً ما كانت غير واقعية أو مضللة نوعاً ما، إذ تخفي حقائق كثيرة ويسودها الغموض كما يختلط فيها الواقع بالنظري (Ibraheem,2006). وقد قام بوضعها في معظم الأحيان الأجانب المستعمرون أيام الاحتلال كما هو الشأن لمعظم خرائط التربة كما استقدمت بعض الدول العربية في النصف الثاني من القرن الحالي خبراء من الولايات المتحدة، والاتحاد السوفيتي سابقاً، وفرنسا لدراسة تربتها وتصنيفها ورسم خرائط لها، معتمدين في السنوات الأخيرة على معلومات تقدمها لهم الأقمار الصناعية الأمريكية أو الأوروبية. ولعل أهم ما يلفت الأنظار في تصنيف التربة في العالم العربي هو صعوبة تطبيق التصنيفات الأجنبية والأوروبية والأمريكية، ذلك لشدة تنوع التربة في البلدان العربية ومنها العراق وما يميزها عن كثير من التربة في العالم، لذلك يكون من الضروري دراسة وتصنيف ورسم خرائط التربة في العراق من أجل معرفة استخدام هذا التصنيف للإغراض الصناعية (Longley,2005).

إن تصنيف التربة ضروري لكي يسهل التعامل معها ويكتمل استعمالها فإن مشكلة التصنيف لازالت قيد الأخذ والرد والنقاش، وذلك لعدة أسباب، منها: كثرة العوامل المشكلة للتربة، ثم لعدم وجود فواصل واضحة بين المراحل الاستمرارية لتطویر التربة، فمن تعريفنا للتربة على أنها النتاج الأخير

لعوامل : طبيعية وحيوية ، ظلت تعمل متعاونة ، مدة طويلة من الزمن لتشكيلها ، يظهر لنا أن هذه العوامل كثيرة ومتنوعة وأن إدخالها كلها في التصنيف قد يؤدي بنا إلى بلوغ أرقام من الأنواع يصعب إدراكه (Gilbrook, 1999).

1-2 تصنيف التربة

في هذا البحث تم تجميع المعلومات من التقارير المختبرية التي أنجزت من قبل المركز الوطني للمختبرات الإنشائية لمختلف مناطق العراق (N.C.C.L., 1986). و نظراً للكم الهائل من المعلومات أصبح من الصعوبة التعامل معها واستيعابها والاستفادة منها. إلا إذا نظمت وصنفت وفهرست واختزلت رقمياً وخُزنت في قواعد بيانات يمكن التعامل معها آلياً والاستفادة منها دون أن يخل هذا الاختزال والإيجاز بدقتها وصحتها ودالاتها. فدعت الحاجة إلى استعمال نظم المعلومات الجغرافية لما يمتاز به هذا البرنامج من حفظ كميات هائلة من البيانات والتي تترتب في جداول مع مساحة كبيرة من خرائط الموقع الجغرافية والتي لا يمكن حفظها بصورة أمينة على الورقة، ويتم حفظ البيانات مع الخرائط بطريقة مترابطة بحيث يسهل على المستخدم عرض البيانات الجدولية مع الخرائط وبعده أساليب بالإضافة إلى إجراء عمليات معالجة حسابية عليها لاستخراج النتائج بوقت وجهد قليلين والاستفادة منها في اتخاذ القرارات بالسرعة المناسبة (ESRI, 2008). وفي هذا البحث تم الاعتماد على العديد من الصور الفضائية التي تبين تضاريس ونوعية التربة لأغلب مناطق العراق، وكذلك خرائط ورقية على سبيل المثال ، تم مسحها ضوئياً لكي يسهل التعامل معها في برنامج نظم المعلومات الجغرافية. ويوضح الشكل (1) فتح الخريطة في برنامج نظم المعلومات الجغرافية وبعد ذلك تتم عملية الإرجاع الجغرافي للخارطة المدخلة ثم عملية الترفيق الإلكتروني فإدخال الإحداثيات ثم إنشاء الطبقات حيث يظهر كل نوع من التربة على شكل طبقات (عودة، 2005). والشكل (2) يوضح إحداثيات و موقع كل نقطة بالنسبة إلى الخارطة الأصلية (المدخلة).

ومن خلال معرفة الإحداثيات الحقيقية للخارطة من خلال الشبكة الموجودة على الخارطة وهي الشبكة الجغرافية خط الطول وخط العرض كما موضح في الجدول (1) وتم اختيار المسقط المناسب للحصول على أقل عملية تشوه للتحويل من الإحداثيات الجيودسية "الكروية" إلى الإحداثيات التريبية "المترية" حيث تم استخدام المسقط الاسطوانى المستعرض أو ما يعرف (Universe Transverse Mercator UTM) الذي استخدم في البرنامج لعملية تحويل الإحداثيات من النظام الجغرافي إلى النظام كارتيزي (Y=Northing, X=Easting).

2-2 تصنيف التربة باستخدام نظم المعلومات الجغرافية:

بعد عملية ادخال كل المعلومات المتوفرة الى البرنامج وتحليل النتائج تم تصنيف اهم أنواع التربة التي صنفت باستخدام نظم المعلومات الجغرافية هي كما موضحة بالأشكال من الشكل (3) الى الشكل (15) حيث تظهر كل تربة في موقعها بالنسبة الى خارطة العراق بشكل مستقل، والشكل (17) يوضح الخارطة النهائية للعراق بعد أن تم جمع البيانات وتحليل النتائج من شكل (1-15) من اجل الحصول على افضل توزيع صناعي للمواقع هذه التربة التي يمكن ان تستثمر بشكل صحيح وهي كالتالي:

1-2-2 التربة الفسفورية Phosphorite Soil: وتكون هذا النوع غني بمعدن الفسفور ويتواجد في شمال وغرب العراق. ويكون انتشاره في العراق كما موضح في (الشكل 3).

2-2-2 التربة الرملية (Sand Soil): تتكون هذه التربة بصورة رئيسية من السيليكا (SiO_2) ويستخدم النقي منها في صناعة الزجاج اما النوع الذي يكون غني بالحديد والذي يسمى (Ferruginous Sand Soil) ذو اللون الاحمر او بني يكون ذو اهمية اقتصادية ويمثل خام الحديد وتستهلك التربة الرملية في البناء والانشاء حيث تستعمل في الخرسانة المسلحة كما تمتاز بمسامية ونفاذية عالية. (العكدي، 1996) ويكون انتشاره في العراق كما موضح في (الشكل 4).

3-2-2 التربة الجيرية (Lime Soil): وتتكون من كربونات الكالسيوم والمغنسيوم $\text{CaMg}(\text{CO}_3)_2$ ويعتبر هذا النوع من التربة ذات اهمية اقتصادية حيث يستعمل في صناعة الاسمنت ويستعمل أيضاً في البناء والإنشاءات واكساء الشوارع وان

هذه التربة اذا ما تعرضت الى دفن داخل الارض (حرارة وضغط) تتحول صخر المرمر الذي يعتبر من الصخور الاقتصادية المستخدمة في البناء والإنشاءات وعمل الأرضيات (خضر، 2001). ويكون انتشاره في العراق كما موضح في (الشكل 5).

4-2-2 التربة الطينية (Clayey Soil): هي من التربة الفتاتية ناتجة من عمليات التجوية الكيميائية تتكون من سيليكات الألمنيوم المائية $(AlSi)_3O_4$ ذو أهمية اقتصادية كبيرة حيث تستخدم في صناعة الطابوق والسيراميك وصناعة الأسمنت والأنواع منها ذات جودة عالية تستعمل في صناعة الفخار وإطباق ومستحضرات التجميل اما الأنواع التي تكون ذات درجات انصهار عالية تستعمل في صناعة الحراريات والأفران والصناعات الكهربائية وخاصة في خطوط نقل الطاقة العالية وفي عمل فلاتر تصفية المياه (الجبوري، 2002). ويكون انتشاره في العراق كما موضح في (الشكل 6).

5-2-2 الصخور المتحولة (Metamorphose Rocks): من أشهر الأنواع هو الذي يدخل في تركيب المرمر والذي بدوره يدخل في البناء والإنشاءات التي تستعمل في عمل السقوف والأرضيات ويحوي هذا النوع من التربة على معادن ذات قيمة عالية مثل (Kyanite) الذي يستعمل في صناعة المواد الحرارية (خضر، 2001). ويكون انتشاره في العراق كما موضح في (الشكل 7).

6-2-2 التربة الملحية (Salty soil): يتكون هذا النوع من معدن (Halite) الذي هو كلوريد الصوديوم NaCl وهو يترسب من مياه البحيرات ويبلغ وزنه النوعي (2.16) وغالبا ما يحتوي على شوائب من أملاح البوتاسيوم (KCl) ويعتبر من المعادن المهمة في حياة الإنسان حيث يستخدم الملح للطعام مثال عليه مملحة السماوة جنوب العراق. (العكدي، 1996) ويكون انتشاره في العراق كما موضح في (الشكل 8).

7-2-2 الصخور المتكتلة (Conglomerates): وهي الناتجة من ترسيب قنوات الأنهار وتكون ذات حجم كبير يصل حجم قطر حبيبتها من (3-60) ملم وتكون الحبيبات متماسكة بمواد لاحمة مختلفة مثل السيليكا أو أكاسيد الحديد أو كربونات الكالسيوم وتستعمل في البناء والإنشاءات وفي رصف الطرق (خضر، 2001). ويكون انتشاره في العراق كما موضح في (الشكل 9).

8-2-2 المارل (Marl): يعتبر من النوع الطيني ولكن يحتوي على نسبة عالية من الجير (كربونات الكالسيوم $CaCO_3$) وتستعمل في صناعة الاسمنت وفي صناعة الفخار (الجبوري، 2002). ويكون انتشاره في العراق كما موضح في (الشكل 10).

9-2-2 التربة الغرينية (Silty Soil): وتكون فتاتية ذات حجم حبيبي اقل من حجم الرمل ويستعمل في البناء والإنشاءات وأيضاً يعتبر من رواسب الأنهار والبحيرات وتكون غنية بالمعادن الثقيلة. ويكون انتشاره في العراق كما موضح في (الشكل 11).

10-2-2 صخور صلتالية (Shale): وهو نوع طيني متعرض الى ضغط حيث فقد كل محتوياته المائية وتصلب على هيئة طبقات رقيقة او صفائح وله نفس استعمالات الطين (خضر، 2001). ويكون انتشاره في العراق كما موضح في (الشكل 12).

11-2-2 الصخور النارية (Igneous Rocks): ويتكون من صخور كبيرة مثل صخرة (Basalt & Granite) وهما من اكثر الصخور الرئيسية التي تستخرج منها معظم خامات المعادن الفلزية منها مثل الحديد والنيكل والكروم والزنبق والذهب والبلاتين والنحاس والرصاص والألمنيوم وغيرها من الفلزات حيث تترسب هذه المعادن بصورة مباشرة من الصهير كما ايضا تحتوي هذه الصخور على معادن نفيسة مثل الماس ومعدن الزمرد والعقيق وغيرها (العكدي، 1996). ويكون انتشاره في العراق كما موضح في (الشكل 13).

12-2-2 التربة المزيجية: تكون خليط ما بين الغرين والطين من ناحية حجم الحبيبات والاستعمالات وقد تحتوي على ترسبات لبعض الفلزات والمعادن النفيسة كما انها تعتبر مفيدة للزراعة وتشكل الجزء الاكظم من السهل الفيضي لنهري دجلة والفرات ويكون انتشاره في العراق (العكدي، 1996). كما موضح في (الشكل 14).

13-2-2 Gypsum and Alanhaedraat: ان الانهايدرايت كبريتات الكالسيوم اللامائية (CaSO_4) وعندما يمتص الماء يتحول الى كبريتات الكالسيوم المائية ($\text{CaSO}_4 \cdot 2\text{H}_2\text{O}$) حيث يأخذ جزيئي ماء وهو يترسب من مياه البحار الضحلة والبحيرات الشاطئية ان الاهمية الاقتصادية له هو يستخدم بصورة رئيسية في عمل الجص المستخدم في البناء كما يدخل في خلطة الاسمنت كما انه يستعمل في عمل التماثيل (خضر، 2001). ويكون انتشاره في العراق كما موضح في (الشكل 15).

3- حساب المساحات :-

لغرض حساب المساحة تم اختيار المسقط المناسب للحصول على اقل عملية تشوه للتحويل من الاحداثيات الجيودسية "الكروية" الى الاحداثيات التربيعية "المتريية" وهناك مساقط متنوعة مثل المخروطي والاسطواني والمستوي والشائع هو الاسطواني المستعرض او ما يعرف (Universe Transverse Mercator UTM) المسقط العالمي الاسطواني المستعرض والذي يقسم العالم الى قطاعات Zone كل واحد محصور بـ 6 درجات طول مع العلم ان نقطة الانطلاق لخطوط الطول هو خط Greenwich وخط العرض الرئيسي هو خط الاستواء وتقاطع خط الطول الرئيس لكل قطاع وخط الاستواء يمثل نقطة الانطلاق لنظام الاحداثيات في هذا القطاع ويعرف كل قطاع كالاتي. خط الطول الرئيس Central Meridian والذي هو 45 درجة لقطاع 38 والذي يغطي حوالي 90% من العراق و 51° درجة لقطاع 39 والذي يغطي مساحة قليلة جدا من العراق في محافظة البصرة قرب الحدود الايرانية و 39° درجة لقطاع 37 والذي يغطي منطقة غرب الانبار ، (العبادي، 2006).

ويوضح الجدول (2) النسبة المئوية لمساحة كل تربة بالنسبة الى مساحة العراق الكلية ، وكذلك يوضح مساحة كل تربة ويظهر ذلك بشكل اوضح .

اما في الشكل (16) الذي تم رسمه بالاستعانة ببرنامج (Excel) حيث يظهر المساحة التي تشغلها كل طبقة نسبة الى الطبقات الأخرى. ان رسم طبقات التربة هو عبارة عن رسم مضلع (polygon) لكن الامر ليس بهذه البساطة إذ ان هناك مجموعة من المشاكل ستواجهنا مثل مشكلة التجاور بين الطبقات حيث ان دقة الرسم مهما كانت عالية ستكون هنالك اما تداخل (overlab) او فراغات (gaps) بين الطبقات ولتجاوز هذه المشاكل تم استخدام برنامج (Arctoolbox) الذي له إمكانية مسح جزء من طبقة متداخل مع طبقة اخرى لتنتج طبقة جديدة غير متداخلة مع الطبقة الأخرى أما الطبقة القديمة فيمكن مسحها لان الطبقة الجديدة تعوض عنها، (Iraq G.S.I.Institute, 2012).

والآن وبعد أن تم حساب المساحة لكل طبقة من طبقات التربة (أنواع التربة) يمكننا أن نجمع كافة البيانات في خريطة يمكننا ان نسميها خريطة تصنيف التربة في العراق للإغراض الصناعية ويمكن أن تستخدم قسم منها في الإغراض الهندسية لأننا استخدمنا بعض المعايير الهندسية في التصنيف حيث تم الاعتماد على تقارير هندسية صادرة من المركز الوطني للمختبرات الإنسانية. والشكل (18) يوضح خريطة تصنيف التربة في العراق للإغراض الصناعية .

4- الاستنتاجات:

- أ- يمكن الاستفادة من هذا البحث في تحديد الموقع الأمثل لإنشاء المعامل الصناعية حسب تواجد المواد الأولية والتي تم تحديد موقعها من خلال اعداد قواعد البيانات المكانية للتربة.
- ب- أعطينا فكره أولية عن أنواع التربة المتوفرة ومعرفة مساحاتها ونسبها المئوية ومواقع انتشارها في العراق بواسطة استخدام البرامج الحديثة والتحليلات الإحصائية.
- ت- تم في هذا البحث التعامل مع المعلومات والبيانات الكبيرة ومعالجتها وادرتها وتحليلها وتحديثها، خاصة وأنها تعتمد بشكل أساس على معطيات الاستشعار عن بعد الواسعة الدقة، لتسهيل عملية دراستها وتحليلها

ومقارنتها واتخاذ القرارات المناسبة للتخطيط والتنمية في منطقة الدراسة، وبذلك استطاعت تمثيل هذا الكم المعلوماتي في خرائط موضوعية كمية ونوعية وبدقة عالية، وسهولة تحليلية للقارئ المتلقي خاصة عند استعمال الرموز البيانية فيها.

ث- من خلال هذه البيانات التي اعدت باستعمال برنامج نظم المعلومات الجغرافية يمكننا أضافتها الى بيانات اخرى لتمكين العاملين في هذا المجال الاستفادة منها في اتخاذ القرارات المناسبة في تصميم وإنشاء المصانع حسب تصنيف التربة فانه سوف يوفر اقل وقت واقل كلفة لإنتاج اي مشروع مستقبلاً.

REFERENCES

- Ali Hussian, Z. M., 2008, The effect of Grading of Aggregate on Properties of Self-Compacting Concrete, MSC. Thesis, College of Engineering, Department of civil engineering, AL-Mustansirya University, January.
- Barzanji, A.F., 1984, Infiltration Rate Characteristics of Gypsiferous Soil in Northern Iraq Al-Jazirah-Area, M.Sc. Thesis, Irrigation and Drainage Engineering Department, College of Engineering, University of Mosul.
- Chang, K.T., 2006, Introduction to Geographic Information System, 3d .Ed. McGraw Hill international Edition.
- ESRI Arc GIS 9.3 Help Manual, 2008, Environmental System Research Institute Inc, Redlands, California.
- Gilbrook, M.J GIS Paves the way, 1999, Civil Engineering, Vol.69, No.11.
- Ibraheem, A. Th., 2006, The application of geographic information system (GIS) in civil engineering, 4th International Forum on Engineering Education - IFEE2006 / Integrating Teaching and Research with Community Service / 25-27 April 2006, Sharjah, United Arab Emirates.
- Iraq Geological Surveying Institute, 2012, Geosurv-Iraq and maps of Iraq, Baghdad.
- Konecny ,G., 2003, Geo information: Remote sensing ,Photogrammetric and Geographic Information System, Taylor& Francis, London and New York.
- Longley,P.A.,Goodchild,M.F., Maguire, D.J., and Rhind, D.W., 2005, Geographical nformation Systems and Science" , 2nd Edition, England, John Wiley & Sons Ltd, USA.
- N.C.C.L.. A Study of The Engineering Soil Characteristics of Iraq Area, 1986, Report No.67,68,69,70and 71, Baghdad, Iraq.

المصادر العربية

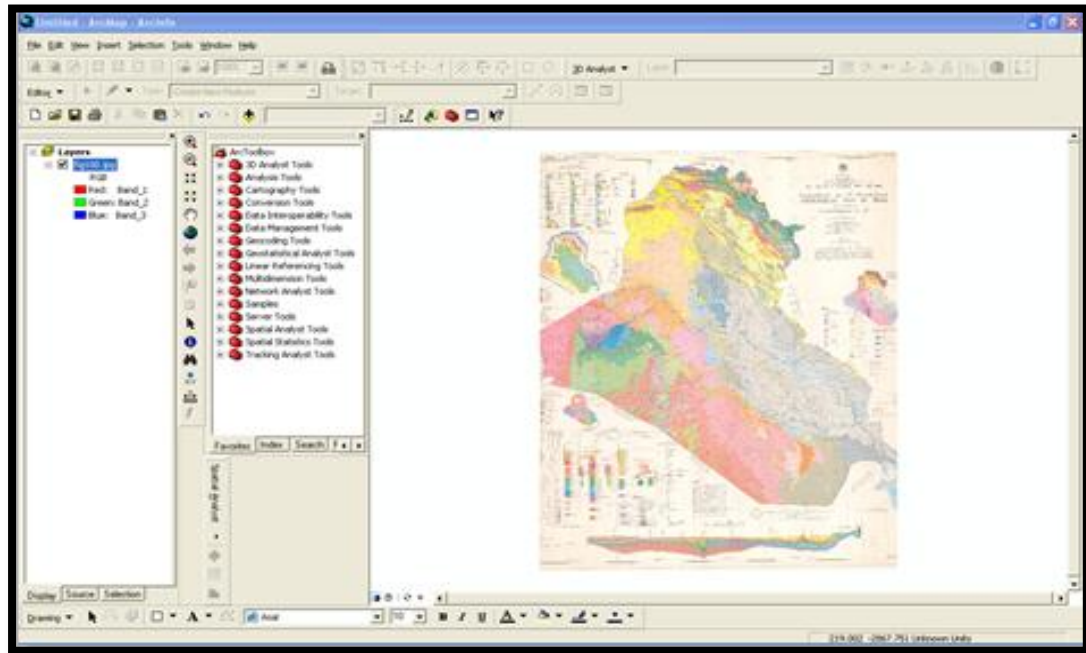
- ألبادي، خضر خشن، "مساقط الخرائط"، مطبعة جامعة بغداد، بغداد، 2006.
- العكيدي، وليد خالد، "نظام تصنيف الترب العراقية"، مجلة العلوم الزراعية العراقية المجلد 27، العدد 1، 1996.
- الجبوري، حامد حسن عبدالله، "الخرائط الجيوتكنيكية الأولية للتربة في المحافظات وبعض المناطق المجاورة"، اطروحة ماجستير كلية العلوم _ جامعة بغداد، 2002.
- خضر، سالار علي، "دور العوامل الجغرافية في تكوين التربة وتغير صفاتها"، اطروحة ماجستير كلية التربية (ابن رشد) _ جامعة بغداد، 2001.
- عودة، سميح احمد محمود، "أساسيات نظم المعلومات الجغرافية وتطبيقاتها في رؤية جغرافية"، دار المسرة للنشر، عمان، الاردن 2005.

الجدول (1) . إحداثيات النقاط المختارة حسب موقعها على الخارطة.

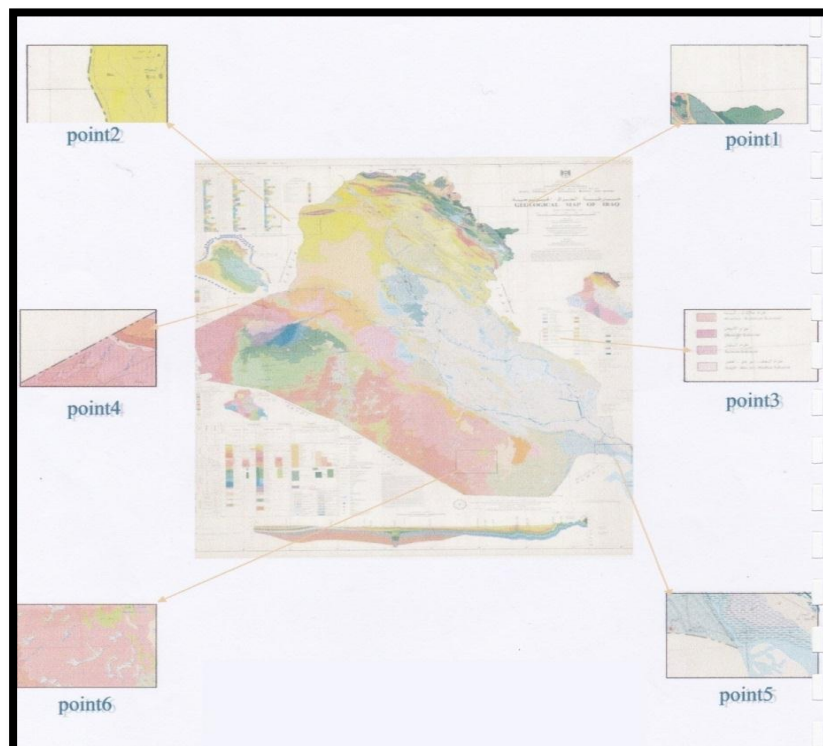
رقم النقطة	خطوط العرض α (Northing)	خطوط الطول λ (Easting)
1	46° 23' 11"	36° 30' 10"
2	44° 33' 41"	35° 46' 16"
3	47° 42' 52"	32° 55' 26"
4	40° 12' 31"	33° 20' 42"
5	48° 22' 43"	29° 10' 55"
6	45° 13' 12"	29° 23' 34"

الجدول (2). يوضح المساحة لكل طبقة مع النسب المئوية لها تم حسابها من خلال البرنامج.

اسم الطبقة	نوع الطبقة	المساحة بالمتري المربع	النسبة المئوية
Main river	Polygon	2153662902	0.47739
Sub river	Polygon	448290669.2	0.09937
Lakes	Polygon	5276990657	1.16972
Silty soil	Polygon	32483547010	7.20044
Marl	Polygon	27110374840	6.00940
Medley soil	Polygon	104053826800	23.06501
Metamorphosed	Polygon	3408308349	0.75550
Phosphorite soil	Polygon	3078169361	0.68232
Salty soil	Polygon	13863536690	3.07305
Clayey soil	Polygon	54673687010	12.11920
Conglomerate	Polygon	18822208040	4.17221
Gypsum	Polygon	94805604280	21.01501
Igneous	Polygon	41073837450	9.10460
Lime	Polygon	3797726187	0.84182
Sandy soil	Polygon	45687572650	10.12730
Shale	Polygon	396004377	0.08778
المجموع		451132805917	100



الشكل 1. يوضح الخطوات الاولى للبرنامج نظم المعلومات الجغرافية مع الخارطة



الشكل 2. يوضح الخارطة المدخلة موضح عليها موقع كل نقطة بالنسبة الى الخارطة الاصلية.



التربة الرملية

الشكل 4. يوضح عليها أماكن تواجد التربة الرملية



التربة الفسفورية

الشكل 3. يوضح عليها أماكن تواجد التربة الفسفورية.



التربة الطينية

الشكل 6. يوضح عليها أماكن تواجد التربة الطينية.

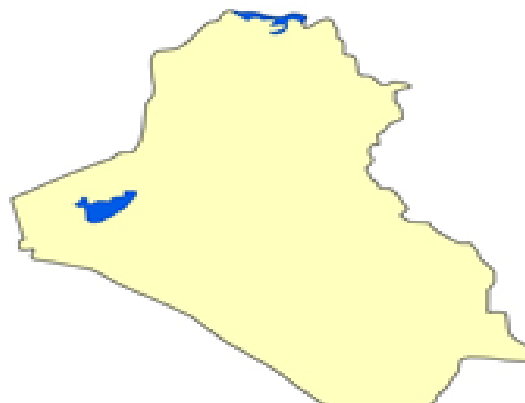


التربة الجيرية

الشكل 5. يوضح عليها أماكن تواجد التربة الجيرية.



الشكل 8. يوضح عليها أماكن تواجد التربة الملحية



الشكل 7. يوضح عليها أماكن تواجد الصخور المتحولة .



الشكل 10 . يوضح عليها أماكن تواجد المارل.



الشكل 9 . يوضح عليها أماكن تواجد الصخور المتكتلة



التربة الصلصالية

الشكل 12. يوضح عليها أماكن تواجد الصخور الصلصالية



التربة الغرينية

الشكل 11. يوضح عليها أماكن تواجد التربة الغرينية .



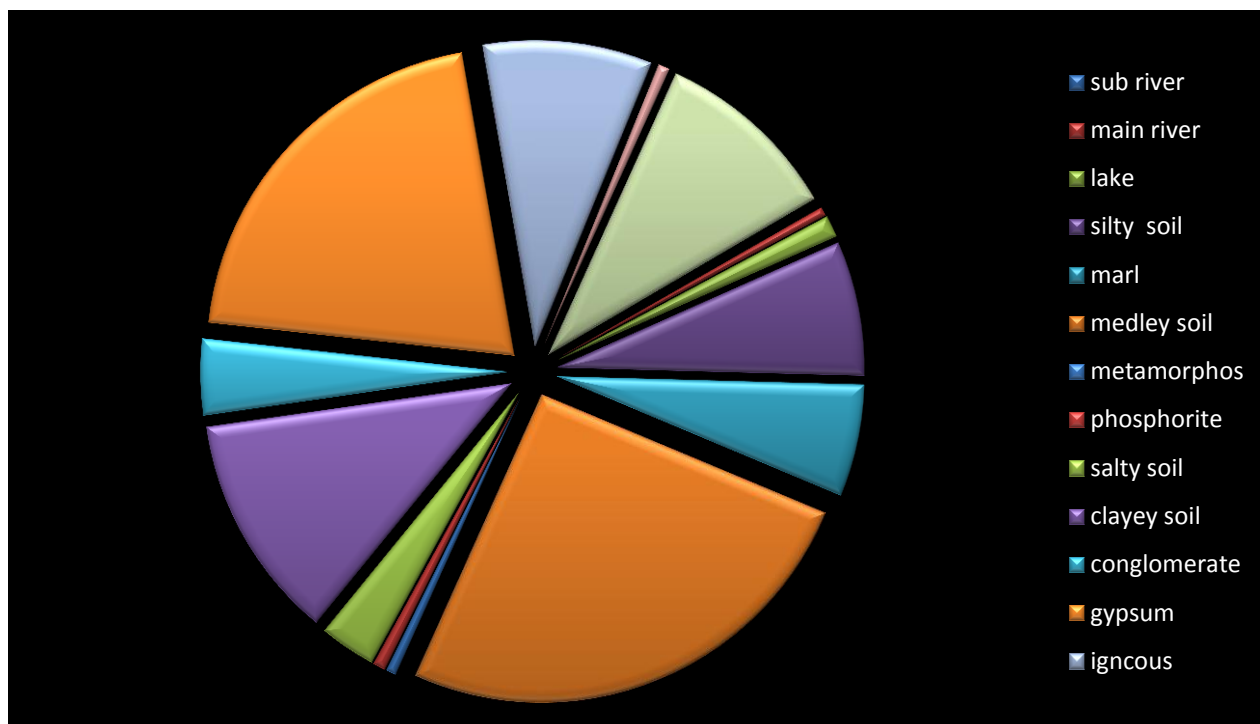
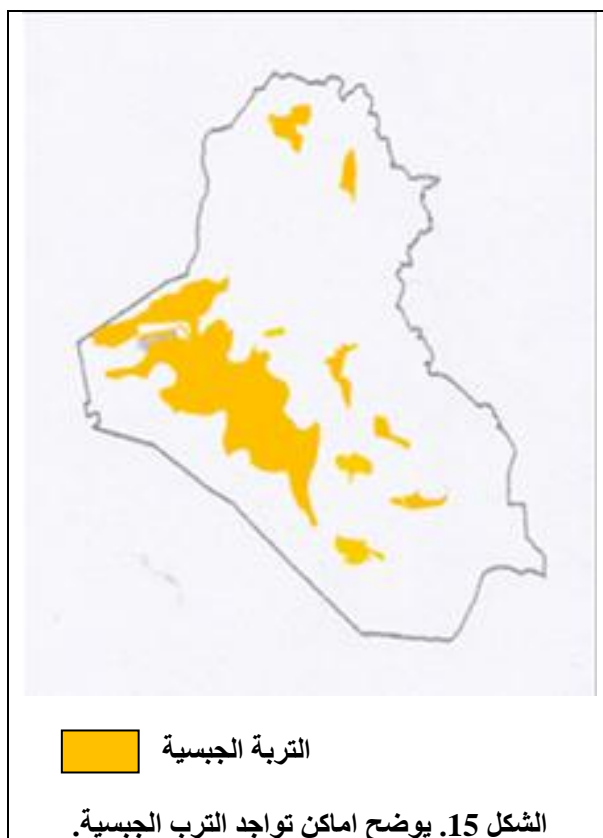
التربة المزيجية

الشكل 14. يوضح أماكن تواجد التربة المزيجية.

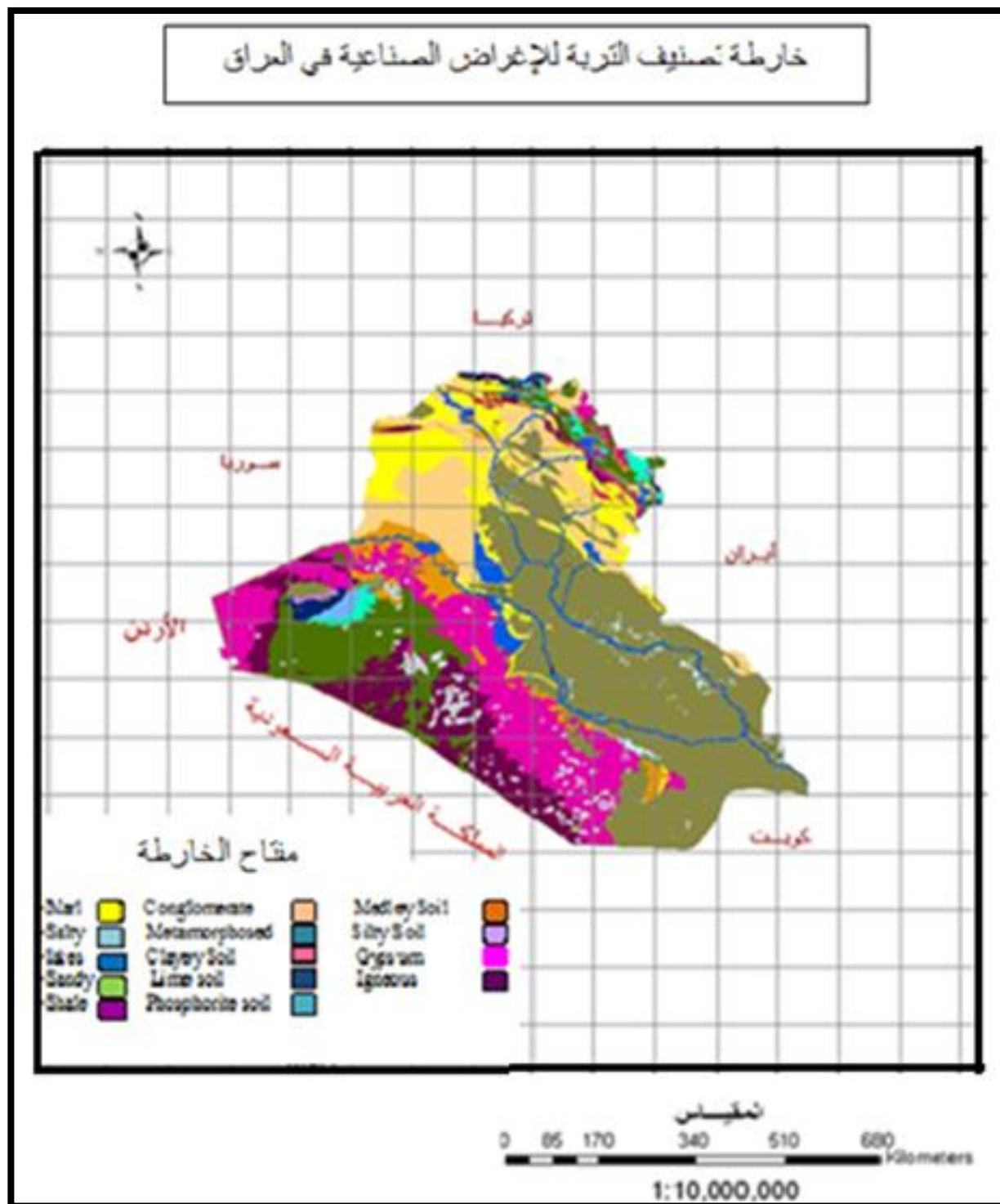


التربة النارية

الشكل 13. يوضح أماكن تواجد التربة النارية.



الشكل 16. يعطي نظرة عامة عن المساحة التي تشغلها كل طبقة نسبة الى الطبقات الاخرى



الشكل 17. خارطة تصنيف التربة لإغراض الصناعية في العراق.

List of Contents

English Section:

Page

**Enhancing Performance of Self–Compacting Concrete with Internal Curing Using
Thermostone Chips**

1 - 13

*Amar Yahia Ebrahim AL-Awadi
Prof. Dr. Nada Mahdi Fawzi*

**Influence of Temperature Upon Permanent Deformation Parameters of Asphalt
Concrete Mixes**

14 - 32

*Aliaa Faleh Hamd Al.ani
Dr. Amjad Hamad Albayati*

Regulations Enforcement Mechanisms for Sustainable Housing Projects

33 - 49

*Dr. Sawsan Rasheed Mohammed
Ibtisam Abduljabbar Abdulridha*

**Adsorption of Mefenamic Acid From Water by Bentonite Poly urea formaldehyde
Composite Adsorbent**

50 - 73

*Dr.Basma Abbas Abdel Majeed
Dr.Raheem Jameel Muhseen
Nawras Jameel Jassim*

**Performance Evaluation of a PID and a Fuzzy PID Controllers Designed for
Controlling a Simulated Quadcopter Rotational Dynamics Model**

74 - 93

*Laith Jasim Saud
Rasha Shehab Mohammed*

**Simulation of Groundwater Movement for Nuclear Research Center at Al-Tuwaitha
Area in Baghdad City, Iraq**

94 - 107

*Ayad Sleibi Mustafa
Ahmed Hazem Abdulkareem
Rasha Ali Sou'd*

Aluminium Matrix Composites Fabricated by Friction Stir Processing A Review

108 - 126

Hussein Burhan Mohammed

E-ISSN 2520-3339

P-ISSN 1726-4073



Journal of Engineering



**A Scientific Refereed Journal
Published by
College of Engineering
University of Baghdad**

**July
2017**

**Number 7
Volume 23**

E-ISSN 2520-3339

P-ISSN 1726-4073



مجلة الهندسة



مجلة علمية محكمة تصدرها
كلية الهندسة - جامعة بغداد

العدد 7
المجلد 23

رقم الايداع في دار الكتب والوثائق ببغداد
2231 لسنة 2017

قائمة المحتويات

القسم العربي:

العنوان

الصفحة

1 - 13

اعداد قواعد بيانات المكانية للترب وحساب مساحاتها في العراق للإغراض الصناعية باستخدام نظم المعلومات الجغرافية (GIS)

نعم عامر عبد اللطيف